UNIVERSITÀ
DEGLI STUDI
FIRENZE

DOTTORATO DI RICERCA TOSCANO IN NEUROSCIENZE

CICLO XXXII

COORDINATORE Prof. Renato Corradetti

Identification of prognostic and therapeutic tools for cortical stroke treatment in mice

Settore Scientifico Disciplinare MED/26

Dottorando
Dott. Irene Busti

Tutore
Prof. Ubaldo Bonuccelli

Tutore

Prof. Matteo Caleo

Coordinatore
Prof. Renato Corradetti

Anni 2016 /2019

Index

Abstract

Stroke is the third cause of death in Italy and it affects 196'000 new patients per year. Around 70-80% of patients survive the ischemic attack, however around three fourths of them do not recover completely. Currently, there are only few effective therapies to treat this pathology in the early phases. Great is therefore the need for (i) reliable biomarkers predictive of spontaneous recovery and (ii) novel approaches to stimulate the recovery of lost functions.
Given this background, the aim of my project was to develop novel prognostic and therapeutic tools in preclinical mouse models of stroke.

I took advantage of two different mouse models, the Middle cerebral artery occlusion (MCAO), which shows a higher variability and is thus closer to the human condition, and the photothrombosis, that is more reproducible and allows to better identify benefits of new therapies.

In the first part of the project, I characterized behavioral and anatomo-physiological impairments occouring in the MCAO model. By means of histology, I analyzed the ischemic lesion and its evolution. In this context, a novel quantitative method was implemented to evaluate lesion size, location and shrinkage in histological brain sections obtained 30 days after injury. Particularly, evaluating the exact lesion location for each subject allowed me to measure the percentage of the lesioned portion of the Caudal Forelimb Area (CFA), possibly an important index underling post-stroke recovery. We demonstrated that the focal site of the lesion involved predominantly somatosensory areas, whereas the motor areas, including the CFA, were only partially affected or represented a perilesional site. Indeed, a robust damage in the CFA has been found only in a minority of animals that presented a larger lesion. Then, I conducted behavioural tests to assess whether a measurable motor deficit was induced by MCAO and the extent of the associated spontaneous recovery. I exploited GridWalk test, skilled reaching test and motor performance in the M-platform, a robotic device that permits to quantitatively evaluate several kinetic and kinematic parameters related to forelimb movement. Permanent MCAO determined a clear motor deficit at the level of the contralesional forelimb, as we observed in the GridWalk test and also an impairment in the performance during fine grasping behavior, by means of the skilled reaching test. In addition, kinetic and kinematic features of the motor performance during robotic tasks showed a large variability of motor outcome in the late phase, with a complete, mild or without any degree of recovery. Making advantage of this observed variability, we conducted a preliminary correlation analysis between anatomical measures and indices of motor recovery in our set of behavioural tests. In parallel with behavioural tests, we performed also electrophysiological measures both in freely moving condition and during the retraction task onto the M-platform. We found that, after stroke induction, some alterations in bands (de)synchronization took place, especially in the affected hemisphere.

For the second part of the PhD project, I characterized the therapeutic potential of *in vitro* generated neurons to promote functional recovery after stroke. The differentiation protocol designed by our collaborators allows to reliably produce neurons of specific regional identity, i.e. cortical excitatory neurons and hippocampal neurons. First of all, I assayed the behavior

and projection patterns of these neural precursor cells after grafting in vivo, into hippocampus and motor cortex. The two types of cells were co-injected into the dentate gyrus or in the healthy motor cortex of adult mice. Both hippocampal and cortical precursors survived and fully differentiated in mature neurons after grafting in adult hippocampus and isocortex. However, they showed different capacity for axonal projection. In intact hippocampus, only grafted hippocampal cells were able to extend long-range projections, while isocortical cells failed in sending far-reaching processes. Instead, after transplantation in adult intact moto cortex, cortical cells were also able to extend processes. Then, we assessed the integration and projection patterns of isocortical cells in a mouse model of ischemic lesion induced by photothrombosis in the primary motor cortex. In this case, cells were injected three days after stroke and the assessment of recovery was based on a well established motor task (Gridwalk Test). The quantification of fibers demonstrated that cortical-like neurons transplanted in ischemic lesion displayed a higher number of projections with respect to the healthy, naïve brain. The possibility to successfully transplant neural precursors originated in vitro into damaged cortex has opened new opportunities for therapeutic approaches for cortical stroke. With this purpose, we showed that grafting cortical-like cells promoted some functional restoration of forelimb function after ischemic damage to the motor cortex.

.

Introduction

1- Introduction to stroke

Stroke is one of the major causes of mortality and disability-adjusted life years (DALYs) worldwide. Despite considerable improvement in primary prevention, diagnostic workup and treatment (i.e. stroke units, thrombolysis, and thrombectomy) and an overall decrease in mortality over the last years, the number of stroke incidents in Europe is increasing by 30% between 2000 and 2025 (Truelsen et al. 2006).
The term “stroke” is used to describe any kind of brain injury caused by an abnormality of the blood supply to the brain or one of its areas. Stroke symptoms tend to appear suddenly and relate to focal deficits and/or global brain function lasting more than 24 hours (Mackay and Mensah, 2004). Brain functioning strictly depends on a constant supply of glucose and oxygen to work normally. A sudden block of such supply determines suppression of neural function within 20-60 seconds, primarily due to interference with synaptic functions (Hofmeijer and Van Putten, 2012). If the event is limited in time, blood deprivation can cause only reversible damage but when reperfusion does not promptly occur, the damage becomes permanent (Krnjević, 2008).

1.1 Haemorrhagic vs ischemic stroke

There are two main types of stroke: hemorrhagic stroke, which accounts for 13% and ischemic stroke, which accounts for 87% of all stroke incidents (**Fig.1**). Haemorrhage refers to bleeding inside the skull, either into the brain or at the level of meninges. Bleeding into the brain parenchyma tears and disconnects important grey and white matter connections and pathways. When a hematoma forms, it exerts pressure on brain regions adjacent to the collection of blood and can injure these surrounding tissues. Oedema often develops around the hematomas, further adding to the extra volume of abnormal tissue. Large haemorrhages are often fatal because they increase pressure within the skull, squeezing vital regions in the brainstem.
Bleeding into the fluid around the brain is referred to as subarachnoid haemorrhage, in which the blood collects under the arachnoid membrane that lies over the pia mater. In contrast to the situation in intracerebral haemorrhages, where a localized haematoma causes loss of function related to a specific area, in patients with subarachnoid haemorrhages more systemic symptoms (e.g. headache, vomiting, seizures, decreased consciousness, etc…) are reported. Also, subdural and epidural haemorrhages can occur: they are most often caused by traumatic head injuries and the consequent damage to blood vessels.
The second major types of stroke are ischemic. Ischemia refers to the insufficiency of blood supply to an organ, so it indicates not only a lack of oxygen (anoxia) and glucose but also a block in the removal of potentially toxic metabolites. There are three main categories of brain ischemia, referred to as thrombosis, embolism, and systemic hypo-perfusion, each indicating a different mechanism of blood vessel injury or reason for decreased blood flow. 1) Thrombosis refers to a local problem within a blood vessel that supplies a portion of the brain. The process is often a disease of the blood vessel, which narrows blood flow through that vessel. Often, a thrombus is superimposed on the localized vascular process. 2) Embolism refers to a breaking loose of materials (often thrombi, but occasionally bacteria,

cholesterol crystals, fat, foreign bodies, etc.) from a proximal source to block a distant vessel farther along the circulatory path. The vessel blocked downstream causes infarction to a localized brain region in the same way that a primary vascular lesion (i.e. thrombosis) does. 3) Systemic hypoperfusion is characterized by a global decrease in blood flow to the head rather than a localized decrease as occurs in thrombosis and embolism. Abnormally slow or fast heart rhythms, cardiac arrest and failure can all diminish blood flow to the head and brain. Another cause of diminished circulatory function is a lowering of blood pressure due to an inadequate amount of blood and fluid in the vascular compartment. Bleeding, dehydration, and loss of fluid into body tissues (shock) can all lead to inadequate brain perfusion. Hypotension from any cause can lead to global brain ischemia and syncope (Zigmond et al. 2015).
Ischemic stroke remains the most frequent and it represents the second single most common cause of death in Europe, with almost 1.1 million deaths in Europe each year ("World Heart Day: New European statistics released on heart disease and stroke," European Heart Network, www.escardio.org); moreover, projections show that by 2030, an additional 3.4 million people aged ≥18 years will have had a stroke (Mozaffarian et al., 2014).

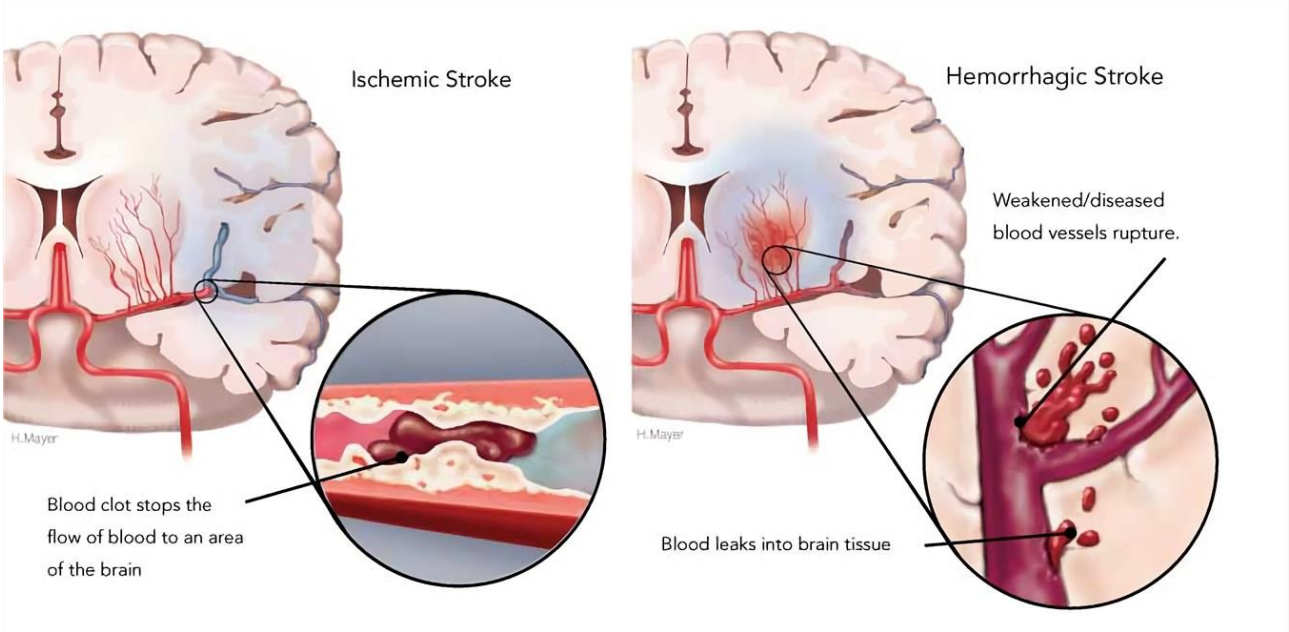

***Figure 1**: **Schematic representation of the two principal types of stroke**. Hemorrhagic stroke (left) is caused by a vessel rupture while ischemic stroke (right) is the consequence of blood vessel occlusion. Taken from http://heart.arizona.edu/*

Ischemic lesions are defined by two main areas: a central ischemic zone, "core", and the surrounding area, "penumbra" (**Fig. 2**). The core is the area severely affected by the lesion and is characterized by decreased blood supply and necrosis of neurons and glial cells (irreversible damage). Among the tissues normally perfused and those involved in the ischemic phenomenon, however, there is usually the presence of a defined area, the penumbra, which is the subject of several studies, both clinically and in basic research. This phenomenon has been described for the first time in 1981 by Astrup and refers to an area of brain tissue in which the reduction of blood flow is severe enough to cause hypoxia and physiological deficits but not so severe to cause an irreversible arrest of cellular energy metabolism and subsequent tissue necrosis (Paciaroni et al., 2009). It is, therefore, a zone not yet irreversibly damaged, and thus a target for acute therapies (Fisher, 1997). Studies

with 2-photon microscopy on a mouse model of stroke reported that reperfusion (i.e., restoration of blood flow) of the penumbra promotes the recovery of dendritic structures of the damaged neurons (Sigler and Murphy 2010). However, the response of the penumbra after an ischemic event relies on the residual blood supply and the duration of vascular dysfunction. That is why this area might be a target for acute therapies, in which the intervention time window is the first and crucial point for the treatment of the injured area.

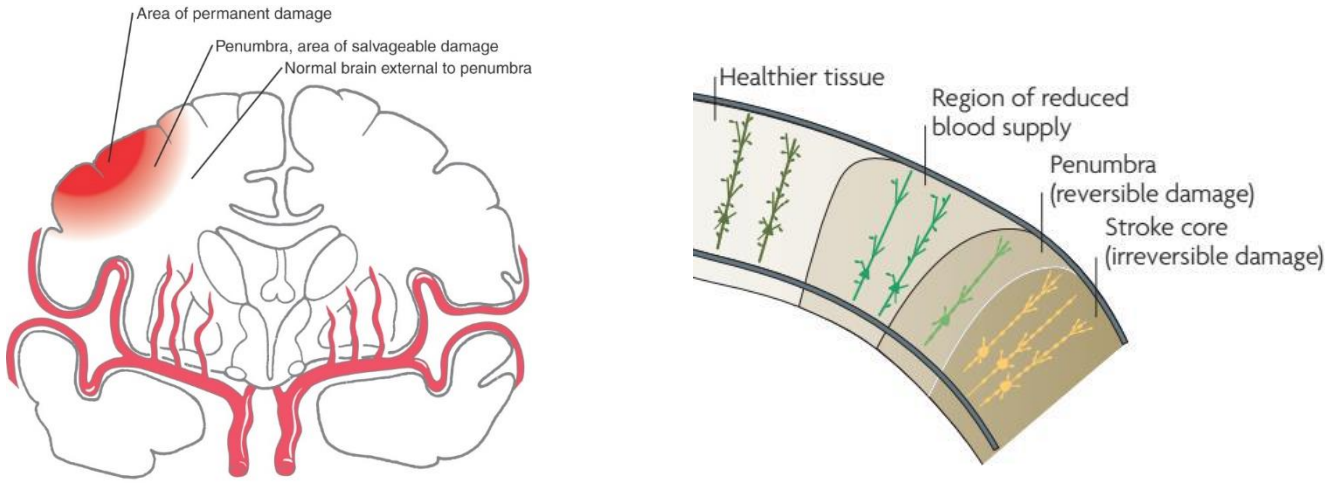

Figure 2: Ischemic stroke*: ischemic core is colored in dark red while the surrounding light red zone represents the penumbra in human brain (left). Rodent cortex showing the stroke core (darker brown) and penumbra (lighter brown) after occlusion of the middle cerebral artery (right). Taken from (Murphy and Corbett 2009)*

2- Pathophysiology of ischemic stroke

Focal ischemia produces impaired blood flow in the distribution of an artery supplying a portion of the brain. Here, there is a gradient of energy failure, maximum in the ischemic core and less critical in the ischemic penumbra. The impairment of a specific area is reflected in focal abnormalities of the body, such as weakness of the limbs on one half of the body.
The sudden lack of blood flow triggers a cascade of cellular and molecular events such as excitotoxicity, peri infarct neuronal depolarization, production of free radicals like reactive oxygen species and nitric oxide, and inflammation leading to cell death (involving both necrosis and apoptosis). This process is specifically known as the ischemic cascade (**Fig.3**). Reduction in the amount of available nutrients, particularly oxygen and glucose, leads to failure in maintaining ionic gradients thereby causing a breakdown in normal cellular function and homeostasis. One of the most prominent features of the ischemic tissue is excitotoxicity, which refers to the pathological effect of excitatory neurotransmitters, particularly glutamate. The increased glutamate concentration results from depolarization-induced synaptic release, as well as from reversal of astrocytic glutamate uptake.
Extracellular glutamate binds to NMDA receptor, particularly the extrasynaptic receptors containing an NR2B subunit. Its activation produces an influx, which is further increased by the contribution of voltage-gated Ca^{2+} channels (Lai et al., 2014). In addition, anaerobic

metabolism results in lactate accumulation and acidosis in the ischemic brain regions (Siesjo et al. 1996). The presence of acidosis activates Ca^{2+} permeable, acid-sensing ion channels, further exacerbating calcium dysregulation. Overload of intracellular calcium leads to activation of neuronal nitric oxide synthase, with resultant production of reactive oxygen species (Samdani et al., 1997). Since mitochondria and endoplasmic reticulum buffering systems are not able to cope with calcium overload, cell death pathways are mobilized. The cell membrane of the affected neuron is degraded, inflammatory mediators and free radicals are released from the neuron triggering activation of microglia. Damage to mitochondria triggers DNA damage and necrotic and apoptotic cell death.

In addition, ischemia leads to spreading depolarization (SD) which induces a wave of strong excitation followed by a wave of suppression of all spontaneous or evoked electrical activity in the affected region. Consequences of SD include propagated loss of ion homeostasis, altered vascular response, changes in synaptic architecture and subsequent depression in electrical activity across the cortex.

In the ischemic core, where blood flow is most severely disrupted, cell death is likely to occur as early as 5-10 minutes after the onset of stroke.

Rapid cell death occurs by the process of necrosis, with cell and organelle swelling, membrane rupture, and spilling of cellular contents into the extracellular space with consequent inflammation. Organelle swelling results in cytoplasmic microvacuolization (Arumugam et al. 2018). In the penumbra, cell death occurs in a slower, energy-dependent, and more regulated way, characterized by apoptosis. The intrinsic pathway of apoptosis is the most prominent in stroke. Here, in contrast to necrosis, affected cells demonstrate shrinkage, membrane blebbing without rupture, aggregation of chromatin about the nuclear membrane, preservation of intracellular organelle integrity with subsequent dispersal of cell contents in membrane-bound apoptotic bodies, and finally DNA fragmentation. This surrounding area remains partially buffered by collateral blood flow and therefore still represents a salvageable tissue only for as long as energy metabolism and membrane function are preserved. Unless blood flow is restored as early as possible after stroke onset, this tissue will eventually form part of an extended infarct core due to excitoxicity. At later stages, cell death in the extended infarct area occurs via mechanisms such as apoptosis and inflammation. The subsequent progression of the injury depends on different factors such as type of ischemia, duration of occlusion and degree of reperfusion.

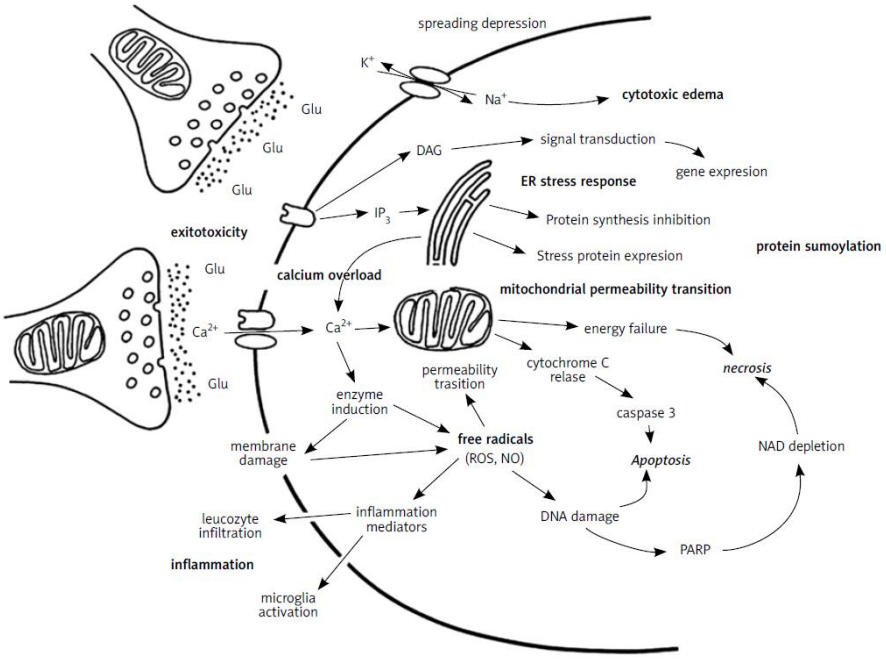

***Figure 3**: **Ischemic cascade**: schematic representation of ischemia-induced molecular injury pathways (Hossman 2012).*

In the clinical progression of stroke in humans, four different phases can be identified: 1) hyperacute phase (0-24 hours), when cell death occurs, 2) acute phase (1-7 days), characterized by inflammation and scar formation, 3) subacute phase (further divided into early subacute 7 days-3 months and late subacute 3-6 months), when plasticity phenomena and recovery take place, and 4) chronic phase (> 6 months) (Bernhardt et al. 2017) (**Fig.4**).

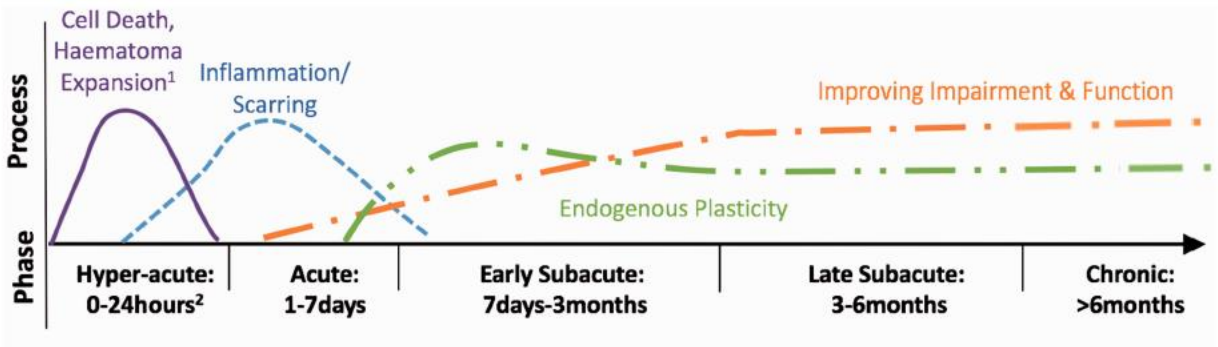

***Figure 4**: Framework of critical timepoints post-stroke that link to the currently known biology of recovery (Bernhardt et al. 2017).*

3- Role of inflammation, microglia and reactive astrocytes

In addition to ischemic cascade, stroke also triggers an inflammatory cascade. Although many aspects of post-ischemic inflammation, that is, the response of the immune system to disruption of tissue homeostasis, manifest themselves days and weeks after the event, the inflammatory cascade is activated immediately after vessel occlusion has occurred.
This process involves damage to blood brain barrier, leukocyte invasion, release of pro-inflammatory factors such as cytokines and danger-damage-associated molecular patterns (DAMP) from injured and dying neurons which activate pattern recognition receptors on microglia, the brain resident immune cells, and astrocytes (Singh et al., 2016).
Following an ischemic insult, resident microglia respond to changes in neuronal integrity, synaptic inputs and activity by rapidly switching morphology and migrating towards the injury (Pocock and Kettenmann, 2007; Morrison and Filosa, 2013;). Specific interactions between microglia and neurons are shaped by an intricate dynamic pattern of environmental cues, resulting in transient changes in the exact nature of microglial activity and morphology, which can influence the evolution of stroke lesion pathology in the acute, subacute and chronic stages in a positive or detrimental manner (Hanisch and Kettenmann, 2007; Ekdahl et al., 2009; Morrison and Filosa, 2013). Microglial cells can be beneficial or detrimental for stroke recovery, depending on their phenotype and on the features of the local environment (**Fig.5**).

Similar to microglia cells, astrocytes react quite rapidly with changes in morphology, proliferation, and gene expression, and form a glial scar that separates the injury site from healthy surrounding tissue (Choudhury and Ding, 2016, Liu and Chopp 2016). The functional role of glial scar after stroke is controversial. In the scar, reactive astrocytes express a broad range of inhibitory molecules against axonal regeneration, such as chondroitin sulfate proteoglycans (CSPGs) (McKeon et al., 1991; Smith and Strunz, 2005), which have been recognized as major barriers to CNS axon extension and thus regeneration failure in the CNS, at least in mammals. However, the glial scar may also seclude the injury site from viable tissue, preventing a cascading wave of uncontrolled tissue damage (Faulkner et al., 2004), and may also restrict diffusible factors secreted from the damaged region. However, astrocytes have clearly a dual role as they may participate in repair by producing or recycling neurotrophic factors, thus stimulating plasticity of spared networks. Because neurons are not viable without astrocytes, neuroprotective therapeutics should consider being beneficial for protecting both neurons and astrocytes (Chen and Swanson, 2003). Astrocytes are generally more resistant than neurons to oxygen-glucose deprivation (OGD) in the culture media, an in vitro model of ischemia. Most neurons in astrocyte-neuronal co-cultures will die after 60-90 min of OGD, while astrocytes are irreversibly injured after 4-6 hours (Goldberg and Choi, 1993; Almeida et al., 2002;). Reactive astrogliosis is a hallmark of various pathologies, including stroke. Reactive astrocytes are traditionally thought to be detrimental to neurological outcome after stroke. Within minutes after injury, reactive astrocytes produce and release inflammatory mediators such as cytokines and chemokines, cytokines including IL-6, TNF-α, IL-1α and β and interferon γ (Orzylowska et al., 1999; Basic et al., 2008; Tuttolomondo et al., 2008). However, in addition to the detrimental role during the early stage of ischemic onset, reactive astrocytes may also play a beneficial role in the brain. Indeed, it has been demonstrated in animal model of stroke an involvement of reactive astrocytosis in behavioral recovery following brain injury (Hayakawa et al., 2010; Liu et al., 2014). In a first report, Hayakawa et al. (2010) used fluorocitrate, a metabolic inhibitor of astrocytes, to reduce reactive gliosis. They showed a worsening of the behavioral deficits in the treated animals. A second study employed mice lacking two major astrocytic intermediate filament proteins, glial fibrillary acidic protein (GFAP) and vimentin. These animals displayed an attenuated astrocytic reactivity following photothrombotic stroke in the

forelimb motor area, and motor functional recovery was significantly reduced as compared to wild-type mice (Liu et al., 2014). Altogether, these data suggest that reactive astrogliosis may play a role in aiding functional restoration after stroke.

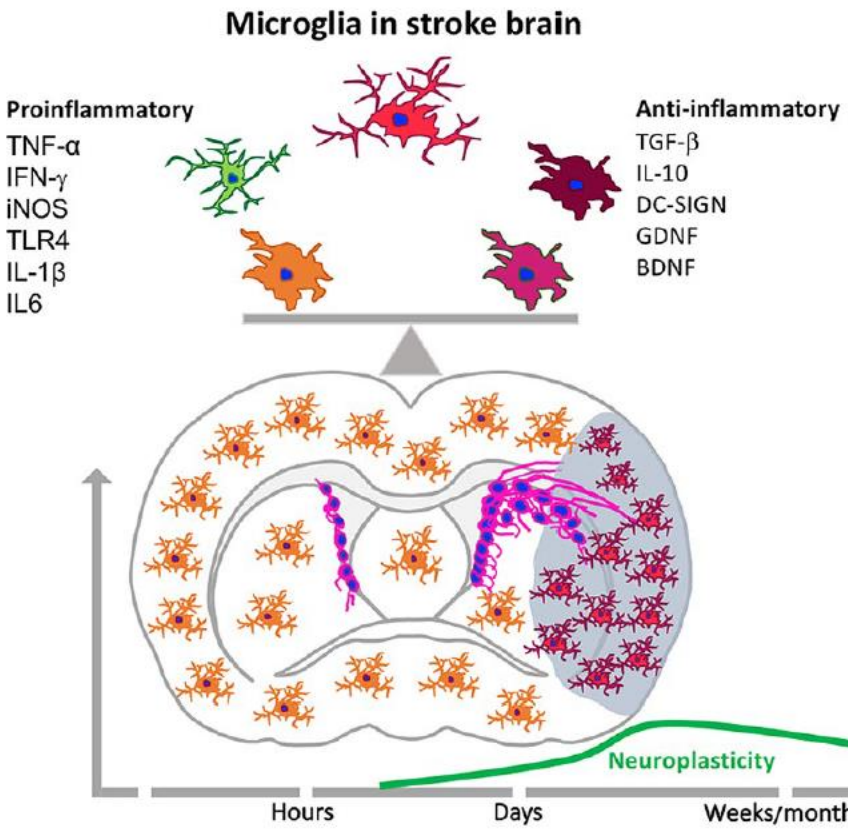

***Figure 5**: Overview of key roles of microglia after ischemic injury (Sandvig et al.,2015)*

4- Epidemiology and clinical measures

Almost 200'000 people in Italy experience a stroke each year, 20% of which represent relapse of previously-affected subjects. In Italy, stroke is the third cause of death, after cardiovascular diseases and cancer (10-12% of all deaths occur after an ischemic attack), and represents the main cause of disability.
In our country, the number of stroke survivors is around 913'000. Up to one year after stroke, one third of patients show a consistent level of disability, such that these subjects are not independent in their activities of daily living. This phenomenon is constantly increasing due to the progressive ageing of the Western population. On a global basis more than 90%of the stroke burden can be attributed to modifiable risk factors related to lifestyle (e.g. smoking, poor diet and low physical activity) and the physical environment (e.g. air pollution and lead exposure).

The ictus prevalence in the elderly (65-84 years old) is 6,5%, slightly higher in men (7,4%) than in women (5,9%). The incidence progressively increases with age and peaks beyond 85 years of age. Thus, 75% of cases are +65 year patients. (Società Italiana dell'Ipertensione Arteriosa, http://siia.it). Among the stroke subtypes, brain ischemia is much more common than hemorrhage: about four strokes out of five are ischemic.
If an ischemic insult occurs in the motor cortex, one or more body parts contralateral to the infarct result impaired or paretic. The degree of the motor impairment depends on many factors, such as the extent of the infarct, the identity of the damaged region and the effectiveness of the initial neuroprotective interventions. In the first weeks after stroke, limited spontaneous recovery can occur. About 26% of stroke survivors are able to carry on everyday activities (Activity of Daily Living or ADLs, i.e. eating, drinking, walking, dressing, bathing, cooking, writing) without any help, but another 26% is forced to shelter in a nursing home (Carmichael, 2005). Impairments of upper and lower limbs, are particularly disabling as they make very hard to have a sufficient degree of independence in ADLs.
To perform a better diagnosis and design the best therapy for each patient is important to know with high precision the location and extension of the ischemic damage. For this purpose, many techniques have been developed in the last years.

4.1 Tools for neurological investigation

Diagnostic imaging of the brain is an invaluable tool in clinical stroke medicine because it provides information about the nature, location and volume of the stroke lesion. The standard imaging technique used to acquire anatomical information is computed tomography (CT), however, owing to its superior soft-tissue contrast, magnetic resonance imaging (MRI) is also more frequently being used to acquire details about the stroke physiology beyond lesion structure. The technique originally used for the identification of the ischemic borders and identification of penumbra is the "Positron Emission Tomography" (PET), which provides data on the cerebral blood flow (CBF) and cerebral volume (CV). This technique is extremely accurate but also complex and expensive, so often it cannot be applied in time for the patient. Today, many health centres use magnetic resonance imaging (MRI) to study perfusion (Perfusion-Weighted or PW) and diffusion phenomena (Diffusion-Weighted or DW). MRI has been particularly useful as a technology in acute stroke patients, because it is widely available and provides a breadth of anatomical and physiological measurements in a brief exam (less than 20 min). Among MRI, functional magnetic resonance imaging (fMRI) measures brain activity by detecting changes associated with blood flow. This technique relies on the fact that cerebral blood flow and neuronal activation are coupled: when an area of the brain is in use, blood flow to that region also increases. This technique can be used also to study how stroke incidence affect brain function.
Currently, the diagnostic method most widely used on stroke patients is the Perfusion Computed Tomography (CT) that has been tested in acute stroke by Wintermark et al., who evaluated the clinical relevance of both perfusion-weighted CT and DWI, founding that perfusion-weighted CT allowed the accurate prediction of the final infarct size and clinical prognosis for acute stroke patients at the time of their emergency evaluation (Wintermark et al., 2002). Perfusion-weighted CT can be used not only as a tool to distinguish between various types of stroke or between an ischemic phenomenon and a brain tumor but also to study changes that characterize the ischemic area in the early post-stroke period. In particular, the "Dynamic Perfusion CT" consists in the acquisition of sequential images using a contrast medium previously administered to the patient, allowing to estimate measures for CBF, CBV, and the mean transit time (MTT). A prolonged MTT and increased CBV indicates that a brain region is compromised at hemodynamic level. Often there are regions that show

vasodilatation and recruitment of collateral vessels, meaning they have preserved a certain level of self-regulation and are considered "Tissue at risk" (Paciaroni et al., 2009).

Stroke diagnosis and prognosis can be supported by measures of brain electrical activity by means of electroencephalography (EEG), magnetoencephalography (MEG) and recording of evoked potentials. In particular, electrophysiological recordings can provide insights about underlying cellular and network phenomena. In many respects, the temporal resolution (milliseconds) of these techniques is optimal for non-invasively capturing the precise timing of stroke-related activity. EEG acquisition allows detecting the signal originating mainly from extracellular currents resulting from the integration of excitatory and inhibitory post-synaptic signals in dendrites of cortical pyramidal cells. Synaptic transmission impairments due to neuronal loss after ischemic stroke generate electrical alterations in neural signals that could be detected by a quantitative EEG (QEEG). Quantitative EEG can detect changes in brain activity a thousand times faster than most biochemical indices, and they are not measures of cell metabolism but the summation of cortical postsynaptic potentials themselves. After initial conflicting results (De Weerd et al., 1988), this technique has been widely evaluated and adjusted and, in the last few years, it has shown a good predictive potentiality for ischemic stroke pathophysiology (Murri et al., 1998; Luu et al., 2001; Finnigan et al., 2004, 2007). Indeed, one of the most relevant parameters that can be extracted from EEG signal is the power spectral density. This index is computed for specific bands of frequency isolated by Fourier transform and represents signal intensity for that specific range of frequencies. Ischemic stroke produces abnormal, slow EEG activity – particularly in the delta frequency range (1–4Hz) – and attenuation of faster activity, particularly in the alpha frequency range (8–12 Hz; e.g., Jordan, 2004; Hirsch et al., 2013). Indices sensitive to the power of delta relative to faster activity which have proven particularly informative for clinical applications are: relative delta power, delta/alpha power ratio (DAR) and (delta + theta)/(alpha + beta) power ratio (DTABR). All these indices are able to accurately classify stroke patients from control, with DAR alone being the optimal classifier (Finnigan et al. 2016). I will come back on this point later on to describe the utility of spectral bands as possible biomarker.

Several recent studies have assessed also the potentialities of evoked potentials (EP) as a useful, objective prognostic test in terms of predicting post-stroke functional recovery. The evaluation of motor and sensory evoked potentials (MEP and SEP) allows, indeed, assessing the integrities of cortico-spinal and somatosensory pathways (Tzvetanov et al., 2005). SEPs are recorded from the somatosensory cortex and consist of a series of waves that reflect sequential activation of neural structures along the somatosensory pathways. SEPs can be elicited by mechanical stimulation of sensory receptors or electrical stimulation of peripheral nerves, which gives larger and more robust responses. MEPs recording are acquired at the muscular level and requires a safely, not invasive stimulation of the brain cortex, specifically of the motor area. Transcranial magnetic stimulation (TMS), developed by Barker et al. in 1985 (Barker et al., 1985), is a painless (Merton and Morton, 1980), non-invasive technique that uses magnetic fields to stimulate motor cortex. Nowadays, TMS is amply used to obtain information about the function of motor pathways (Theodore, 2002; Bembenek et al., 2012). Parameters obtained from MEPs, such as latency or amplitude, in the limb contralateral to the motor cortex stimulation have been shown to represent good mirrors of the integrity and functionality of the corticomotor pathway, as SEPs are for sensory motor system (Ziemann et al., 1999; Lai et al., 2015). These findings have encouraged several studies about the use of MEPs as an index of motor function and recovery after stroke (Binkofski et al., 1996; Escudero et al., 1998; Stinear et al., 2007).

4.2 Tools for functional outcome

Several scoring systems are exploited in the clinic to objectively quantify the impairment caused by a stroke. One of them is The National Institutes of Health Stroke Scale (NIHSS) that is widely used to assess the severity of acute ischemic stroke. It has been used in many trials and it is a validated tool to predict stroke outcome. (Fischer and Mattle, 2005). The National Institutes of Health Stroke Scale (NIHSS) is a systematic assessment tool that provides a quantitative measure of stroke-related neurologic deficit. The NIHSS was originally designed as a research tool to measure baseline data on patients in acute stroke clinical trials. Now, the scale is also widely used as a clinical assessment tool to evaluate acuity of stroke patients, determine appropriate treatment, and predict patient outcome. The NIHSS can be used as a clinical stroke assessment tool to evaluate and document neurological status in acute stroke patients. The stroke scale is valid for predicting lesion size and can serve as a measure of stroke severity. The NIHSS has been shown to be a predictor of both short and long term outcome of stroke patients. Additionally, the stroke scale serves as a data collection tool for planning patient care and provides a common language for information exchanges among healthcare providers. The scale is designed to be a simple, valid, and reliable tool that can be administered at the bedside consistently by physicians, nurses or therapist. The NIHSS is a 11-item neurologic examination stroke scale used to evaluate the effect of acute cerebral infarction on the levels of consciousness, language, neglect, visual-field loss, extraocular movement, motor strength, ataxia, dysarthria, and sensory loss. A trained observer rates the patent's ability to answer questions and perform activities. Ratings for each item are scored with 3 to 4 grades with a score of 0 typically indicates normal function in that specific ability, while a higher score is indicative of some level of impairment. The individual scores from each item are summed in order to calculate a patient's total NIHSS score. The maximum possible score is 42, with the minimum score being a 0. The single patient assessment requires less than 10 minutes to complete. The evaluation of stroke severity depends upon the ability of the observer to accurately and consistently assess the patient (nihstroke scale.org).

Another scale that is widely utilized in the field is the Fugl-Meyer Assessment which is more specific for sensory motor function. The Fugl-Meyer (FM) Assessment is considered by many in the field of stroke rehabilitation to be one of the most comprehensive and quantitative measures of motor impairment following stroke, and its use has been recommended for clinical trials of stroke rehabilitation (Gladstone et al., 2002).

The FM scale is a 226-point multi-items and it is divided into 5 domains: motor function, sensory function, balance, joint range of motion, and joint pain. Each domain contains multiple items, each scored on a 3-point ordinal scale (0 = cannot perform, 1 = performs partially, 2 = performs fully). The motor domain includes items measuring movement, coordination, and reflex action about the shoulder, elbow, forearm, wrist, hand, hip, knee, and ankle. The motor score ranges from 0 (hemiplegia) to a maximum of 100 points (normal motor performance), divided into 66 points for the upper extremity and 34 points for the lower extremity. Similarly, there is a maximum of 24 points for sensation, 14 points for sitting and standing balance,44 points for joint range of motion, and 44 points for joint pain. The FM assessment is best administered by a trained physical therapist on a one-to-one basis with the patient. It takes approximately 30 minutes to administer (Gladstone, et al., 2002).

5- Post stroke reorganization and spontaneous recovery

Although stroke damage can be devastating, many patients survive and undergo some spontaneous recovery. Indeed, the uninjured brain has mechanisms for reorganization and plasticity associated with retraining or experience. A stroke presents the brain with a much more difficult challenge. A plastic reorganization of the spared brain tissue is crucial for recovery to occur.

Post-stroke plasticity has been thoroughly investigated in the primary motor cortex (M1), a region located in the dorsal portion of the frontal lobe of the brain. Together with other motor and subcortical regions (e.g., parietal reach region and dorsal premotor cortex), M1 is involved in planning and executing voluntary movements (Shenoy, Sahani, and Churchland 2013). Furthermore, this area is the primary output of the cerebral cortex to the spinal cord, with direct projections to spinal circuits via the pyramidal tract (corticospinal neurons; Rathelot and Strick 2009). The motor cortex (as the sensory cortex) shows a topographical organization. It means that it consists of a map of movement clustered for different body parts. These maps are quite stable, but they can change after experience-dependent plasticity or brain injury.

There is very strong evidence that structural changes occur in the uninjured cortical tissue surrounding the stroke (Gerloff et al., 2006; Nudo 2006).

The destruction of neural networks, in fact, usually stimulates a rewiring and a reorganization of the connections and this plastic environment is highly sensitive to the experience following the damage (Stroemer et al., 1993; Li and Carmichael, 2006).

Particularly such phenomena involve the perilesional tissue and the surrounding brain areas of the injured hemisphere. There is mounting evidence that the return of function observed after cortical injury is largely attributable to adaptive plasticity in the remaining cortical and subcortical motor apparatus (Chollet et al., 1991; Liepert et al., 2000). In the search for neural substrates for adaptive plasticity, studies to date have focused on cortical motor structures adjacent to the site of injury. For example, both neurophysiologic and neuroanatomic studies in experimental animals (Nudo and Milliken 1996; Jenkins and Merzenich 1987;) and both neuroimaging and noninvasive stimulation studies in humans (Cramer et al. 1997; Traversa et al. 1997; Rijntjes and Weiller 2002) confirm functional, seemingly adaptive alterations in the healthy tissue immediately adjacent to a cortical infarct. These examples of adaptive plasticity are consistent with a long-held belief that functions lost due to cortical injury may be “taken over” by tissue immediately adjacent to the injury (Frost 2003, Nudo 2006). Studies on primates have demonstrated that following an ischemic injury in the hand area of M1, there is a significant reduction of hand representation if no rehabilitative training is applied. However, if the monkey undergoes rehabilitative exercises, the area of the hand is preserved; it is possible that the training, encouraging the re-acquisition of a degree of motor skills in the injured limb, maintains the effectiveness of the projections of spared neurons to spinal motor neurons of the hand (Nudo, 2007). Moreover, following ischemic injury in M1, secondary motor areas can survive and remain functional and can contribute to the recovery (Nudo, 2007). Indeed, it is proven that after a small cortical lesion, peri-infarct areas could actually vicariate lost or damaged functions (Murphy and Corbett, 2009; Dancause and Nudo, 2011). Nevertheless, plastic phenomena can occur also in some portions of the contralateral hemisphere, subcortical and spinal regions. In the contralateral hemisphere neuronal connections appear to be altered as a result of cortical damage. Human functional imaging studies on post-stroke patients, using PET and functional MRI, have identified a role of the healthy hemisphere in recovery. In particular, the reorganization process in the intact hemisphere seems to be important for vicariating the impaired functions of damaged areas, thus promoting the processes of recovery after stroke (Calautti and Baron, 2003). An enhanced activity in the contralesional hemisphere has been

reported in patients in the first 10 days post injury, followed by an increase in the ipsilesional one (3-6 months). This sequential activation was related to improvements in motor performance (Marshall et al., 2000; Ward et al., 2003).
Similarly, in rodents, the activity of the contralesional hemisphere was enhanced immediately after stroke (when the deficit was more pronounced) and was followed by perilesional activation at later stages during the recovery phase (Dijkhuizen et al., 2001).
Pharmacological or electrical silencing of the healthy hemisphere after stroke improves motor function in the late phase (Mansoori et al., 2014; Spalletti et al., 2017).
These results could indicate an involvement of the healthy hemisphere in functional alterations following an injury in the contralateral one. However, whether the healthy hemisphere has a positive or negative impact on the recovery is still controversial. In fact, there are many evidence that in some cases the activity of the healthy hemisphere can worsen motor recovery. For example, a recent QEEG study in stroke survivors showed that the increase of contralesional hemisphere activity, during the acute phase, is related to negative final outcome. In fact, the increase of the contralesional power associates to an interhemispheric communication breakdown (Assenza et al., 2013).
A possible hypothesis takes in consideration the lesion volume: when the lesion is sufficiently small to allow the reorganization of spared adjacent motor areas, the contralesional hemisphere activity would have a negative impact on the recovery; conversely, when the lesion extent is so vast to involve most of motor areas, the healthy hemisphere could be important to vicariate lost functions (Di Pino et al., 2014).
In keeping with this idea, acute inactivation of the healthy hemisphere (via injection of lidocaine), induced different effects in ischemic rats, depending on the lesion size. Animals with large lesions were dramatically affected by lidocaine administration as shown by a worsening of the performance in a reaching task (Biernaskie et al., 2005).
These results are in line with a mechanism of interhemispheric competition, meaning that there is a mutual inhibition between the hemispheres and after a unilateral stroke the intact hemisphere gains control and suppresses homotopic areas across the midline (Murase et al. 2004). Indeed, the interaction between the two brain hemispheres before and after stroke is a widely investigated topic. The neural activity in the brain motor areas is functionally coupled between the two hemispheres (Kinsbourne, 1974) and the lateralization of neural activity during movements is likely to be related to interhemispheric inhibition between motor areas exerted via transcallosal connections (Bütefisch et al., 2008). After a cortical injury, the subjects recovering from stroke showed changes in these interhemispheric influences (Kobayashi and Pascual-Leone, 2003; Mohajerani et al., 2011) which are thought to be caused by an imbalance in the mutual interhemispheric inhibition between the two motor cortices (Murase et al., 2004) that could be an obstacle for motor recovery (Dancause et al., 2015).
Overall, these findings indicate that the recovery of motor functions after stroke and brain remapping involve changes in local and distant sites.
Several studies suggest that also the environment is important for the spontaneous recovery (Risedal et al. 2002; Biernaskie 2004; Hinman, Rasband, and Carmichael 2013). Enriched environments and motor learning in adult animals are associated with dendritic growth, increases in dendritic spines, and synaptogenesis. These same structural neuronal changes are seen after a brain injury and form the theoretical basis for neuroplasticity post stroke (Teasell 2005). In support of this hypothesis many genes, expressed at high levels during early brain development, involved in neuronal growth, synaptogenesis, and proliferation of dendritic spines, are re-expressed for a limited period of time after stroke (Cramer 2000; Carmichael 2005; Carmichael 2006). This “critical period” after the injury can last a few months in humans and about one month in rodents (Nakayama et al. 1994; Cramer 2008; Zeiler and Krakauer 2013). Because of the re-activation of these processes, this “critical

period" may constitute the ideal time window for the therapeutic intervention. In this time window, behavioural training has its maximum effect: early evidence of this was provided by Biernaskie and colleagues (Biernaskie et al. 2004), who found that rats that started motor training of the affected forelimb starting at 30 days post stroke exhibited little improvement when compared with those whose treatment started earlier, at 5–14 days post stroke. The causal role of the lesion itself in initiating spontaneous biological recovery was furtherly confirmed by Zeiler and colleagues (Zeiler et al. 2015), who showed that intensive reach training was not able to promote full recovery in a mouse when commenced 7 days after stroke. However, when a second stroke was induced in the same animal and training was commenced 2 days later (presumably within the critical period), recovery was substantially improved, and performance levels approached those seen before either stroke. Clearly, focal brain damage sets in motion a series of biological events that, when combined with appropriate type and intensity of behavioural training, can support a consistent recovery.

This period of post-stroke heightened plasticity is related to the spontaneous recovery that is observed in stroke patients. Brain responses to stroke in humans can be divided in three different groups (Cassidy and Cramer 2017), based on timing of occurrence. Within few hours after stroke are the immediate changes; this time window represents the best opportunity to save the damaged tissue of the penumbra, for instance via reperfusion or neuroprotection. The observed mechanisms of early functional recovery are associated with a reduction of acute effects, such as edema or inflammation, and to an improvement of metabolic and vascular activity of the injured area (Teasell, Bayona, and Bitensky 2005). The second group of changes starts few days after stroke and last for several weeks; it corresponds to the peak of spontaneous neural recovery and endogenous repair. During this time, spontaneous recovery appears to rely on the central nervous system (CNS) reorganization and plasticity (Nudo 2003). Particularly, animal experiments showed that this time period is characterized by growth of synapses and dendrites (Jones and Schallert 1992; Jones, Kleim, and Greenough 1996;), axonal remodeling and angiogenesis (Ding et al. 2008; Teng et al. 2008), and increased expression of growth-related genes (Li and Carmichael 2006). These cellular and molecular changes can facilitate neural protection and recovery (Overman and Carmichael 2014), but can also lead to the development of maladaptive functional responses when not correctly directed (Takeuchi and Izumi 2013). Maladaptive responses might lead to the pathogenesis of dystonia and phantom pain (Flor 2008; Quartarone, Siebner, and Rothwell 2006) or they can limit the recovery and weaken motor functions (Murase et al. 2004; Kerr, Cheng, and Jones 2011). The third group begins weeks to months after stroke when the spontaneous recovery has reached a plateau, it represents a stable chronic phase of brain repair, but modifications in brain structure and function are still possible. Since these groups are related to different biological states and delineate windows of neuroprotection and repair, they are crucial in the choice of the timing for rehabilitation therapies.

In humans, the majority of functional gains occur within the first 3 months post-stroke (Nakayama et al. 1994; Kwakkel et al. 2003;) and the degree of this spontaneous recovery depends on the infarct size and location, age, and pre-stroke health conditions (smoke, obesity, diabetes, previous ischemic events; (Cramer 2008)).

However, in many cases recovery is variable and difficult to predict: in one study, only 38% of patients who showed an initially paralysed upper limb regained some dexterity by 6 months (Kwakkel et al. 2003), and in general two-thirds of patients perceived that loss of arm function was still a major problem after 4 years (Broeks et al. 1999). Several factors are associated with poor outcomes, however the dominant one for predicting long-term upper limb outcome is initial severity of motor impairment (Coupar et al. 2012). Additional factors

that have independent predictive power over and above their association with this initial severity are being intensively investigated, but still require additional evidence to become useful in the clinical practice.
The ability of initial severity to predict upper limb recovery was first quantified as the “proportional recovery” rule (Prabhakaran et al. 2008). For example, by 3 months, patients will regain ~70% of the upper limb motor function that had been lost on day 3 after stroke. In other words, the more severe is the deficit, the more the patient will recover, with a constant factor of 70%. However, initial upper limb impairment predicts later upper limb outcome accurately only in patients who present with mild to moderate impairment. On the contrary, among patients who present with high severity, recovery is proportional to the initial severity in approximately half cases, whereas no substantial recovery is seen in the other half. Importantly, this finding tells us that the causes of initial impairment are probably independent from the biological factors that are important for the subsequent recovery process (Ward 2017) (**Fig.6**).
The proportional recovery rule has been confirmed in the motor domain several times. Evidence also suggests that proportional recovery applies to nonmotor areas, such as language (Lazar et al. 2010) and hemispatial neglect (Nijboer et al. 2013). Moreover, these recent findings suggest that studies exploring the effect of any post-stroke therapy need to be contextualized in a proportional recovery framework.
This striking clinical phenomenon provides a framework for investigating potentially modifiable biological factors that are necessary for maximizing recovery of function and raises several clinical questions: 1) can we help patients with stroke to regain more than 70% of lost function and how, 2) can we predict the long-term motor outcome, regardless the initial impairment, 3) can we predict if a patient will respond to a treatment, in order to customize the therapy and 4) how can we turn poor recoverers into proportional recoverers?

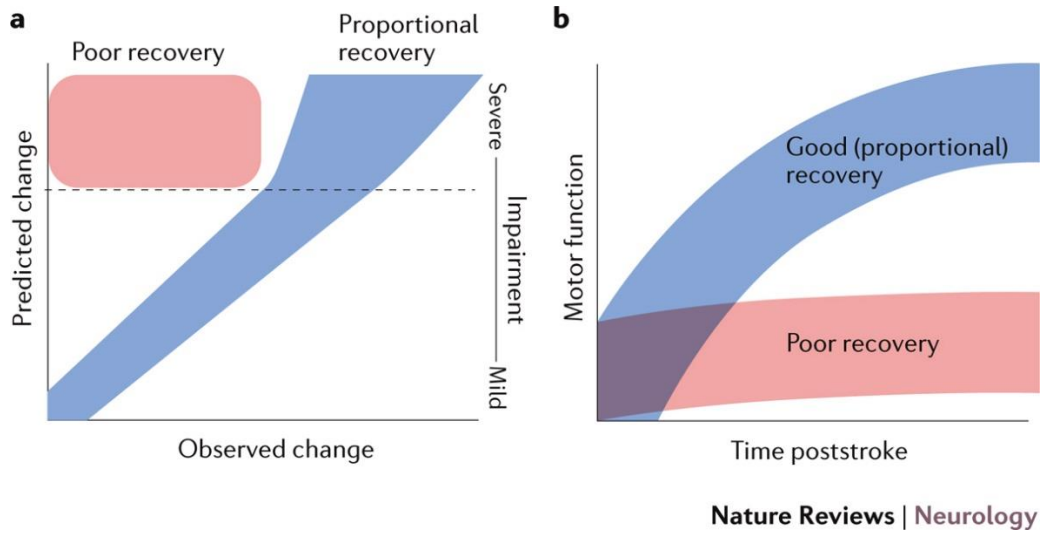

Figure 6: A) *Upper-limb impairment plotted against observed change at 3 months poststroke: Patients in the blue area have proportional recovery as predicted. Patients in the red area recover less well than predicted. Patients above dotted line all have initially severe levels of impairment, and roughly equal numbers of patients have good (proportional) or poor recovery.* ***B****) Illustration of different recovery curves of patients with initially severe upper limb impairment. (Ward 2017)*

6- Biomarkers for stroke recovery

The unpredictable timing and extent of motor recovery after stroke highlights the crucial need to define the pathophysiological mechanisms underlying this process.
Ideally, accurate prognoses for recovery after a stroke should allow clinical teams, patients, and families to optimize rehabilitation plans with realistic goals and appropriate allocation of time and resources. However, accurate prediction of the extent of an individual patient's motor recovery can be difficult for clinicians. This prognostic challenge has led to a growing interest in biomarkers of motor recovery and outcomes (Stinear et al., 2017, Westlake et al., 2012). A stroke recovery biomarker (SRB) can be defined as an indicator of disease state that could be used to understand outcome or predict recovery or treatment response. Motor outcomes, in contrast to motor recovery, are measured at a single time point, and are therefore insensitive to whether the patient's motor performance has improved, remained stable, or deteriorated over time after stroke. This limitation can be addressed by evaluating motor recovery over time, which is typically measured as the absolute difference between baseline and subsequent clinical scores.
In practical terms, biomarkers should improve our ability to predict long-term outcomes after stroke identifying whom and when to target, and in some instances at which dose, with interventions for promoting stroke recovery (Cramer 2007). Unpredictable outcomes after stroke, particularly in those who do not follow the proportional recovery rule (Krakauer et al. 2015), mean that clinical trials of rehabilitation interventions need hundreds of patients to be appropriately powered. Use of biomarkers would allow incorporation of accurate information about the underlying impairment, and thus the size of these intervention trials could be considerably reduced, with obvious benefits (Winters et al. 2016). Indeed, use of appropriate biomarkers for patient stratification may foster developments in new therapies and improve clinical trial efficiency through better patient selection or stratification. Tailoring of therapies for individual patients based on their capacity for neural reorganization and recovery will facilitate personalized interventions, guiding the delivery of effective treatment to the right people, at the right time (Bernhardt et al 2017).
In order to be useful, a possible biomarker needs to explain recovery beyond that denoted by initial impairment, i.e. more than it is currently achievable using the proportional recovery rule. To fully understand the predictive capacity of biomarkers, there is a need to conduct mechanistic studies, for which preclinical models are fundamental. Furthermore, conducting longitudinal studies would provide useful data to better predict outcome or treatment response.

6.1 Structural markers

Scientists have used many different neurophysiological and imaging techniques in their attempts to identify the major predictors of motor outcome in stroke. Results of structural imaging studies have suggested that both lesion size and lesion location correlate with impairment and that the involvement of motor-related cortical regions (both primary and nonprimary motor areas), corona radiata, and internal capsule progressively decrease the probability of upper limb functional recovery (Zhu et al., 2010).
In a series of experiments conducted in monkeys, a relationship has been found between lesion size and the reorganization of motor representations in the ipsilesional cortex (Frost et al., 2003; Dancause et al., 2006). In each animal, lesions were made to selectively target different proportions of cortical gray matter in the hand area of M1. After recovery, there was a reorganization of the hand representation in the ventral premotor cortex (PMv), and the

cortical area evoking movements of the paretic hand in the PMv was proportional to the size of injury. Several studies also support the idea that there is a relationship between lesion size and contralesional plasticity. For example, in the days following middle cerebral artery occlusions (MCAO) in rats, there is shift of activation toward the contralesional hemisphere and atypically high hemodynamic activity in M1 and the primary somatosensory cortex (Dijkhuizen et al., 2003). The increase in contralesional activity is greater in animals with larger lesions. Many neuroanatomical changes are also observed in the contralesional hemisphere after brain injuries, and they are greater in animals with larger lesions (Hsu et al., 2006; Kim et al 2010). The size of lesion may also affect the role of the contralesional hemisphere in the recovery of the paretic limb. Reversible inhibition of the contralesional hemisphere induces more profound motor impairments with the paretic forelimb in rats that recovered from large lesions than in those that recovered from small lesions (Biernaskie et al., 2005). Along the same lines in humans, a treatment based on contralesional inhibition that improves the control of the paretic arm for mildly impaired patients with relatively small damage can have detrimental effects for patients with greater deficits and more extensive damage (Bradnam et al., 2012: Touvykine 2016).
In humans it has been demonstrated that infarct size correlates with motor outcome (NIHSS), but this relationship is attenuated with increasing leukoaraiosis severity (Helenius 2015). The extent of existing white matter disease (i.e. leukoaraiosis) has been associated with acute lesion size, degree of lesion expansion and stroke severity indicated by initial NIHSS score (Henninger et al., 2013). These findings underscore the point that biomarker performance varies across different stroke subgroups.
However, the lesion size explains only 15% of the variance, indicating also the importance of the different brain areas involved. Small pilot studies have demonstrated that integration of lesion location and size can estimate stroke severity better than volume alone (Wu et al., 2016). In particular, it has been found that injury to the motor pathway (i.e. posterior limb of the internal capsule, corona radiata) and white matter tracts, were associated with greater severity of acute stroke symptoms and poor long-term outcome (Fink et al., 2005; Wu et al 2016). In addition, also concerning the ischemic penumbra, recent data suggest that the site of ischemic penumbra, rather than volume, is the most informative parameter. As a matter of fact, infarction of an extremely well localized area of the periventricular white matter and the adjacent internal capsule is related to poor outcomes after MCA stroke. This cross-road of tracts is located extremely close to the initial ischemic core: interestingly, good motor outcome is related to the salvaging of this penumbral area by early arterial recanalization (Rosso et al 2014).

Neurophysiological and structural imaging studies also showed that motor outcome is strongly dependent on the integrity of the motor fibers, and the extent of corticospinal tract (CST) damage limits motor performance and recovery (Stinear et al., 2006; Schaechter et al., 2009; Sterr et al., 2010; Puig et al., 2013; Stinear et al., 2014; Sterr et al., 2014; Puig et al., 2017). In fact, the CST constitutes the major motor output pathway. Voluntary limb movements originate primarily from the contralateral motor cortex, which receives input from frontal and parietal areas that play an important role in higher-order sensorimotor processing. The motor cortex is divided into the primary motor cortex (M1), premotor cortex (PMC), cingulate motor area (CMA), and supplementary motor area (SMA). The CST is formed by large pyramidal neurons from M1, which converge with fibers from SMA, PMC, the somatosensory cortex, and the posterior parietal cortex (Davidoff 1990). The CST passes through the corona radiata, the posterior limb of the internal capsule (PLIC), and the cerebral peduncles and crosses at the level of the pyramidal decussation in the medulla into the lateral spinal cord. A small portion (10%) of the CST also descends anteriorly into the ipsilateral spinal cord.

Growing evidence shows the potential of diffusion tensor imaging (DTI) as a noninvasive magnetic resonance imaging (MRI) technique for in vivo quantification of microstructural damage to white matter tracts following stroke. This technique is based on the concept that water tends to diffuse more rapidly in the direction aligned with the internal structure that contains it, e.g. bundles of axons, and more slowly as it moves perpendicular to the preferred direction. Thus, it is possible to derive directional information of white matter tracts brain-wide.

Measurement of CST integrity in the acute phase via diffusion tensor imaging, which reflects fibre number, predicts motor recovery (Fugl-Meyer score) at 12 months. In particular, for patients with severe stroke, initial Fugl-Meyer score was not correlated with motor recovery, suggesting that they did not follow the proportional recovery rule. However, initial fiber number showed strong correlation and, in multivariate analysis, it improved prediction compared with using only initial Fugl-Meyer, age, and stroke volume (Bigourdan et al. 2016). Similar results were previously obtained using as biomarker the CST lesion load, calculated by overlaying the patient's lesion map on magnetic resonance imaging with a probabilistic CST constructed from healthy control subjects (Feng et al. 2015). Several studies have found that even when measured in the late subacute-chronic stage (> 4 months), the extent of CST injury also helps in predicting subsequent treatment response. For instance, Nouri et al. showed that those patients benefitting more from an epidural motor cortex stimulation had a smaller fraction of CST compared to those who did not (44% vs 72%), and rarely had severe tract injury (Nouri et al. 2011). Recently, it has been identified that the integrity of the corticospinal tract and corticocortical connections between the ventral premotor cortex and primary motor cortex have a significant role in the residual motor output of people with sub-acute stroke (Schulz et al., 2017). Additionally, an intact sensory afferent signal is important for driving cortical remapping which is key for motor recovery (Murphy and Corbett, 2009). Thus, the somatosensory modalities may play an important role in modulating motor control processes as well (Bodmer and Beste, 2017). After stroke, voxel-based lesion-symptom methodology showed a lack of integrity of brain structures such as the superior thalamocortical radiation and the parietal operculum cortical regions, and associated with behavioral somatosensory deficits (Meyer et al., 2016). Therefore, the assessment of both motor and somatosensory factors could increase the percentage of accurate prediction of upper limb outcome. Multivariate machine learning methods have recently been applied to neuroimaging data with the aim of providing individual predictions based on an approach that integrates features extracted from brain voxels from multiple brain areas, rather than one area (Mah et al., 2014). In patients presenting with severe upper limb impairment, classification of a subsequent good or poor recovery was more accurate using lesion information from a range of cortical and subcortical motor-related regions compared to just using CST (87% compared to 73% accuracy respectively) (Rondina 2017). This proof of concept approach highlights the importance of considering different anatomical structures in order to better predict motor recovery.

6.2 Functional markers

The structural predictors mentioned above are limited to isolated studies of tract injury and do not reflect the full extent of injury or the underlying influence of functional plasticity as a whole brain network. Advances in functional neuroimaging technology provide the opportunity to assess a baseline of residual neural activity to enhance current structural predictors. Neuroimaging studies using functional magnetic resonance imaging (fMRI) are useful to understand the interaction between the affected cortex and its contralateral counterpart. They clearly show brain activity associated with movement of the upper extremity after stroke reflects a displacement of activity, excess recruitment, and/or altered

hemispheric balance of activity (Feydy et al., 2002; Ward et al., 2003; Hamzei et al., 2006; Calautti et al., 2007). In general, improved sensorimotor function is paralleled by focused activity of the residual ipsilesional motor cortex (Marshall et al., 2000; Ward et al., 2003), which depends, in part, on the integrity of the corticospinal tract (Stinear et al., 2007). Poor recovery, on the other hand, is associated with greater contralesional motor cortex activation (Calautti et al., 2007; Schaechter et al., 2008). This hypothesis is supported by the enhanced activity of the affected primary motor cortex induced by motor training and acute pharmacological interventions, in parallel with improved motor function (Calautti et al. 2003). Indeed, defining the percent of spared critical functional tissue within the primary motor cortex improves the prediction of recovery (Crafton et al., 2003; Westlake et al., 2012). Apart from measuring activity from precise brain areas during a particular behaviour, fMRI allows to study functional connectivity among different regions, looking at the coherence of activation between them during resting state. In humans, resting state functional connectivity (rsFC) provides a promising means of assessing the intrinsic transfer of information within a widespread neural network (Greicius et al., 2003; Fox et al., 2007). Resting state functional connectivity findings in the early and late subacute phases converge on the conclusion that interhemispheric connectivity is particularly important for motor control. Acute disruption of rsFC at the level of specific networks was shown to correlate with higher initial deficit (Carter et al. 2010, Baldassarre et al. 2016) as well as poor recovery at six months (Park et al. 2011). Therefore, characterizing the impact of a stroke-induced lesion on local and remote resting-state connectivity can broaden the understanding of restorative mechanisms after stroke (James et al., 2009; Guye et al., 2010; van Meer et al., 2010; Wang et al., 2010).

There is broad consensus that the presence of an upper limb Motor Evoked Potential (MEP) in response to transcranial magnetic stimulation (TMS) at the hyperacute and acute stages strongly predicts good motor outcome and that shorter MEP latencies and central motor conduction times are associated with better outcome (Talelli et al. 2006,). The presence of a MEP has been found to identify which patients will follow the proportional recovery rule in a cohort of 93 patients. However, among MEP-negative patients, some proportional recoverers can be found, leaving part of the problem unsolved (Byblow et al. 2015). Prediction of recovery is more challenging for patients without a MEP and combining TMS with MRI biomarkers may be useful in this context (Stinear et al., 2012; Byblow et al., 2015,). The presence or the absence of a MEP in the first three days after stroke has been suggested to predict between a good and a limited or poor motor recovery respectively. TMS at the chronic stage helps explain the relationship between corticomotor function and motor performance in cross-sectional studies, and those who have a MEP are more likely to benefit from physical interventions.
Also, Lai et al. showed that the effectiveness of transcranial magnetic stimulation therapy for post stroke motor enhancement depends on the presence of MEPs (Lai et al. 2015).

However, apart from TMS and MRI methodologies, electrophysiological measures to guide sub-group stratification has been identified as a developmental priority at a Stroke Recovery and Rehabilitation Roundtable (Boyd et al., 2017).
Electroencephalography (EEG) records brain electrical fields using surface electrodes on the scalp while magnetoencephalography (MEG) records brain magnetic fields using sensitive magnetometers (Cohen et al., 1972). Both applications are close in methodologies since they have the same source of signals from ionic currents generated by biochemical processes at the cellular level (Lopes da Silva, 2013) and also have superior temporal resolution (Shiner et al., 2015). MEG has higher spatial resolution in separating cortical

sources than EEG (Hari, 2011) but it is more expensive and highly sensitive to external disturbances of the tiny magnetic fields measured (Triccas et al., 2019).
A valid alternative method is represented by quantitative Electroencephalography (qEEG): a non-invasive, easy applicable technique characterized by a high temporal resolution but low spatial resolution. qEEG is very sensitive in detecting abnormalities of cerebral rhythms that are typical of stroke.
Specific band power activities are considered to be linked to brain functions and in case of stroke, are associated to different degrees of neuronal survival in the ischemic regions and therefore can assume a prognostic value. The increasing power of slow rhythms and decreasing power of fast rhythms are directly linked with neuronal metabolism and reflect ischemic injury (Foreman and Claassen, 2012; Wu et al., 2016). In one of the first studies, Cuspineda et al showed that qEEG might be a powerful tool to predict short-and long-term outcome in patients with an acute ischemic stroke, when the examination is performed within the first 72 hours after infarct onset. In particular, theta spectral power, along with alpha power is associated with short-term outcome (6-15days at hospital discharge), while long-term outcome (3 months of clinical evolution) was better predicted by the values of delta frequencies (Cuspineda et al.,2007).
The central role of these frequency bands led to the identification of the quantitative index called Delta/Alpha ratio (DAR), and (delta+theta)/(alfa+beta) ratio that have been used for the correlation between spectral bands alteration and initial deficit.
For instance, Wu et al. employed a regression analysis of spectral power with behavioural impairment scores (NIHSS), and established that higher delta power and reduced beta activity correlate with more severe NIHSS scores. More crucially, this relationship of high delta/low beta was prominent in electrode clusters overlying the ipsilesional sensorimotor cortex (Wu et al. 2016).
Several studies showed that an increase in Delta power and/or decrease in Alpha power (greater DAR) was related to poorer outcome in acute and sub-acute stroke patients (Claassen et al., 2004; Finnigan et al., 2007; Sheorajpanday et al., 2011; Finnigan et al 2013; Schleiger et al 2016;) and in chronic acquired brain injury (Leon-Carrion et al., 2009).
As for fMRI studies, EEG allows to explore the connectivity between different brain area, looking at functional networks. Nicolo et al. recorded resting EEGs within 3 weeks of stroke symptom onset and coherence in the beta frequency band between the ipsilesional primary motor cortex and the rest of the cortex was evaluated. A higher coherence was correlated with improvements in a composite score of upper-limb motor performance during the first 3 months after stroke (Nicolo et al. 2013).
Moreover, also the inter-hemispheric balance could be studied with qEEG metrics as the brain symmetry index (BSI), that provides a measure of inter-hemispheric EEG power asymmetry not specific to single frequency bands (van Putten and Tavy, 2004; van Putten, 2007). The BSI is mainly used in the research field for the purposes of stroke prognosis: literature shows that in acute stroke patients a high BSI is positively correlated with a worse neurological status (van Putten and Tavy, 2004; van Putten, 2007) and with a weaker motor recovery 2 months after the acute event (Agius Anastasi et al., 2017; Fanciullacci et al., 2017).
In addition to resting state recording, EEG/MEG measurements can be performed also during the execution of a task. For instance, a movement-related desynchronization in the beta band at the level of primary motor cortex is observed when a subject produces an unimanual movement. When compared to control subjects, stroke patients exhibit a significantly reduced movement related beta desynchronization (MRBD). Interestingly, within the patient group, smaller MRBD was seen in those with more motor impairment (Rossiter et al. 2014).

The potential for translation of EEG biomarkers to patients is high, as EEG is already part of standard clinical practice. However, further work is needed to develop automated data processing for an easier use by clinicians and to identify other EEG biomarkers that can make individual predictions rather than for groups of patients.

7- Therapeutic Strategies

Currently, the only approved therapeutic strategies that are available for stroke management are aimed at the removal of the thrombi that occlude cerebral arteries, i.e. thrombolysis and thrombectomy. However, when the functional impairment after stroke remains even after the first pharmacological interventions, other kinds of strategies need to be considered. These interventions fall into two broad mechanistic categories: (1) physical interventions, that take advantage of experience and learning-dependent plasticity (e.g. motor rehabilitation), and (2) treatments that enhance the potential for experience and learning-dependent plasticity to maximize the effects of behavioral interventions.

7.1 Treatment in the acute phase

The improvement of the techniques mentioned above is essential to reduce as much as possible the time interval that precedes the application of the treatment; one of the key elements for the success of a clinical intervention in acute stroke, in fact, is the timeliness of treatment. Treatment strategies vary depending on the type of stroke; stroke bleeding should usually be treated with surgery aimed at repairing the damaged vessel while thrombotic occlusions are dissolved through the activation of human tissue plasminogen activator (recombinant tissue Plasminogen Activator or rt PA), a potent thrombolytic agent.
Currently, this is done within three hours from the ischemic episode, while, within six hours of the attack, interventions of intra-arterial (IA) thrombolysis are usually performed. In fact, a randomized trial by Berkhemer's group demonstrated that in patients with acute ischemic stroke functional recovery could be obtained with surgical intra-arterial treatment when performed within 6 hours after stroke onset (Berkhemer et al., 2014). Continued improvements in radiology and in the design of more effective tools, including clot retrievers and stents, have allowed increasingly applicable interventions of intra-arterial recanalization, allowing secure access to main intracranial blood vessels (Saletti et al., 2011).

7.2 Neuroprotective treatment

Recently, new drug therapies have been developed to limit the neuronal damage in brain areas affected by stroke. Despite the above-mentioned actions of thrombolytic therapy, indeed, the percentage of deaths and the development of disability following ischemic events remains very high. Therefore, scientific research continues to focus on increasing the functional recovery following ischemic attack. One of the approaches that have received much interest in this field is the study of the neuroprotective factors.
Neuroprotection can be defined as 'any strategy which directly targets the brain parenchyma with the aims of antagonizing the harmful molecular and cellular events responsible for the ischemic damage, allowing brain cells to survive, to reduce cerebral blood flow and to stabilize the penumbra (Moretti 2015). In particular, the potentiality of these substances to preserve neurons affected by the ischemic event from an irreversible functional damage is currently subject of study. This treatment could be particularly important if applied to the

tissues included in the ischemic penumbra that, although interested by the hypoperfusion, are still potentially viable and subject to phenomena of structural and functional recovery after reperfusion, as demonstrated in animal models (Murphy et al., 2008). Also in this case, the timing of intervention is decisive because these tissues are highly dynamic and always at high risk of apoptosis and tissue necrosis. In animal studies, many of these substances have been applied to interfere with these adverse biochemical changes. Preclinical studies indicate a period of at least 4 hours after onset of complete ischemia in which many potentially viable neurons exist in the ischemic penumbra. In humans, the time window may be longer, depending on the severity of the infarct. Given the number of neurons lost within a short time period after onset of stroke, research on neuroprotection has been focused on the different factors that influence neuronal death.

Neurotrophic factors, anti-apoptotic agents, inhibitors of excitotoxicity, hyperpolarizing agents, anti-inflammatory drugs and cytokine inhibitors are only some examples of neuroprotective factors that have been tested in the last years. However, although many neuroprotective agents have produced good results in animal models of stroke, the application on humans is not free of risks and they are used, in some cases, as an attempt to save ischemic neurons in the brain from irreversible injury (Green, 2004).

Considering the multiple pathways involved in the pathophysiology of ischemia, effective neuroprotection might require a combination or addition of drugs that target distinct pathways during the protracted development of ischemic injury. So, one of the most common approaches related to neuroprotection is to reduce phenomena of excitotoxicity in the damaged areas. For this, the effect of antagonists of N-Methyl-D-aspartate (NMDA), glutamatergic receptor, responsible of the excessive entry of calcium into cells, is subject of several studies. Excitotoxicity is important during the initial 1-2 hours after the onset of stroke and the difference in timing of neuroprotective treatments between animal models and in clinical trials may be part of the explanation for the lack of translational success of neuroprotective agents. Indeed, clinical studies have shown that some NMDA antagonists are poorly tolerated and determine the occurrence of side effects such as hypertension, sedation, hallucinations, until catatonia. Many of these trials have been discontinued for lack of evidence about a satisfactory relationship between risks and benefits (Lees, 1997).

Another, complementary, experimental approach to decrease excitotoxicity is to reinforce the main inhibitory neurotransmitter in the central nervous system (CNS), the γ-amino-butyric acid (GABA). Pre-clinical studies using a GABA agonist, Clomethiazol, have demonstrated its protective effect that is, however, strictly dependent on a prompt intervention, not later than 1 hour after occlusion. However, in the clinical trial of acute stroke involving this strategy, it has been possible to apply the treatment only 12 hours from the onset of symptoms, so it is not surprising that these studies have yielded negative results (Ginsberg, 2008). Conversely providing a benzodiazepine inverse agonist immediately after the ischemia induction, determines an increase of the lesion volume (Clarkson 2010).

Therapeutic hypothermia appears to be a promising technique for the treatment of ischemic stroke whose effectiveness as a neuroprotective factor has already been established in animal models of stroke but also of patients suffering from cardiac arrest (Shintani et al., 2010). However, this therapeutic strategy is obviously quite complex to apply in humans. The management of the patient must be highly accurate and sedation, tremor and intubation can lead to adverse effects such as respiratory problems, arrhythmias and clotting disorders. Thanks to recent advances in instrumentation and application techniques, this therapy may become accessible to clinical application in the future (Ginsberg, 2008; Froehler and Ovbiagele, 2010; Hong et al., 2014).

All these approaches might help to limit the functional deficit and to increase neuronal survival but despite this, the full recovery is not assured and the consequences of stroke can be severely disabling, anyway. In fact, even if a recovery of synaptic function can be

obtained in the ischemic penumbra following reperfusion, the areas that suffer the major vascular damage (Core) does not show this kind of recovery (Li and Murphy, 2008). And however, even if it were possible to facilitate the survival of the cell bodies of neurons in spared tissues using neuroprotective factors, the functional recovery of the circuits might be hindered by a lack of recovery of dendritic arborisation.
Therefore, complete recovery of the functionality of the brain areas involved in stroke is quite difficult and trying to increase cell survival in the acute phase to limit neurodegeneration in the penumbra could be not enough.

7.3 Rehabilitative strategies

Majority of stroke patients are unable to perform daily activities after the injury (Hummel et al. 2005; Hummel and Cohen 2006). Standard therapy aimed to enhance recovery of motor function is functional rehabilitative training. The traditional approach is physiotherapy that consists of a series of specific physical exercises guided by a therapist that promotes the execution of correct movements; physiotherapy usually starts when patients' conditions are stable and lasts also after their de-hospitalization. Plateau of the beneficial increment in motor performance is achieved in about 6 months (Hendricks et al. 2002). However, even after completing the rehabilitation protocol, 50-60% of patients still experiences some degree of deficits, and about 50% reaches only a partial level of independence in the daily activities G et al. 1998). A crucial aspect of rehabilitation is the choice of when to begin it in order to maximize its effectiveness. Many studies suggest that delays in initiating rehabilitation are associated with a poorer outcome and a longer stay in hospital for patients (Weinrich et al. 2004; Teasell et al. 2008;). This can be explained by the plastic processes that characterized the semi-acute phase after stroke ("critical period", see above) that diminish with time. Obviously, the rehabilitation is not able to cancel the effects of stroke but primarily aims at increasing strength and effectiveness of parts that were not affected by the damage and also the confidence of patients with their deficits, which they often must learn to live with.

7.3.1 Robot-mediated Rehabilitation

The effectiveness of post-stroke rehabilitation techniques seems to be strictly related to the duration and intensity of the therapy sessions. Timing, repeatability and intensity of treatment are the key words to regain some motor function and to induce a reorganization of neural circuits. This treatment results very complex, tiring (for both the patient and the rehabilitator) and expensive (Posteraro et al., 2010). These are some of the reasons which led the medical research to focus on the effects of using robotic instruments in rehabilitation after damage of the nervous system. The robotic therapy is usually administered by means of a mechatronic device that helps a patient to perform a specific motor task.
The first robotic device used for post-stroke rehabilitation was the MIT-Manus system developed by Aisen and collaborators, for the recovery of motor functions of the upper limb (Aisen et al. 1997). The MIT-manus is a robot that allows patients to perform reaching movements in the horizontal plane and it enables unrestricted movements of the shoulder and elbow joints. Implementation of this device for the rehabilitative training showed positive outcomes suggesting that robotics might be a useful tool for post stroke rehabilitation.
When compared to standard therapies, robotic devices show two fundamental advantages (Caleo 2015; Lum et al. 2012; Masiero et al. 2007; Posteraro et al. 2009; Raffin and Hummel 2018): i) high levels of precision and accuracy ii) accurate, quantitative, and immediate assessment of motor performance. Moreover, robotic devices can be tailored to the specific

needs of the patients, allowing a personalized therapy. For example, it is possible to adjust the exercise in terms of degree of assistance provided by the robot during the training, “assist as needed” approach. Recent studies have also attempted to improve patient’s motivation using these robotic devices coupled with elements of virtual reality (i.e., audiovisual elements, cognitive challenges and score displays; Novak et al. 2014).

Devices for upper limb rehabilitation can be broadly classified into two types, based on their mechanical structure: end-effector- and exoskeleton-based systems (Maciejasz et al., 2014). In end-effector-based devices, only the most distal part of the robot (i.e., end effector) is attached to patient’s upper limb extremity (hand or wrist). Movements of the end effector change the position of the upper-limb extremity, but also indirectly affect the position of the other segments of the patient’s upper-limb. Exoskeleton-based systems have a more complex mechanical structure that mimics the structure of patient’s limb. They allow for independent and concurrent control of many robot joints, which directly affect the position of correspondent joints of patient’s arm. The mechanical and control algorithm complexity of such devices is usually higher than the end effector- based devices, because of the need to adjust lengths of particular device’s segments to the lengths of the patient arm’s segments or to manage the high number of degrees of freedom allowed.

A protocol of intensive rehabilitation is able to provide long-term benefits in patients with moderate or severe damage, even years after the onset of a stroke (Lo et al., 2010) and robotic devices seem to be particularly suitable for this purpose. In a recent study, an exoskeleton robot that allows task-specific training in three dimensions has been used on patients having motor impairment for more than 6 months and moderate-to-severe arm paresis. They found that after 8 weeks of treatment, patients assigned to robotic therapy had significantly greater improvements in motor function of the affected arm over the course of the study as measured by Fugl-Meyer assessment (FMA-UE) than those assigned to conventional therapy (Klamroth-Marganska et al., 2014). Moreover, some studies on chronic or sub-acute patients survived from ischemic attack have shown how the use of robotic therapy can actually improve the functionality of the upper limbs thanks to an intensive treatment in both chronic and sub-acute post-stroke populations (Volpe et al., 2000; Fasoli et al., 2003; Brewer et al., 2013; Poli et al., 2013). In particular, it has been shown that this type of therapeutic approach is able to improve muscle strength and motor coordination in patients with neurological deficits (Barreca et al., 2003; Micera et al., 2005). Furthermore, data on the kinetics and kinematics collected from robotic tools can be useful for implementing new markers of progression in motor recovery. With robotic devices, in each session the patient can carry up 1000 voluntary finalized movements in about 45 minutes; such amount of treatment would be physically very heavy for a physiotherapist (Posteraro et al., 2009).

Despite all these findings and potentialities, however, in literature there are not studies that demonstrate without any doubts the efficacy and the actual benefits of these technologies, especially considering their relatively high cost (Dickstein, 2008). It remains also unclear what are the neural mechanisms underlying the possible improvement provided by this therapeutic approach. For this reason, recently some robotic devices designed for interaction with rodents, in particular rats, have been developed to study a particular task or training, demonstrating the successful integration of mechatronics and robotics with such animal models. Using robotics in animal models doesn’t mean to develop new devices for animals and then translating them to new systems for humans – since devices for patients have already reached a high level of technology and complexity. Rather, the robot developed to interact with animals aims to mimic human robot devices to try to investigate mechanisms at the basis of robot-based rehabilitation as well as
providing quantitative, reliable and accurate data where qualitative and experimenter-biased tests are still intensively used.

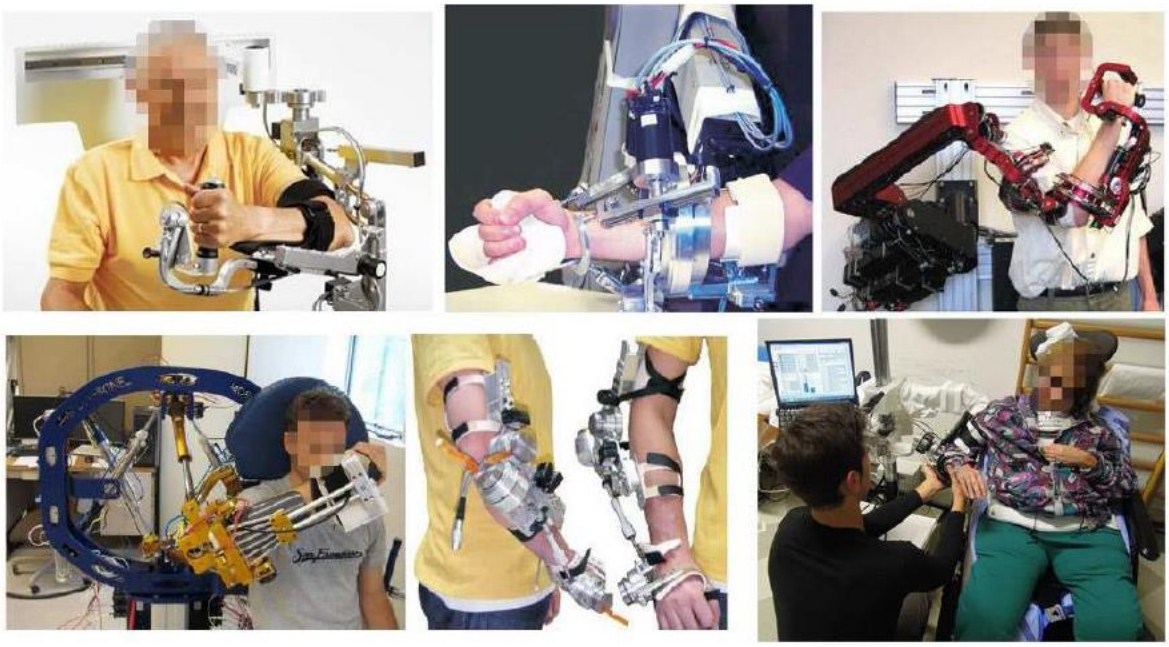

***Figure 8**: Some examples of upper-limb robots for motor rehabilitation*

7.4 “Plasticizing” treatments

There is a general consensus in the literature that physical rehabilitation should be coupled with interventions that render the spared CNS networks more susceptible to experience-dependent modifications. Specifically, a major focus of current research is on the delivery of ‘‘plasticizing” treatments that enhance the modifiability of spared circuits and the formation of novel neural connections, that can then be selected and strengthened by physical rehabilitation (Caleo 2015). In the past few years, several other approaches have been explored to increase the adaptive plasticity in the subacute stage of recovery, where much of the neural reorganization supporting the recovery is expected to occur.

A series of rodent studies have examined the effectiveness of various combinations of treatments and the optimal timing for their administration. In particular, the use of pharmacological manipulation to increase arousal and learning during training and the use of pharmacological agents to increase sprouting and anatomical plasticity have been investigated by several groups. As an example, some drugs as erythropoietin, fluoxetine and neurotrophic factors have been successfully tested on animals and are used to aid the post-stroke recovery of neural injuries, both through neuroprotective and neuroplastic effects (Wahl et al 2014, Lee et al 2004, Fang et al, 2010, Jeffers et al 2014, Soleman et al 2012, Overman et al 2012). However, their systemic administration in humans is often related to side effects (Saver, 2010).

For this reason, another strategy under intensive investigation is the use of cortical stimulation to increase or decrease the activity of targeted brain areas. The use of stimulation has the potential advantages of manipulating the function of specific targeted areas to favor recovery with few, if any, side effects. In humans, transcranial direct current stimulation (tDCS; Fregni et al., 2005; Nitsche et al., 2005) or TMS (Hummel and Cohen, 2006) have been used to promote recovery. Whereas the precision of the stimulation site is

lower and duration of stimulation treatment is more limited, these approaches have the great advantage of being noninvasive, lowering the potential for complications.
The use of tDCS in stroke patients as many advantages in comparison to TMS, such as its low cost, the ease of use and the fact that it can be combined with rehabilitative treatments. tDCS delivers weak direct currents to the cortex via two electrodes that polarize the neural tissue. The active electrode, either the anode to increase or the cathode to decrease excitability, is placed on the scalp over the brain area to modulate (Nitsche et al.,2003, 2007). In chronic stroke patients, a single treatment including the activation of the lesioned hemisphere with anodal tDCS can increase the excitability of the ipsilesional M1 and produce transient improvements in motor performance (Hummel et al., 2005). The application of tDCS over the course of several days prolonged this effect (Boggio et al., 2007). In addition, cathodal tDCS delivered to the contralesional hemisphere can also result in an improvement in motor functions (Fregni et al., 2005; Hummel and Cohen, 2005). Although these studies reported positive results, not all the clinical trials involving these technologies have achieved good motor outcomes (Lotze et al. 2006; Seniów et al. 2012). Therefore, the potential usage of these approaches has to be further evaluated, even so it is worth underlying that tDCS and TMS have the advantage to be combined to other rehabilitation techniques, such as robotic technologies.

8- Cell-based Therapy

Besides physical rehabilitation and plasticizing treatments, stem cell-based approaches hold much promise as potential novel therapies to restore brain function after ischemic stroke (George and Steinberg, 2015). Cell-based therapy has been pioneered in the therapy of Parkinson Disease (PD) and initial studies showed that fetal dopaminergic neurons grafted in the striatum ameliorated PD symptoms, both in animal models (Herman and Abrous, 1994) and in patients (Lindvall et al., 1990; Kordower et al., 1998). Since fetal transplantation poises both ethical issues and technical challenges (Robertson, 2001), mesenchymal stem cells (MSCs) may represent a more accessible alternative. MSCs can be readily derived from various sources, show a low immunogenic effect and proved to be beneficial in stroke treatment (Eckert et al., 2013; Zhang and Chopp, 2013). Notably, MSCs-conditioned medium alone is sufficient for a similar therapeutic effect, suggesting that the beneficial effect is likely due to a bystander effect and trophic support, rather than actual cell replacement (Eckert et al., 2013). In the last decade, transplantation of stem cells of different origin and stage of development has been shown to lead to improvement in experimental models of stroke through several mechanisms including neuronal replacement, modulation of cellular and synaptic plasticity and inflammation, neuroprotection and stimulation of angiogenesis. Several clinical studies and trials based on stem cell delivery in stroke patients are in progress with goal of improvements of functional recovery through mechanisms other than neuronal replacement. These approaches may provide therapeutic benefit, but generation of specific neurons for reconstruction of stroke-injured neural circuitry remains ultimate challenge (Lindvall and Kokaia, 2011). The ultimate goal for stem cell research in stroke, which would give rise to optimum, long-term recovery, should be to provide the stroke-injured brain with new cellular elements, including specific neurons for reconstruction of damaged neural circuitry. For this reason, in vitro differentiation of pluripotent stem cells derived either from cells of the pre-implantation human or mouse embryo (embryonic stem cells (ES cells), or from somatic cells that are induced to a primitive pluripotent state (termed induced PSCs (iPSCs) seem particularly attractive for the generation of neurons for cell replacement in stroke (Takahashi and Yamanaka, 2006).

8.1 Pluripotent stem cells

The promise of using pluripotent stem cells (PSCs) dates back to 1998 when James Thomson first derived human embryonic stem cells (hESCs) from the inner cell mass of developing embryos (Thompson 1998). Embryonic stem (ES) cells, in particular, possess a nearly unlimited self-renewal capacity and developmental potential to differentiate into virtually any cell type of an organism, thus providing functional replacement or trophic support to worn-out or dysfunctional cells and tissues in a range of diseases (Trounson et al 2016). Embryonic stem cells (mESCs) derive from the inner cell mass of the developing blastocyst and give rise to all cell lineages. In vitro, ES cells can be propagated indefinitely in an undifferentiated and pluripotent state, maintaining the ability to differentiate when induced by the appropriate signals.
Mouse ES cells, which are established as permanent cell lines from early embryos, can be regarded as a versatile biological system that has led to major advances in cell and developmental biology. Human ES cell lines may additionally serve as an unlimited source of cells for regenerative therapy. Before therapeutic applications can be realized, important problems must be resolved. Ethical issues surround the derivation of human ES cells from in vitro fertilized blastocysts. However, the alternative methods of establishing ESC lines from single-cell embryo biopsy without interfering with the developmental potential of embryos have been proposed (Chung et al. gage). The common practice of obtaining hESCs is the use of leftover fertilized embryos from in vitro fertilization that were not implanted and were discarded.
Because of their strong capacity to self-renew and propagate, transplanted ESCs can form tumours in the host (Erdo et al. 2003; Pomper et al. 2009); thus, the risk of adverse outcome after transplantation is high. To reduce the tumour-forming potential, hESCs can be pre-differentiated in vitro in committed precursor cells or neural precursor cells (NPCs).
In recent years, the use of pluripotent stem cells has allowed the production of neurons with specific identities. This has been made possible by the modification of existing methods of in vitro neuralization and patterning of pluripotent cells, by fine-tuning the signaling pathways that normally orchestrate the acquisition of distinct types of neuronal identities during embryonic brain development (Hansen et al., 2011; Lupo et al., 2014).
Several in vitro protocols have been developed to derive NPCs from ESCs and many factors which can steer the anterior-posterior (A/P) identity of murine and human ESC-derived neurons have been investigated. Particularly, several FGFs, BMPs and WNTs act as caudalizing factors and repress the expression of anterior neural markers (Hendrickx et al., 2009). Consistently, the synergistic inhibition of WNT and BMP signaling upregulates isocortical and hippocampal markers in mESC-derived neurons (Bertacchi et al., 2015, Terrigno et al 2018).
The ability to obtain virtually any particular type of neuronal identity starting from pluripotent cell cultures has generated new expectations of feasible and reliable protocols of neuronal cell transplantation for the potential treatment of many different neurodegenerative diseases. In fact, neurons suitable for transplantation must be able to integrate into the host tissue, produce the appropriate type of neurotransmitter and neurotransmitter receptors, and develop functional synapses with the host neurons.
Many works have focused also on induced pluripotent stem cells (iPSCs), which can be transplanted into the injured brain, either directly or after they have been fated to neural progenitor cells (NPCs) or to specific neuron types. Similar to embryonic stem cells, iPSCs can generate tumours (Kawai et al., 2010), but if iPSCs are fated to neural phenotype, tumorigenicity is virtually abolished. Hitherto, it is not clear whether iPSC-derived neurons

can express the complete functional phenotype of the neurons they are going to replace, which is a crucial point for a translational perspective. In recent years, several studies have demonstrated the feasibility of the reprogramming approach to produce cells for transplantation in experimental stroke models. Mouse and human skin derived iPSCs have been transplanted in mouse and rat brains subjected to different types of ischemic stroke. The reprogrammed cells have been transplanted directly as iPSCs or, more often, after they have been pre-differentiated or transformed into neural lineage cell lines such as NPCs or long-term neuroepithelial-like stem cells (lt-NESCs). The relative safety of reprogrammed cells generated from lt-NESCs and iNSCs is supported by findings that their implantation in immunedeficient mice and rats revealed no transplant overgrowth or tumour formation (Tornero et al., 2013; Yao et al., 2015).
Transplanted iPSCs have been detected in the rodent brain 4–5 months after transplantation with variable survival rate depending on host strain and species as well as immunosuppression mode (Sauter and Rudin 1995; Majid et al. 2000; Braeuninger and Kleinschnitz 2009; Oki et al. 2012). All published studies clearly indicate that when human iPSCs are transformed into iPSC-NPCs or iPSC-lt-NESCs after transplantation in the stroke-damaged brain, they become prone to develop into cells with neuronal phenotype.
Interestingly, iPSC-derived lt-NESCs cells have been shown to survive transplantation also into the stroke-damaged brain of aged rats. More than 90% of reprogrammed cells differentiated to mature neurons expressing the marker HuD. Moreover, a population of transplanted cells (19%) expressed GABA (Tatarishvili et al., 2014). Since the majority of stroke patients are elderly people, the ability of reprogrammed somatic cells to give rise to neurons also in the aged brain tissue environment is important from a translational perspective.

8.2 The fate of transplanted cells

Once obtained the cell type(s) of interest, the next step is to evaluate if these cells can properly integrate in the host tissue, sending short and long projections to their natural targets and rebuilding damaged circuitry.
Initial reports showed that the outgrowth from grafts of fetal neurons in adult host brain was limited and dependent on the site of injection (Gonzalez et al., 1988; Isacson et al., 1988; Fricker et al., 1999). The first consistent observation of long-distance axons and extensive innervation of the host brain by fetal transplants following experimental deletion of cortical projection neurons was reported by Hernit-Grant and Macklis (1996) and Fricker-Gates et al. (2002). However, in these studies the specificity of efferent projections from the grafted cells toward appropriate host target sites was not assessed.
One of the first interesting paper in which the reconstruction of damage cortical circuitry is characterized by long-range projection in the appropriate target regions is represented by Gaillard et al 2007. They grafted embryonic cortical neurons into the damaged motor cortex of adult mice and two months after the transplantation they observed a set of projections toward most of the cortical and subcortical targets normally contacted by motor cortex neurons. Interestingly, this pattern of projections was detected also in distant target such the internal capsule and the spinal cord tract, suggesting that they properly follow the corticalspinal tract. The commitment of transplanted cells in developing efferent projections corresponding to their cortical site of origin was underlined also by the fact that visual grafts do not seem competent to replace de degenerating motor pathways. Altogether, these initial reports showed that transplanted embryonic neurons are able to extend long-range projections to distant targets with great specificity, suggesting that guidance cues persist in the adult brain or are re-expressed after injury, although no electrophysiological and/or

behavioral evidence was provided to corroborate the anatomical observations (Gaillard et al., 2007).
More recently, Falkner et al. (2016) performed in vivo 2-photon imaging of embryonic cortical neurons transplanted in lesioned visual cortex, evaluating longitudinal structural maturation, morphology, dendrite elongation and spine refinement of grafter neurons.
They demonstrated the possibility to transplant embryonic neurons that integrate adequately into the adult cerebral cortex, mature over time and reestablish a normal pattern of projection according to their original positional identity (Falkner et al., 2016).
However, in the last decade several groups worked to overcome the ethical and technical challenges of using fetal tissue, developing protocols to differentiate pluripotent stem cells into neurons with appropriate cellular identity and area specification.
Among the first, Pierre Vanderhaeghen and collaborators showed that murine and human PSC-derived neurons transplanted in a model of visual cortex lesion in adult mice display layer-specific patterns of projection in accordance with their molecular identity and consistent with the pattern of projection of native neurons of the visual cortex. Interestingly, these results were only obtained following homotopic transplantation in visual and not in motor cortex, as also confirmed by transplantation of fetal visual and motor cortical neural precursors (Espuny-Camacho et al., 2013; Espuny-Camacho et al., 2018).
In one of the first reports of mouse PSC used as cell therapy in animal models of stroke, Bühnemann et al. (2006) found that PSC-derived neural precursors transplanted into an Endothelin-1 (ET-1)-induced corticostriatal ischemic lesion, or in the perilesional striatum in rats, survived for up to 12 weeks and differentiated into distinct neuronal subtypes without expressing a specific cortical area-specific identity.
The generation of cortical neurons and reconstruction of cortical neuronal networks are major issues for the development of cell based therapies in stroke. Tornero and collaborators transplanted human IPSCs-derived, cortically committed or non-committed neural precursors, in the perilesional somatosensory cortex of a rat stroke model obtained by middle cerebral artery occlusion (MCAO). The cortically fated cells survived, differentiated to functional neurons, and improved neurological outcome in stroke-subjected nude rats (Tornero et al., 2013). In support of their cortical phenotype, they also demonstrated pyramidal morphology of the grafted, fated cells and expression of the cortex-specific marker TBR1 in a certain layered pattern.

8.3 Functional integration of transplanted cells

Although functional integration of grafted neurons in injured host neural circuitry will most likely lead to optimum functional recovery after stroke, evidence that neuronal replacement really occurs is still limited. Functional integration requires the formation of electrophysiologically and morphologically competent neurons but also of efferent projections to the appropriate targets and establishment of functional synaptic inputs on the grafted neurons from host brain. Several studies showed that neurons transplanted in the cortex differentiate and mature in functional neurons, which are characterized by appropriate electrophysiological properties of resting membrane potential, spontaneous and induced action potentials (APs) and spontaneous post-synaptic activity in voltage or current clamp configuration (Bühnemann et al., 2006; Daadi et al., 2009; Oki et al., 2012; Espuny-Camacho et al., 2013, 2018; Tornero et al., 2013; Michelsen et al., 2015).
Interestingly, many of these studies reported both excitatory and inhibitory spontaneous post-synaptic activity of transplanted cells. This activity was totally blocked using AMPA, NMDA or GABA antagonists (CNQX, APV and Gabazine, respectively), indicating that transplanted cells successfully receive inputs from resident neurons.

However, direct experimental data demonstrating that transplanted stem cell or reprogrammed cell derived neurons receive synaptic inputs from stroke-injured host brain are scarce. Neurons, derived from transplanted mouse or human NSCs or human ES cells, have been shown to be surrounded by structures expressing synaptic markers and to exhibit spontaneous excitatory postsynaptic currents (Buhnemann et al., 2006; Daadi et al., 2009). Some ultrastructural data indicate synaptic connections between host axon terminals and grafted neurons (Daadi et al., 2009; Muneton-Gomez et al., 2012). Tornero and collaborators have shown that stimulation of the mouse intact cortical region adjacent to the transplant triggered monosynaptic evoked responses from the intracortically grafted neurons, generated from human iPSC-derived lt-NESCs, which indirectly suggested that the host neurons had established afferent synaptic contacts on the grafted cells (Tornero et al., 2013).
A recent report has demonstrated for the first time that the host brain regulates the activity of grafted, cortically fated human lt-NESC-derived neurons, providing strong evidence that these transplanted cortical neurons can become incorporated into injured cortical circuitry (Tornero et al., 2017). In this study, the authors used the rabies virus-based trans-synaptic tracing method and showed that the grafted neurons receive direct synaptic inputs from neurons in different host brain areas located in a pattern similar to that of neurons projecting to the corresponding endogenous cortical neurons in the intact brain. Immunoelectron microscopy confirmed that neurons of stroke-injured host brain establish excitatory axodendritic synaptic contacts with the grafted human cortical neurons. In vivo electrophysiological recordings from the cortical transplants showed that mechanical stimulation of nose and paw evokes spikes or inhibits spontaneous activity in the grafted neurons, indicating that some of the afferent inputs to these neurons are functional. Confirming the functionality of the synaptic inputs, using patch-clamp recordings, they showed that the grafted neurons respond to photostimulation of virally transfected, channelrhodopsin-2-expressing thalamocortical axons in acute brain slices. Although these data clearly demonstrate that the reprogrammed grafted neurons can become part of injured host neuronal circuitry, it remains to be demonstrated that this repair mechanism contributes to long-term amelioration of functional impairments after stroke.

8.4 Beneficial Impact of transplanted cells

The final goal of cell-based therapies is to improve recovery from functional deficits. In this context, beneficial effects of grafted cells can be ascribed to two, not mutually exclusive, mechanisms: (i) transplanted neurons could properly rebuild damaged circuitry, reestablishing lost sensorimotor synaptic connections; (ii) grafted cells could enhance functional recovery by secreting trophic factors and molecules with a neuroprotective/neuroplastic effect (also known as bystander effect) (Alia et al., 2019).
Consistently, a main focus in cell therapy for stroke has been cell replacement attempting to mitigate neuronal loss in the immediately affected brain area, i.e. the ischemic core. This approach is however confounded by major challenges, not least the extensive tissue damage and lack of blood supply and nutrients in the ischemic core, which results in poor transplant survival, as reported in several animal studies (de la Rosa-Prieto et al, 2017). Another challenge is that stroke lesions are very complex and evolve over time to affect more and more interconnected brain areas. This phenomenon is called diaschisis (von Monakow, 1914) and can explain why an initially focal ischemic lesion spreads over time to affect other brain regions. As a result of disrupted connectivity, loss of tissue and function will also occur in brain regions distant to the one immediately affected by the stroke (Kokaia and Darsalia, 2018). Indeed, the fact that in several reports grafted cells were not detected in transplanted animals, despite an apparent functional improvement, indicates that: (i) the

beneficial effect of the grafting was not related to long-term cell integration in the host neuronal circuitry and was exerted in the initial phase before the cells degenerated and (ii) the effect might be due to secretion of beneficial molecules released from grafted cells, or from resident cells stimulated by the grafting, in early post-implantation phase (Ramos-Cabrer et al., 2010; Oki et al., 2012; Hermanto, 2017). Several experimental studies, have demonstrated the potential of neural cell grafts alone or in combination with pharmacotherapeutics and *in situ* engineering approaches to promote transplant mediated repair with some degree of functional restoration after stroke (Lindvall and Kokaia, 2011; Kokaia and Lindvall, 2012; Tornero et al, 2013; Medberry et al., 2013; Massensini et al., 2015; Jendelová et al., 2016; Sandvig et al. 2017, Kokaia and Darsalia, 2018). Data from these studies indicate that the grafted reprogrammed cells induce functional improvement in stroke models by mechanisms other than neuronal replacement: this phenomenon is known as the bystander effect. In most of these studies, the beneficial effect of transplantation was first observed within 1–2 weeks, i.e., before any functional neurons could have developed from the grafted reprogrammed cells. It is inconceivable that this early improvement is due to neuronal replacement.

The majority of these studies seem to suggest that the observed functional outcomes, which tend to be transient, involve processes such as trophic action, neuroprotection, modulation of inflammation, and stimulation of angiogenesis. As such, improved outcome may be attributed to paracrine effects exerted by the cell transplant, i.e. cell-cell communication mediated by the transplant which induces a response in nearby cells which mediates ameliorating effects within the host tissue (Kokaia and Darsalia, 2018). In support, using mouse-derived iPSCs, Chen et al. (2010) demonstrated decreased levels of the proinflammatory cytokines IL-1b, IL-2, IL-6, TNFa, and iNOS mRNA concomitant with increased level of the antiinflammatory cytokine IL-4 and increased expression of IL-10 mRNA in the hemisphere ipsilateral to stroke. Similarly, decreased inflammation was observed when human-derived iPSCs were transplanted in stroke-damaged brain (Chang et al., 2013; Tatarishvili et al., 2014). Mohamad et al. (2013) described increased BDNF mRNA levels in the stroke-injured brain of mice grafted with iPSC-NPCs. It has also been observed that neurons derived from human neural stem cells express high levels of vascular endothelial growing factor (VEGF) and improve animal performance in the rotarod and limb placement tests when transplanted in the perilesional tissue after a hemorrhagic lesion, with early effects (8 days post-transplantation) (Lee et al.,2007).

A major currently unmet challenge is that for (sustainable) functional recovery to occur, a neural cell transplant must functionally integrate with the stroke lesioned brain, i.e. receive inputs and extend axons and establish long-range, target-specific connections with relevant neuronal assemblies. This entails structural and functional integration within a complex multi-nodal neural circuit, i.e. the neural transplant needs to become embedded in the brain connectome, in a patient-specific manner.

The latter is very important, given that there is major variation between patients with regard to stroke lesion profile and severity, but also spontaneous recovery mechanisms as well as response to intervention. This underlies the importance to identify prognostic factors that are able to predict long-term motor outcomes in order to stratify the patients selecting whom and when to target with specific therapeutic approaches. Considering the cell-based therapy, little is known about the exact mechanisms underlying the integration process, while the manner in which cell transplantation could be assisted by targeted rehabilitation approaches to promote sustainable functional outcomes is unknown. Moreover, direct empirical evidence supporting functional integration of engrafted cells in human patients is currently lacking (Kokaia and Darsalia, 2018). It follows that to determine whether neural cell therapy can indeed become a viable therapeutic option for stroke in the clinic, preclinical models of stroke are needed. Moreover, preclinical models of stroke should have predictive value in

terms of responsiveness of individual subjects to cell therapy, also in the context of tailored rehabilitation regimes. A corollary to the above is that such models must consider the large stratification of stroke patients and relevant lesions observed in the clinic.

9- Animal models of stroke

Several animal models have been developed in the recent years to study molecular and cellular mechanisms following a focal ischemic insult in the brain and to evaluate possible therapeutic approaches for the restoration of function (Wittenberg, 2010).
In particular, rodent models allow a coordinated electrophysiological, behavioral, biochemical, and anatomical analysis of post stroke recovery. Despite there are some differences in the organization of cortical areas and in the distribution of corticospinal neurons, intracortical connections between different areas of the somatosensory cortex are very human-like. This makes the rodents a reasonably good model for understanding the changes in the intracortical communications following a brain injury (Nudo, 2007). Mice (Mus musculus), in particular, offer the possibility to carry out various genetic manipulations. Using Knock-out mice is possible to carry out studies aimed at identifying the molecules involved in the pathophysiology of stroke and related neuronal events such as neuroprotective phenomena, ischemic tolerance and ischemia induced neurogenesis (Wang et al., 2007). Moreover, it is possible in mice to express optogenetic and/or chemogenetic receptors linked to specific promoters (i.e. targeted to highly selective areas of the brain or even neuronal populations) to finely modulate neuronal activity.
Of course, animal models that reproduce human stroke have several limitations, some of which are difficult to overcome. The human clinical stroke is often a result of a number of predisposing factors such as depression, diabetes, obesity and circulatory problems (Nudo, 2007; Pearson- Fuhrhop et al., 2009). In the animal models, stroke is induced in young and healthy individuals and in strictly controlled experimental conditions, that cannot reproduce the complexity and heterogeneity of a human stroke. In addition, the corticospinal tract (CST) is very different in the two species. In mammals, this descending path from the layer V of the motor cortex to the spinal motor neurons is the main motor output. Primates, however, present a higher number of corticospinal neurons than rodents. Moreover, there is no direct corticospinal connections to motor neurons located in the spinal cord in rodents (Alstermark et al., 2004, Alstermark and Ogawa, 2004), where instead motor commands conveyed by the CST are transmitted to spinal motoneurons by segmental interneurons and propriospinal neurons (Lemon, 2008). Another striking difference is the amount of CST decussation: in primates, fibers that cross to the contralateral side of the spinal cord prevail, while in rodents the ipsilateral component is greater and represents a potential compensatory pathway. For this reason, rodents often show a better and faster recovery after injury than humans (Nudo, 2006). Finally, every stroke induction model requires anesthesia, which is well-known to impact on neuroprotection and stroke outcome (Kitano et al. 2007). The possibility to control and standardize factors like age, location of lesion and its extension is a great advantage in terms of experimental results but it also introduces a difference from humans where all those aspects are often variable.

9.1 Middle cerebral artery occlusion (MCAO)

Since the majority of human stroke lesions are located in the territory of the middle cerebral artery, many experimental models consist in variants of MCA occlusion (Carmichael 2005). The MCA is one of the major arteries that provides blood supply to the brain. In humans, it arises from the internal carotid artery, routes along the lateral sulcus where it then branches and projects to the basal ganglia (lenticulostriate arteries) and the lateral surfaces of the temporal (inferior division) and fronto-parietal lobes (superior division), including the primary

motor and sensory cortex. The right and left MCA are connected to the anterior cerebral arteries and the posterior communicating arteries, which connect to the posterior cerebral arteries, creating the Circle of Willis (Fig.9). In rodents, the MCA follows a very similar path.

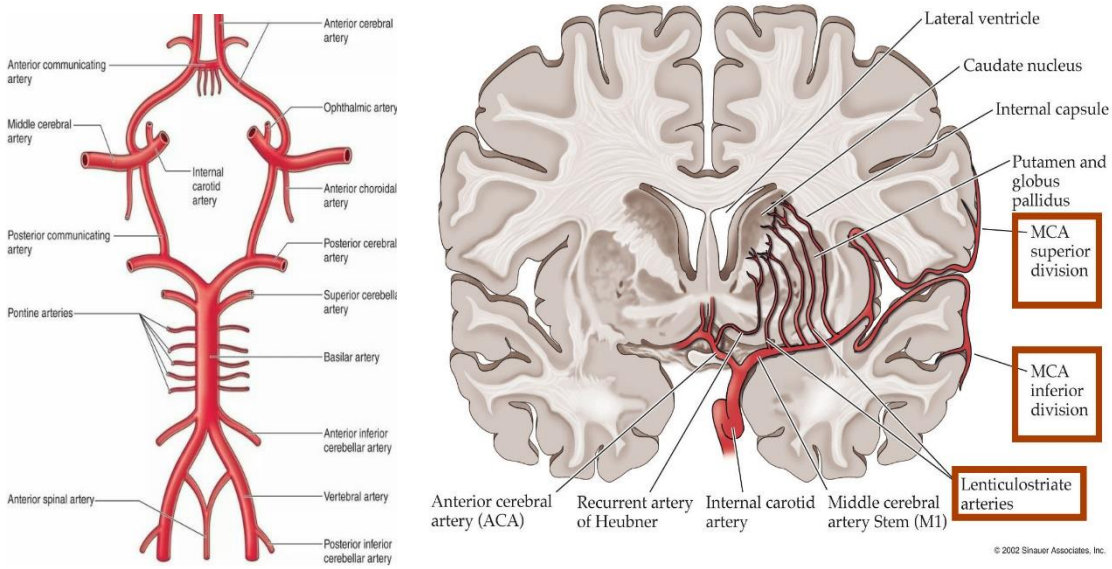

***Figure 9**: Schematic representation of the Willis circle (left) and the MCA and its ramifications (right)*

9.1.1 Intraluminal filament model of stroke

One of the most commonly used stroke models is the “filament model”. In order to induce MCAO, an intraluminal filament (silicon coated or heat blunted) is introduced into the internal carotid artery (ICA) and advanced until it occludes the origin of the MCA (Longa et al., 1989). Following insertion of the filament, it can be left in place permanently or withdrawn after a defined period of time (usually after 60, 90 or 120 minutes) to induce reperfusion of the MCA. With the filament model of MCAO, there is typically damage to the striatum and depending on the length of occlusion time cortical damage will also be present. In terms of ischaemic penumbra, the intraluminal filament model has been demonstrated to produce a considerable volume of potentially salvageable penumbra with the presence of comorbidities such as hypertension resulting in significantly less penumbra (McCabe et al., 2009, Meng et al., 2004, Shen et al., 2003). This makes it a useful model for studies investigating the impact of therapeutic approaches on either the volume or lifespan of the penumbra or tissue salvage following reperfusion (Henninger et al., 2007a, Henninger and Fisher, 2007).
One area of criticism is that MCAO does not represent the clinical stroke population where typically gradual recanalization of the occluded vessel will occur: in the animal model there is prompt reperfusion right after filament removal (Hossmann, 2012). Thrombolysis with rtPA (see above) results in a gradual breakdown of the clot which can take anywhere from 30 min to up to several hours to fully lyse and therefore may induce a gradual reperfusion (Alexandrov et al., 2001). However, with the recent advent of endovascular thrombectomy, in which the thrombus is surgically removed, the filament model has found a new clinical relevance. Surge reperfusion observed with removal of the filament will be similar to that observed with endovascular thrombectomy (Sutherland et al., 2016).

9.1.2 Electrocoagulation model of MCAO

The electrocoagulation model of MCAO in rodents was originally developed by Tamura and colleagues (Tamura et al., 1981). In this model, a craniotomy is performed to expose the MCA on the brain surface. Electrocoagulation forceps are used to coagulate a particular portion of the MCA in order to permanently occlude the vessel. One of the advantages of this model is that the section of the MCA that is occluded can be varied (i.e. a distal or proximal occlusion) in order to induce a stroke affecting cortical or both cortical and sub-cortical territory. A distal occlusion of the MCA will induce a cortical lesion whereas a proximal occlusion (at the origin of the MCA), which includes the lenticulostriate branches irrorating the basal ganglia, will induce a larger sub-cortical and cortical infarct and thus results in a lesion similar to the filament model. Typically, mortality is low owing to the craniectomy required to visualise and occlude the MCA, which limits the effects of edema. One limitation with this particular model is that it induces permanent MCAO and therefore reperfusion is not possible. Due to the location of the craniectomy, damage to the temporalis muscle may occur, particularly if a distal occlusion is carried out. With this model, it has been demonstrated that there is a measurable region of penumbra, which gradually becomes incorporated into the infarct over the first 3–4 h after MCAO (Tarr et al., 2013). Infarcts modelled by the distal Middle Cerebral Artery Occlusion (MCAO) model in mice encompass about 10-15% of the hemisphere, thereby mimicking a majority of human stroke lesions which are located in the cortical MCA territory (Carmichael 2005, Howells et al 2010).

9.2 Photothrombosis

Another ischemic model for rodents that has become quite popular in the scientific field is the phototrombotic stroke. Photothrombosis is a technique that allows to induce a cortical infarct by means of systemic injection of a photosensitive dye and the subsequent irradiation of a specific cortical area with a light beam (Watson et al., 1985). The most used dye used for this purpose is the Rose Bengal, that can be administered directly in the tail vein or intraperitoneally. Rose Bengal has its peak of absorption in the green part of the spectrum (560 nm) and the size of the infarct volume induced (with the same concentration of the dye) could be adjusted by regulating the field aperture and the intensity of the light source (Wang et al., 2010). The illumination can be delivered directly from the skull, so that this technique is not only quick, precise and reproducible but also minimally invasive. The local activation of the dye induces the generation of singlet oxygen that leads to focal endothelial damage, aggregation of platelets and ultimately the formation of thrombi (Watson et al., 1985). The coagulation cascade determines the occlusion of the small vessels but not the generation of a penumbra, because of the rapid induction of oedema and breakdown of the blood brain barrier (Dietrich et al., 1986). The lack of penumbra could be disadvantageous for preclinical studies of early interventions aimed at preserving the survival of the instable tissue. Also, reperfusion cannot take place, due to the irreversible damage to blood vessels. On the contrary, phototrombotic ischemic model is highly useful for investigations involving cortical plasticity and remapping induced by ischemic injury, restorative drugs and neuronal repair (Durukan and Tatlisumak, 2007), due to the high reproducibility of the resulting ischemic lesion in terms of position and size. Based on the original protocol for rats introduced by Watson et al. (1985), the phototrombotic model has
been simplified and adapted for mice by Schroeter et al. (2002). The main advantage introduced by this work is the validation of irradiation parameters with a conventional cold white light source that simplifies the application of this technique (Schroeter et al., 2002).

Aim of the study

The aim of this thesis project was developing new prognostic and therapeutic tools in preclinical models of stroke. I took advantage of two different mouse models, the Middle cerebral artery occlusion (MCAO), which shows a higher variability and is thus closer to the human condition, and the photothrombosis, that is more reproducible and allows to better identify benefits of new therapies.

In the first part of the project, I started characterizing the MCAO model. By means of histology, I analysed the ischemic lesion and its evolution in time. I conducted behavioural experiments to assess whether a measurable motor deficit existed. After confirming the presence of a motor deficit at the level of the forelimb, I further investigated this aspect, utilizing (1) the skilled reaching test, which provides a readout of finer motor skills, and (2) the M-platform, a robotic device that allows to quantitatively and objectively evaluate several kinetic/kinematic parameters related to a retraction movement.

Given the presence of a forelimb motor deficit, I focused on electrophysiological alterations of the cortical area that controls this body part, namely the caudal forelimb area. I studied changes in spectral bands longitudinally, before and after stroke induction. In addition, I exploited electrophysiology to characterize the retraction movements onto the M-platform, in terms of power spectral density changes and event-related potential. Later on, I studied how these mechanisms are altered by stroke.

Finally, I combined behavioural and anatomical data in order to reveal possible biomarkers that predict long-term motor recovery.

In the second part, I transplanted two different kind of neurons derived from embryonic stem cells (hippocampal and isocortical neurons) in order to evaluate the different projection pattern. Moreover, I focused on analyzing the effect of a cell-based therapy to promote functional recovery after photothrombotic stroke. First of all, I studied the behaviour of in vitro-generated cortical neurons when transplanted either in healthy or in ischemic brain regions, then I assessed the impact of transplanted cells into the ischemic stroke by means of gridwalk test in order to test the presence of functional recovery.

Materials and Methods

Experimental design (1)
Assessing anatomical and behavioural biomarkers to predict motor recovery after MCAO-induced stroke

All procedures were performed according to the guidelines of the Italian Ministry of Health for care and maintenance of laboratory animals, and in strict compliance with the European Community Directive n. 2010/63/EU on the protection of animals used for scientific purposes. Animal experimentation at the CNR Neuroscience Institute was approved by the Italian Ministry of Health. All surgical procedures were performed under deep anesthesia and all efforts were made to minimize suffering of animals. In order to investigate electrophysiological and behavioral changes that occur upon MCAO induction, a total of 39 C57BL6J mice were used (22-27 g, age 8-12 weeks).
First, animals were trained in a skilled reaching test (Lai et al. 2015, Alia et al. 2016, Spalletti et al. 2017) for two weeks: only left-handed mice were selected and underwent electrode implant (see below). Then, animals were trained for an additional week in order to allow them to re-habituate to the grasping task after the surgery. During this re-habituation period, animals were also shaped on the robotic platform. At the end of the week, the baseline performance in the skilled reaching, GridWalk test and on the M-platform was acquired. MCAO surgery was induced in the right hemisphere. Finally, animals underwent behavioural testing in the GridWalk, skilled reaching test, M-platform at day 2 and 30 post MCAO lesion.

Moreover, to investigate possible post-stroke electrophysiological changes, the animals were recorded both in freely-moving condition and during a retraction task on the M-platform. After 30 days, in order to perform anatomical analyses, animals were transcardially perfused and immunohistochemistry was carried out on brain coronal sections.

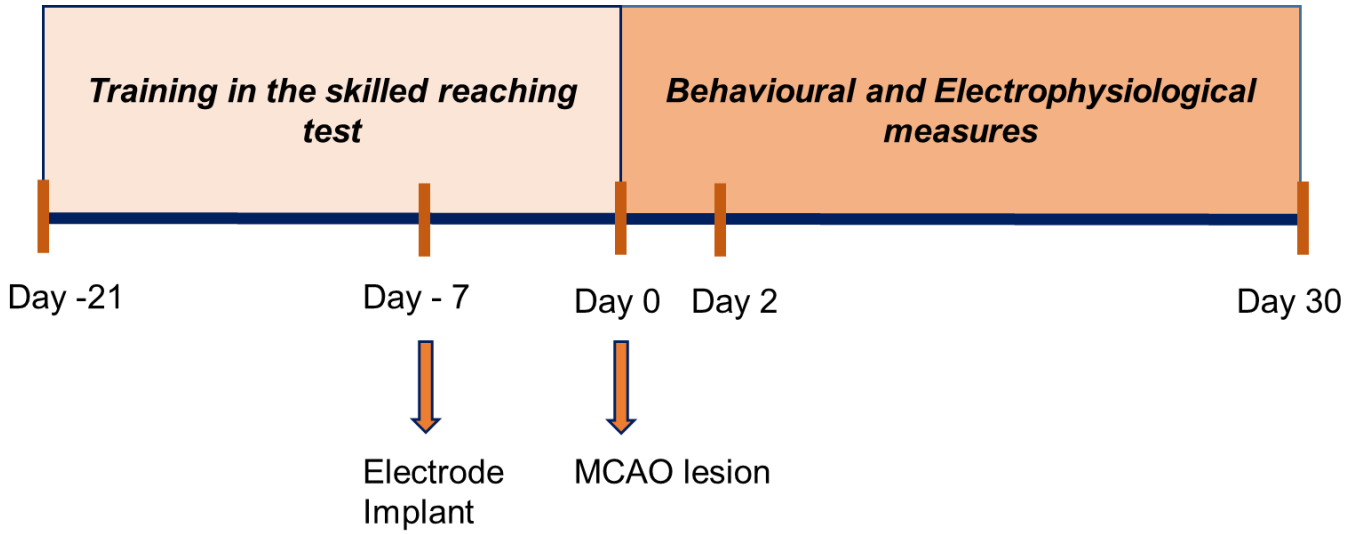

Figure 1: Timeline of experimental procedure

1.1 Electrode implant

Animals were anesthetized with avertin (20ml/kg, 2,2,2 tribromoethanol 1.25%; Sigma-Aldrich, USA), placed in a stereotaxic apparatus and the skull was exposed through a midline incision. Then, two burr holes were drilled in both hemispheres at the level of Bregma, 2 mm lateral. This way, the electrodes were implanted in the caudal forelimb area (CFA; Tennant et al. 2011, Alia et al. 2016). A surgical screw was tightened at the center of the occipital bone and was used both as ground reference and to give more stability to the recording implant. Bipolar electrodes were assembled prior to the surgery: a couple twitched insulated tungsten wires (700µm spaced in length at the tip) were soldered at the channel and reference pins of the connector (Elitalia).
With the aid of a micromanipulator, the electrode was stereotactically inserted in the centre of the drilled holes at 700 µm of depth and the ground pin was connected to the occipital screw. A first layer of dental cement (Optibond) was distributed to secure all the components to the skull surface. After the first layer of cement was dried, an aluminium post, used later to head-fix the animal, was cemented onto the skull. Finally, a second layer of cement (Paladur, Pala, Germany) was distributed to enclose all the electrical components. After the surgical procedure, animals were treated with paracetamol (100 mg/kg) for 4 days post-operation in drinking water.
Animals were allowed to habituate to the implant for one week before undergoing any further procedures.

1.2 Permanent Middle Cerebral Artery Occlusion

Animals were anesthetized with avertin (20ml/kg, 2,2,2 tribromoethanol 1.25%; Sigma-Aldrich, USA), transferred onto a heat blanket in lateral position and immobilised with adhesive tape for medical use. A skin incision was performed between the ear and eye using fine surgical scissors. Then, the temporal muscle was exposed, detached from the bone and cut vertically to reveal the underlying skull. The MCA was identified below the semitransparent bone and a circular craniotomy was drilled above it.
Once it was exposed, the MCA was occluded with electrocoagulation forceps (2biological instruments, bipolar mode, 12W). If the artery was bifurcated, the coagulation was performed both proximally and distally to the branching and, if necessary, also the single branches were coagulated. When there was no bifurcation, the MCA was coagulated at two sites of approximately 1 mm of distance. If spontaneous recanalization occurred, the electrocoagulation was performed again. Finally, the temporal muscle was relocated to its position, glued with cyanoacrylate and the wound was sutured. Intraoperative rectal temperature was kept at 37.0 ± 0.5°C using a heating pad.
Sham animals underwent the same procedure but without the electrocoagulation step.
After the surgical procedure, animals were treated with paracetamol (100 mg/kg) for 4 days post operation in drinking water.

1.3 Immunohistochemistry

For immunohistochemistry, brains were collected after transcardial perfusion of deeply anaesthetized mice with PBS (5 min) followed by 4% PFA. Brains were then post-fixed in 4% PFA for 2 hours and then kept 30% sucrose in Phosphate Buffer at 4 °C. Then, they were sectioned on a sliding microtome (Leica, Germany) into 50 µm coronal sections, which were kept free-floating for further processing. Brain slices were incubated in a blocking

solution for 1 hour (10% horse serum; 0,3% Triton X-100 in PBS) before applying the primary antibodies, dissolved at the proper concentration in 1% horse serum and 0.2 % Triton X-100 in PBS. The following primary antibodies were used: guinea pig anti-NeuN (1:1,000, Millipore), rabbit anti-GFAP (1:500, Dako). After washing, slices were incubated with species-specific secondary antibodies, dissolved in 1% horse serum and 0.2% Triton X-100 in PBS, for 2 h at room temperature. Nuclear staining was performed with (1:500) Hoechst 33342 (Sigma). Coverslips were mounted on glass slides with Vectashield (Vector Labs). Images were acquired with epifluorescence microscope (Axio Imager. Z2, Zeiss) equipped with Apotome.2 (Zeiss).

1.4 Anatomical and structural measures

1.4.1 CFA localization and quantification

In order to create masks that show the exact CFA localization in brain coronal sections at different anteroposterior (A-P) levels, we merged information from a forelimb motor map previously obtained using intracortical microsimulation (ICMS) (Alia et al 2016) and coronal sections derived from the Mouse Brain Atlas (Paxinos, George, and Keith B.J. Franklin. The mouse brain in stereotaxic coordinates) (**Fig. 2A**). In Alia et al., 2016, the cortex of anesthetized mice was exposed and intracortical electrical stimulations were systematically performed following a grid with nodes spaced 250µm. Then an averaged map showing the probability (p) to observe a forelimb movement for each site was built (**Fig**. **I**). Thus, according to the spatial resolution used to obtain ICMS motor maps, our masks were built using intervals of 250µm at the A-P level.
In order to delineate CFA borders on coronal section masks, we binarized ICMS maps to obtain a red area with high movement probability (p>0.8) and a yellow area with a medium movement probability (0.5<p<0.8). Then, we approximated the yellow area to p=0.5 (i.e. that area is responsible for a forelimb movement in the 50% of tested animals) and the red area to p=1 (i.e. that area is responsible for a forelimb movement in the 100% of tested animals).

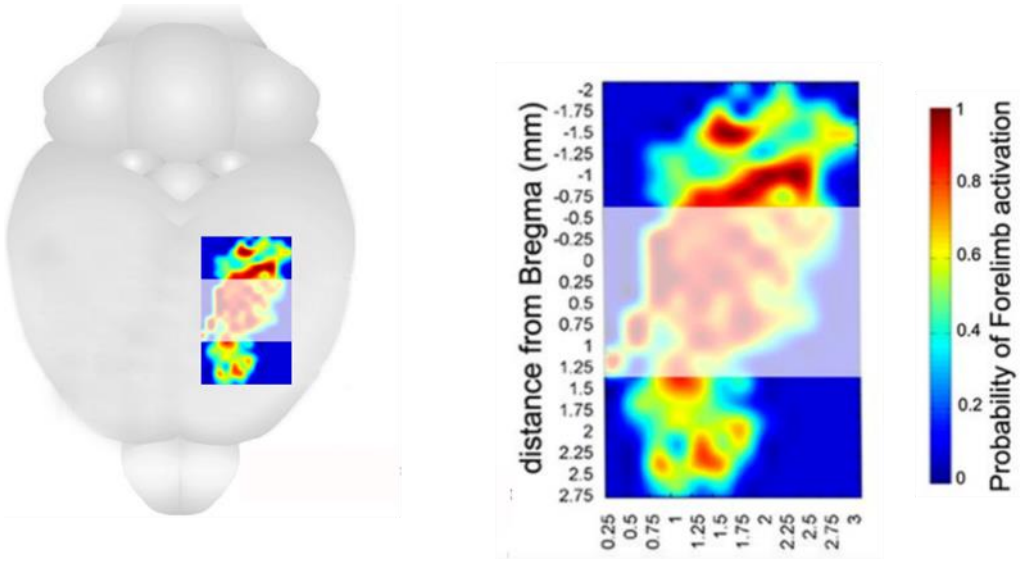

Figure I: ***CFA rearrangement.*** *Scheme of the average map obtained by ICMS technique following a grid of stimulation site of 250 µm in healthy animals. For each pixel in the maps, a color code indicates the probability (high – red; low – blue) to elicit movement of a body part (contralateral forelimb) after stimulation with a train of cathodal pulses (current, 30 µA) (Alia et al.,2016).*

Then, we reported the position of yellow and red areas boundaries on each mask along the anteroposterior axis (**Fig. 2B**). Subsequently, each CFA representing mask was superimposed and adapted to the corresponding histological brain slice for the entire extension of the CFA, (from approximately -1.00mm posterior up to +1.25 anterior to Bregma suture). The adaptation of the masks to the histological brain slices was reached using Photoshop filters in order to highlight the CFA area despite the distortion of slices caused by the MCAO lesion and the shrinkage due to slice preparation (**Fig. 2C**). Then, using a digital elaboration software (ImageJ), the lesion contour was drawn (**Fig. 2D**), thus lesion area and the percentage of CFA affected were measured. The volume and location of the lesion were assessed as follow. To quantify the lesion volume, 1 out of every 6 sections was stained with NeuN and GFAP. Quantification of area values were obtained with ZENpro software (Zeiss). The lesion volume and the volume of the affected CFA for each animal were calculated by summing up all damaged areas and multiplying this number by section thickness and by 6 (the spacing factor). To avoid an underestimation of the lesioned volume due to the brain shrinkage that takes place in the ipsilesional cortex after the stroke, each damaged area in each single brain slice was normalized by its cortical shrinkage before summation (see below for the calculation of the cortical shrinkage) as follows:

$$\textit{Normalized Area of the Lesion} = \frac{\textit{Measured Area of the lesion}}{1 - \textit{Cortical Shrinkage}}$$

A total infarction volume and the volume of the affected and total CFA was given in mm^3. The area in the yellow region was weighted for the probability of forelimb involvement, thus it was multiplied by 0.5. Finally, the volume of the affected CFA was divided for the total volume of the CFA for each animal, thus giving a % of the affected CFA.
We also measured the CFA and cortical shrinkage, another possible parameter that could predict motor recovery in absence of a direct ischemic damage to the CFA. To obtain a reliable value of the shrinkage, we firstly computed a volumetric factor (Vf) accounting for the dimension of the brain with respect to the standard Paxinos atlas. We used as healthy cortical area the measure of the contralateral cortex in a section far away from the lesion.

$$Vf = \frac{\textit{Healthy Cortical Area}}{\textit{Corresponding Area from Paxinos}}$$

$$\text{Paxinos x Vf} = \text{Healthy Cortical Area}$$

Then the ipsilesional cortical area was measured for each section and subsequently converted in cortical volume (Cv) as previously described. Then we calculated the % of Cortical shrinkage as follows:

$$\% \text{ Cortical Shrinkage} = \frac{Sn - Cv}{Sn} \times 100$$

$$Sn \times \text{Cortical Shrinkage} = Sn - Cv$$

where Sn is the volume of the standard cortical tissue from the Paxinos multiplied for Vf. As the same, we computed the % of the CFA shrinkage:

$$\text{CFA Shrinkage} = \frac{CFAn - CFAv}{CFAn} \times 100$$

where CFAn is the volume of the standard CFA multiplied for the Vf and CFAv is the total volume of the CFA for each animal.

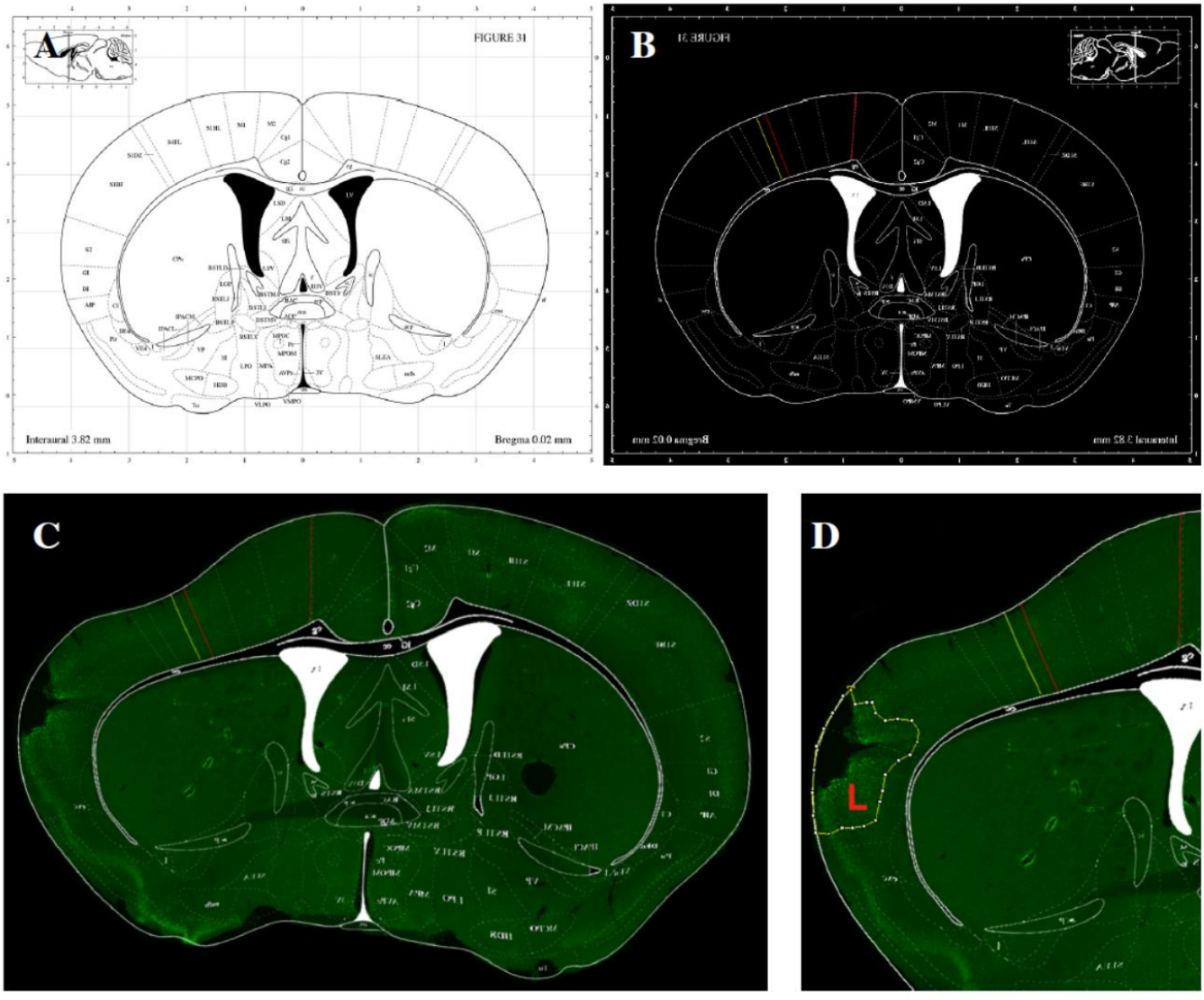

Figure 2: Mouse Brain Atlas slices and mask A) *Slice obtained from Paxinos et al: The mouse brain in stereotaxic coordinates.* ***B)*** *Prototype of mask to highlight CFA in histological brain slice.* ***C)*** *Mask adapted to histological brain slice using Photoshop filters.* ***D)*** *Lesion caused by MCAO (the area of the lesion 'L' is delimited by dotter line).*

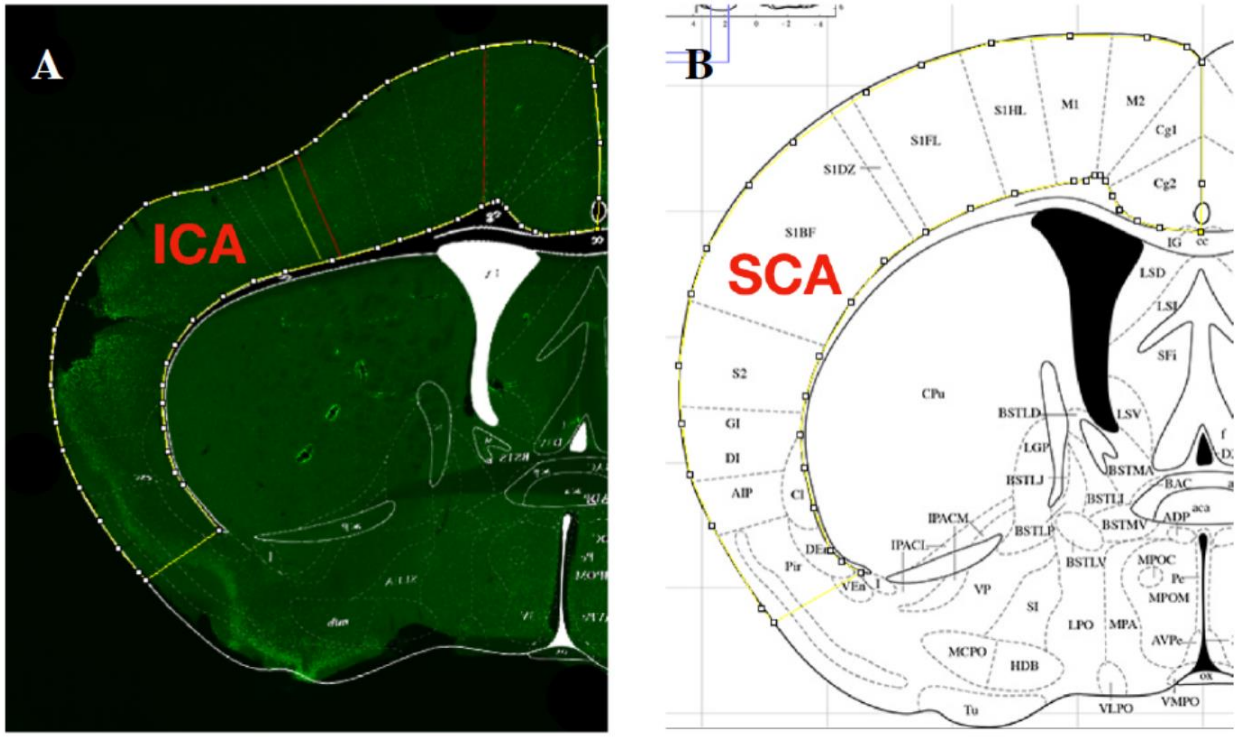

Figure 3: Calculation of Cortical Shrinkage. *To obtain the Cortical volume (Cv), Ipsilesional cortical areas (ICA marked with dotted line in figure* ***A)*** *of analyzed brain slices, were summed and multiplied by section thickness and by 6 (the spacing factor). The same was done for the standard cortical area (SCA marked with dotted line in figure* ***B),*** *but before summing each SCA they were normalized using a volumetric factor. Finally, to obtain the % of Cortical Shrinkage the difference between the normalized standard volume (Sn) and the Cortical volume were divided for Sn as follow:*

1.4.2 CFA neuronal counting

To assess the neuronal density of the CFA, the same histological brain slices used for the CFA localization and quantification were employed. Anti-NeuN immunolabelled slices with their corresponding adapted masks were analyzed with ImageJ (**Fig. 4A**). To avoid neuronal counting biases due to the damage produced by the electrodes at anteroposterior bregma 0 level, we analyzed brain slices 0.50mm posterior to bregma.
First, each image was binarized with a manual threshold to obtain the maximum contrast between cells and their background (**Fig. 4B-4C**). The image was then converted to a mask and round shapes were contoured with a line of single pixel using the ImageJ "watershed function" (**Fig. 4C**). At this point the number of particles with an area greater of 20 pixel,

were automatically counted (**Fig. 4D**), analyzing a 0.6x0.6mm square (**Fig. 4B**) in two different positions inside the CFA. we then averaged the results and calculated the number of neurons contained in 1mm^2.

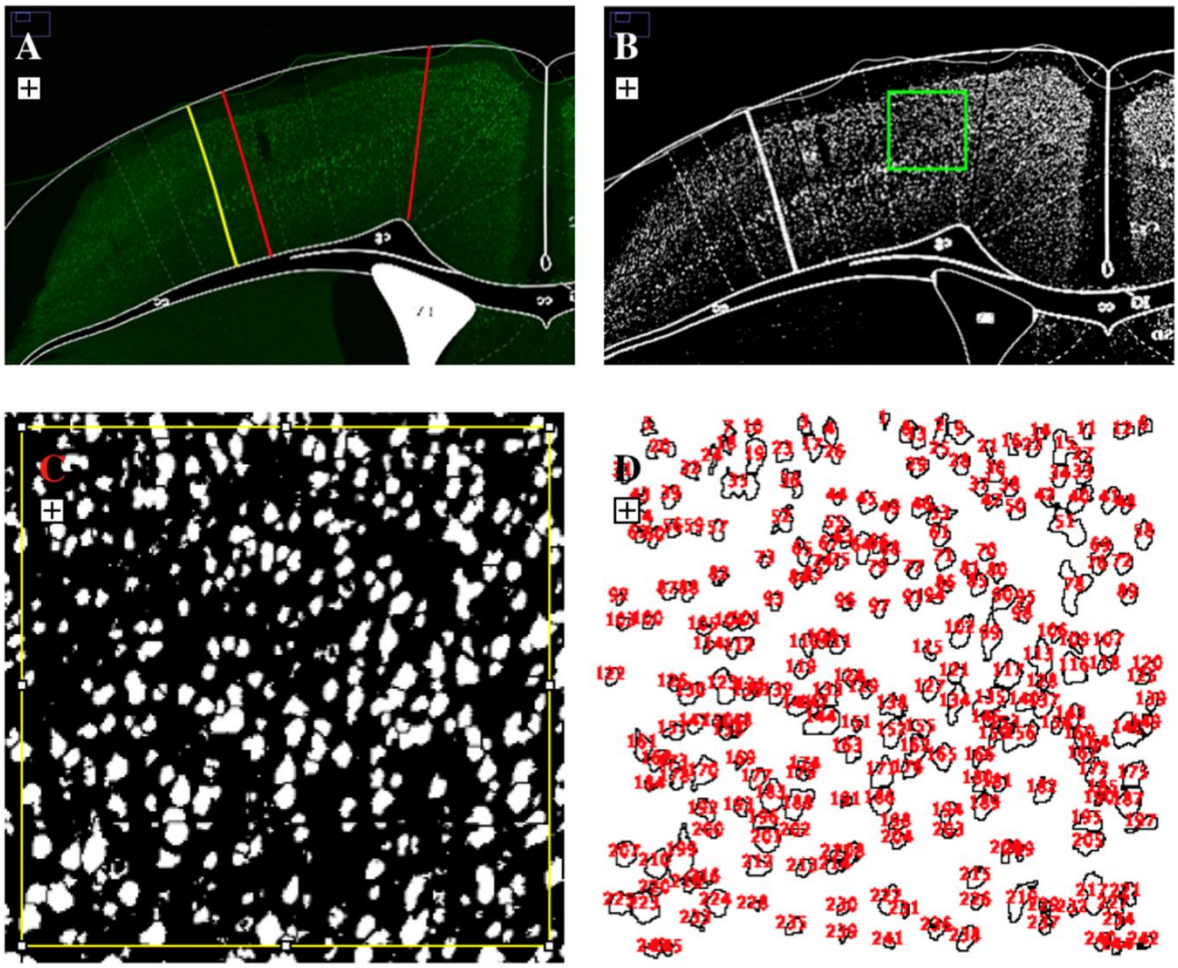

Figure 4. CFA neuronal density A) *CFA mask adapted on histological brain slice immunostained for NeuN* ***B)*** *Binarized image obtained by splitting colors, removing background and using watershed function, the green square represent the area analyzed during the counting.* ***C)*** *Magnification of the* ***(B)*** *image in the CFA* ***(D)*** *Counted cells of field in panel* ***(C).***

1.4.3 White Matter Integrity

In order to test the hypothesis that impairments in the descending motor pathways, measured at the level of internal and external capsule, would determine motor deficit after a cortical stroke, the integrity of the white matter was measured using a Luxol fast blue staining. For each animal 2 50um-thick coronal brain slices located at 0.5 mm (AP1) and 1mm (AP2) posterior to Bregma were chosen. These slices were mounted on a gelatin-coated slide, then were rehydrated in distillate water for 1 minute, ethanol 50%, ethanol 70%, ethanol 96% for 3 minutes each, so, slides were incubated at 60°C with a Luxol fast blue solution overnight. Then slices were left to cool, after that they were placed in: ethanol 96% 2 minutes for 2 times, ethanol 70% and ethanol

50% for 3 minutes each, distilled water 3 minutes for 2 times, lithium carbonate for 10 minutes, distilled water 3 minutes for 2 times, periodic acid for 8 minutes, distilled water 3 minutes for 2 times and sulfur dioxide solution 1 minute for 3 times. Slices were rinsed in running water for 15 minutes, then they were dehydrated in ethanol 50%, ethanol 70%, ethanol 96%, ethanol 100% for 3 minutes each and xylene for 5 minutes. Slices were mounted with DPX. An Olympus BX61 microscope,
inter-faced with VS-ASW-FL software (Olympus Tokyo, Japan) was used to acquire the entire brain sections at 20x of magnification, with a pixel size of 0.346 mm. Acquisition was done over 10 micron thick stacks, with a step size of 2 microns. The different focal planes were merged into a single stack by mean intensity projection to ensure consistent focus throughout the sample. Images were analyzed using Fiji software. The ipsilateral and the respective contralateral stained areas (IC and EC) were assessed blindly and delineated by tracing the stained area on a video screen (**Fig.5A-B**).

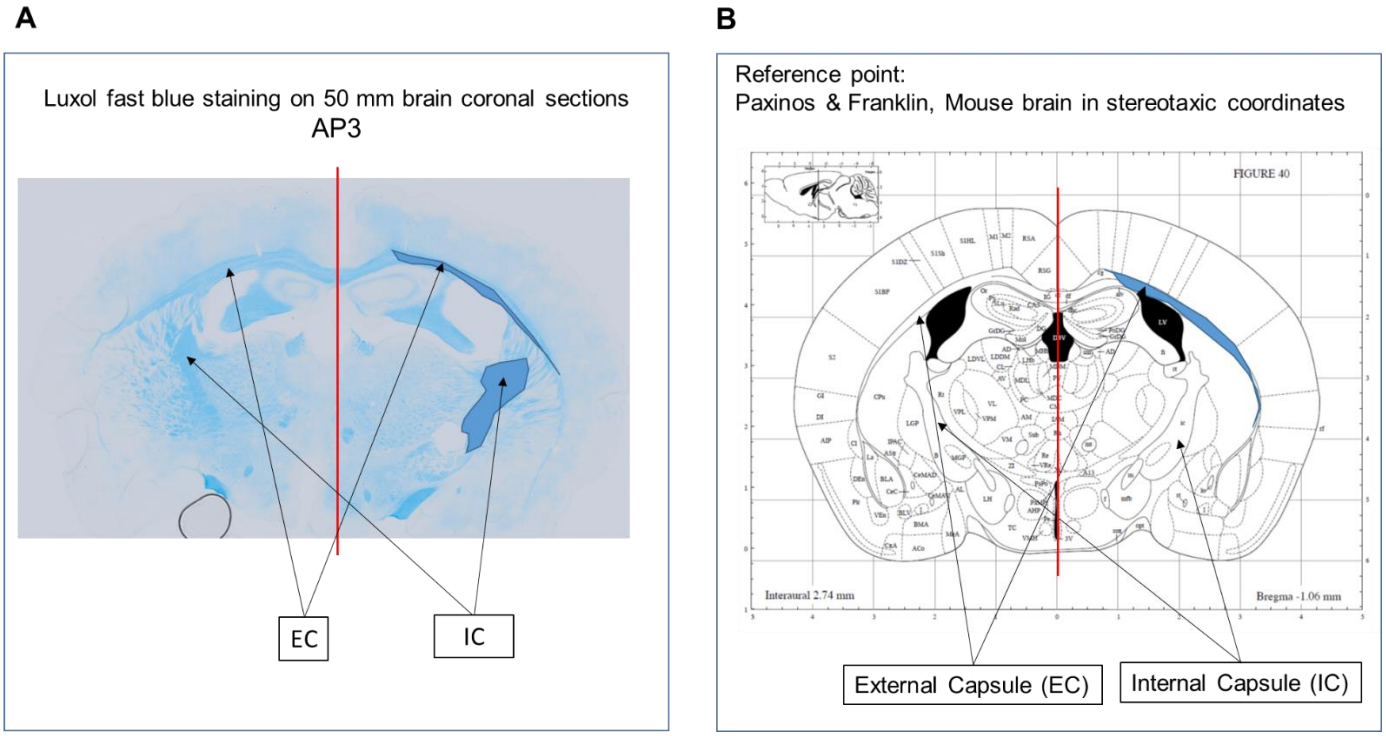

Figure 5. Histological brain slice stained with luxol fast blue protocol A) *Histological brain slice located at 1.00mm (AP2) posterior to bregma stained with luxol fast blue in order to highlight myelin sheaths.* ***B)*** *Reference point from Paxinos et al correspondent to AP2 in which it is possible to visualize the external capsule (EC) and the internal capsule (IC).*

1.5 Behavioural Tests

1.5.1 Gridwalk test

Animals were allowed to walk freely for 5 minutes on an elevated grid (32 x 20 cm, with 11 x 11 mm-large openings) and the task was video-recorded. The video recordings were analysed off-line by means of a custom-designed Graphical User Interface implemented in Matlab (Lai et al., 2015), to assess correct steps and foot-faults, i.e. steps not providing body

support, with the foot falling into grid hole, blind to the experimental group. The percentage of foot faults for each limb was then calculated as following:

$$\% \text{ Foot Faults} = \frac{\text{\# foot faults}}{\text{\# correct steps} + \text{\# foot faults}} \times 100$$

1.5.2 Skilled Reaching Test

The animals (food deprived for 15 hours) were placed in a testing chamber with plastic walls and trained to perform a skilled reaching task with their preferred paw, which had to pass through a small frontal rectangular aperture (0.5 x 1.3 cm) to grasp and retrieve food pellets. Given that the robotic platform is designed for left-handed animals, right-handed ones were excluded. The task was video-recorded from the side of the tested forelimb, thus allowing for a sagittal view of the animal.
Each session comprised around 60 trials; each trial started as soon as the pellet was placed in position and ended when it was displaced from it. Each attempt was classified as follows:

- Correct: the pellet was grasped, taken directly to the mouth and eaten;
- Dropped: the pellet was grasped but it fell right before entering the chamber or inside of it;
- Displaced: the pellet was not grasped but just displaced from its position;
- Missed: the paw crossed the frontal window but the pellet was not displaced.

Then the percentage for the single categories was calculated over the total attempts, i.e. each time the mouse crossed the frontal window with its paw. Also, a cumulative score of the performance was calculated as follows:

$$ReachingScore = \%Correct + \mathbf{0.6} \cdot \%Dropped + \mathbf{0.3} \cdot \%Displaced + \mathbf{0} \cdot \%Missed$$

1.5.3 Motor Assessment onto Robotic Platform

We measured forelimb performances in a robotic device, the M-Platform **(Fig. 6)**, where the animal had to pull back a handle in order to get a liquid reward (Spalletti et al., 2014, 2017) thereby allowing the assessment of kinetic and kinematic parameters.
The main components of the robotic platform, namely the M-platform, are a linear actuator (Micro Cylinder RCL, IAI, Germany), a 6-axis load cell (Nano 17, ATI Industrial Automation, USA) and a custom designed handle that was fastened to the wrist of the mouse and placed on a precision linear IKO slide (IKO BWU 25-75, USA). Furthermore, an actuated system (Pasquini et al. 2018) precisely set the level of static friction at a level of 0.3 N (**Fig. 6A**). During experiments, the animal was kept in a U-shaped restrainer (interior dimensions 35 × 80 × 30 mm) and head-fixed on the platform by means of a post cemented to the skull. Its left wrist was blocked to the slide through the handle. The task was a pulling/retraction movement and included two phases: a passive phase and an active phase. During the first phase the linear actuator pushed the slide, where the wrist of the animal was blocked, to extend its forelimb parallel to the sagittal plane. Then, the active phase started and the motor was quickly decoupled from the slide and the animal could voluntarily pull back the slide to

the rest position. Animals were water-deprived for 15h and receive a milk droplet as a reward for each complete retraction.
During the task, force signals were acquired by the load cell and digitalized using the USB DAQ board, while the position of the slide during the active phase was monitored by a high-resolution webcam (Zyno Full HD, Trust, Netherlands) with a frame rate of 25 Hz. Signals were synchronized off-line with a custom-made algorithm. Time to perform each trial was calculated, peaks of force were detected using a threshold method (**Fig.6B**).
Based on these variables, several robot parameters were evaluated: (1) the latency to the first retraction (i.e. the time elapsed before the first force peak) (2) the t-target, i.e., the time spent by the animal to accomplish a single retraction task; (3) the number of sub-movements needed to complete the task; (4) the number of attempts, i.e., the number of force-peaks not corresponding to a submovements (i.e. below the static friction force). For each session, a number of 25-30 trials, i.e. full extension-retraction cycles, were performed. During each trial, the above-mentioned parameters were measured and then averaged across trials to obtain a single value for each session. Given that the distribution of the single values across different trials rarely passed the normality test, we took the median instead of the average as a representative value for that specific session.
In addition, the M-platform allows to perform an isometric task, consisting in 40 seconds during which the mouse forelimb was kept extended by the actuator. Two other parameters were extracted: (1) the mean force, i.e. the mean of the values of the force peaks, and (2) the Area Under the Curve (AUC) of force-peaks.

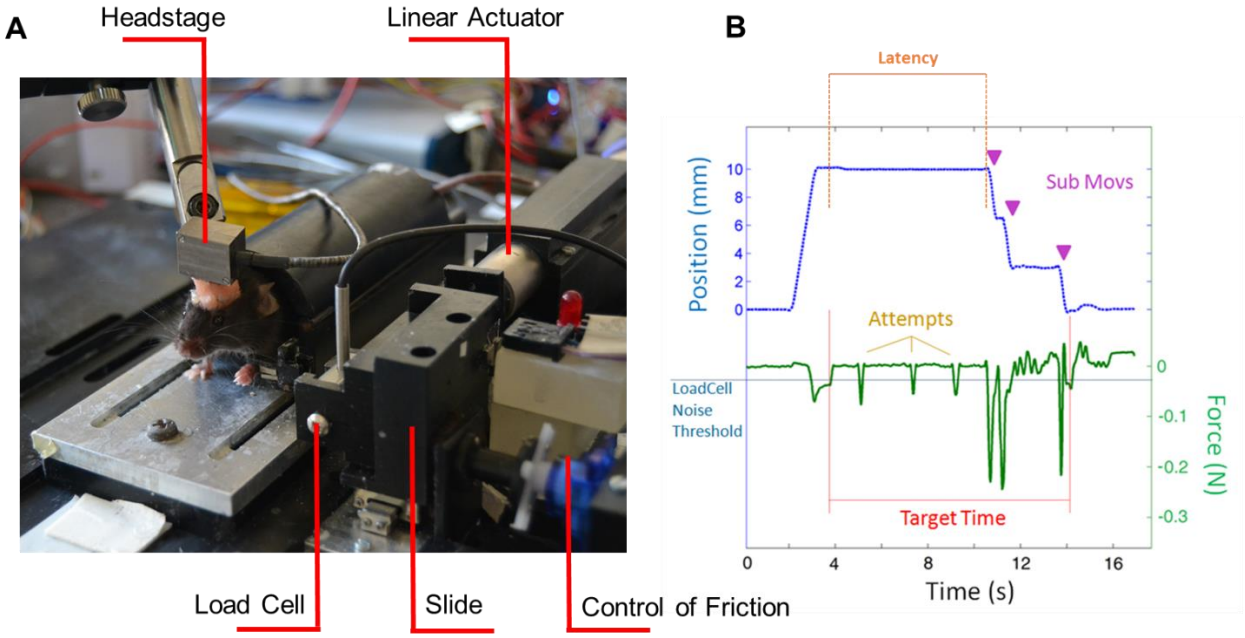

Figure 6 M-Platform A) *Main components of the M-Platform* ***B)*** *Parameters extracted from retraction movement*

1.5.4 Motor Score

in order to combine all the obtained behavioral data, we implemented a global motor score, that includes the outcomes of all behavioural tests in a single total score. To calculate the global motor score, the readouts of each behavioural test (gridwalk, skilled reaching task, robot – including retraction parameters and isometric task) were firstly converted in a scale

from 0 to 10. Score 0 was assigned to animals showing a bad performance, while score 10 to represents maximal performance. For each readout, the dynamical range where the greatest variance was observed was manually selected. The readout was converted though a linear transformation (see table). Values exceeding the previously selected dynamical range were converted to either 0 or 10, according to whether it was below the lower bound or above the upper bound respectively. Finally, the converted readouts were summed up to obtain the global motor score.
For each test the score was assigned as follow:

- **Gridwalk test:**
  score= $0.2 \cdot (100 - \%err) - 8$ where %err= percentage of foot faults

  10% - 60% → 10(max)-0(min) score
  < 10% errors → 10 (max) score
  > 60% errors → 0 (min) score

- **Reaching test:**
  score= $score_{reaching}(in\ percentage)\ /\ 10$

  The entire dynamic range (0-10) was maintained:
  0 → 0 (min) score
  100% → 10 (max) score

- **Robot task:**

  <u>Latency:</u>
  score= (-10· $latenza/\ 1000\ ) + 10$

  0-1000 → 10(max)-0(min) score
  > 1000 → 0 (min) score

  <u>T-Target:</u>
  score= (-10· $ttarget/\ 1000\ ) + 10$

  0-2500 → 10(max)-0(min) score
  > 2500 → 0 (min) score

  <u>Attempts:</u>
  score= (-10· $attempts/\ 5) + 10$

  0-5 → 10(max)-0(min) score
  > 5 → 0 (min) score

The same classification was applied for the isometric measures:

Amplitude:
score= $(10 \cdot amplitude) / 0.8$

0-0.8→ 10(max)-0(min) score
> 0.8 → 10 (max) score

AUC:
score= $(10 \cdot AUC) / 15$

0-15→ 10(max)-0(min) score
> 15 → 10 (max) score

1.6 Neurophysiological Recordings

1.6.1 Electrophysiology in freely moving mice

Spontaneous neuronal activity was recorded for 30 minutes in both controls and ischemic animals during freely moving behaviour before surgery and then at 2dpl and 30dpl. The animals were placed in a recording chamber, where, after a one-hour habituation, local field potential (LFP) recording sessions were performed. Signals were acquired by a miniature headstage (NPI, Germany) connected to an amplifier (EXT-02F, NPI). Signals were amplified (10,000 fold), filtered (high pass 0.3; low pass, 100 Hz), digitized with a sampling rate fs = 200 Hz (National Instruments Card) and conveyed to a computer for a storage and analysis.
The power spectrum of the signals was estimated by using the Welch method, in which the signal is split into half-overlapping segments (periodograms) and the spectral density averaged over them. We focused on estimating the power content of the standard neurophysiological spectral bands: δ = (0.5 − 4) Hz, θ = (4.1 − 8) Hz, α = (8.1 − 12) Hz, β = (12.1 −30) Hz, γ = (30.1−50) Hz of the LFP signal (Vallone et al., 2016).

1.6.2 Electrophysiology onto the Robotic Platform

Recordings of local field potentials (LFPs) were performed from both hemispheres during the retraction task in the M-Platform. Signals has been bandpass filtered (3 - 100Hz), amplified and fed to recording system (Plexon). Recordings were carried out before and at 2 and 30 days after MCAO. Neural signals were recorded during the retraction phase, the isometric task and in a resting phase in which the animal was still head-fixed onto the platform and secured with the handle to the slide. These data were processed with NeuroExplorer Software to obtain the power spectral density (PSD) during the retraction task (see above) and the event-related potentials (ERPs) associated with the force peak generation. Regarding the PSD, Fourier analysis was performed during (PostM, orange) and before (PreM, yellow) the generation of a force peak. PSD for each interval was averaged among intervals of the same time and then compared to the PSD obtained in

resting condition, i.e. when the mouse was not generating a force (Empty; magenta **Fig.7).** Moreover, we also distinguished between force peaks generating or not a submovement (above or under the 0.3N friction threshold respectively) (**Fig.7**).

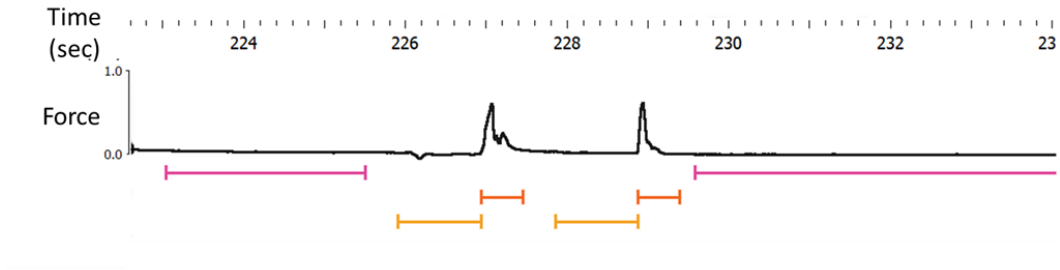

Considered intervals:
Empty = from 0.5s after the end (EVT08) up to 1.5s before the beginning (EVT07) of the force peak (FP);
PostM = from 0 to 0.512 from the beginning of the FP (resulting in a submovement);
PreM = from -1.024 to 0 from the beginning of the FP (resulting in a submovement);
PostNM = as Int_mPost but regarding attempts (no submovement generation);
PreNM = as Int_mPre but regarding attempts (no submovement generation);

Figure 7: Scheme of how the extracted file from retraction task was subdivided into different time intervals

The short time intervals in which the force peaks are generated did not allow us to analyse the delta band. Also, the software allowed to divide the power spectrum in the following spectral bands: θ = (3.9 – 7.8) Hz, α = (7.8 – 11.7) Hz, β = (11.7−29.29) Hz, low γ = (29.29−40) Hz, high γ (62-99.6) Hz.
Regarding the event-related potential (ERP, i.e. the averaged activity around a force peak), neural signals were aligned on the onset of the force peak and latency and amplitude parameters were extracted by means of a Matlab custom-made graphical user interface (GUI). The ERP shape shows an early positive peak (peak1) followed by a negative, more prominent one (peak1-to-peak2) as showed in the Figure below.

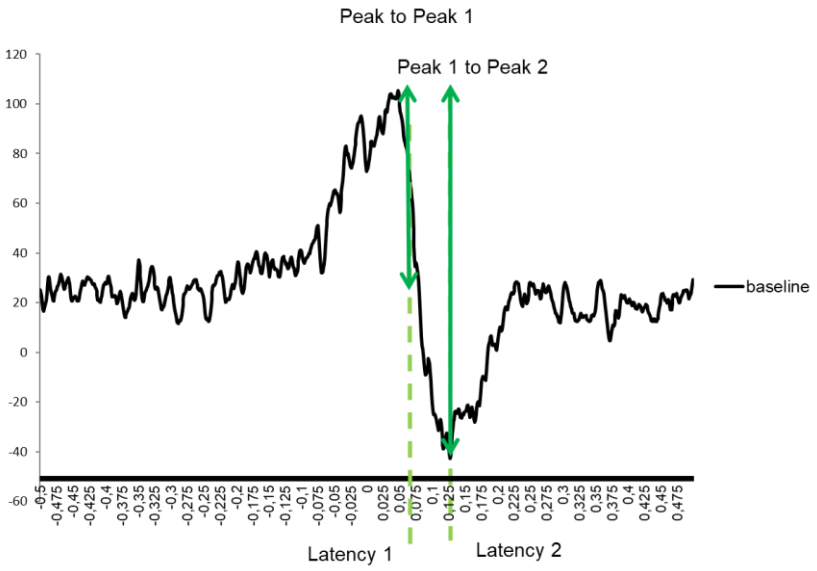

Figure 8: Typical ERP obtained by aligning the LFP traces around the force peak

Experimental design (2)
Transplant of neurons derived from mouse embryonic stem cell (mESCs) and their projection patterns in the stroke brain

All procedures were performed according to the guidelines of the Italian Ministry of Health for care and maintenance of laboratory animals, and in strict compliance with the European Community Directive n. 2010/63/EU on the protection of animals used for scientific purposes. Animal experimentation at the CNR Neuroscience Institute was approved by the Italian Ministry of Health (authorization #129/20002A). All surgical procedures were performed under deep anaesthesia and all efforts were made to minimize suffering of animals.
In order to evaluate the effect of cell transplantation, CD1 mice of the age of two months were employed. Animals were analyzed in healthy condition and after ischemic stroke. In this case, animals underwent photothrombotic infarction and were injected with either neural progenitors or vehicle 3 days after. Then, their behaviour was assessed weekly, starting from day 2 to day 23, with the gridwalk test. The analysis of projection pattern of transplanted cells was performed one month and two months after transplantation.

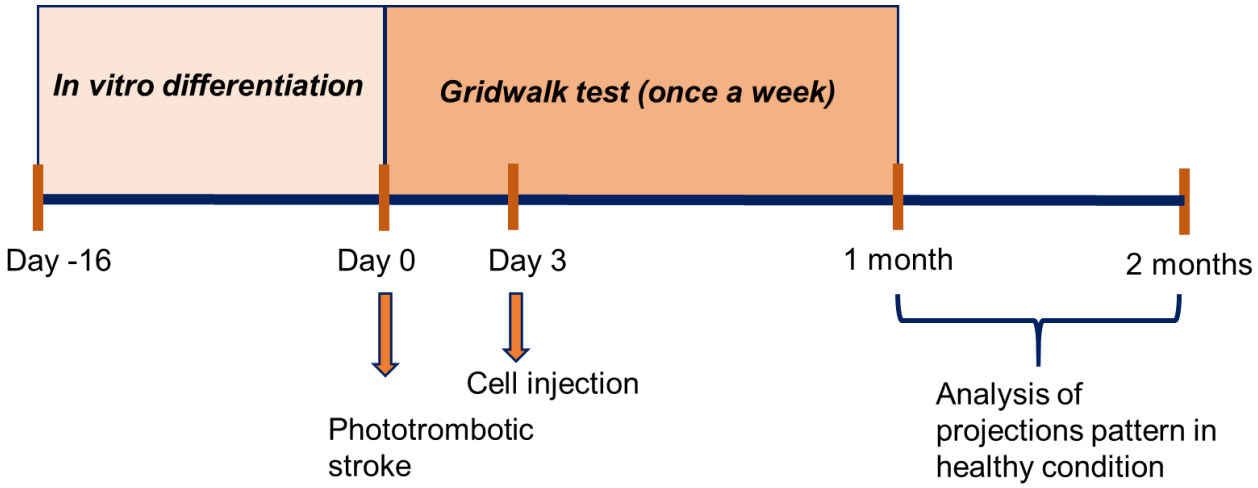

Figure 8**: **Timeline of experimental procedure

2.1 Neuronal progenitors preparation

The protocol of cortical progenitor differentiation is thoroughly described in Terrigno et al. (2018). Briefly, the protocol consisted of three steps. In Step-I, dissociated murine ES cells were seeded and cultured in chemically-defined minimal medium (CDMM) plus 2.5μM Wnt inhibitor (53AH, Cellagen Technology) and 0.25μM BMP inhibitor (LDN193189, Sigma) for 3 days. In Step-II, ES cell were dissociated and seeded on Poly-ornithine (Sigma; 20 μg/ml in sterile water, 24 hours coating at 37°C) and natural mouse Laminin (Invitrogen; 2.5 μg/ml in PBS, 24 hours coating at 37°C). Cells were cultured for 4 additional days in CDMM Plus Wnt/BMP inhibitors, changing the medium daily. In Step-III, cells were dissociated, seeded on Poly-ornithine and Laminin coated wells and kept in CDMM Plus Wnt/BMP inhibitors for four additional days. ES cells were differentiated into isocortical (WiBi 11) and hippocampal (CHIR 8) neurons, as previously described. On day 9, WiBi- and CHIR-treated neurons were

transduced, respectively, with a lentivirus carrying a membrane-bound form of GFP and mCherry for 6 hours at 37°C. To eliminate undifferentiated ES and cycling cells, gamma-secretase inhibitor 10μM (DAPT, Sigma) was added to the culture medium on day 14 and 15 and Aracytin 5μM (AraC) on day 15. After 16 days of differentiation, ES cells were dissociated and resuspended at a concentration of 150'000 cells/μL in DMEM/F12 supplemented with 10% FCS. In co-transplantation experiments, WiBi- and CHIR-treated cells were pooled and injected together in equal proportions.

2.2 Phototrombosis

The photothrombotic lesion was induced as previously described (Lai et al 2015; Alia et al, 2016). Animals were anesthetized with avertin (20ml/kg, 2,2,2 tribromoethanol 1.25%; Sigma-Aldrich, USA), placed in a stereotaxic apparatus and the skull was exposed through a midline incision. Then, Rose Bengal (0.2 ml of a 10mg/ml solution in PBS; Sigma Aldrich) was injected intraperitoneally. After 5 minutes, necessary for the compound to spread systemically, a cold light source (ZEISS CL 6000, Germany) linked to a 20X objective was used to shine light through the intact skull for 15 min. The light was centred on the caudal forelimb area (0.5 mm anterior and 1.75 mm lateral from Bregma, Tennant et al., 2011). At the end of the surgery, the skin was sutured and mice were allowed to awaken from anaesthesia.

2.3 In vivo grafting

Mice were anesthetized with Avertin (20ml/kg, 2,2,2 tribromoethanol 1.25%; Sigma-Aldrich, USA) and placed in a stereotaxic apparatus. Injections were performed within the right hemisphere. The stereotaxic coordinates were defined according to the mouse atlas by Paxinos and Franklin and previous intracortical mapping studies. For injections in normal animals the motor cortex (+0.5mm antero-posterior, +1.75mm medio-lateral from Bregma and 750μm cortical depth), or the hippocampus (-2mm antero-posterior to bregma; 1.5mm lateral and 1.7mm from the cortical surface) were targeted. In the ischemic mice, two injections were performed three days after stroke: one in the centre of the photothrombotic lesion(+0.5mm antero-posterior, +1.75mm medio-lateral from Bregma and 750μm cortical depth, and the other in the perilesional area posterior to the stroke (-1.75mm antero-posterior, +1.75mm medio-lateral from Bregma and 750μm cortical depth).
100,000-150,000 cells/μl were injected per each site using a syringe pump (Legato™ 130, KD Scientific, infusion speed: 0.5μl/min; total volume 1μl).
For the study of functional restoration, an additional group of stroke animals were injected with vehicle (i.e. cells medium) or only cortical progenitors using the same two coordinates as described above. They were used for the behavioural assessment of motor deficits after ischemia using the Gridwalk test.
At the end of the surgery, the skin was sutured and mice were allowed to awaken from anaesthesia.

2.4 Axonal projection imaging and quantification

For immunohistochemistry, brains were collected after transcardial perfusion of deeply anaesthetized mice with PBS (5 min) followed by 4% PFA. Brains were then post-fixed in 4% PFA for 2 hours and then kept 30% sucrose in Phosphate Buffer at 4 °C. Then, they

were sectioned on a sliding microtome (Leica, Germany) into 50 µm coronal sections, which were kept free-floating for further processing. Brain slices were incubated in a blocking solution for 1 hour (10% horse serum; 0,3% Triton X-100 in PBS) before applying the primary antibodies, dissolved at the proper concentration (see below) in 1% horse serum and 0.2 % Triton X-100 in PBS. The following primary antibodies were used: rat anti-mCherry (1:1000, Life Technologies) and goat anti-GFP (1:800, Abcam) (see experiments). After washing, slices were incubated with species-specific secondary antibodies, dissolved in 1% horse serum and 0.2% Triton X-100 in PBS, for 2 h at room temperature. Nuclear staining was performed with (1:500) Hoechst 33342 (Sigma). Coverslips were mounted on glass slides with Vectashield (Vector Labs).
Images were acquired with epifluorescence microscope (Axio Imager. Z2, Zeiss) equipped with Apotome.2 (Zeiss). Z-stack images (2.5-mm z-step size) of three different sections were acquired with the ZENpro software (Zeiss) and then processed with ImageJ 1.48p software. Projection density was calculated as the total number of pixels above threshold normalized on the average area (expressed in millions of pixels) of the graft from which the fibers originated. For detailed experimental procedures see Terrigno et al., 2018.

2.5 Electrophysiological recordings

For electrophysiological analyses of functional integration, we used lesioned mice transplanted with mESC-derived neurons previously transfected with a AAV vector carrying the gene of the transmembrane protein channelrodopsin 2 (ChR2). After 3 months, each animal was anesthetized with avertin, placed in a stereotaxic apparatus and a midline incision was made to expose the skull and the sutures. A 1x1 mm craniotomy centered over the transplantation site was performed in the transplanted hemisphere. The dura mater was left intact and a 4x4mm recording chamber was made using a dental cement (Ivo-clar Vivadent Inc., USA). A ground screw was implanted above the cerebellum, and an aluminium post, used later to head-fix the animal, was cemented onto the skull. Then, the skull over the recording chamber was covered by agarose and Kwik-Cast (WPI) and a thin layer of the dental cement was used to cover the entire exposed skull. Animals were allowed to recover from the surgery and treated with paracetamol (100 mg/kg) for 4 days post-operation in drinking water.

Starting from 2 days following the surgery animals were habituated to stay headfixed in the recording apparatus. At the beginning of the recording session, agarose and Kwik-Cast were removed and the tip of the optic fiber was positioned stereotactically over the injection site. Optogenetic stimulation was delivered by means of PlexBright Optogenetic Stimulation System (PlexonInc, USA) with a PlexBright LD-1 Single Channel LED Driver (PlexonInc, USA) and a 456 nmTable-top LED Module connected to a 200um Core 0.39 NA optic fiber (ThorlabsInc, USA). The maximum emission power of the fiber optic was assessed before each experiment with PlexBright Light Measurement Kit; for each experiment the maximum emission power was about 10 mW (79.55mW/mm2). Stimulation parameters were controlled by a custom-made software developed in LabWindows/CVI (National Instruments, USA) through a USB DAQ board (NI USB-6212BNC, National Instruments, USA). Neuronal activity was recorded in the perigraft tissue by means of 16 channels linear probes (NeuroNexus, USA), connected to the OmniPlex D Neural Data Acquisition System (PlexonInc, USA). Wide Band (WB) signals were acquired at 40,000 Hz, amplified 1K, and band-pass filtered (0.03–12,000 Hz). Continuous spike signals (SPKC) were computed online by band-pass filtering the WB signals (0.03–300 Hz and 300–10,000 Hz, respectively) and referred to the ground electrode in the cerebellum. Multi-unit activity was computed

offline by further processing the SPKC signals using the OFFLine Sorter Software. With this configuration, we recorded neuronal activity stimulating grafted neurons with 100ms light pulses at 90% of maximum light power. Stimulations were repeated 50 times for each power intensity, spaced by 5 s. In order to verify the post-synaptic nature of the recorded spiking activity, the AMPA receptor antagonist NBQX (Tocris, UK) was topically applied over the craniotomy, without removing the electrode. Data were analyzed offline with Offline Sorter and NeuroExplorer software (PlexonInc, USA) and with custom made Matlab User Interfaces (Matlab, Matworks).

3- Statistical Analysis

Statistical analysis was performed using Sigmaplot 12.0 software (Systat Software Inc., Chicago, IL), considering the value of significance at $P < 0.05$.
For comparisons between different groups and between different time points, a Two-Way Repeated Measures ANOVA was used followed by appropriate post-hoc tests. For comparison of a single measure, Student t-test was used. For comparison between the ipsilesional and contralesional side of each animal, a paired t-test was used. The analysis of correlation was made by using the linear regression model with the Matlab fitlm function. All statistical analyses were performed on raw data (alpha value 0.05), if not differently indicated. The different number of animals reported in the measured data was related to technical and/or methodological issues (histological tissues, animals death and other). In all graphs, data are reported as mean ± standard error. Graphs were obtained using GraphPad Prism6.

Results

Part 1

Assessing anatomical and behavioural biomarkers to predict motor recovery after MCAO-induced stroke

1- Anatomical alterations after MCAO-induced stroke

A model of cerebral focal ischemia (permanent Medial Cerebral Artery Occlusion, MCAO) was implemented to investigate the mechanisms underlying spontaneous motor recovery. First, we characterized anatomical changes that occur 30 days after the lesion. In particular, we assessed the targeted cortical areas and the volume of the lesion via immunohistochemistry for a neuronal and an astroglial marker, i.e. NeuN and GFAP respectively.
The ischemic tissue included mostly somatosensory areas, whereas motor areas, including the CFA, were only partly affected or represented a perilesional site (**Fig. 1A-C**). In fact, a consistent variability in terms of lesion location along the anteroposterior axis was present (**Fig. 1D**). At 30 days post-lesion (dpl) the ischemic tissue was completely lost while in the perilesional regions NeuN signal could still be detected, but neurons were shrunken (**Fig.1E**). An intense astrogliosis was present in a large portion of the ipsilesional hemisphere, specifically along the lesion contour, while the lesion itself was devoid of astrocytes. In order to exactly quantify the extent of the lesion and the involvement of relevant functional areas (CFA), custom-made histological masks were adapted on acquired NeuN-immunolabeled brain slices.
To obtain a reliable value of the lesion volume, ischemic area of each single brain slice was normalized for its ipsicortical shrinkage as described in Materials and Methods. Briefly the normalized area of the lesion was obtained as follows:

$$\textit{Normalized Area of the Lesion} = \frac{\textit{Measured Area of the lesion}}{1 - \textit{Cortical Shrinkage}}$$

The cortical shrinkage corresponds to the contraction of the ipsilesional cortex respect to a reference normalized for the brain dimension of each animal.

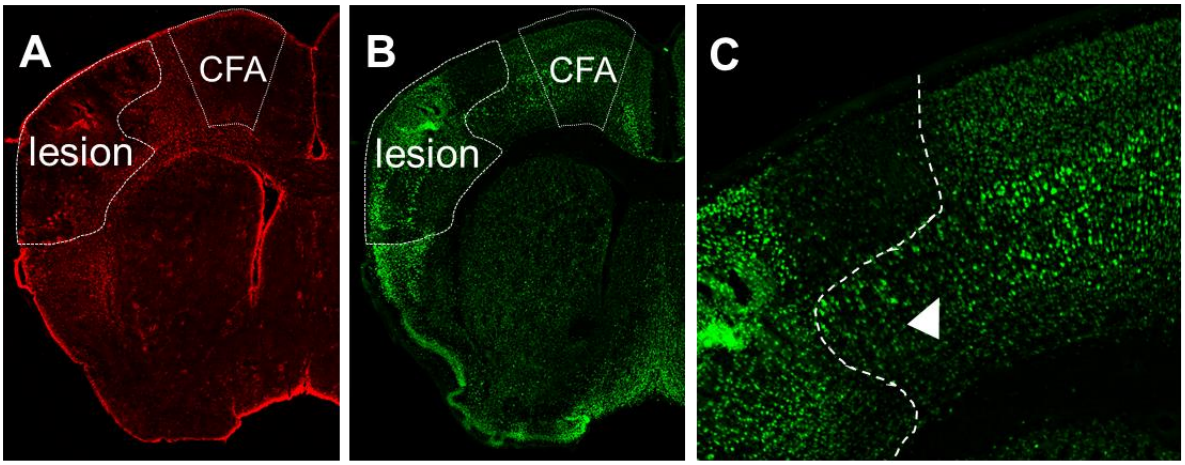

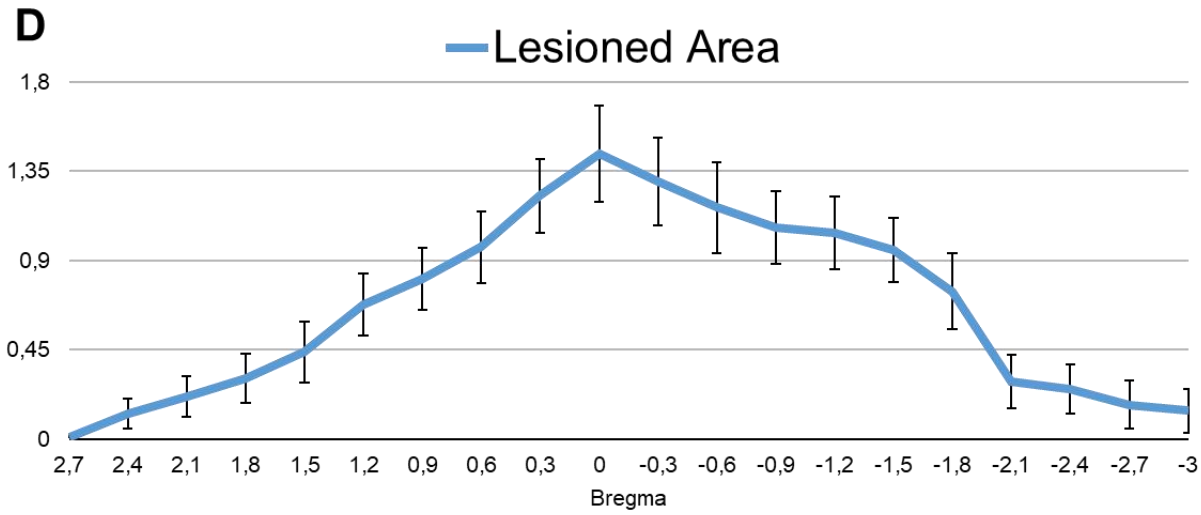

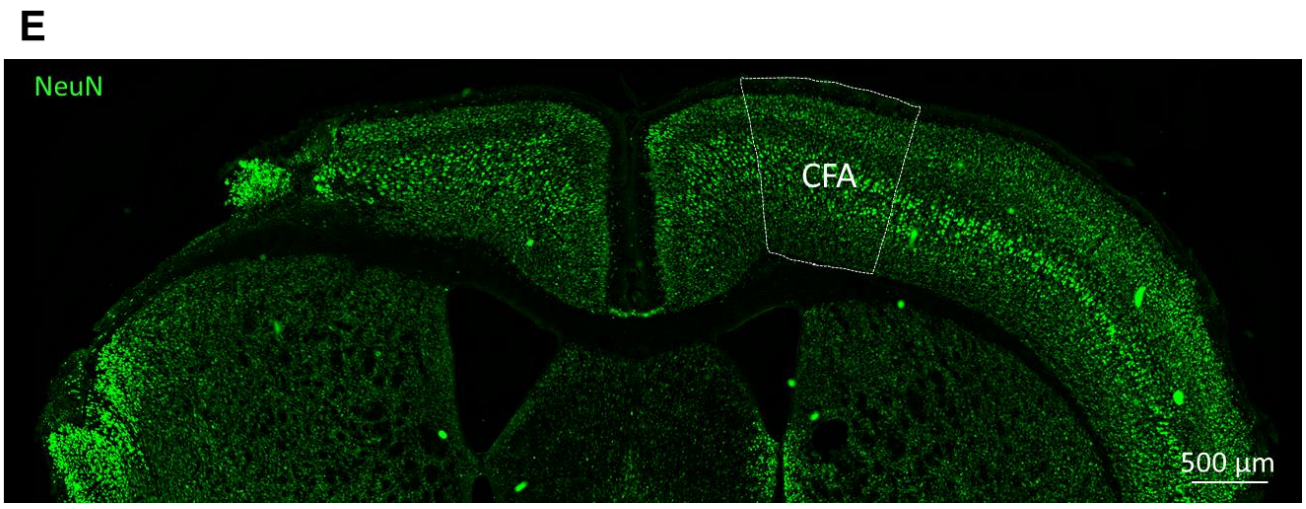

***Figure 1**: **Histological characterization of MCAO lesion**. (**A)-(C)** NeuN and GFAP immunohistochemistry at 2dpl. (**C)** Detail of the lesion. Dashed line indicates the border between the ischemic tissue (left) and the healthy tissue (right). Arrowhead indicate the presumptive penumbra. **(D)** Representation of lesion extension at 30 dpl along the anteroposterior axis. Data represented mean±SEM (n=15). **(E)** Immunohistochemistry 30 days after MCAO induction. CFA is drawn in the contralesional site according to Alia et al. (2016)*

Among animals (n=15) the lesion extended on average approximately from 2.4 mm anterior to Bregma to 2.1 mm posterior to Bregma, had a peak of lesioned area around Bregma suture and had a volume of 4.00 ± 0.625 mm^3. However, the high variability of the lesion localization can be easily appreciated by comparing the same brain coronal slice from different animals that underwent MCAO (**Fig.2**).

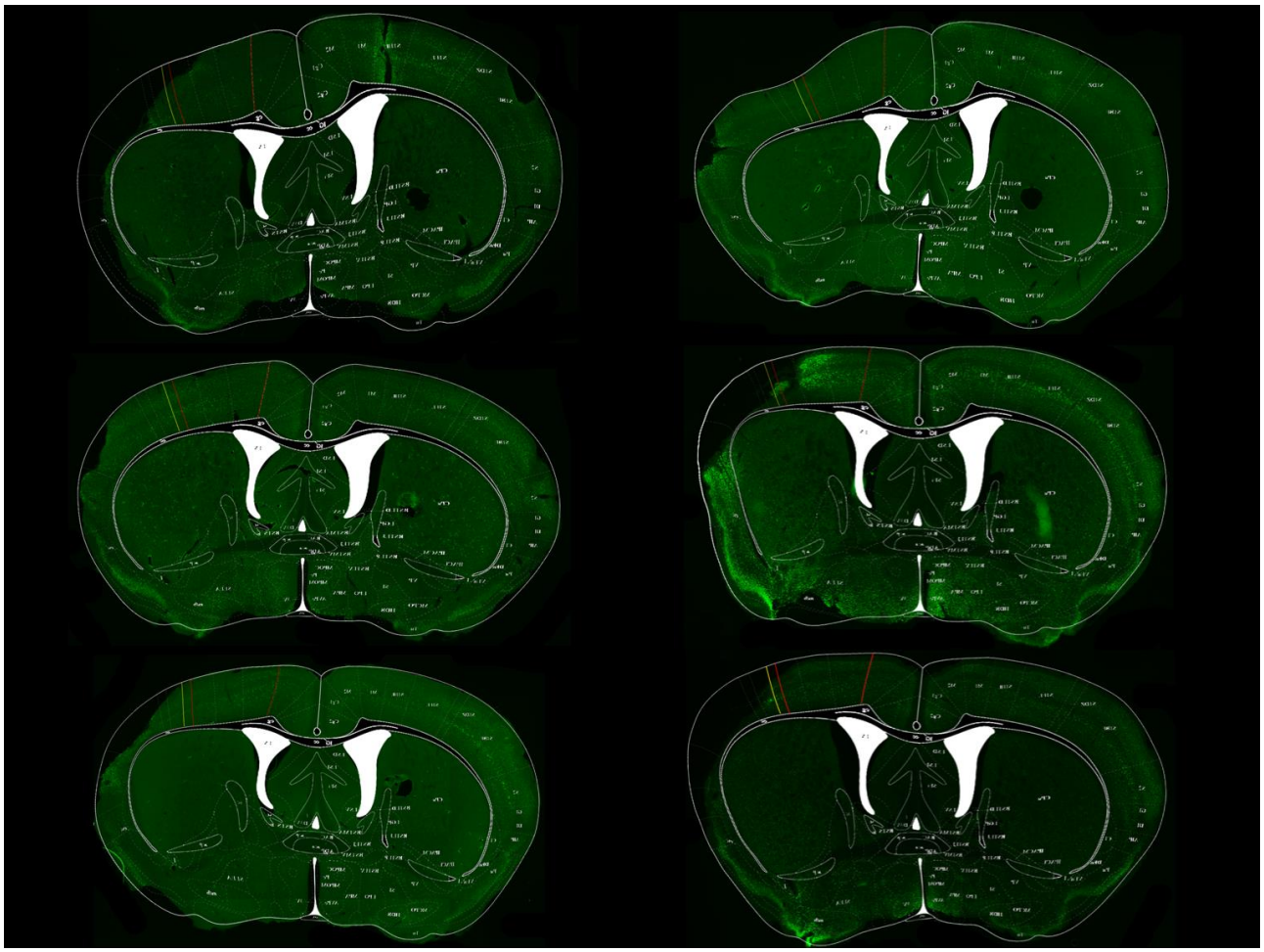

Figure 2: NeuN staining of at bregma level in six different animals. The same mask was superimposed on each slice to highlight Caudal Forelimb Area location.
The same mask on the same anterioposterior coronal section of different mouse after MCAO highlight the high variability of the extent of the lesion and its location. Moreover, the adapted mask localize the CFA despite the slice distortion.

The distortion caused by the shrinkage is an important parameter not only for normalizing the volume of the lesion, but can itself contribute to the neural impairment due to compression of the tissue.
Thus, it could be taken into consideration as a possible biomarker. On average the lesion shrank the ipsilesional cortical area of 19,36 ± 2,25 %, and the contraction of the neural tissue was tendentially greater around Bregma where the area of cortical damage is larger (**Fig.3A**). As expected, among animals the percentage of ipsicortical shrinkage, strongly and

positively correlated with the extent of the lesion volume (R=0.778716; p= 0.000625) (**Fig.3B**). Indeed, after a stroke, the ischemic area is rapidly filled with scar tissue, that, following the reduction of the initial edema, tends to shrink, leading to the stretch of the perilesional tissues and the eventually worsening of the initial damage.

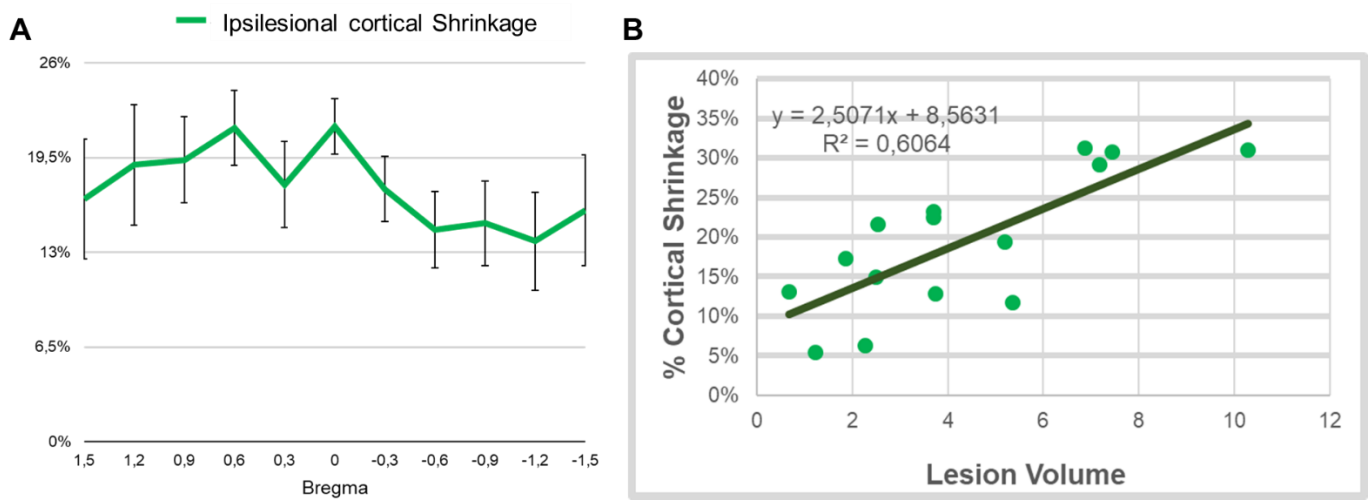

Figure 3: Ipsilesional cortical shrinkage at 30dpl. A) *Percentage of ipsilesional cortex shrinkage along the anteroposterior axis. Data represent mean ± SEM (n=15).* ***B)*** *Correlation among cortical shrinkage and lesion volume (linear regression R=0.7787 and p=0.000625 (n=15). The graph shows its* R^2 *and the linear equation.*

1.1 Caudal Forelimb Area impairment after MCAO

As described above, the ischemic injury hit mostly somatosensory areas, whereas motor areas, including the CFA, were only partially affected since they frequently reside in the perilesional area. A lesion in the CFA is supposed to directly affects the motor performance of the contralateral forelimb. However previous studies highlighted the great potential of the perilesional tissues to partially regain the lost motor function trough the remapping of the surrounding motor cortex (Alia et al. 2016). Given the importance of the CFA in the voluntary movement of the contralateral anterior limb and in recovery-related plasticity after stroke, we set up a method to quantify the percentage of the damaged CFA, to evaluate its possible exploitation as a biomarker to predict recovery. This method allowed to obtain the exact location, area of the lesion and the distortion that it induces on the nearby tissues (for details, see Materials and Methods). Among 15 animals that underwent MCAO, only 5 of them showed a significant (percentage of lesioned CFA > 5%) ischemic damage in the CFA (**Fig.4A**). The same five animals had also the most extended lesions. Among these animals (n=5) 12.86% ± 1.95% of the CFA was lesioned, with a greater damage posterior to Bregma suture (**Fig. 4B**). Moreover, these 5 animals had also a cortical shrinkage that was statistically greater than animals with an intact CFA (t-test, p= 0.0012), probably due to the extension of their lesions (**Fig.4C**). Additionally, the percentage of lesioned CFA positively correlated with the lesion volume (R=0.934 and p=0.02) (**Fig. 4D**).

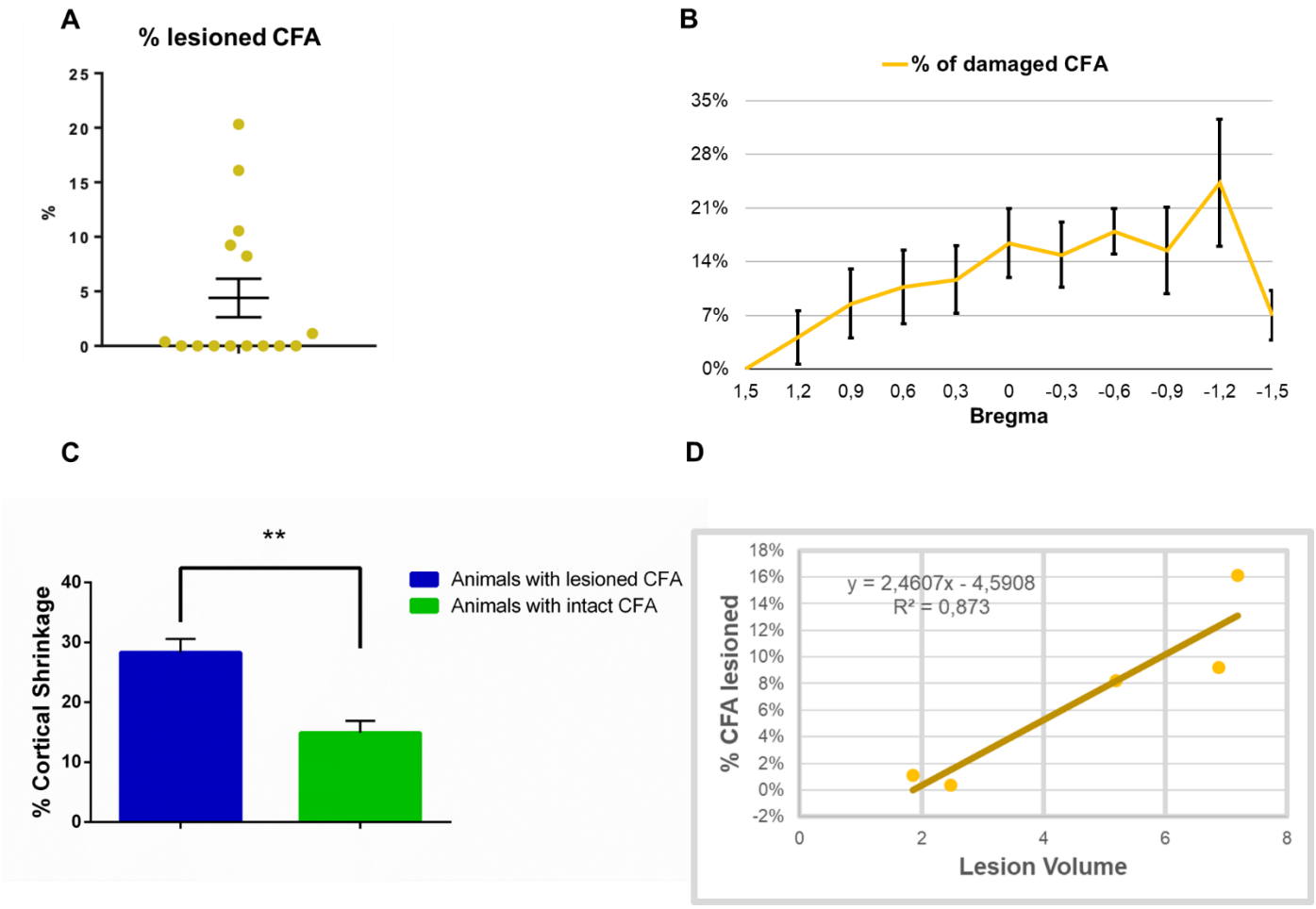

***Figure 4**: **CFA lesion on 30dpl histological brain slice. (A)** Percentage of lesioned CFA among MCAO mice (n=15). **(B)** Percentage of damaged CFA along anteroposterior axis in animals that reported a consistent (>5%) damage in CFA. Data represented mean ± SEM (n=5). **C)** Percentage of cortical shrinkage among animals with a robust CFA damage (n=5) and non CFA lesioned mice (n=10). (t-test; ** p=0.0012.) **D)** Correlation between the percentage of lesioned CFA and lesion volume (linear regression R= 0.934 and p=0.02). The graph shows its R^2 and the linear equation.*

Another possible biomarker that could predict motor recovery in absence of a direct ischemic damage of the CFA is the shrinkage of the CFA after MCAO. We can, therefore, hypothesize that a strong distortion of this area could affect its function, leading to a dampening of recovery after MCAO. Indeed, the percentage of the shrinkage in the CFA was highly variable among our population (n= 15), with an average of 9.11% ± 12% SD (**Fig.5A**).

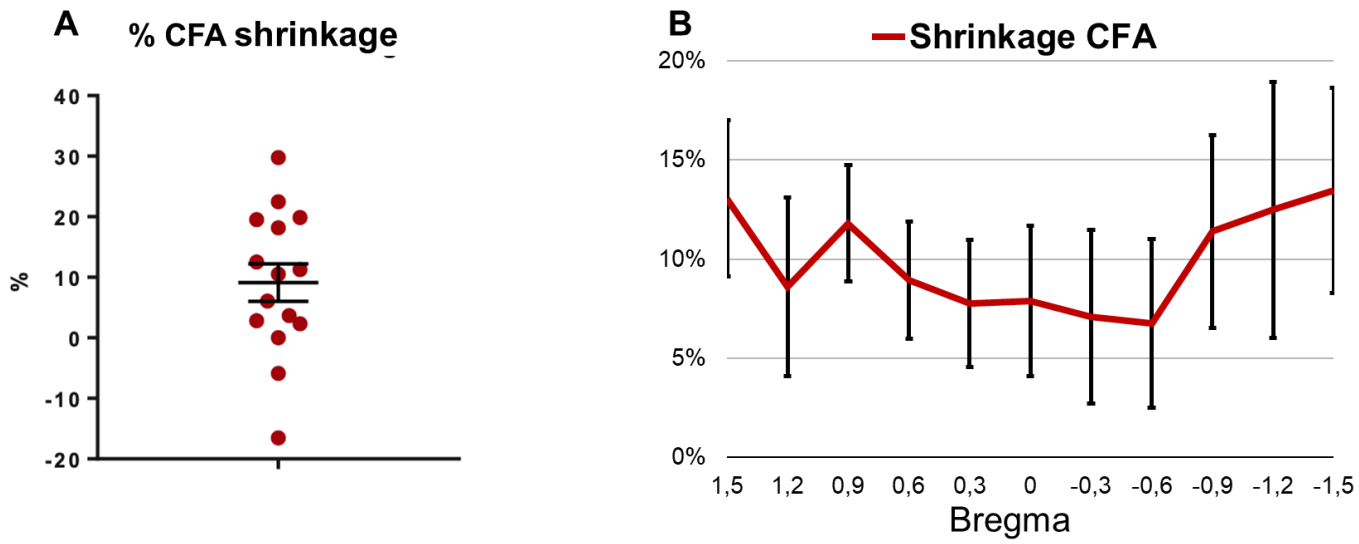

Figure 5: CFA shrinkage on 30 dpl histological slices. A) *Percentage of CFA shrinkage among MCAO mice. Data represent mean ± SEM (n=15).* ***B)*** *Percentage of CFA shrinkage along anteroposterior axis among MCAO mice (n=15)*

Similar to what happens with cortical shrinkage, animals with more extended lesions that further involve the CFA, have higher compression of the CFA volume. The CFA shrinkage in CFA lesioned animals was generally different from animals in which the CFA was not affected, even if not significant higher (t-test; p=0.08) (**Fig.6A**). Indeed, also the shrinkage of the CFA volume, like the cortical shrinkage, positively correlates with the volume of the lesion, but with a lower coefficient of correlation (R= 0.564 and p= 0.0286) (**Fig.6B**). This could be explained by the high variability in the position of the lesion and its volume, that can affect the distortion of the CFA in different ways.

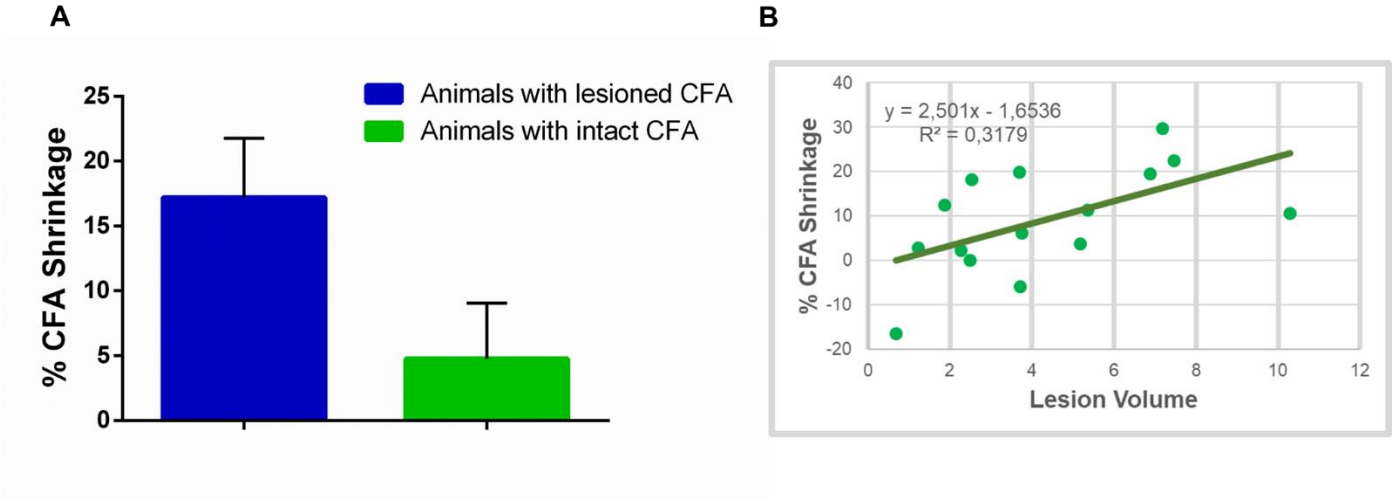

Figure 6: CFA shrinkage comparison and correlation A) *Percentage of CFA shrinkage among animals with a lesioned (n=5) or intact (n=10) CFA. (t-test; p=0.08).* ***B)*** *Correlation among cortical shrinkage and lesion volume (linear regression R=0.564 and p=0.0286) (n=15). The graph shows its R^2 and the linear equation.*

1.2 Decrease of neuronal density in ipsilesional CFA

To better characterize the anatomical changes in the CFA, the neuronal density inside this area was analyzed after MCAO. In order to obtain a reliable value, masks were superimposed on 30dpl brain slices images to highlight the CFA. Then, we applied a protocol to count neurons automatically (see Materials and Methods) and we found a significant difference in neuronal density between the CFA on the ipsilesional side (normalized for its cortical shrinkage) and the CFA on the contralesional side of mice that underwent MCAO (paired t-test p= 0.0472) (**Fig.7**). Moreover, a decrease in the density of neurons can be also appreciable if we compared animals with a robust lesion on the CFA respect to intact CFA animals (unpaired t-test p = 0.0517, data not shown). These data showed a quantitative change in the primary motor cortex that was present even in the absence of a direct lesion to the CFA, suggesting a possible explanation for the motor impairment in animals that appear to have an intact CFA.

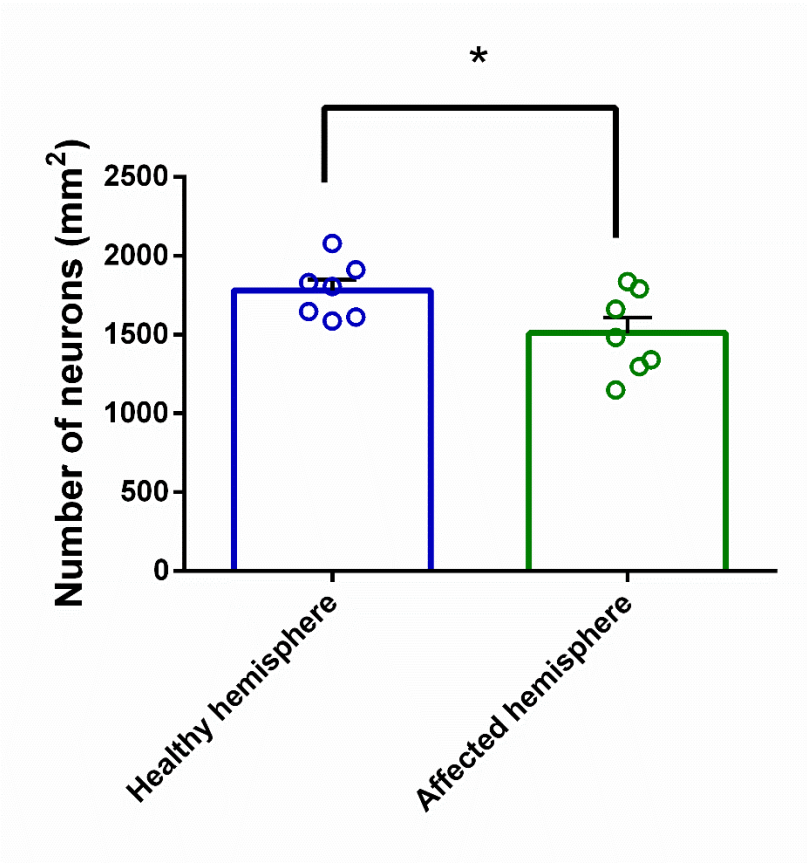

***Figure 7: CFA neuronal density**. Number of neurons per mm^2 among ipsilesional and contralesional CFA. (paired t-test; p= 0.0426; * p<0.05) (n=7)*

1.3 White Matter integrity

Today, the most robust imaging biomarkers to predict motor recovery and outcome in humans after stroke are measures of white matter integrity of the corticospinal tract (CST). To study this aspect on the murine MCAO model, the integrity of the white matter was measured in the internal and external capsule on histological slices of the brain obtained 30 days after the induction of the lesion. The white matter was stained with Luxol fast blue and

measurements were performed on coronal brain slices at two anterior-posterior levels (AP1 and AP2), i.e. 0.5mm (AP1) and 1mm (AP2) posterior to the Bregma suture (see Materials and Methods).
The area of stained white matter in the ipsilesional and contralesional Internal and External capsules was measured for each animal of the MCAO group. A statistically significant difference was found for the external capsule for both the anatomical points and also for the internal capsule (Paired t-test p<0.001) (**Fig.8A-B**). The same analysis was also conducted in a small subgroup of control animals (sham surgery) in order to confirm that no changes in the integrity of the white matter were present (data not shown p=0.294).

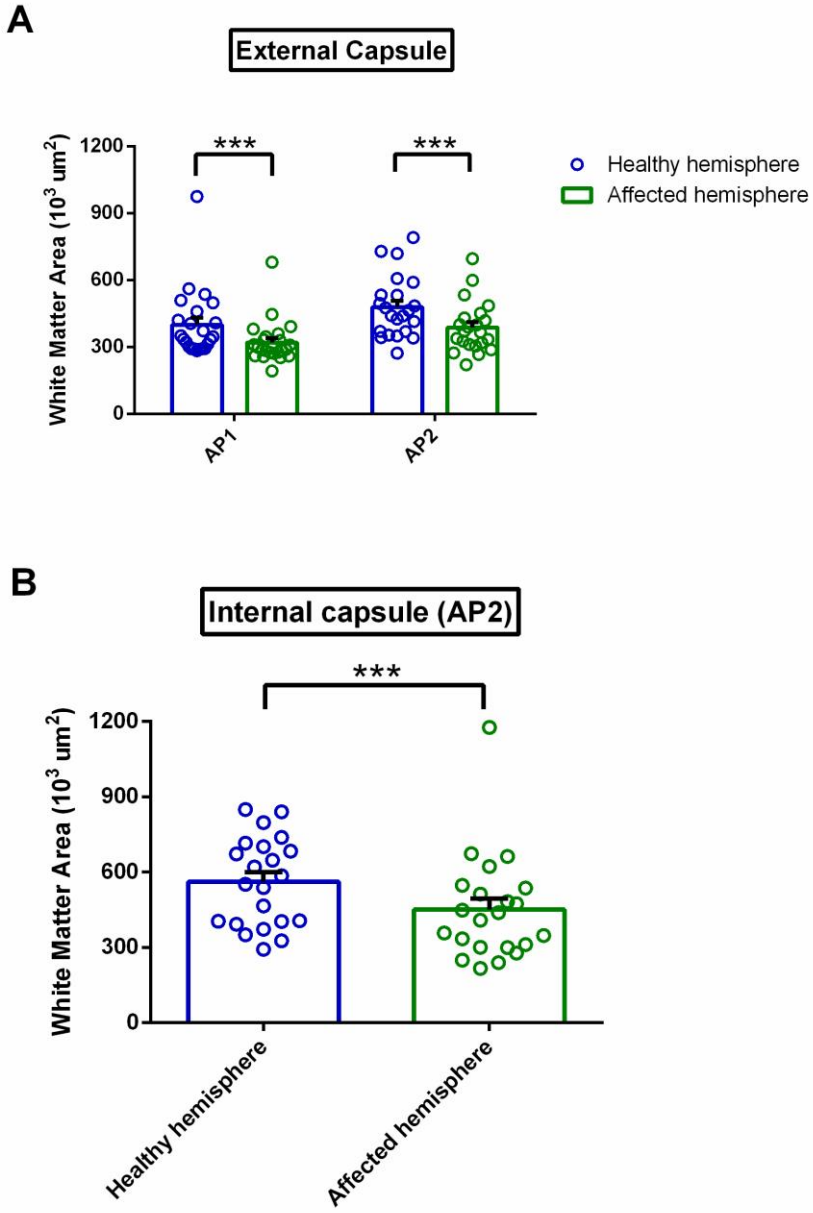

***Figure 8: White Matter Integrity in MCAO group**: (**A)** White matter area of External Capsule at AP2 (n=23) and AP3 (n=22) and **B)** White matter area of Internal Capsule at AP3 (n=22). A significant decrease of white matter area was found in the affected hemisphere with respect to healthy side in every anatomical points considered. (Paired t-test with Wilcoxon signed rank test). *** p<0.001. Each point represents one animal. Histograms indicate mean ± SEM*

2- Post-stroke behavioural deficits

2.1 Performance in general and fine motor tests

In order to assess the deficit induced by MCAO lesion at behavioural level, two main motor tests were exploited, skilled reaching test and GridWalk test, to evaluate, respectively general and fine anterior movements.

The skilled reaching test allows the analysis of fine motor performance, i.e. the grasping of a food pellet. To examine this, animals were pre-trained for 2-3 weeks pre-stroke, when the baseline performance was measured and then tested again after 2dpl (acute phase), and 30 dpl (chronic phase). During the scoring procedure, “correct” movements and errors were evaluated. In addition, errors were further divided into “dropped”, “displaced” and “missed” (see Materials and Methods). As expected, after the lesion, there was a significantly decrease in the number of “correct” movements at 2dpl in MCAO group (n=25), whereas the sham group (n=13) did not show significant differences (Two-Way RM ANOVA $p<0.001$ from baseline and between groups) **(Fig. 9A)**. At the behavioural level, it has been observed that lesioned animals started to generate “clumsy movements” in which the forelimb was barely extended beyond the testing chamber window, preventing animals to grasp the pellet and that were thus classified as “missed”. It is reasonable to believe that this “missed” category represented the most severe type of error, given that in this case the animal is not even able to reach or displace the pellet. Indeed, percentage of errors and in particular the proportion of ‘missed’ movements was significantly increased after stroke and remain different from baseline performance up to 30dpl (Two-Way RM ANOVA $p<0.001$ from baseline and between groups) (**Fig. 9B**)

The sham group did not show significant differences. Given that motor performance in the skilled reaching task appeared quite variable even within the same animal, we used a cumulative score in which a fixed value is attributed to each class of movements: 1 for “correct”, 0.6 for “dropped”, 0.3 for “displaced” and 0 for “missed” (see methods). This scoring method revealed more robust than just considering the number of ‘correct’ and we observed a functional decrease at 2dpl with a spontaneous recovery at 30dpl (Two-Way RM ANOVA $p<0.001$ from baseline and between groups) (**Fig. 9C**).

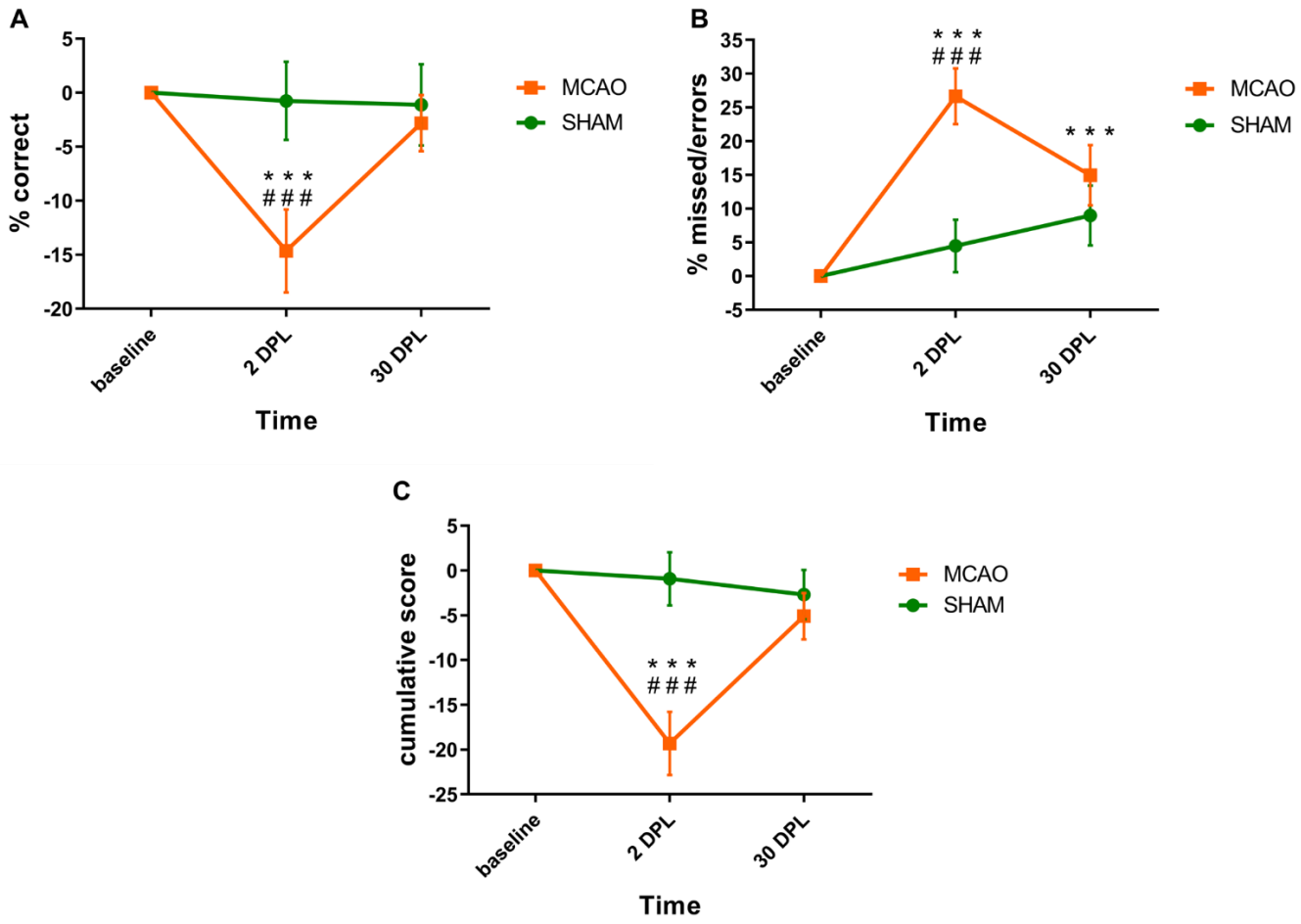

Figure 9: Analysis of skilled reaching test performance. A) *Percentage of 'correct' movements among MCAO (n=25) and sham (n=13) animals. The observed decrease was significant at 2dpl.* ***B)*** *Proportion of "missed" over the total number of "errors". We observed a significant worsening of the performance within the MCAO group that last until 30 dpl, while a worsening for sham animals is not present.* ***C)*** *Cumulative score. The MCAO group showed a robust functional decrease at 2dpl that was significantly different also from sham group. A spontaneous recovery was present at 30dpl. For all panels, Two-way RM ANOVA, followed by Holm-Sidak method. (*) represents significant difference from the baseline, *** p < 0.001. (#) represents significant difference from the sham group, ###, p < 0.001). Data were normalized on baseline value and represented as mean ± SEM.*

Another way used to assess motor damage of all the four limbs is the GridWalk test in which an animal is placed on an elevated grid with openings (see Materials and Methods). Animals without brain damage usually put their paws precisely on the wire frame to hold themselves while moving along the grid. Each time a paw slips through an open grid, a "foot fault" is recorded. Sham animals generally show few foot faults for both forelimbs. The percentage of foot faults in both the affected (i.e. contralateral to the lesion) and healthy (i.e. ipsilateral) forelimb was evaluated. After the induction of MCAO, there was a significant deficit in the use of the affected forelimb at 2dpl (Two-way RM ANOVA $p < 0.001$ from baseline and between groups), which did not recover up to 30dpl. A significant difference was also present with respect to the sham group for both time points considered (**Fig. 10A**).
When looking at the healthy forelimb, an unexpected progressive worsening of the performance was observed in the MCAO group already at 2 dpl with a further aggravation at 30 dpl (Two-Way RM ANOVA $p<0.001$ from baseline and between groups). This effect was instead completely lacking in Sham group (**Fig. 10B**). A similar decrease in the dexterity

of the healthy forelimb has been observed in the clinic (F. Molteni, personal communication). Hence, the MCAO model provides a measurable deficit in the GridWalk test, however it induces also some other features, e.g. the deficit in the unaffected side, that makes it truly similar to the clinical condition.

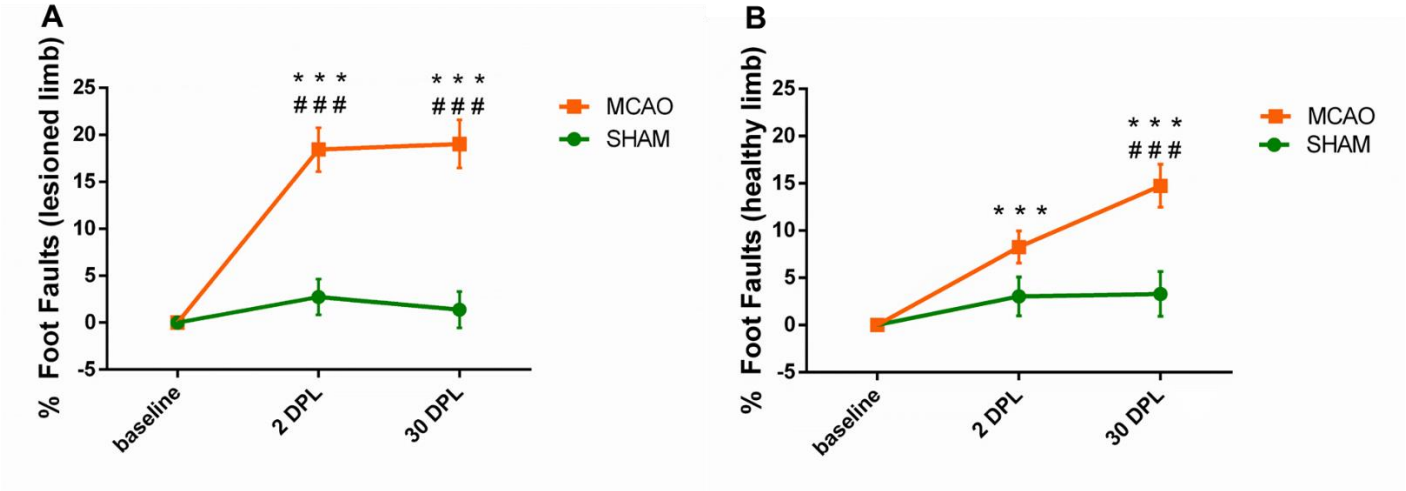

Figure 10: Analysis of gridwalk test performance. A) *Percentage of affected limb foot faults for MCAO (n=25) and sham group (n=14). The deficit in MCAO group was significant for all the time points and differed significantly from the sham group* ***B)*** *Percentage of healthy limb foot faults for MCAO (n=25) and sham group (n=14). The deficit in MCAO was significant for all the time points and differed significantly from the sham group at 30 dpl. For all panels Two-way RM ANOVA, followed by Holm-Sidak method. (*) represents significant difference from the baseline, *** p < 0.001. (#) represents significant difference from the sham group, ###, p < 0.001. Data were normalized on baseline value and represented as mean ± SEM.*

2.2 MCAO-related motor impairments tested on the M-platform

In order to add a quantitative and reliable measure of the MCAO-induced motor deficit, we exploited a robotic platform that has been developed in our lab, i.e. the M-platform. This device (i) provides a quantitative assessment of forelimb flexion movement, (ii) is sensitive to detect deficits in performance after a localized cortical infarct, and (iii) measures functional improvements during post-stroke training (Spalletti et al. 2014, Pasquini et al. 2018). Mice were allowed to habituate to the setup for one week, before measuring baseline performance. Animals were tested again onto the robotic platform at 2, and 30 days post-lesion. Four different parameters were analysed: latency, t-target, submovements and attempts (**Fig. 11**) (see Materials and Methods).
By using this protocol, we observed that while in the sham group there was a progressive improvement, probably linked to learning, in the MCAO group a worsening of the motor performance was noticed. In particular, the difference between 2dpl and baseline performance was significantly higher in MCAO animals than in sham for latency, t-target and attempts. Indeed, the MCAO group took longer to start performing the task (Two-way RM ANOVA; p= 0.015 from baseline) (**Fig.11A**), spent more time to accomplish the retraction task (Two-way RM ANOVA; p= 0.001 from baseline and p=0.04 from sham group) (**Fig.11B**) made more attempts (abortive tries not resulting in a movements) at 2dpl showing an improvement trend a 30dpl (Two-way RM ANOVA; p= 0.006 from baseline and p=0.028 from sham group) (**Fig.11C**). The number of submovements did not show a significant change in

both groups (Two-way RM ANOVA; p>0.05) (**Fig.11D**).

The M-platform allowed also to perform an isometric task (45s of duration), in which the forelimb is kept extended and the amplitude of the exerted force and its relative area-under-the-curve (AUC) of each peak were measured with the idea of evaluating the maximum force of the animal (**Fig.12A-B**). Even in this case, sham animals tended to improve their performance in terms of force peak amplitude, even though they worsened at last time point. This improvement was completely abolished in MCAO group where their performance was reduced soon after the lesion (2dpl) and remained significantly different until 30dpl (Two-way RM ANOVA; p=0.007 from baseline). Coherently, the AUC in lesioned animals significantly decreased 2 days post-stroke (Two-way RM ANOVA; p=0.005 from baseline) and remained significantly affected up to 30dpl (Two-way RM ANOVA; p=0.005 from baseline).

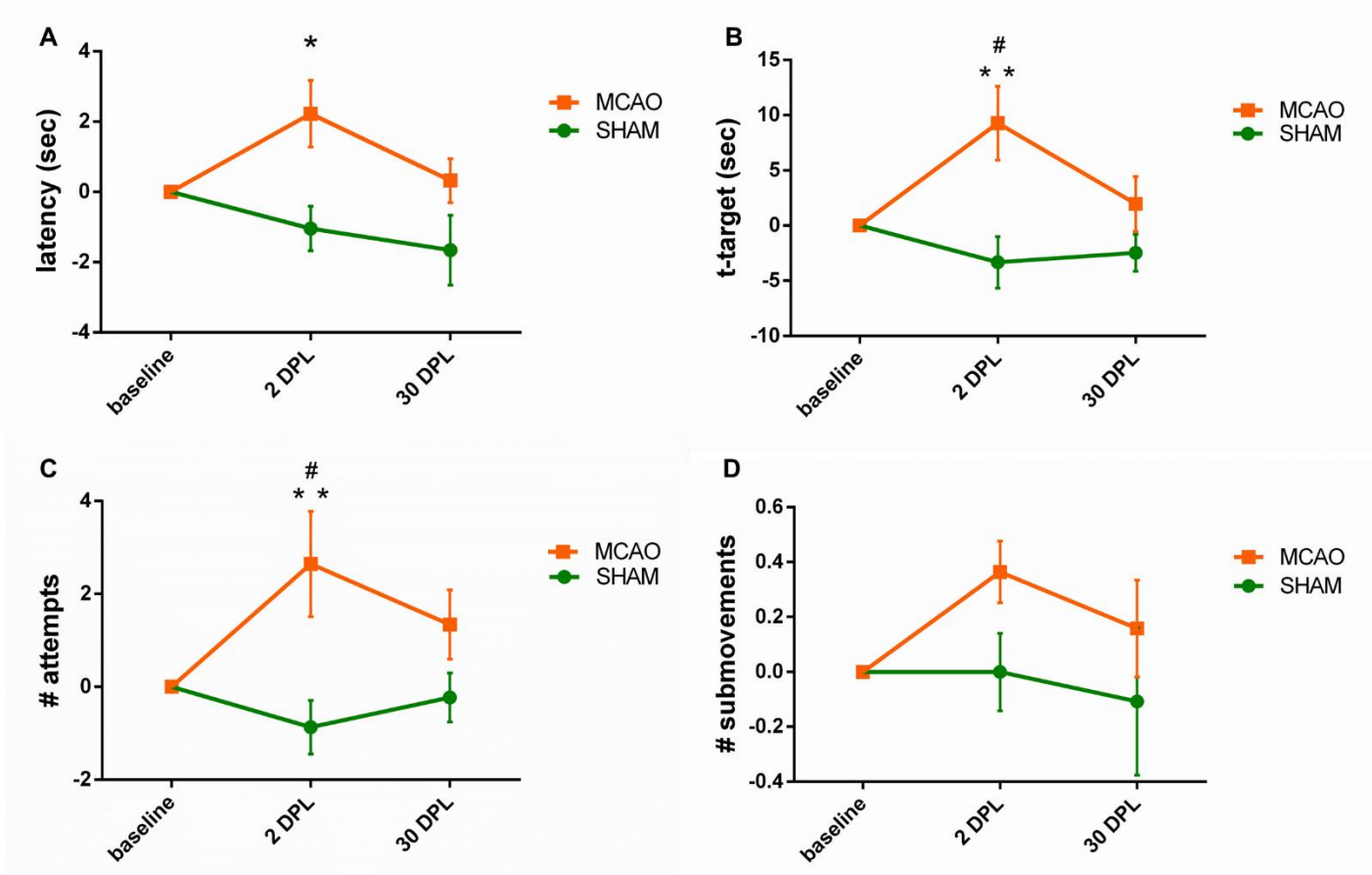

***Figure 11**: **Motor performance onto the robotic platform. A**) Latency**; B)** t-target**; C)** Attempts; **D)** Submovements**. (Two-way RM ANOVA, MCAO group (n=18) vs sham animals (n=13) followed by Holm-Sidak method). (*) represents significant difference from the baseline, * p < 0.05; ** p < 0.01. (#) represents significant difference from the sham group, # p < 0.05. Data were normalized on baseline value and represented as mean ± SEM.*

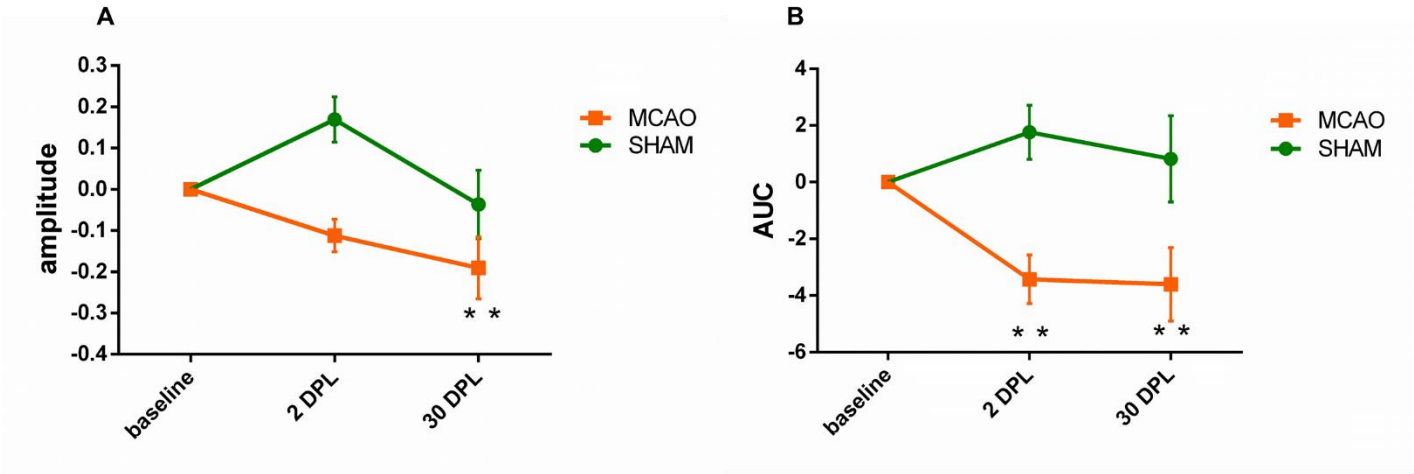

***Figure 12: Performance in the isometric task**. **A)** Amplitude of exerted force and **B)** AUC during the isometric task (Two-way RM ANOVA, MCAO group (n=18) vs sham animals (n=13) followed by Holm-Sidak method). (*) represents significant difference from the baseline, ** p < 0.01. Data were normalized on baseline value and represented as mean ± SEM.*

2.3 Establishing a novel clinical-like motor score

To combine all behavioural results, a global motor score was established, including all motor tests together for the different time-points considered. This was done to mimic clinical scales such as the Fugl-Meyer which typically assess motor function by the sum of the scores in different tasks. To this end, performance relative to each behavioural tests (Gridwalk, reaching, M-platform) was converted in a range from 0 to 10 (see Materials and Methods). The differences between sham (n=14) and MCAO groups (n=26) were showed as a radar plot, where each item (i.e. parameter obtained in a specific task) is represented on one axis. We observed a retraction of the orange area in MCAO group due to loss of motor function, while the green area relative to sham group remained almost unchanged over time (**Fig.13**).


baseline
attempts
t-target
amplitude
latence
AUC
reaching
gridwalk
0
1
2
3
4
5
6
7
8
9
10
MCAO
SHAM


2 days
attempts
t-target
amplitude
latence
AUC
reaching
gridwalk
0
1
2
3
4
5
6
7
8
9
10
MCAO
SHAM

Figure 13: Global motor score*: All motor tests were included together and presented for all the three time points considered (baseline, 2 days after lesion, 30 days after lesion)*

Then, for each animal, we calculated the total score as a sum of values for each sub-task, mimicking what is done with clinical scales for humans. A significant decrease of the overall motor function was found in the MCAO animals at 2dpl (Two-Way RM ANOVA $p<0.001$ from baseline and between groups) with a trend of improvement observed at 30dpl that remained significantly different from baseline (Two-Way RM ANOVA $p=0.019$ from baseline). To the contrary, sham animals showed no longitudinal differences in the overall motor performance (**Fig.14**).

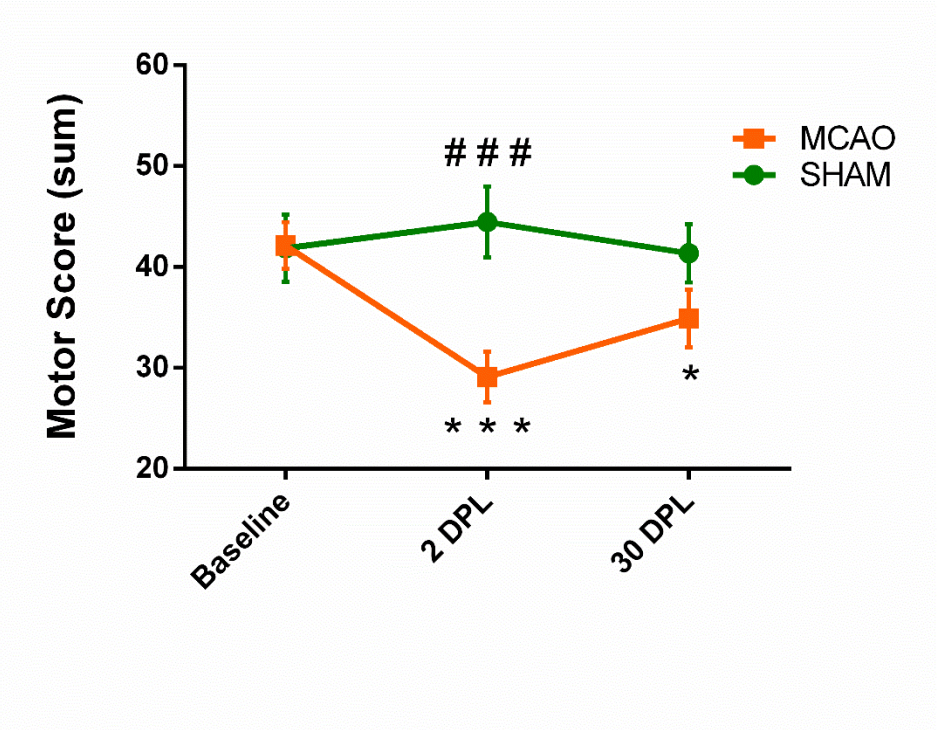

Figure 14: Motor score sum: *the total score obtained from the sum of each motor tests indicated a significant decrease in MCAO animals (n=22) at 2dpl that was not present in sham group (n=12). (Two-way RM ANOVA, followed by Holm-Sidak method). (*) represents significant difference from the baseline, *** p < 0.001, * p < 0,05. (#) represents significant difference from the sham group, # # #, p < 0.001. Data were normalized on baseline value and represented as mean ± SEM.*

2.4 Individual variability in recovery of MCAO stroke animals

As first step, since our starting goal was to establish a stroke model characterized by a large variability in order to mimic the human stroke condition, we evaluated the individual motor recovery of animals in our MCAO groups (n=20). Thus, we considered the global motor score including the performance of all used motor tests. We found that after normalizing performance on the baseline values, the acute motor function (assessed at 2 days after stroke) was greatly variable among animals showing a range of motor deficit going from a really mild (acute performance close to 100%) to a severe (close to 25%) impairment **(Fig.15A)**. Moreover, considering the chronic time point (i.e. 30dpl), we found a relevant variability in terms of recovery. In fact, some mice increased their global motor score with respect to the acute performance (2dpl). **(Fig.15A green lines)** while other mice did not recover or even worsened their motor function in the chronic phase **(Fig.15A red lines)**. To go deeper in this analysis we tried to mimic time-course clinical computations, expressing acute and late performances as % of the initial deficit as follows:

Performance at time X= (Xdpl-baseline)/(2dpl-baseline)*100.

Then, we settled a threshold to quantitatively subdivide “recovers” and “poor recovers”, considering as “recovers” those animals that in the chronic phase regained at least 50% of their initial deficit **(Fig. 15B)**. In our dataset, we found 11 “recovers” (green dots) out of 20 animals (55%), while 9 subjects (red dots) showed a poor or not recovery over time (45%). Despite we cannot draw final conclusions due to the relatively low number of subjects, the

fact that we can distinguish between “recovers” and “poor/not recovers” strengthen the translational value of our model that appears to share some important features with the clinical cases.

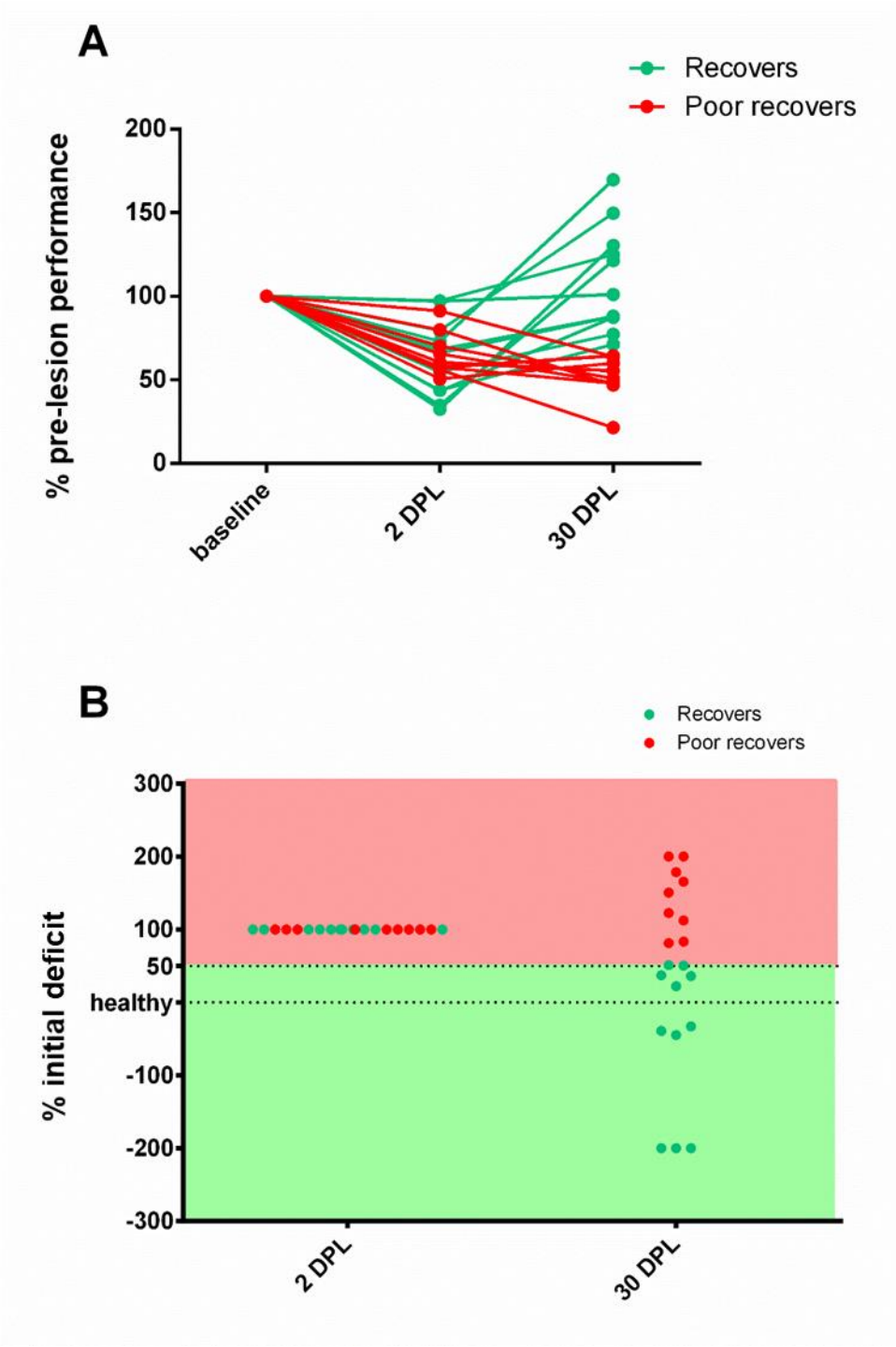

Figure 15: Preliminary analysis on individual recovery. A) *Global motor score was used to analyze the percentage of individual recovery showed by MCAO animals after stroke, normalized on the baseline performance.* ***B)*** *Performance expressed as %of the initial deficit. We considered “recovers” those animals that in the chronic phase regained at least 50% of their initial lost function*

(green dots in the green field), and "poor recovers" those who did not (red dots in the red field). Healthy dotted line represents the baseline condition: animals between under the "healthy line" have a chronic performance that is even better than before stroke.

Then, once verified that individual variability in our model resembles that one observed in the human condition, we investigated if the individual late recovery was proportional to the acute post-stroke performance. Indeed, in humans it has been suggested that the acute deficit could be a strong predictor of chronic motor improvement (Prabhakaran et al., 2008). Here, we obtained acute and chronic performance by subtracting the baseline from the performance at 2 and 30dpl respectively.
Considering the general motor score, linear regression analysis showed that even in our dataset the acute performance can explain 20% of chronic performance variability (**Fig.16A** R= 0.438 and p= 0.041). Moreover, considering only the performance in the reaching test, acute performance seems to predict even better the chronic functionality (**Fig. 16B** R= 0.8400; p= 0.0000627). These results suggest that in our stroke model the early deficit is a good predictor of final motor outcome.

A

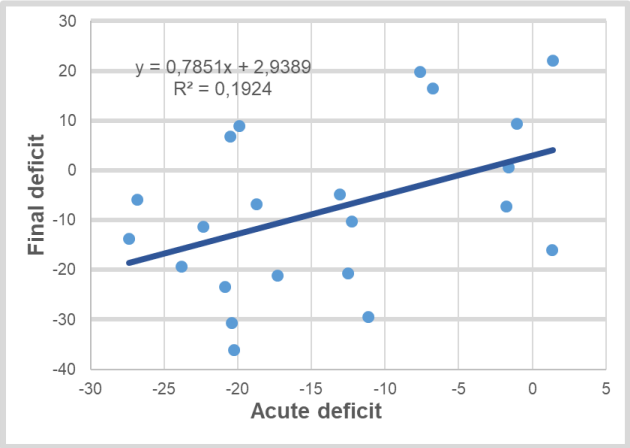

B

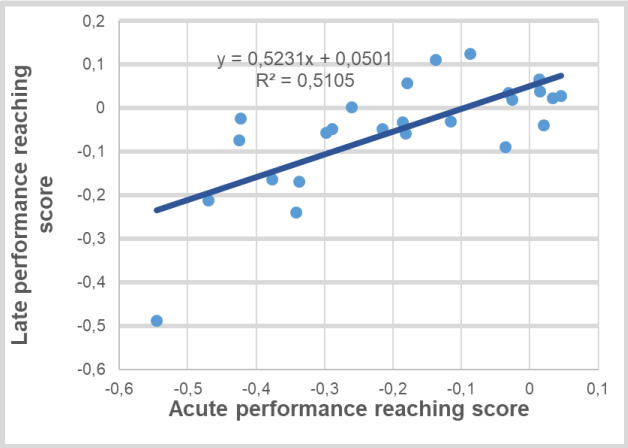

Figure 16: Linear regression between acute and late performance. *Linear correlations between acute and late performance using general motor score (n=22; p= 0.041), **A**) and reaching score (n=25; p= 0.0000627 **B**) in mice that underwent MCAO. Each graph shows its R^2 and the linear equation*

2.5 Correlation among functional and anatomical changes

We then exploited the behavioural and anatomical data collected so far to find possible correlations between the anatomical measures and acute deficit/late residual deficit. To this aim, we performed simple linear correlations between the performance of analyzed animals in different behavioral tasks and each anatomical change that we quantified. As before, we considered acute and chronic performance by subtracting the baseline from each data point.

We found that the most informative anatomical parameters with a predicting value were the lesion volume and the %of the lesioned CFA (**Fig.17 A-B**). Indeed, a good correlation has been found between the score obtained in the reaching test and the volume of the lesion, both for acute (R= 0.6292 and p= 0.0283) and late performance (R= 0.601 and p= 0.0383).

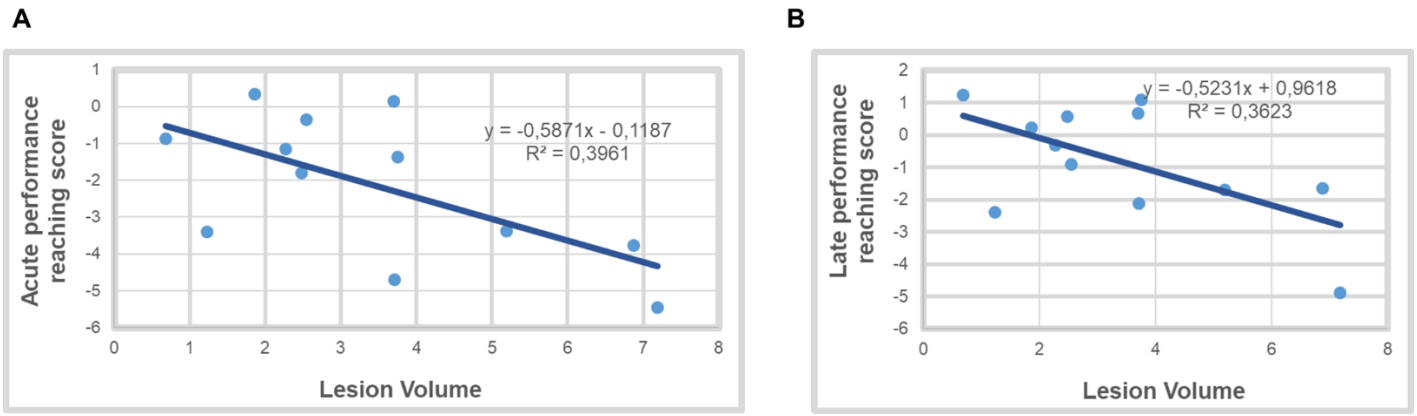

Figure 17: Simple linear correlations between reaching test and lesion volume.
*Linear correlations between acute (**A**) or late (**B**) performance in reaching task and lesion volume in mice underwent MCAO (n=12; p=0.0283 for acute and p= 0.0383 for late performance). Each graph shows its R^2 and the linear equation.*

This correlation was even stronger if only the animals with the injured CFA were considered (n=5) (**Fig. 18 A-B**). The same animals presented also a positive correlation between the percentage of lesioned CFA and the acute/late performance in reaching score (**Fig. 19 A-B** R=0.9199 and p=0.0269 for acute performance; R=0.9842 and p=0.00237 for acute performance).

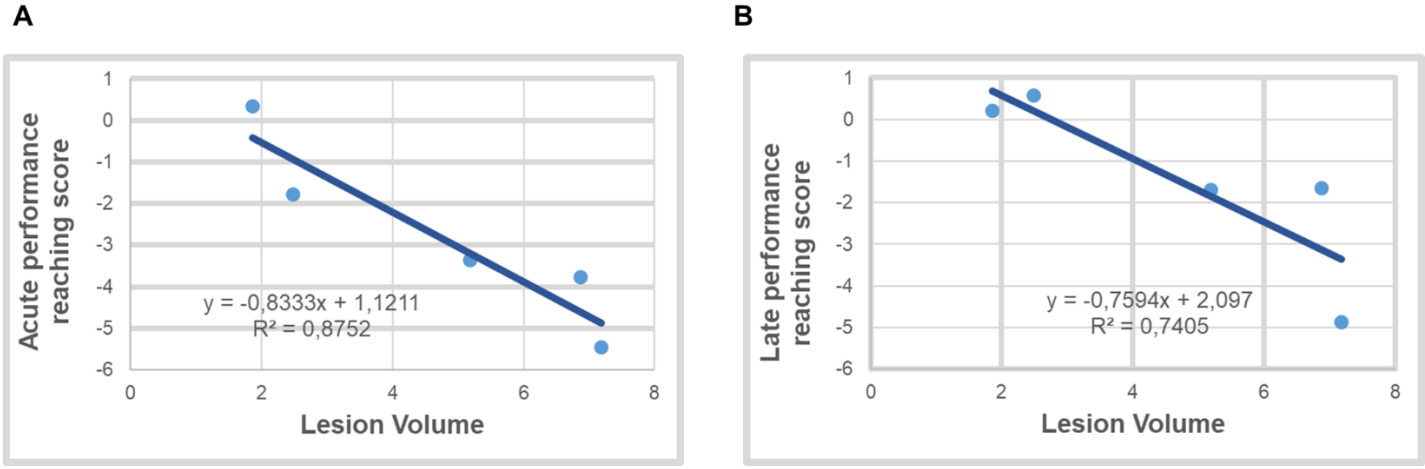

Figure 18: Simple linear correlations between reaching test and anatomical parameters in CFA lesioned mice. (A)- (B) *Linear correlations between acute or late performance in reaching task and lesion volume in MCAO mice that presented a robust damage on the CFA (n=5; p=0.0195 for acute performance; and p=0.06 for late performance). Each graph shows its R^2 and the linear equation*

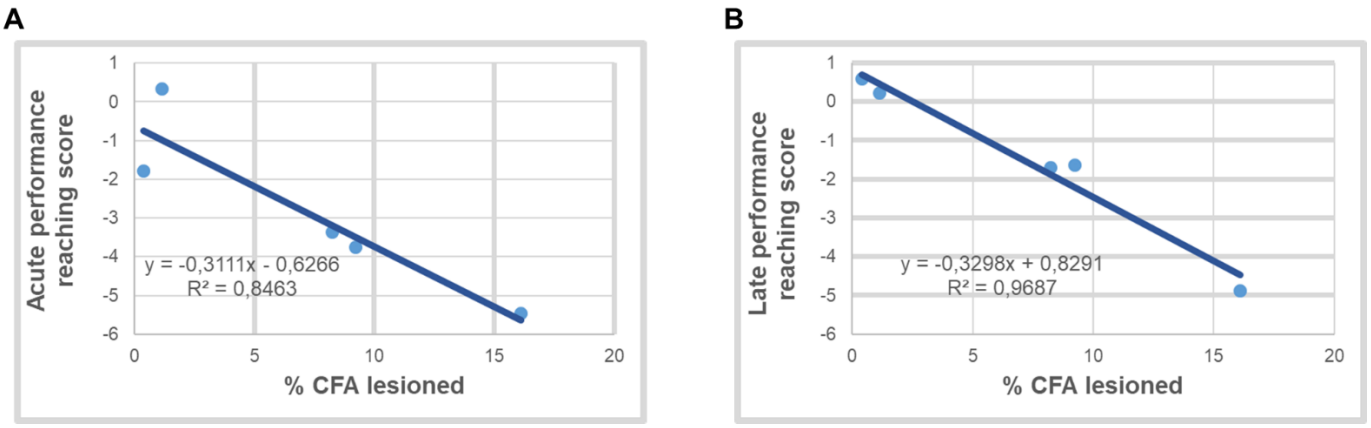

Figure 19: Simple linear correlations between reaching test and anatomical parameters in CFA lesioned mice. (A)- (B) *Linear correlations between acute or late performance in reaching task and the percentage of lesioned CFA in MCAO mice that presented a robust damage on the CFA. (n=5; p=0.0269 for acute performance and p=0.00237 for late performance).*

3- Electrophysiological alterations after MCAO

3.1 MCAO-induced power spectral density changes

Since MCAO spares most of the area of the CFA, it is possible to study electrophysiological alterations in this region in order to correlate them with the behavioural outcome. So, in order to identify possible biomarkers of functional outcome after stroke, we started to consider if induction of MCAO produced measurable electrophysiological changes. For this purpose, we recorded neural signals from animals in freely moving condition by means of chronic electrodes implanted bilaterally in the CFA. The recordings were made longitudinally before the induction of the stroke and then at 2dpl and 30dpl, analysing power spectral density in standard electrophysiological bands (delta, theta, alpha, beta and low gamma, see Materials and Methods). Significant changes have been observed in the affected hemisphere of MCAO animals (n=16) where we found a progressive and significant decrease in the power of the theta (Two-Way ANOVA p= 0.03) and beta (Two-Way ANOVA p<0.001) band at 30dpl. In addition, we noticed an increase in the delta power, which reached a statistical significance at 2dpl and it was maintained until 30 dpl (Two-Way ANOVA p<0.001) **(Fig. 20A)**. For the healthy hemisphere, we observed significant changes at 2dpl for the delta band but also, a total reestablishment in the following days (**Fig.20B**). The same analysis was also conducted in the sham group where no significant changes were noticed (data not shown).

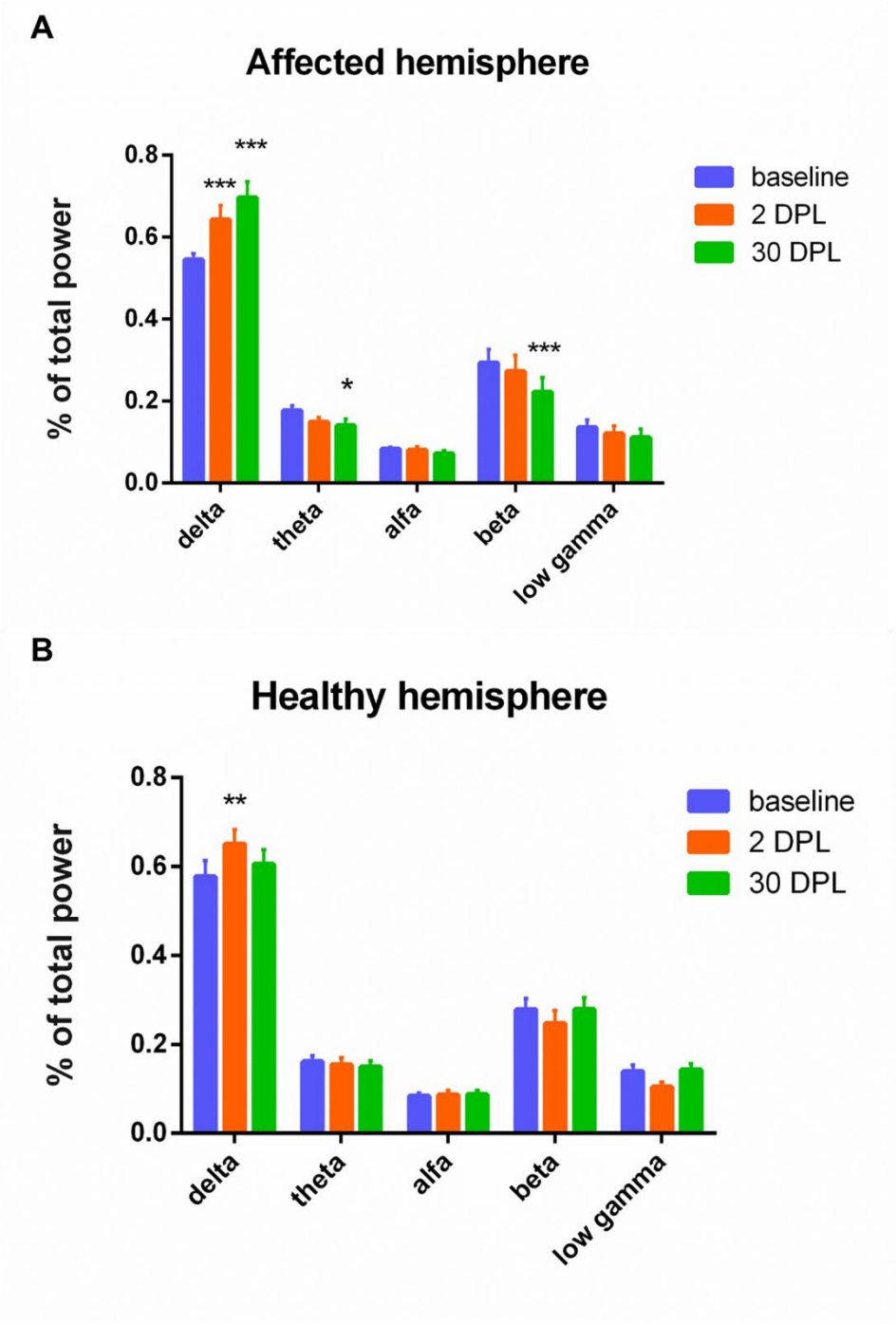

Figure 20: EEG power spectral density changes after MCAO induction *Time course of power spectral density for standard electrophysiological bands in the affected* ***(A)*** *and healthy* ***(B)*** *hemispheres, respectively. In the affected hemisphere, a significant decrease was found for the theta and beta bands, while delta rhythm was increased. (Two-Way ANOVA, followed by Holm-Sidak method, '*' represents significant difference from the baseline. *** p < 0.001 **, p < 0.01, *, p < 0.05). Data were represented as mean ± SEM.*

3.2 Electrophysiological characterization of retraction movement onto M-Platform and related changes after MCAO induction

Next, we wanted to better characterize electrophysiological events associated with the generation of a force peak onto the M-platform, in order to study stroke-induced longitudinal alterations. For this purpose, we first analysed the variation of spectral bands during the different phase of the retraction movement (see Materials and Method for the time intervals). We decided to focus on differences between phases immediately before (Pre) or concomitant (Post) with the force peak in respect to resting phases (i.e. in absence of any forelimb contraction, referred as Empty). Additionally, we also distinguished between force peak generating (M) or not (NM) a submovement.
In baseline condition, during the force peak generation (PostM and PostNM), we observed an increase in the theta band (Two-Way ANOVA $p<0.001$) but a decrease in beta (Two-Way ANOVA $p<0.001$) and low gamma (Two-Way ANOVA $p<0.001$) band relative to the “resting” state (Empty) in the contralateral hemisphere to the used forelimb (**Fig.21A**). A similar phenomenon was observed in the ipsilateral hemisphere, with a synchronization of theta band (Two-Way ANOVA $p < 0.001$ for PostM and $p = 0,001$ for PostNM) and a desyncronization of beta (Two-Way ANOVA $p<0.001$) and low gamma bands (Two-Way ANOVA $p<0.001$ for PostM and $p = 0.0046$ for PostNM) (**Fig.21B**). No changes were found between PostNM and PostM intervals, suggesting that at the cortical level, we are not able to discriminate among attempts and submovements. Moreover, no changes were observed in PreM and PreNM intervals in respect to Empty (data not shown).

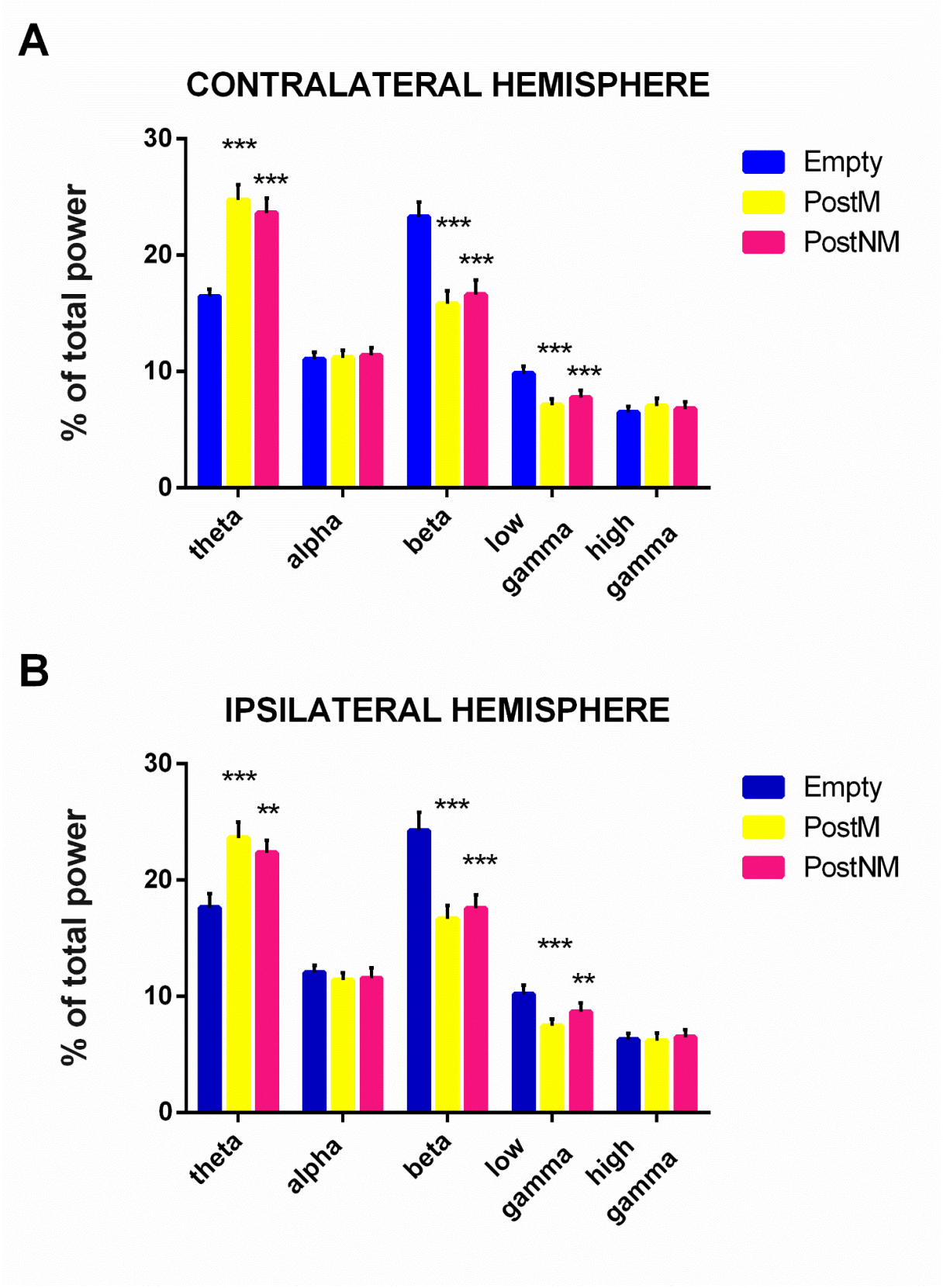

Figure 21: Electrophysiological correlates of force peak generation. (A) *and* ***(B)*** *represent the power spectrum of the neural signal for the contralateral (to the utilized forelimb) and ipsilateral hemisphere, respectively at baseline condition for all animals (n=30). For both hemispheres, an increase in the theta band and a decrease in the beta and low gamma bands is observed. (Two-Way ANOVA followed by Holm-Sidak postdoc method. '*' represents significant difference from the Empty interval. *** p < 0.001, ** p < 0.01). Data were represented as mean ± SEM.*

Later, we wanted to verify if this pattern of syncronization and desynchronization was altered after the stroke. Thus we analyzed the pre/post-stroke differences in both the contralateral (affected) and in the ipsilateral (healthy) hemispheres. Since no differences were found between PostM and PostNM intervals, here we focused only on the ratio between PostM and resting (Empty) states. We observed that this ratio was significantly impaired in the affected hemisphere after MCAO induction with a decrease of theta band synchronization at 2dpl (Two-Way ANOVA $p<0.001$) that was maintained until 30 dpl (Two-Way ANOVA $p= 0.0002$). A significant reduction of synchronization was found also for the alpha band both at 2 dpl (Two-Way ANOVA $p= 0.0183$) and 30 dpl (Two-Way ANOVA $p=0.0406$), while the low gamma desynchronization was disrupted early after stroke (Two-Way ANOVA $p= 0.0294$). Additionally, we observed a transient synchronization of high gamma rhythm immediately after stroke (Two-Way ANOVA $p= 0.0026$) (**Fig.22A**)
Coherently with the tight connections between the two hemispheres, some changes were detected, with a lesser extent, also in the healthy hemisphere (**Fig.22B**).
The same analysis was performed on control animals where we failed to detect any relevant alteration (data not shown).

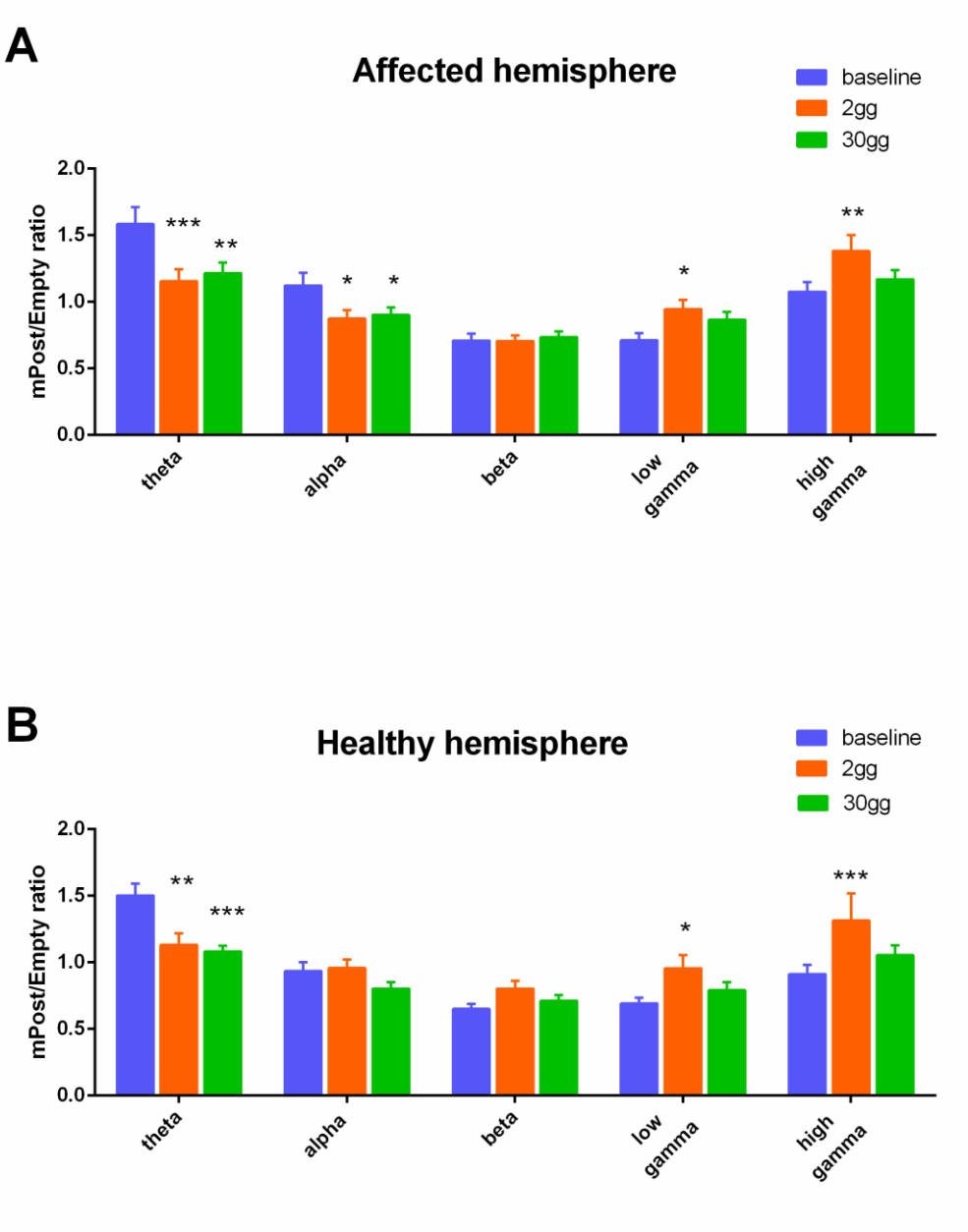

Figure 22: Band-specific alterations of active/resting ratio after MCAO induction. (A) *and* ***(B)*** *show the ratio between the power spectral density during active (PostM) vs. resting state (Empty), for the affected and healthy hemisphere respectively. Only MCAO animals were considered (n=19). Significant changes were particularly present for the theta, alpha and gamma band of the affected hemisphere. In the healthy hemisphere a lower impairment was observed (Two-way ANOVA, followed by Holm-Sidak method, '*' represents significant difference from the baseline *** p < 0,0001, ** p < 0,001, * p < 0.05). Data were represented as mean ± SEM.*

We then focused our attention also on the event-related potential (ERP) associated with the force peak generation. The ERP was computed by averaging the LFP signal in correspondence of the force peaks onset. The ERP was detected in both hemispheres and it is generally composed by an early positive peak ensued by a negative, more prominent one (see Materials and Method). The ERP shape remained stable over time in controls animals while in ischemic mice a robust change in the ERP shape was evident with respect to baseline condition, (**Fig. 23 (A)-(D**). Thus we quantified the latencies and relative amplitudes of each positive and negative components (peak-to-peak1 and 2 respectively).

A

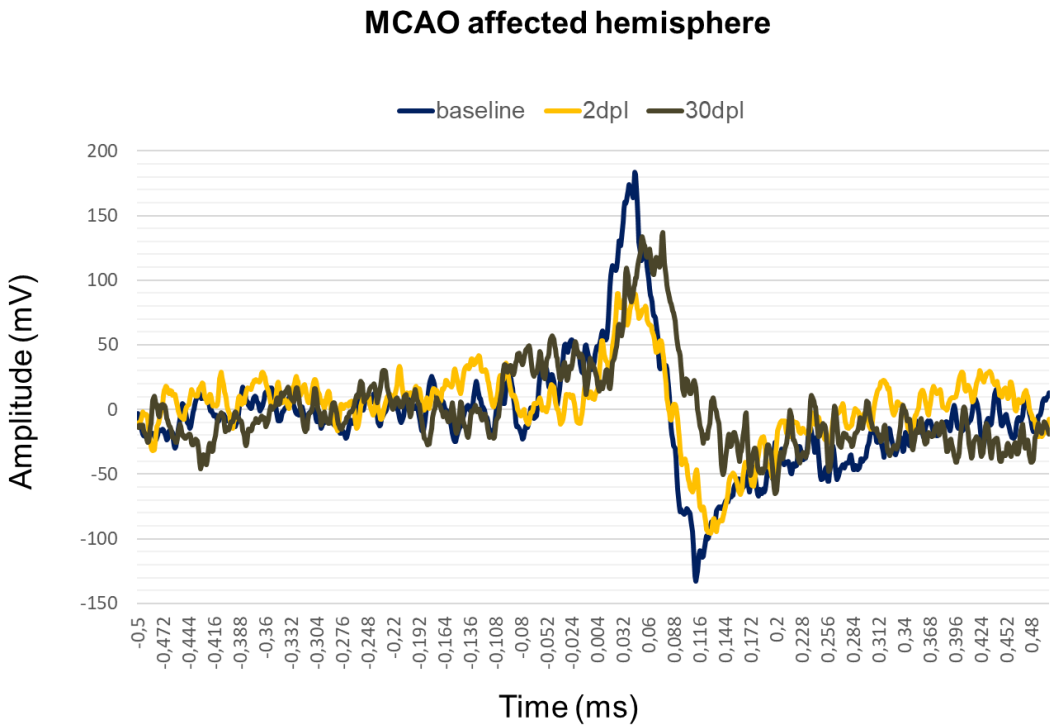
MCAO affected hemisphere
baseline
2dpl
30dpl
Amplitude (mV)
200
150
100
50
0
-50
-100
-150
-0,5
-0,472
-0,444
-0,416
-0,388
-0,36
-0,332
-0,304
-0,276
-0,248
-0,22
-0,192
-0,164
-0,136
-0,108
-0,08
-0,052
-0,024
0,004
0,032
0,06
0,088
0,116
0,144
0,172
0,2
0,228
0,256
0,284
0,312
0,34
0,368
0,396
0,424
0,452
0,48
Time (ms)

B

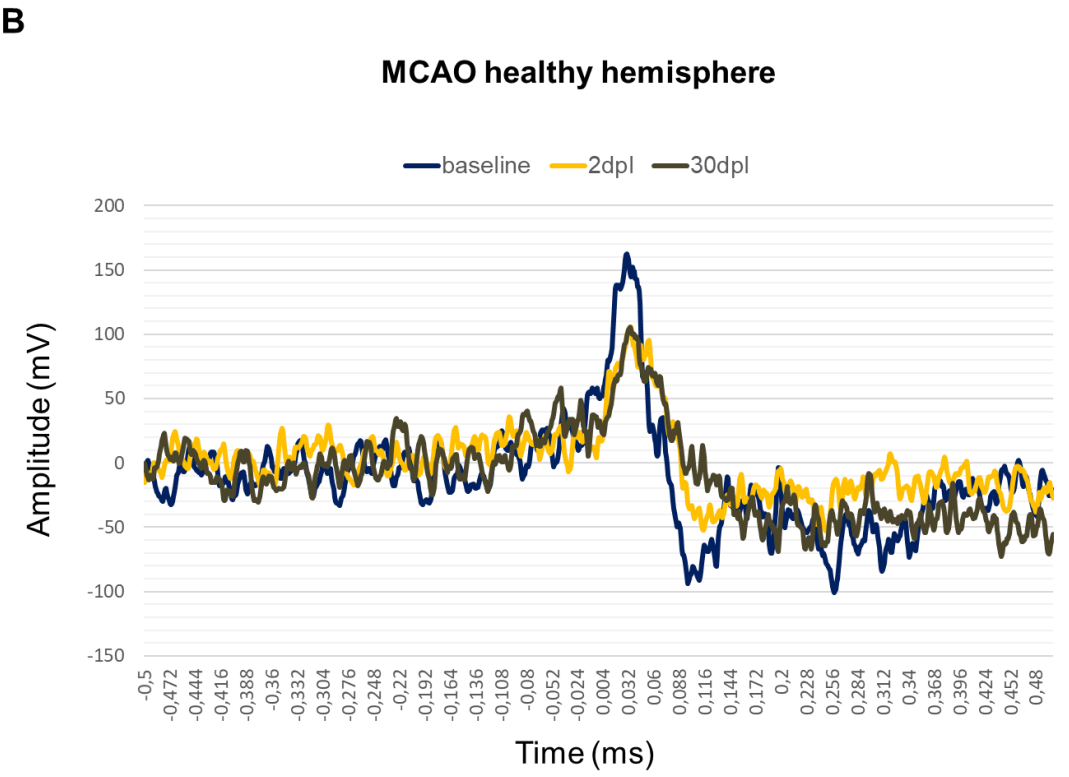
MCAO healthy hemisphere
baseline
2dpl
30dpl
Amplitude (mV)
200
150
100
50
0
-50
-100
-150
-0,5
-0,472
-0,444
-0,416
-0,388
-0,36
-0,332
-0,304
-0,276
-0,248
-0,22
-0,192
-0,164
-0,136
-0,108
-0,08
-0,052
-0,024
0,004
0,032
0,06
0,088
0,116
0,144
0,172
0,2
0,228
0,256
0,284
0,312
0,34
0,368
0,396
0,424
0,452
0,48
Time (ms)

C

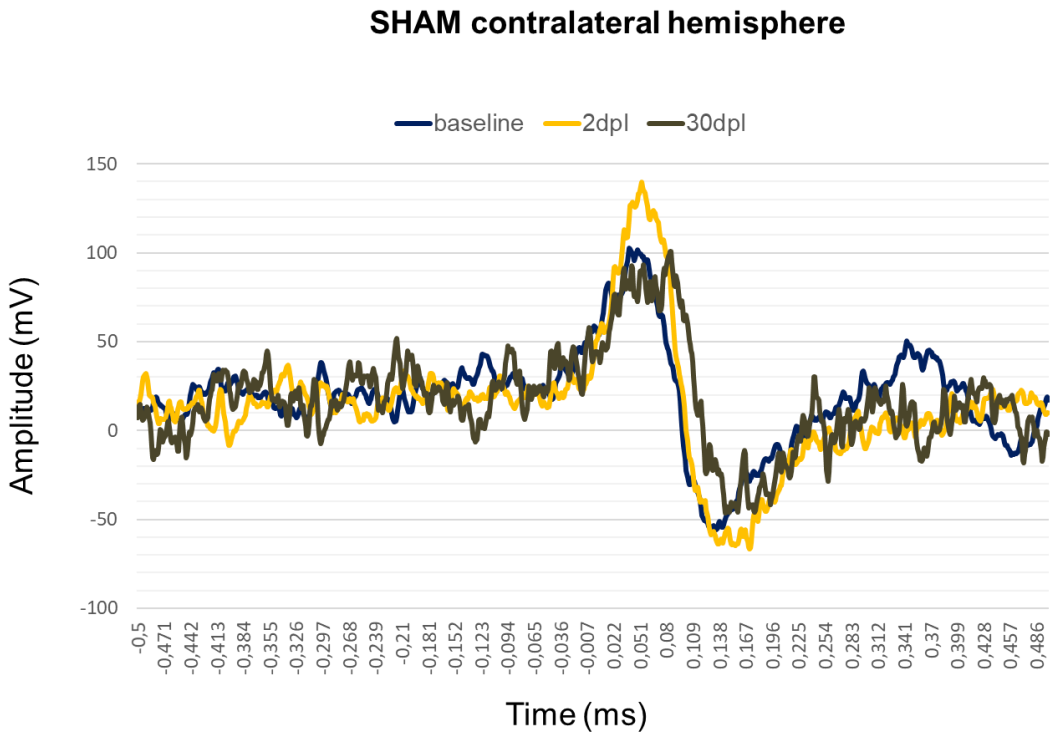
SHAM contralateral hemisphere
baseline
2dpl
30dpl
Amplitude (mV)
150
100
50
0
-50
-100
-0,5
-0,471
-0,442
-0,413
-0,384
-0,355
-0,326
-0,297
-0,268
-0,239
-0,21
-0,181
-0,152
-0,123
-0,094
-0,065
-0,036
-0,007
0,022
0,051
0,08
0,109
0,138
0,167
0,196
0,225
0,254
0,283
0,312
0,341
0,37
0,399
0,428
0,457
0,486
Time (ms)

D

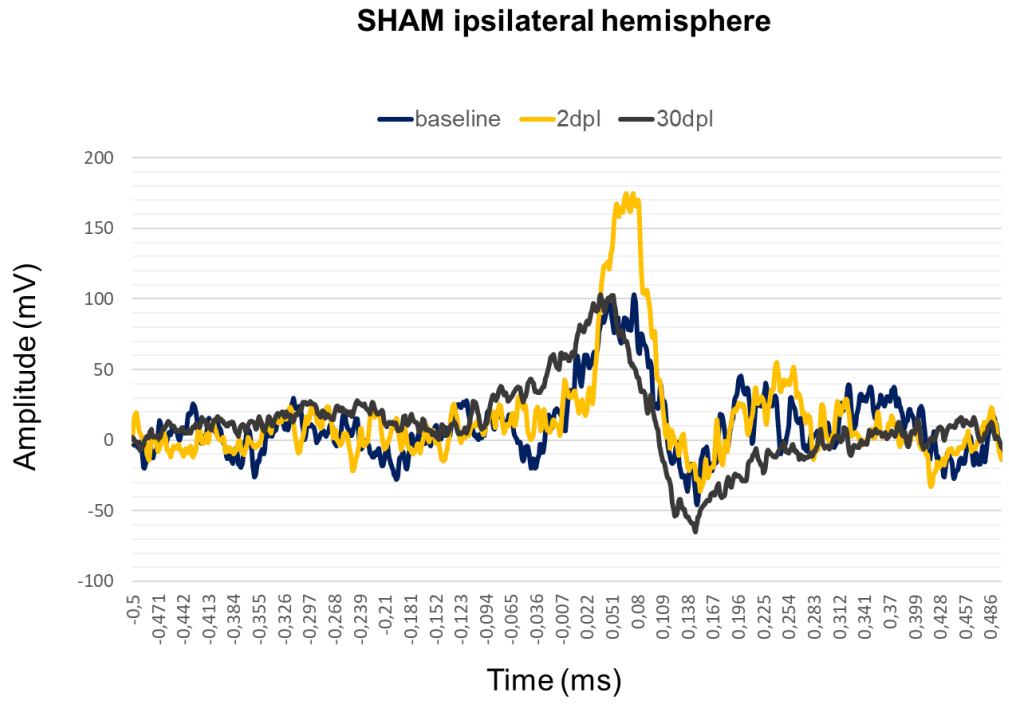
SHAM ipsilateral hemisphere
baseline
2dpl
30dpl
Amplitude (mV)
200
150
100
50
0
-50
-100
-0,5
-0,471
-0,442
-0,413
-0,384
-0,355
-0,326
-0,297
-0,268
-0,239
-0,21
-0,181
-0,152
-0,123
-0,094
-0,065
-0,036
-0,007
0,022
0,051
0,08
0,109
0,138
0,167
0,196
0,225
0,254
0,283
0,312
0,341
0,37
0,399
0,428
0,457
0,486
Time (ms)

Figure 23: Representation of ERP in MCAO and SHAM group. (A)-(B) *Two examples of event-related potentials (ERPs) in the affected* ***(A)*** *and healthy hemispheres* ***(B)*** *of MCAO animals. After the lesion a consistent decrease of amplitude was observed. On the contrary, in SHAM animals, the amplitude remained stable over time both in the contralateral* ***(C)*** *and ipsilateral* ***(D)*** *hemisphere*.

We found that the amplitude of both peak-to-peak 1 and peak1-to-peak2 were significantly diminished at 2 dpl ($p<0.001$) in the affected hemisphere (contralateral to used forelimb), with a recovery in chronic phase (**Fig. 24A**). These results were consistent with the data obtained in the parameters analyzed from retraction task **(Fig. 11)**. This effect was greatly specific for the affected hemisphere; significant changes occurred in the healthy side (ipsilateral) only regarding the peak1-to-peak2 amplitude at 2dpl ($p=0.001$) (**Fig.24B**).
No significant post-stroke variation was observed in latencies neither in the affected and healthy hemispheres (**Fig.24C-D**). As previously mentioned, sham animals showed stable ERPs over time, in fact the quantification confirmed that latencies and amplitudes of both peak1 and peak1-to-peak2 remained unaltered (**Fig. 25A-D**)

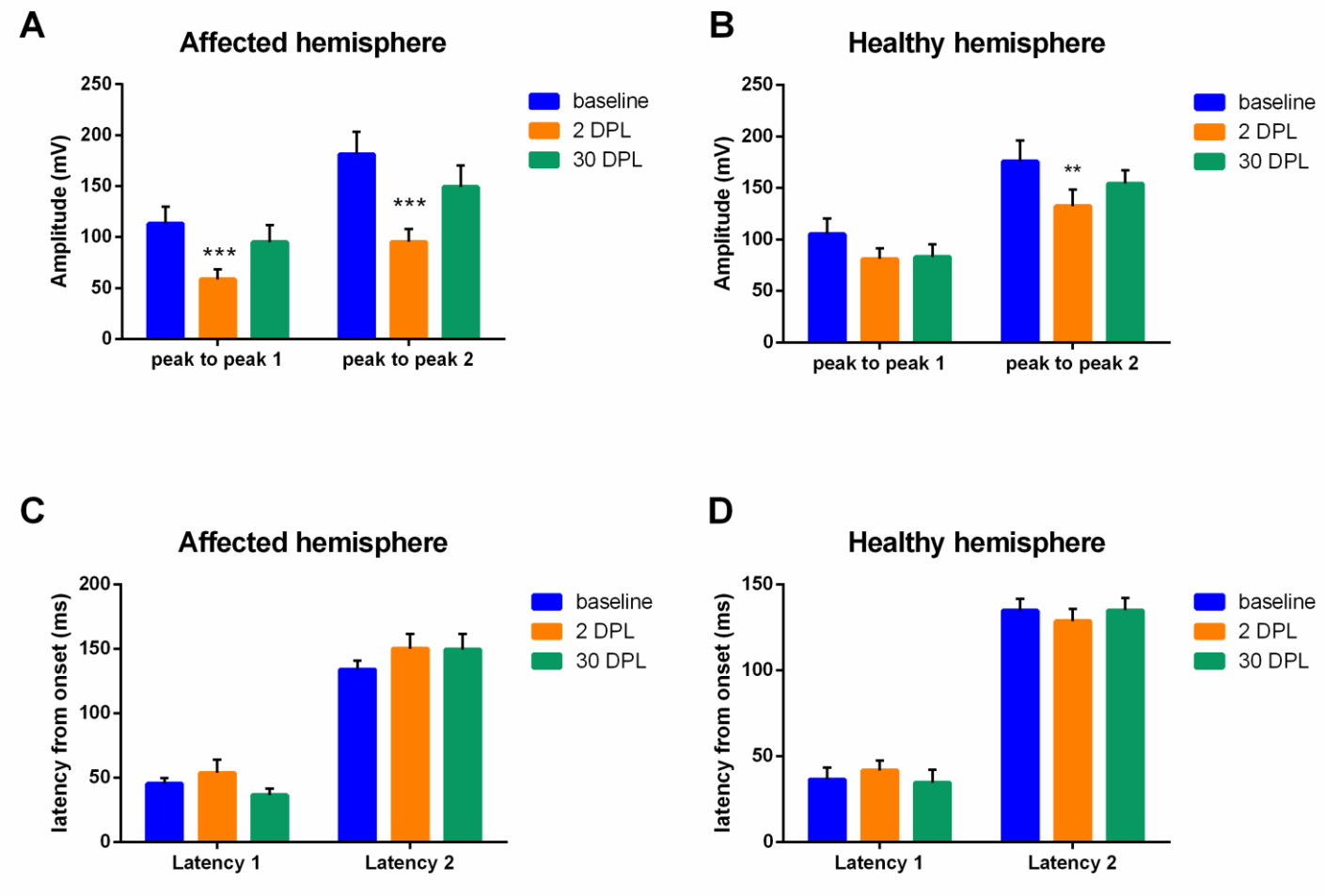

Figure 24: Characterization of force peak generation-related potential before and after MCAO

(A)-(B) *Amplitude of the peak-to-peak 1 and peak1-to-peak2, for the affected (contralateral to used forelimb) and healthy (ipsilateral) hemispheres, respectively in MCAO group (n=21). A significant decrease was observed for both values in the affected side at 2dpl and only in peak1-to-peak2 for the healthy side.* ***(C)-(D)*** *Latency for peak-to-peak1(latency1) and peak1-to-peak2 (latency2), for the ipsilesional and contralesional hemispheres, respectively. No significant variations were observed after stroke induction. (Two-Way ANOVA, followed by Holm-Sidak method, '*' represents significant difference from the baseline, ***, p < 0.001, **, p < 0.01).*

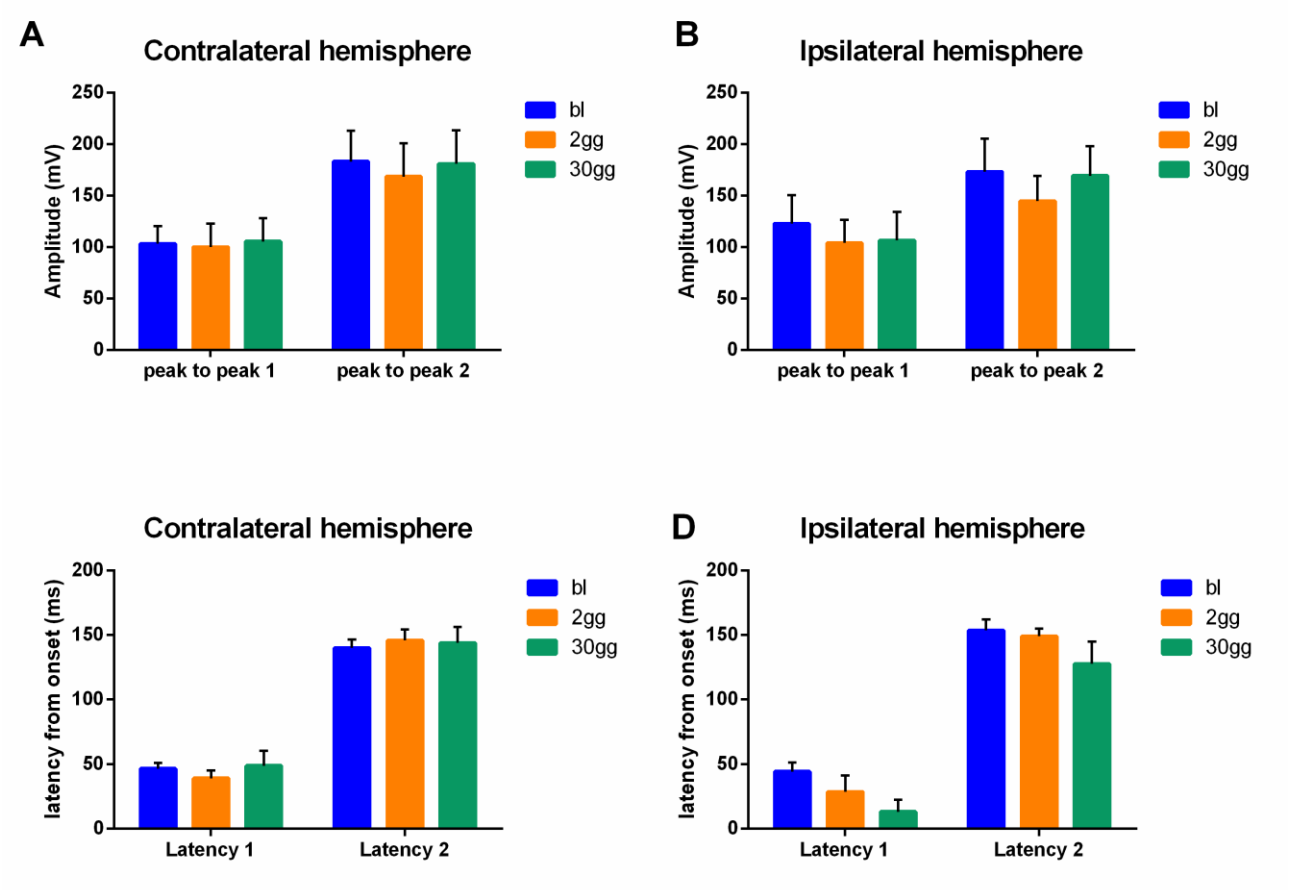

Figure 25: Characterization of force peak generation-related potential in SHAM animals *Amplitude of the peak-to-peak1 and peak1-to-peak2, for the contralateral* ***(A)*** *and ipsilateral* ***(B)*** *hemisphere (relative to the used forelimb), in SHAM group (n=19).* ***(C)-(D)*** *Latency for peak-to-peak1(latency1) and peak1-to-peak2 (latency2), for the contralateral and ipsilateral hemispheres, respectively in SHAM animals (n=19). No significant changes were detected for both amplitude and latency.*

Part 2

Transplant of neurons derived from mouse embryonic stem cell (mESCs) and their projection patterns in the stroke brain.

1- mESCs in vitro differentiation protocol

A crucial aim for cell replacement protocols is the ability to produce the wanted type of neural cell to be replaced. In recent years, the use of pluripotent stem cells has allowed the production of neurons with specific identities. This has been made possible by the modification of existing methods of in vitro neuralization and patterning of pluripotent cells, by fine-tuning the signaling pathways that normally orchestrate the acquisition of distinct types of neuronal identities during embryonic brain development (Hansen et al., 2011; Lupo et al., 2014). Thanks to a collaboration with doctor Federico Cremisi from Scuola Normale Superiore of Pisa, it has been possible to develop a new protocol for the differentiation of mouse embryonic stem cells into neurons with specific molecular identity.
They found that the timely manipulation of Wnt and BMP Signaling during Mouse ESC neuralization generates neural precursor cells with a molecular isocortical or hippocampal identity. In particular, the inhibition of the endogenous WNT and BMP signaling for 11 days of in vitro differentiation (DIV) induced dorsal telencephalic molecular identity (**Fig. 1A**). This was shown by the relative expression of anteroposterior (A/P) embryonic CNS markers, such as FoxG1 and Emx2, (**Fig. 1B**) in Wnt/BMP double inhibited cells (WiBi cells). Notably, double Wnt/BMP inhibition was no longer required after DIV8 to induce the expression of the telencephalic markers FoxG1 and to repress the expression of the posterior markers.
The dorso-medial region of the telencephalon has a fundamental role as signaling center in cortical development. In fact, along the dorsal telencephalic midline there is a high expression of BMPs and WNTs (Hèbert et al., 2002; Shimogori et al., 2004), which are required for the hippocampal field specification (Lee et al., 2000; Yoshida et al., 2006). Accordingly, the reactivation of canonical WNT signaling with a Wnt agonist CHIR99021 (3uM, DBA) from DIV8 increase the expression of the embryonic hippocampal markers Emx1 and Emx2.

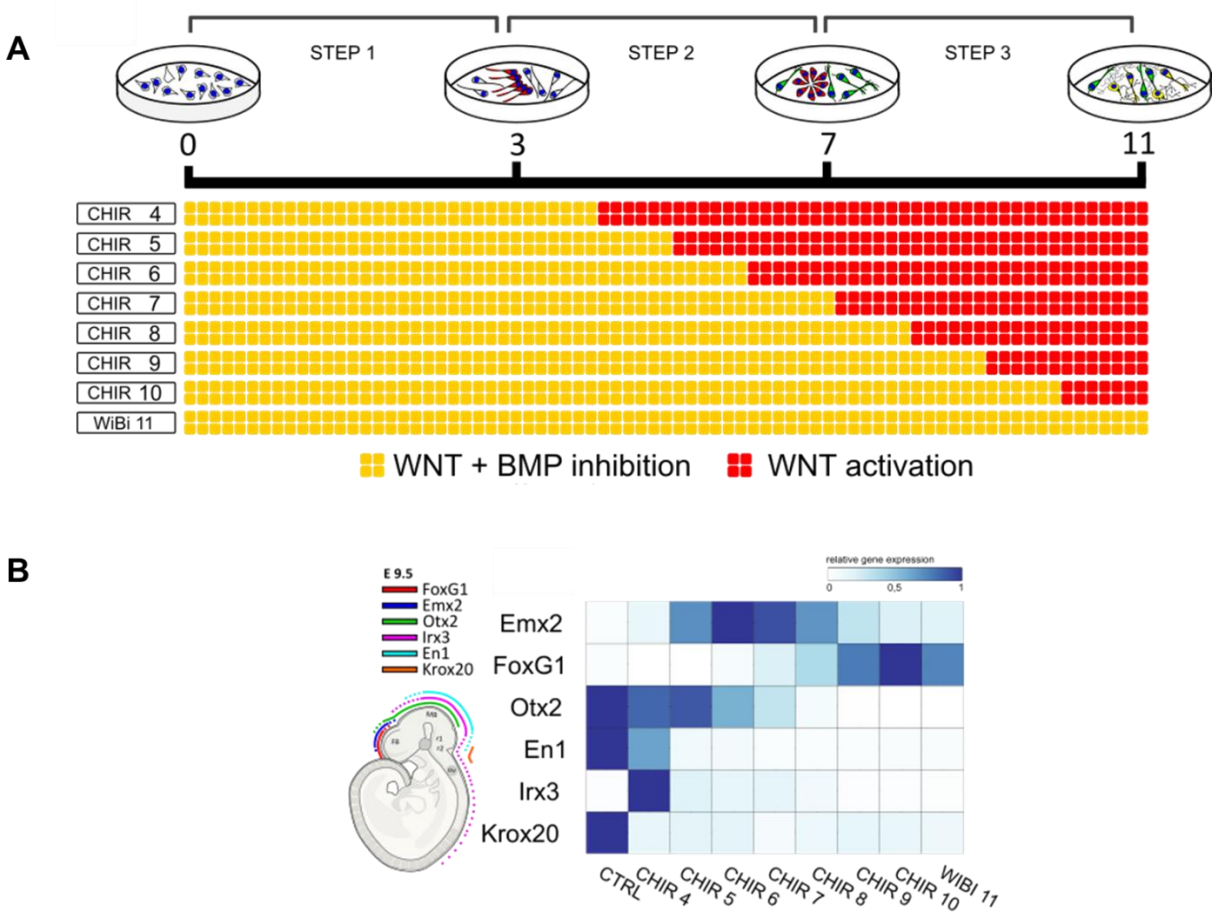

Figure 1: Timely manipulation of Wnt and BMP signaling and regional identity. A) *Scheme of the ESC differentiation protocol. DIV, days of in vitro differentiation.* ***B)*** *The relative expression of anteroposterior (A/P) embryonic CNS markers.*

To further characterize the molecular identity of the cells in which Wnt/BMP signaling was continuously inhibited (WiBi cells) or cells in which Wnt/BMP signaling was reactivated from DIV8 (CHIR8 cells), they compared their global gene expression profiles with the profiles of embryonic cells by principal component analysis (PCA) and clustering analysis (**Fig.2 A-B**). While WiBi-treated cells located closer to isocortex and striatum, CHIR-treated cells were closer to Hippocampus.

In addition, CHIR treated cells showed expression of the dorsal telencephalic markers TBR1, CTIP2, and SATB2 and TBR2 (**Fig. 2C–2E**), as well as expression of the neuronal terminal differentiation markers betaIII TUBULIN, NEUN, and MAP2 (**Fig. 2F and 2G**).

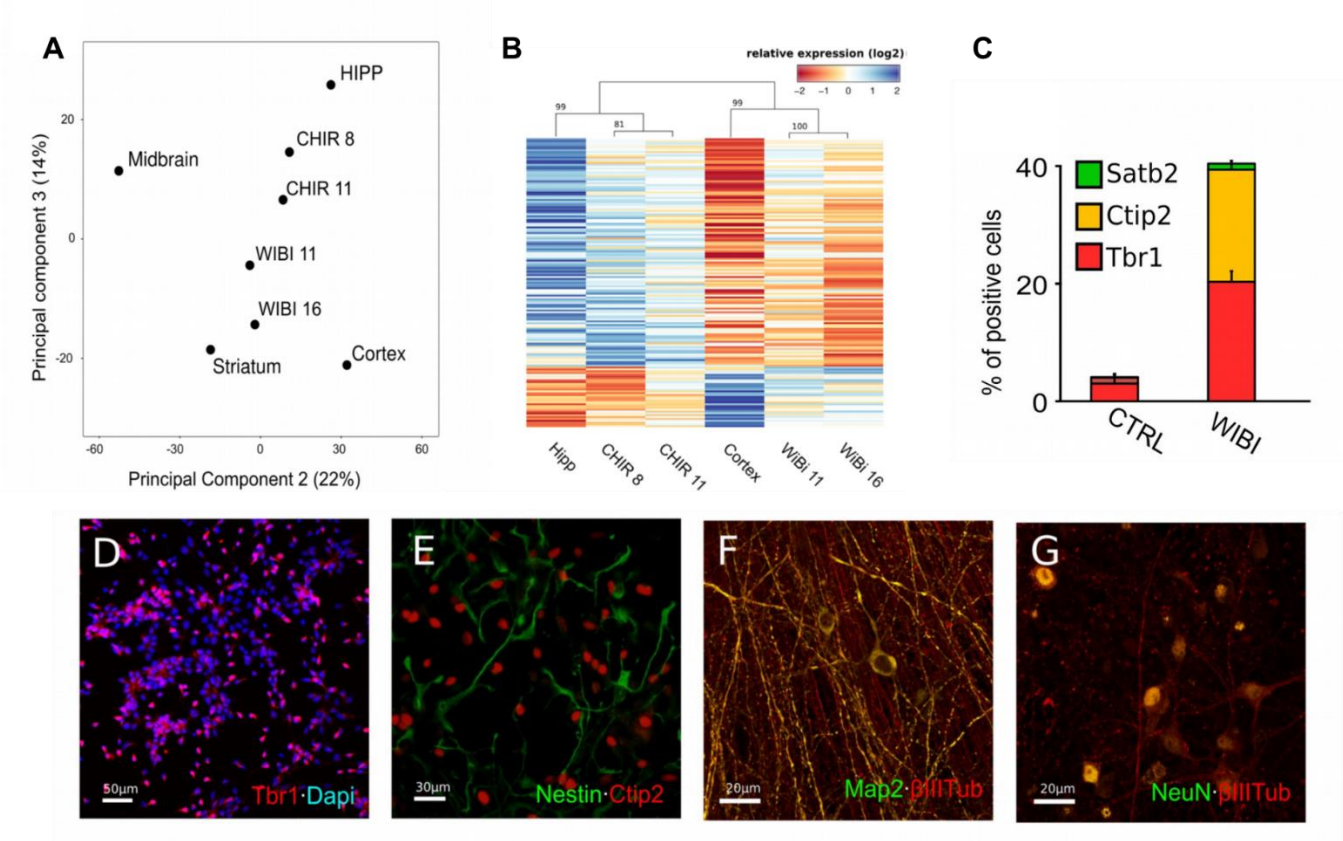

Figure 2: The molecular and neuronal identity of transplanted cells. (A)- (B) *Hippocampal and Isocortical global gene expression profile by principal component analysis* ***(A)*** *and clustering analysis* ***(B); C)*** *Percentage of control (0.1% DMSO) and CHIR8 and WiBi cells positive for the dorsal telencephalic markers SATB2, CTIP2, and TBR1.* ***(D)-(G)*** *Immunocitodetection (ICD) of different neuronal markers in CHIR8 cells. TBR1, CTIP2, and NESTIN: DIV13; bIII TUBULIN, MAP2, and NEUN: DIV25.*

2- mESC derived neurons survive and send projections in different regions of adult brain.

In order to track transplanted cells in the host brain, cortical and hippocampal ESC-derived neurons were labelled with lentiviral vectors carrying membrane-bound forms of GFP and mCherry, respectively, which allowed to visualize long distance projections. Before transplantation, cells were treated with gamma-secretase inhibitor (DAPT) and Aracytin (AraC) to force their differentiation and negatively select dividing progenitors, respectively. In order to evaluate survival and behavior of the cells in vivo, hippocampal (CHIR8) and isocortical (WiBi) cells were pooled and transplanted into the motor cortex and hippocampus of adult mice. One month and two months after transplantation, we performed

neuroanatomical analysis of the grafted cells and their projections (see Materials and Method for general timeline) (**Fig.3**).

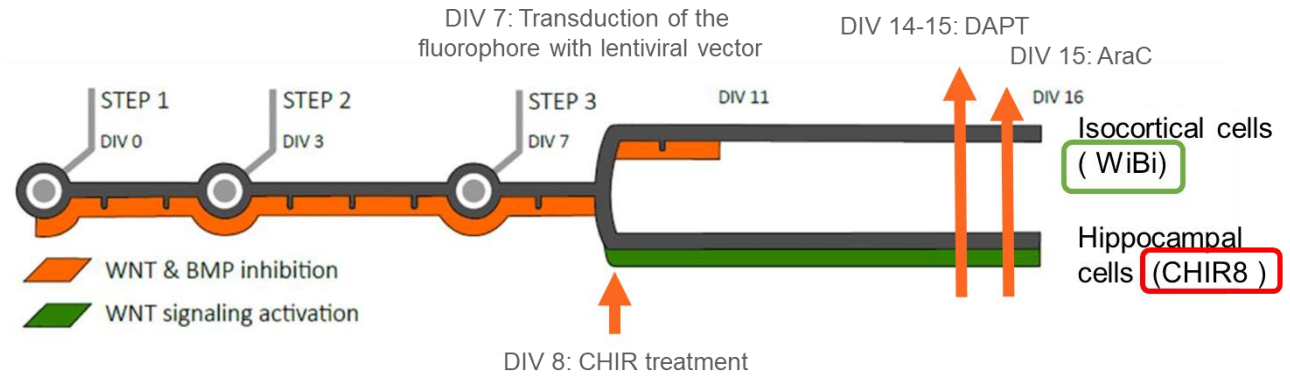

Figure 3: Schematic representation of the experimental protocol implemented in this part of the thesis.

3- In vitro patterned neurons behave differently when grafted in adult hippocampus

The two types of cells were first co-injected into the dentate gyrus (DG) of 2-month-old mice, because this is a niche of adult neurogenesis (Eriksson et al., 1998; Van Praag et al., 2002), and it is also a permissive environment for the extension of new neuronal processes (**Fig.4A**). Both WiBi and CHIR8 cells persisted in the host tissue one and two months after transplantation, showing expression of the terminally differentiated neuronal marker NeuN. However, they presented a different ability to extend neuronal processes. Indeed, only CHIR8 cells were able to send long-range projection reaching the natural target of DG such as CA3, CA1 regions, subiculum and entorinal cortex, while WiBi cells remained in the site of the injection (**Fig.4 (B)- (F)**)

The density of the fibers reaching CA3 was significantly higher than the density of the fibers projecting to other hippocampal structures, especially when analyzed two months after grafting (**Fig.4 G and H**). These observations were consistent with the capability of naïve hippocampal cells to extend new long-range processes contacting CA3 during adult neurogenesis.

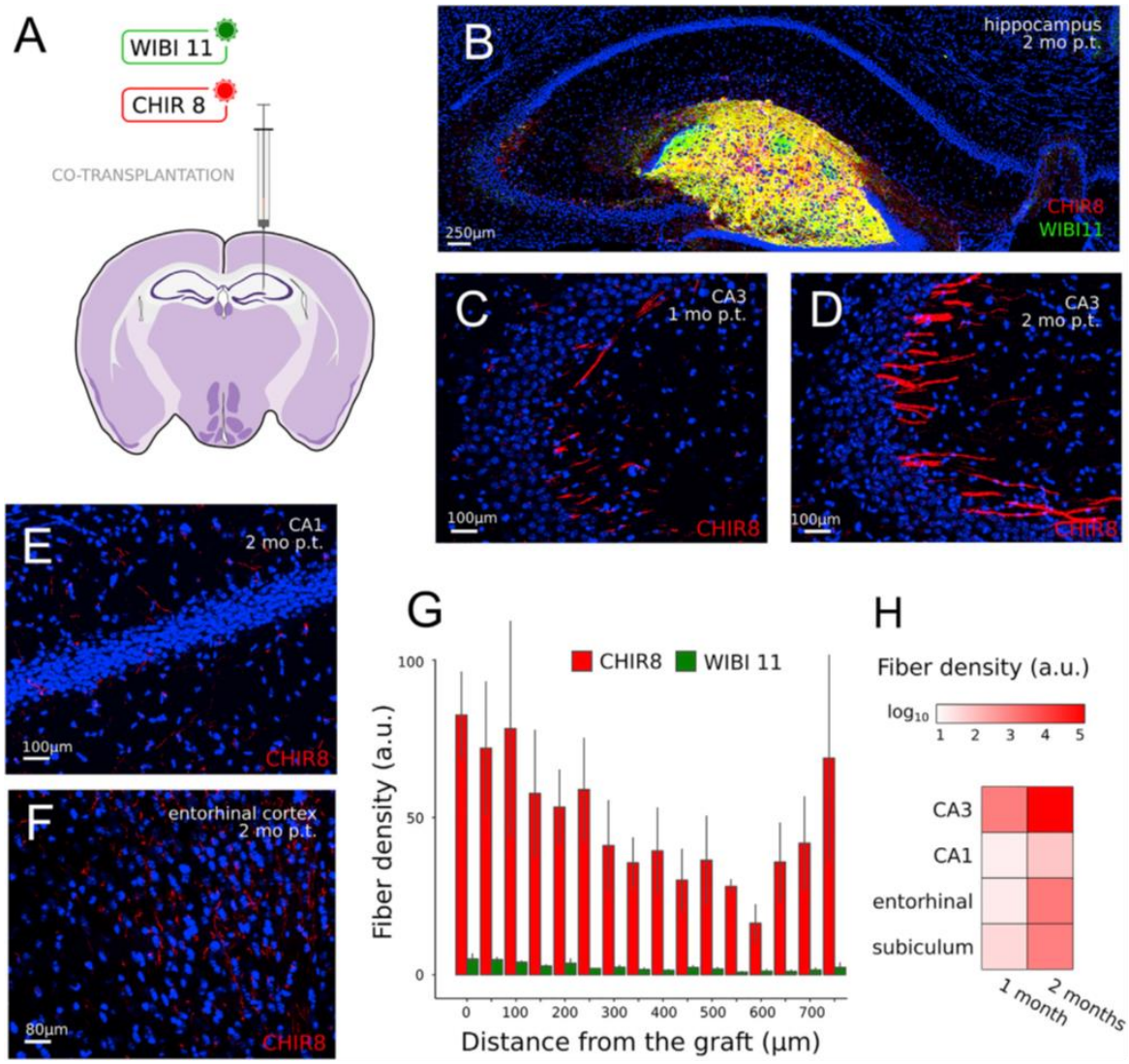

***Figure 4: Cell transplantation in Hippocampus**: **A)** Method and site of cell grafting**. B)** ICD of CHIR8 (red) and WiBi cells (green) 2 months post transplantation (mo p.t.) in hippocampus. Blue, Hoechst nuclear counterstaining. **(C)–(F)** ICD of CHIR8 and WiBi fibers at different times post transplantation and in different regions, as indicated by labels**. (G)** Density of WiBi and CHIR8 fibers at different distances from the graft, 1 month after transplantation. **(H)** Heatmap of CHIR8 fiber density in different hippocampal regions 1 and 2 months after cell grafting. n ≥3 transplanted animals for each time point were analyzed.*

Notably, 30.1% of transplanted CHIR8 cells expressed calbindin1 (CALB1, **Fig.5A and B**), a marker for DG cells (Sloviter, 1989), one month after the transplantation. Moreover, most of the CHIR8 projections found in the Mossy Fiber pathway, which is a natural target of DG (Blackstad et al., 1970; Swanson et al., 1978; Gaarskjaer, 1978; Claiborne et al., 1986), were CALB1 positive (82.0%), while only 8.9% of the projections in CA1 expressed this marker (**Fig.5C and D**). This result suggested that at least a subpopulation of CHIR8 cells displays DG identity and retains the projection pattern of endogenous DG cells.

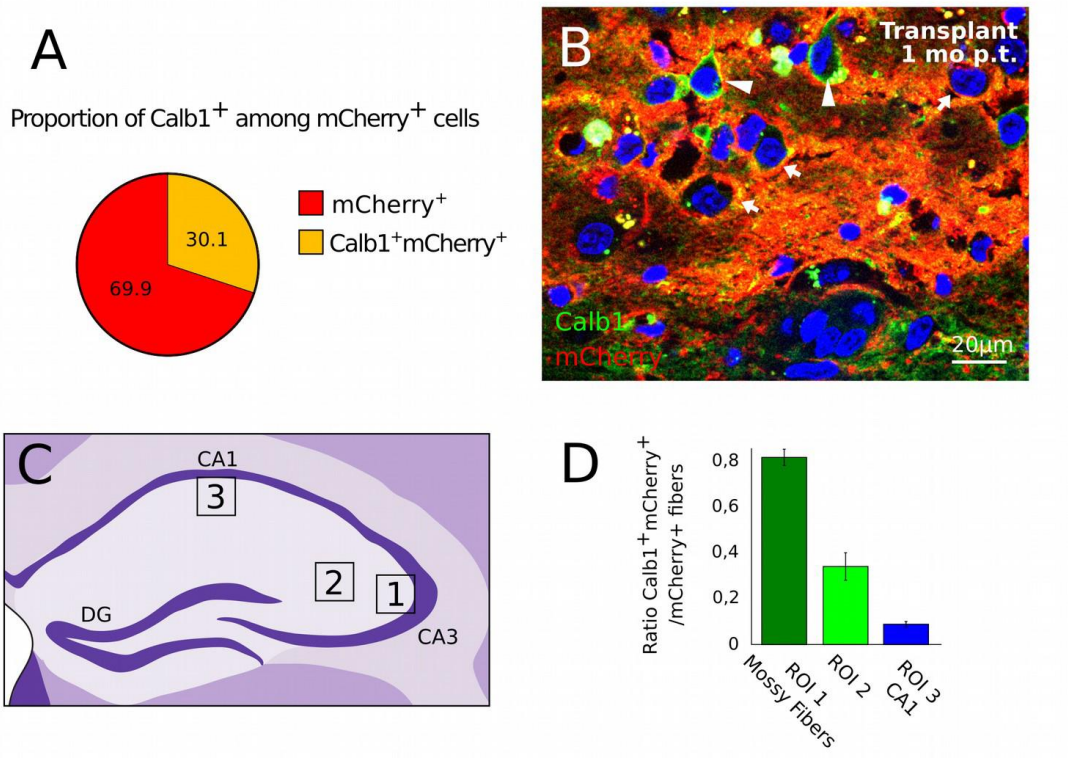

Figure 5: Distribution of CALB1 positive fibers in hippocampus. A) *Percentage of Calb1-positive cells among CHIR8 cells, 1 month p.t.* ***B)*** *ICD of Calb1- and mCherry-positive grafted cells in the hippocampus, 1 month p.t. Arrowheads indicate Calb1/mCherry double positive cells, while arrows point to cells containing only mCherry.* ***C)*** *Schematic representation of the regions of interest (ROIs) analysed for the quantification of Calb1-positive fibers.* ***D)*** *Ratio of Calb1/mCherry double-positive fibers on the total amount of mCherry-stained fibers in each ROI.*

4- Isocortical cells send far reaching projections when transplanted in healthy motor cortex

A different condition was observed after transplantation in adult intact motor cortex. As in the case of transplantations in hippocampus, both WiBi and CHIR8 cells persisted in the host tissue one and two months after transplantation, showing expression of the terminally differentiated neuronal marker NeuN. CHIR8 cells were able to efficiently extend projections, either inside the cortex (**Fig. 6 (C)-(F), 6H, 6I, 6K, and 6L**) or toward extra-cortical regions (**Fig. 6G, 6J, and 6M).** WiBi cells transplanted in adult motor cortex were also able to extend processes. However, they generated far-reaching processes less efficiently than CHIR8 cells one month after transplantation. Interestingly, two months after grafting, WiBi cells were even more effective than CHIR8 cells in extending processes within the motor cortex (**Fig. 6K and 6L**) and almost as efficient as them in sending axons to extra-cortical targets (**Fig. 6M**). Specifically, while WiBi and CHIR8 cells shared most of the cortical and subcortical targets, some regions, such as the piriform cortex ($p < 0.01$), the auditory cortex ($p < 0.01$), the visual cortex ($p < 0.05$), the entorhinal cortex ($p < 0.05$), and the hippocampal formation ($p < 0.01$), were mostly targeted by CHIR8 cells (**Fig. 6L and 6M**), indicating cell-specific axonal outgrowth. We also analyzed other subcortical targets, including the thalamus, midbrain, and corticospinal tract, but we could not detect significant projections for either

cell type. Altogether, these results indicated that cortical cells are slower than hippocampal cells in extending far-reaching axons when transplanted into the isocortex.

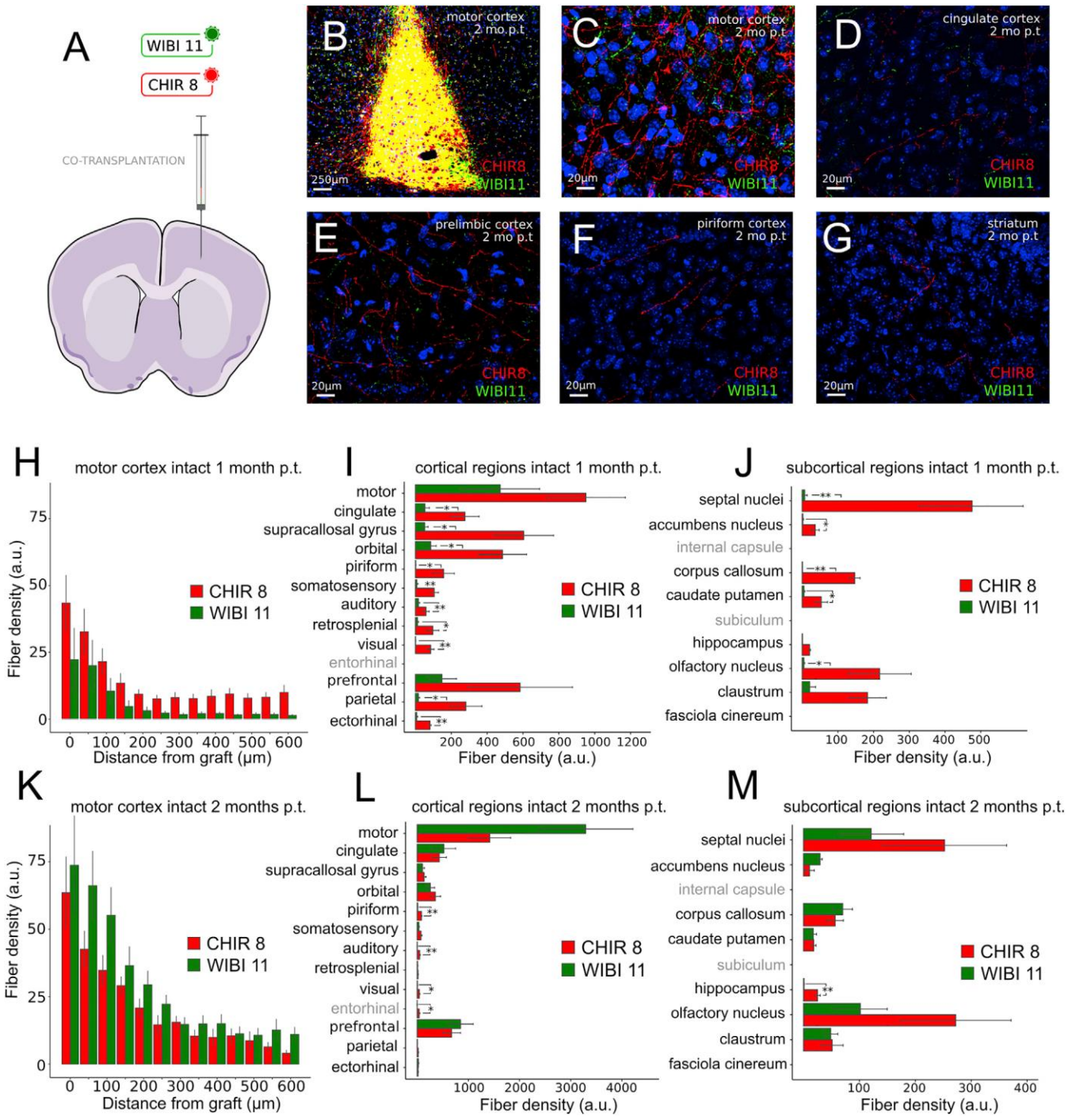

Figure 6: Cell Transplantation in healthy Motor Cortex A) *Scheme of transplantation.**B)** ICD of CHIR8 and WiBi cells 2 months after transplantation in healthy motor cortex. **(C)–(G)** ICD of CHIR8 and WiBi fibers at different times post transplantation and in different regions, as indicated by labels. **(H)-(K)** Density of WiBi and CHIR8 fibers at a different distance from the graft, 1 **(H)** and 2 months **(K)** after transplantation. **(I, J, L, and M)** WiBi and CHIR8 fiber density in cortical **(I and L)** and extra-cortical **(J and M)** regions, 1 **(I and J)** and 2 months **(L and M)** after transplantation. *p < 0.05; **p < 0.01 (two-tailed Student's t test). n ≥3 transplanted animals for each time point were analyzed.*

5- Photothrombotic damage significantly enhances the ability of isocortical cells to extend long range projections

Despite the MCAO model seemed ideal to study prognostic biomarkers for long-term outcome, its variability may hamper studies aimed at revealing beneficial effects of a therapy. For this reason, in this second part of the study, we utilized a photothrombotic model of stroke, which is more reliable in terms of reproducibility of lesion location and functional deficit. In this case, cells were injected 3 days after inducing photothrombotic damage and their survival and pattern of axonal connectivity were analyzed one and two months after stroke (**Fig.7(B)–(N)**)**.** Both WiBi and CHIR8 cells integrated into the host tissue and were detectable at least two months after transplantation, expressing the neuronal marker NeuN. As when transplanted in healthy motor cortex, CHIR8 cells efficiently extended axons into both cortical and extra-cortical regions, one month (**Fig.7H–7J**) and two months (**Fig.7K–7M**) after transplantation. However, WiBi cells formed intra-cortical projections more efficiently than CHIR8 cells already one month after grafting (**Fig.7H and 7I**). This was paralleled by an enhanced ability of WiBi cells to target subcortical regions one month after transplantation.

Finally, the different behavior of WiBi and CHIR8 cells was even more striking considering the total amount of fibers in all the regions analyzed (**Fig.7N**). Interestingly, CHIR8 cells appeared to reach a plateau in projection density already one month after transplantation, and the total amount of fibers was not influenced by the ischemic insult, while WiBi cell projections increased with time and were specifically promoted by the lesion. To conclude, the photothrombotic damage further enhanced the process extension of WiBi cells, but CHIR8 and WiBi cells retained their cell autonomous ability to project toward specific cortical and extra-cortical targets.

The possibility to transplant into damaged cortex has opened new opportunities for therapeutic approaches. For this reason, we tested the impact of cell grafting on motor performance. WiBi cells were chosen to implant since they showed a better long term projection than CHIR8 cells in our stroke model. Thus, mice received WiBi cell transplantation 3 days after experimental stroke, and motor function was assessed longitudinally via the GridWalk test (Lai et al., 2015; Alia et al., 2016). We found that while the motor deficit remained stable in the mice treated with vehicle solution, grafted mice showed a decline (starting from 16 days post stroke) in the number of foot faults made with the contralesional forelimb, indicating functional restoration (**Fig.7O**). However, we speculate that this very early response did not depend on the specificity of WiBi cell target innervation compared with CHIR8 cell, since the differences between the two types of transplants emerged at later times (see Discussion).

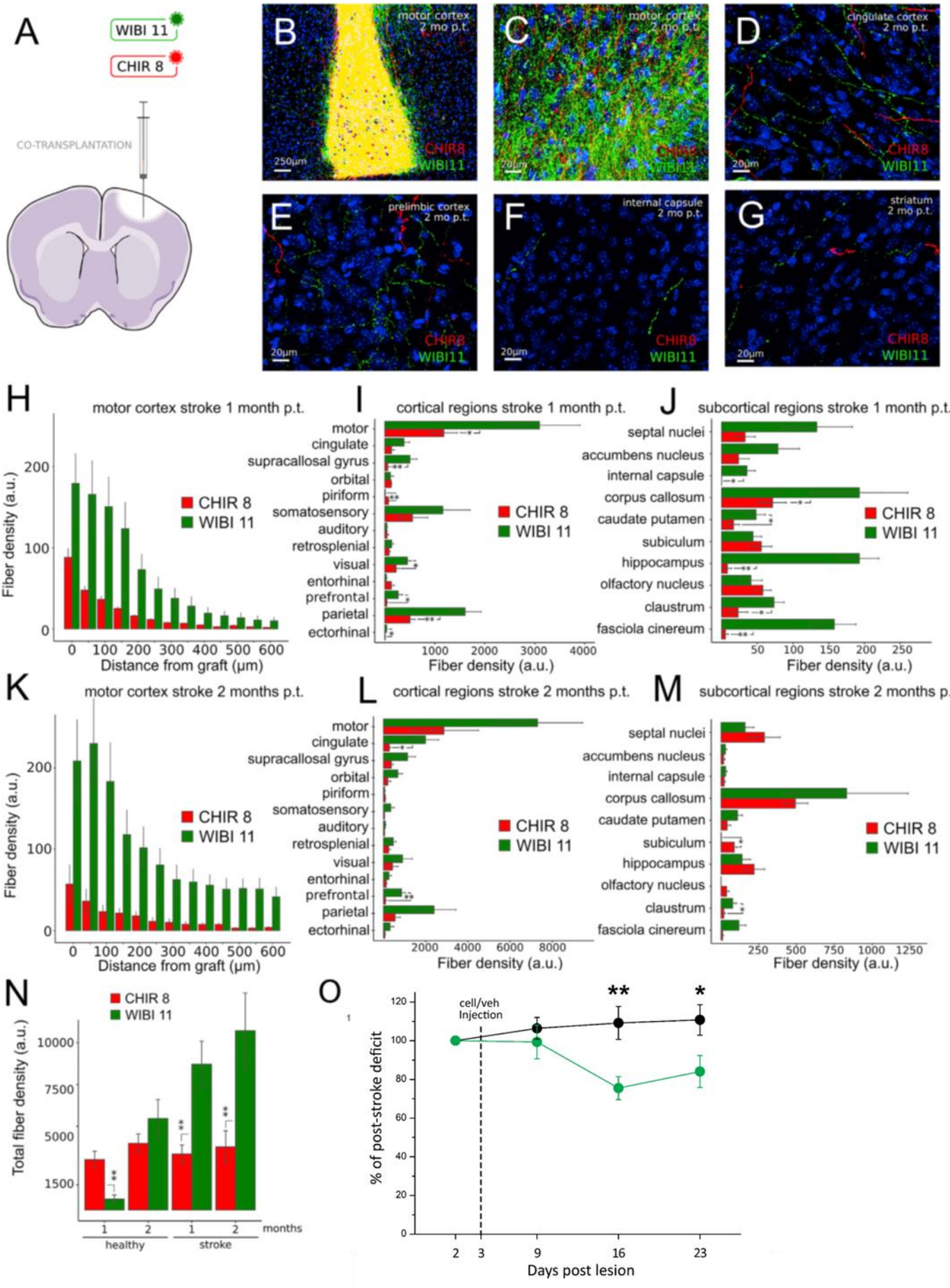
A
WIBI 11
CHIR 8
CO-TRANSPLANTATION
B
motor cortex
2 mo p.t.
250µm
CHIR8
WIBI11
C
motor cortex
2 mo p.t.
20µm
CHIR8
WIBI11
D
cingulate cortex
2 mo p.t.
20µm
CHIR8
WIBI11
E
prelimbic cortex
2 mo p.t.
20µm
CHIR8
WIBI11
F
internal capsule
2 mo p.t.
20µm
CHIR8
WIBI11
G
striatum
2 mo p.t.
20µm
CHIR8
WIBI11
H
motor cortex stroke 1 month p.t.
Fiber density (a.u.)
CHIR 8
WIBI 11
Distance from graft (µm)
I
cortical regions stroke 1 month p.t.
motor
cingulate
supracallosal gyrus
orbital
piriform
somatosensory
auditory
retrosplenial
visual
entorhinal
prefrontal
parietal
ectorhinal
CHIR 8
WIBI 11
Fiber density (a.u.)
J
subcortical regions stroke 1 month p.t.
septal nuclei
accumbens nucleus
internal capsule
corpus callosum
caudate putamen
subiculum
hippocampus
olfactory nucleus
claustrum
fasciola cinereum
CHIR 8
WIBI 11
Fiber density (a.u.)
K
motor cortex stroke 2 months p.t.
Fiber density (a.u.)
CHIR 8
WIBI 11
Distance from graft (µm)
L
cortical regions stroke 2 months p.t.
motor
cingulate
supracallosal gyrus
orbital
piriform
somatosensory
auditory
retrosplenial
visual
entorhinal
prefrontal
parietal
ectorhinal
CHIR 8
WIBI 11
Fiber density (a.u.)
M
subcortical regions stroke 2 months p.t.
septal nuclei
accumbens nucleus
internal capsule
corpus callosum
caudate putamen
subiculum
hippocampus
olfactory nucleus
claustrum
fasciola cinereum
CHIR 8
WIBI 11
Fiber density (a.u.)
N
CHIR 8
WIBI 11
Total fiber density (a.u.)
months
healthy
stroke
O
cell/veh
Injection
% of post-stroke deficit
Days post lesion

Figure 7: Cell Transplantation in the Ischemic Motor Cortex A) *Method and site of transplantation.* ***B)*** *ICD of CHIR8 and WiBi cells 2 months after transplantation in photothrombotic motor cortex.* ***(C)–(G)*** *ICD of CHIR8 and WiBi fibers at different times post transplantation and in different regions, as indicated by labels.* ***(H)-(K)*** *Density of WiBi and CHIR8 fibers at different distances from the graft, 1* ***(H)*** *and 2 months* ***(K)*** *after transplantation.* ***(I, J, L, and M)*** *WiBi and CHIR8 fiber density in cortical* ***(I and L)*** *and extra-cortical* ***(J and M)*** *regions, 1* ***(I and J)*** *and 2 months* ***(L and M)*** *after transplantation.* ***N)*** *Total fiber density of WiBi and CHIR8 cells in healthy and ischemic brains, 1 and 2 months after grafting. (I, J, and L–N) *p < 0.05; **p < 0.01 (two-tailed Student's t test); n >3 transplanted animals for each time point were analyzed.*
O) *Percentage of foot faults made with the contralesional forelimb in the gridwalk test. Values were normalized on the 2 days post stroke value (initial deficit before transplantation). After the injection of WiBi cells (green, n = 9) at day 3, mice showed a significant improvement in the motor performance compared with mice injected with vehicle (black, n = 5) (two-way repeated-measures ANOVA followed by Holm-Sidak method: **p< 0,01 p = 0.004; *p < 0,05 p = 0.015).*

6- Study of functional integration: ongoing experiments

To evaluate if the long-range projections can steer the activity of the host networks after stroke, suggesting a successful integration in the tissue, we are currently exploiting an optogenetic approach. Three days after stroke we injected mESC-derived neurons previously transfected with an Adeno-Associated viral vector carrying the gene of the transmembrane protein channelrodopsin 2 (ChR2) by using the protocol mentioned above. After three months, transplanted neurons were illuminated by using a blue light optic fiber placed above the transplant. Contextually, a 16-channels electrode was inserted in the perilesional and perigraft cortex. In this way, optogenetic stimulation was combined with electrophysiological recordings to study the functionality of the synapses formed by grafted cells with host neurons. A preliminary multi-unit analysis of spiking activity showed multi-units that enhance their firing rate during light stimulation. Considering their late latency and the location of the electrode, this response is supposed to be due, at least in part, to a post-synaptic activity of the host neurons. This hypothesis was confirmed by the fact that, after delivery of an AMPA receptor antagonist (NBQX), light-induced responses were reduced or totally abolished, suggesting that grafted neurons are functional and connected with the host. Future experiments will allow to better clarify these aspects.

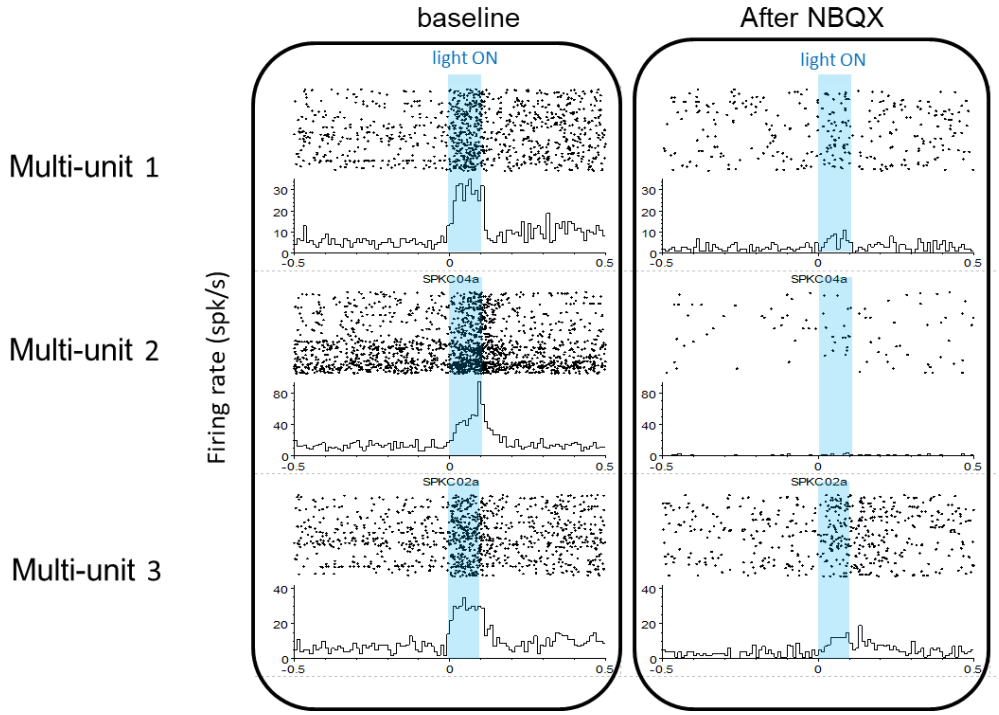

Figure 8: Multi-units spiking activity after transplanted mESCs-derived neurons
Three examples of multi-units spiking activity. During optogenetic light stimulation we observed an increased firing rate, then silenced or reduced by NBQX.

Discussion

Part 1

Assessing anatomical and behavioural biomarkers to predict motor recovery after MCAO-induced stroke

1- Anatomical and behavioral changes after MCAO-induced lesion

In humans, stroke is a very heterogeneous condition, which results in a wide spectrum of functional outcomes. To mimic these features, we needed a preclinical model characterized by such variability. For this reason, we set up in the laboratory a permanent MCAO model of focal stroke which has been previously published (Llovera et al. 2014). The MCAO procedure produced a large ischemic lesion, whose dimensions are consistent with what reported in literature (e.g. Llovera et al. 2014), however it varies significantly in terms of extension and location (**Fig. 1D**). A penumbra area is also present (Carmichael et al. 2005). Both these aspects make the MCAO model reminiscent of the human condition, compared to other models such as the photothrombosis.
Among different anatomical and structural changes induced by the brain lesion, we focused on the possible alterations of the CFA, indeed damages on the cortical representation of the contralateral forelimb movement is expected to be reflected in motor functional impairments. In order to characterize CFA alterations, a novel quantitative method has been developed to evaluate not only the direct damage on the CFA, but also to take in consideration damages that can be derived from the shrinkage of the tissue.
We demonstrated that the focal site of the lesion involved predominantly somatosensory areas, whereas the motor areas, including the CFA, were only partially affected or represented a perilesional site. Indeed, a robust damage in the CFA has been found only in a minority of animals that presented a larger lesion. The linear correlation analysis demonstrated a strong and positive dependence between lesion volume and the percentage of lesioned CFA (**Fig.4D**). Moreover, even in absence of an evident histological deficit, a functional impairment of the CFA can be associated with the distortion caused by cortical shrinkage. Indeed, the cortical shrinkage not only positively correlated with lesion volume but resulted increased in those animals with robust CFA damage (**Fig.3**). As expected, we also found that the shrinkage of CFA region was significantly higher in animals with a lesioned CFA and correlated with lesion volume, although with a lower coefficient (**Fig.6**)

Consistently with previous works (Stinear et al., 2006; Schaechter et al., 2009; Sterr et al., 2010; Byblow et al 2015; Puig et al., 2013; Stinear et al.,2014; Sterr et al., 2014; Puig et al., 2017), we found that the integrity of motor fibers was affected by cortical lesion. Indeed, MCAO-induced lesion produced an imbalance in the integrity of the white matter, between the ipsilesional and the contralesional hemisphere of lesioned animals. These structural changes were statistically significant both in the external and the internal capsule, two important white matter tracts, suggesting the presence of a consistent damage (**Fig.8**).

These anatomical and structural alterations reflected, indeed, a deficit in the contralateral forelimb motor function. Permanent MCAO determined a clear motor deficit at the level of the contralesional forelimb, as we observed in the GridWalk test (**Fig. 10A**). Considering that the lesion affects mainly somatosensory regions, a motor deficit could be unexpected. However, this can be explained by the fact that primary motor cortex, even if not primarily affected, is located in the lesion periphery (in case of largest lesions), or in the perilesional site, where we still detected indirect effect of the stroke. In fact, a quantitative analysis of the neuronal density in the CFA reveled a significant decrease in the number of neurons per mm^2 in the ipsilesional side with respect to the contralateral one, suggesting a possible indirect structural damage that could in part have a role in the observed impairment of motor functions (**Fig.7**).
Another possibility is to consider the high grade of overlap between somatosensory and motor cortex in rodents, where these two areas are less segregated than in primates (Peters et al. 2017). In addition, it is known that the primary somatosensory and primary motor cortices are reciprocally connected. S1 input to pyramidal cells of M1 possesses synaptic and anatomical characteristics ideal for the delivery of strong impulses that can "drive" postsynaptic M1 cells, thereby potentially affecting their output (Petrof et al. 2015). Interestingly, Mathis and collaborators showed that temporally precise photoinhibition of somatosensory cortex applied concurrently with the “perturbation” during a unimanual motor task hampered adaptation of the movement (Mathis et al. 2017). This presumptive function of somatosensory cortex in contributing to motor adaptation may explain other aspects of motor deficit in the MCAO model (see below).

Interestingly, we observed also a progressive impairment of the healthy forelimb (**Fig.10B**). To our knowledge, this aspect has not been reported in the literature so far, thus it constitutes a novel phenomenon that deserves further investigation. The impairment in the healthy forelimb has been observed also by clinicians (F. Molteni, personal communication), but no publications have described it yet. Considering that this deficit progressively develops in time, it is not reasonable to consider immediate and direct effects of stroke induction as the main cause. On the other hand, we speculate that maladaptive plasticity could play a role. It is known that, although some neural plasticity undoubtedly contributes to motor recovery after stroke, injury drives neural plasticity in a maladaptive direction (Takeuchi and Izumi, 2012). For instance, it is common in stroke patients with severe impairment that compensatory or substitutive movements of the less-affected body side are exploited to maximize functional ability. Although compensatory movements may help stroke patients in performing tasks in the short term, the presence of compensation may be associated with long-term problems such as reduced range of joint motion and pain. Specifically, the compensatory use of the healthy part of the body could lead, in the long term, to aberrant motor patterns that result detrimental for global motion.

Following MCAO, forelimb motor deficit extends beyond what can be assessed by means of GridWalk test, in fact we could measure an impairment in the performance, during fine grasping behavior by means of the skilled reaching test. As expected the number of correct movements resulted dramatically decreased in MCAO animals compared with sham animals in which the movements remained unaltered (**Fig.9A**). We also qualitatively observed an increase in “clumsy movements”, in which the animal is not able to grasp the pellet or even to center the frontal aperture (**Fig.9B**). The quality of the movement is not coherent with a paresis of the forelimb. Instead, it is reasonable to conceive a more general defect in sensorimotor coordination. Considering the different kind of fine forelimb movements (correct or not) that animals can realize, a cumulative score has been used to show the trend of motor performance over time (**Fig.9C**). This method allowed to clearly demonstrate a

significant decrease after the lesion that was progressively followed by spontaneous recovery in a chronic phase. This is in keeping with the idea that a damage of somatosensory areas may deprive motor cortex of important inputs for motor adaptation and coordination (Mathis et al. 2017) but that subsequent plastic phenomena can improve the overall function probably via recruiting compensatory strategies.
We also utilized the M-platform to characterize the motor deficit associated with MCAO (Spalletti et al. 2014). In this case, the M-platform was not used for rehabilitation, instead, we exploited this tool for its ability to extract kinetic and kinematic parameters of the retraction movement. Also, the M-platform allows to perform an isometric task, which provides additional parameters associated with the maximal force the animals is able to generate. Kinetic and kinematic features of the motor performance during robotic tasks showed a large variability of motor outcome in the late phase, with a complete, mild or without any degree of recovery (**Fig. 11 and 12**). Together with a deficit in the performance of MCAO group on the robotic platform we observed an increase in the performance of sham animals probably due to learning. However, the deficit in the performance on the robotic platform, resulted limited when compared to other models, such as the photothrombosis (Spalletti et al. 2017). This is in line with our behavioural observations, which lead us to conclude that MCAO may cause a deficit that involves mainly fine aspects of movement.
To further confirm this hypothesis, more refined methods of behavioural analysis could be performed. For instance, Lai and collaborators (2015) developed a semi-automated algorithm for tracking forepaw movements in mice during the execution of the skilled reaching test. This methodology would allow to calculate several kinematic measures for the quantitative assessment of performance, hence it would also be able to reveal more subtle aspects.

Mimicking clinical scale for humans, in this thesis we also implemented a novel global motor score (**Fig.13 and 14**) accounting for all the motor performance evaluated in the single motor tests. This general motor score showed a significant drop in the overall motor performance of MCAO mice, in respect with both baseline condition and sham animals. Consistent with the functional improvement observed in the skilled reaching test and in some kinetic parameters relative to the robotic task, MCAO mice showed a significant increment in their performance at 30 days post lesion (**Fig.14**).

2- Investigations on post-stroke recovery and preliminary correlation analysis

Proportional recovery has become a central aspect of research on post-stroke rehabilitation and therapy. Despite it is a well-recognized phenomenon, a relevant proportion of severe patients do not follow this rule (Hope et al., 2018). Discovering why this happens and how we can predict this condition are very intriguing questions. In this project, we laid the bases to investigate biomarkers that can help predicting whether significant post-stroke recover will occur or not. As a matter of fact, if proportional recovery is valid also in animal models has been poorly addressed so far (Jeffers et al., 2018). Indeed, recently, a study with a large cohort of rats was performed in order to assess the presence of proportional recovery after enodothelin-1 induced stroke. They found that proportional recovery exists with a degree of improvement that is similar to that one observed in humans. However, only a few proportion of animals (30%) demonstrated proportional recovery, while in humans a largest population (80%) of proportional recovers was reported. Among predictive biomarkers

they identified the milder initial post-stroke impairment, smaller infarct volumes, and the cortical damage, demonstrating the concordance between humans and rat. The same biomarkers were investigated also in this project, finding promising results in line with this previous work (Jeffers et al., 2018).

First, we checked whether MCAO mice show different inter-individual degrees of recovery. With this purpose, we implemented a clinical-like scale which combines our behavioural tests and gives a more comprehensive view of motor performance. By using this global scale, we found an interesting segregation into recovers and poor recovers that seems to recapitulate what happens in human patients (**Fig. 15A**). Normalizing these data on the initial deficit, we found that some stroke animals recovered well and sometimes did better than on baseline condition, while others maintained their deficits or even got worse (**Fig.15B**).
Taking advantage of this observed variability, we conducted a preliminary correlation analysis between anatomical measures and indices of motor performance in our set of behavioural tests. The first aspect emerging from our data was that the lesion extension, and particularly the eventual involvement of the CFA, can give valuable prediction of motor performance in the skilled reaching test. The correlation among behavioural impairments and anatomical changes reveled that both volume and percentage of the damaged CFA influenced the finer motor movement assessed by the reaching score, while we failed to detect robust correlations with tests that assessed general coordination (e.g. GridWalk) (**Fig.16-17**).
Interestingly this correlation was even stronger if we took into consideration only the animals that have a damaged CFA, leading the hypothesis that a damage in the CFA strongly impairs finer motor movements while general coordination could be also controlled by other spared areas. More complex was the situation if we took into consideration animals that had a lesion only in the somatosensory area. The complete lack of correlation among any parameter tested and both the acute and chronic performance in different behavioral tests on animals that received a lesion only in the somatosensory area, suggests a highly variable motor impairment that seems to rely more on the quality and not on the quantity of the damaged connections. More interesting was the finding that the extent of the acute deficit is a good predictor for the late motor performance - both considering the reaching test and the global motor score (**Fig.16**). In conclusion we found that quantitative anatomical parameters like the volume of the lesion and the percentage of the affected CFA are able to predict motor recovery of skilled movement when a lesion on the MCA territory affects the primary motor cortex in mice. These results further increased our knowledge on the mechanisms used by the central nervous system to reorganize and rewire the spared motor areas following a stroke, and, could contribute to find reliable biomarkers with high translational potential to predict functional recovery in stroke. However additional analyses are needed to assess the predictive power of our parameters.

3- Investigation of post-stroke electrophysiological alterations

In parallel with behavioural tests, we performed also electrophysiological measures both in freely moving condition and during the retraction task onto the M-platform.
For the freely moving condition, we performed a standard analysis of the relative power of electrophysiological spectral bands (**Fig.20**). We observed affected hemisphere-specific alterations in the power spectrum, in particular a decrease in the beta and theta bands and an increase in the delta band. It has been usually reported, both in humans and in rodents,

that an increase in slow waves and a decrease in rapid waves take place after stroke, i.e. increment of delta band and decline of beta bands observed in our experiments. These results were generally consistent with the data reported in the literature. However, human data often report changes in the alpha band (Faught 1993; Moyanova et al 1998; Finnigan 2007; Luu et al 2001) that was unaltered in my dataset. However, in humans these measures usually represent global indices, i.e. are averaged over the entire set of EEG electrodes, so they can mask some site specific-alterations. For what concerns rodents, in which the small dimensions allow the use of a limited number of electrodes, many studies have focused on the transient model of MCAO, which produces a lesion that involves a great portion of the striatum. This difference with the permanent MCAO model, in which the lesion is confined to the cortex, might account for some model-specific alterations. To our knowledge, few works have been published on the permanent MCAO model (Luu et al., 2001; Lammer et al. 2011). Even in these cases, the expected delta increase and alpha decrease were observed. In Lammer et al., electrodes were inserted directly in the ischemic tissue. Interestingly, at the same time points, the authors could not detect any alterations for the above-mentioned spectral bands when the signal was recorded from electrodes in proximity to the lesion, but outside of it. In this work, no data are reported about theta and beta bands. Instead, Luu et al., they considered different cortical regions and reported that the most important changes occurred in the acute phase of permanent MCAO. Specifically, they found an increase in the delta power accompanied by compensatory decreases in theta, alpha, and beta power. The temporal progression of power distribution varied by cortical regions. For example, by day 7, delta power for pMCAO was still moderately elevated while theta and beta power recovered to approximately 90% of baseline activity in most cortical regions. However, in the ischemic core temporal regions, the alpha power never fully recovered and remained at approximately 60% of the control level. In our view, the apparent discrepancy between our data and the literature is easily reconcilable, when considering the different areas where recording electrodes were placed. Moreover, when we considered the power spectral density analysis during the retraction task, a consistent decrease of alpha band was observed, highlighting how this change is more related to a specific motor performance.

Indeed, we also expanded the repertoire of electrophysiological parameters, characterising the power spectrum changes and the event-related potential of the retraction movement onto the M-platform. First, we analyzed the baseline condition by including all animals. In this case, we observed a movement-related theta synchronization and beta and gamma desynchronization (**Fig. 21**). In humans, it is well established that beta desynchronization occurs during the movement execution, which is consistent with our results (Pfurtscheller and Lopes da Silva, 1999; Pfurtscheller et al., 2003). Beta oscillations have also been linked to the processing of rewards. In a magnetoencephalography (MEG) study of healthy individuals exerting physical effort on a hand grip device to win monetary rewards, the level of beta desynchronization was positively associated with incentive level and a decrease in rest duration, suggesting that beta desynchronization may act as a mechanism that speeds the initiation of effort production in the presence of greater rewards (Meyniel and Pessiglione, 2014). On the contrary, an increase in high gamma synchronization is reported (Nowak et al. 2018). Recently, progress has been made to understand the precise roles of oscillations at different frequencies and their cross-frequency coupling in neural circuit function. Slow (30–50 Hz) and fast (60–120 Hz) gamma bands are sometimes accompanied, or nested hierarchically, by lower-frequency oscillations in the theta band (4–10 Hz) especially in memory-related cortical areas, including hippocampus (Lisman and Redish, 2009). In a study on rats, LFPs were recorded during a push-hold-and-pull movement of a lever, the authors observed the expected increase of the fast gamma band

but, interestingly, a decrease of slow gamma (30-50 Hz), which is in keeping with our observations. Furthermore, they observed also an increase in theta synchronization, which gamma oscillations appear to be nested in (Igarashi et al. 2013). Normally, theta power increases as a result of attention demanding processes preceding movement onset (Popivanov et al., 1999; Turak et al., 2001; Tsujimoto et al., 2006; Christie and Tata, 2009) and during reward presentation and motor initiation in response to reward (Zhu et al., 2019). Overall, our electrophysiological characterization is in line with previous evidence.

After stroke induction, some alterations in bands (de)synchronization took place (**Fig. 22**).
Regarding theta oscillations, little is known about their function in the motor system. Some evidence suggests a role of theta oscillations in the temporal control of action in mammals, however these studies are focused on the medial frontal area and not on the primary motor cortex (Emmons et al. 2016). Hence, how theta oscillations alterations reflect some specific neural phenomena is still unexplored. However, it has been showed that theta oscillatory power was increased by the GABAA receptor antagonists, such as gabazine and picrotoxin, in *in vitro* brain slice. By contrast gamma oscillatory power in M1 was significantly reduced by the $GABA_A$ antagonists gabazine and picrotoxin indicating dependence on and inhibitory synaptic transmission (Johnson et al. 2017). These data are consistent with the decrease, after stroke, of theta band in freely moving condition and with the known inhibitory components of gamma oscillations. However, the precise role of gamma oscillation is still controversial.
The studies of the last years, among the various evidences, have shown that the synchronized oscillations in the highest gamma frequency (60-90 Hz), occur immediately before the beginning of the movement and during the execution of the movement itself. This "motion-related gamma synchronization" seems to reflect the initial activation of primitive motor neurons that make movement possible (Gaetz et al., 2013;Cheyne and Ferrari, 2017). In humans, driving higher range oscillations seems to facilitate motor performance (Joundi et al., 2012); therefore, the role of high frequency synchronized oscillations is to favor plasticity and motor control (Uhlhaas et al., 2011).
In humans, a stroke in the middle cerebral artery territory provokes acute alterations of the neural rhythmic activity at rest in both the damaged and contralesional brain hemisphere (Tecchio et al. 2007). In particular, gamma activity reduction has been recorded in stroke patients together with reduced hand functionality. Lower gamma-band cortico-muscular coherence in performing a reaching task was found in poorly rehabilitated stroke survivors with permanent upper-limb motor deficits. These evidences reveal poor brain-muscle communication (poor EEG-EMG coherence) and poor integration of the signals from the two sources. This “incoherence” could be one of the fundamental mechanisms involved in the failure of the performance (Fang et al., 2009). By contrast, increase in gamma power in the impaired hemisphere was related to a higher probability of total recovery (Tecchio et al. 2007). This seems in contrast with our results. However, it has been demonstrated a direct link between the oscillations in the gamma band and the balance between excitation and inhibition within mutually connected networks of GABAergic interneurons and pyramidal cells localized in the primary motor cortex (Hall et al.2011; Gaetz et al. 2011; Buzsàki and Wang, 2012;). In this perspective and with this background, other studies have suggested that parvalbumin-positive fast-spiking interneurons could be a key tool in this field because they have a central role in gamma band rhythm generation and modulation (Sohal et al. 2009; Cardin et al.2009).
In line with these findings, GABAergic interneuronal activity is known to be critically affected after stroke, particularly it has been shown that GABAergic tone increases after stroke (Clarkson et al. 2010). Thus, our electrophysiological observation might reflect this

underlying alteration of the inhibitory network. On this point, it remains to be assessed if this alteration regards a precise subpopulation of interneurons (e.g. parvalbumin, somatostatin, etc…) or a specific transmission "modality", i.e. tonic vs. phasic signaling. Recently parvalbumin-expressing interneurons have been correlated to spontaneous gamma oscillations, at least in the visual cortex (Chen et al., 2017).
Together with previous finding about theta modulation, it is tempting to hypothesize a role of inhibitory signaling in the observed MCAO-induced alterations.
We characterized also the event-related potential (ERP) associated with forelimb retraction (**Fig. 23**). Even in this case, we observed clear alterations after stroke especially in the affected hemisphere (**Fig. 24A**). In particular, the reduced amplitude of the peaks could be associated with a damage of feedforward connections from the somatosensory cortex (Petrof et al. 2015). Alternatively, we could hypothesize a difficulty in neural recruitment, owing to an excessive inhibitory tone. On the other hand, the constancy in latency values seems to exclude a problem in the velocity of signal transmission (**Fig. 24C-D**).

I now plan to use this large set of electrophysiological data for establishing correlations with both the initial and chronic motor deficit in individual stroke mice. Hopefully, this analysis may reveal early electrophysiological signatures that allow to distinguish "good" and "poor" recovers. In the future, I am planning to analyze also inter-hemispheric interactions, which can be easily implemented given our set up of bilateral electrode recordings. Specifically, we are planning to exploit several quantitative methods of time series analysis (cross-correlation, mutual information and Granger causality analysis) to monitor longitudinal changes in the cross-talk between hemispheres, as already performed by Vallone and collaborators in the photothrombotic model (Vallone et al. 2016). This way, I expect to gain more insights on the role of inter-hemispheric communications in this particular model and extract other parameters to feed in our correlation analysis.

Altogether, these results highlight the potentiality of structural and functional biomarkers to predict the extent of recovery from upper-limb impairment. Considering the great effort employed to identify effective therapy strategies, these data could optimize clinical study.

Part 2

Development of a novel cell-based therapy option for post-stroke treatment

1- Generation of neurons with specific molecular identity

For the second part of the PhD project, we characterized the therapeutic potential of *in vitro* generated neurons to promote functional recovery after stroke. In this study, we preferred the use of the photothrombotic model, which is more reproducible, especially in terms of lesion location and extensions. For our purposes, this aspect was crucial in order to perform transplantations always in the same sites relatively to lesion location.
The differentiation protocol designed by our collaborators allows to reliably produce neurons of specific regional identity, i.e. cortical excitatory neurons and hippocampal neurons. So far, a limited number of studies have addressed the problem of specific regionalization (Kokaia et al. 2017). A number of studies focused on the signaling required in vitro to steer the positional identity of neural precursor cells. Both mouse and human ESCs, or induced pluripotent stem cells (iPSCs), expressed markers of dorsal telencephalic identity upon inhibition of Wnt signaling, or combined Wnt/BMP inhibition, during in vitro neutralization (Bertacchi et al., 2015; Chambers et al., 2009; Espuny-Camacho et al., 2013; Mariani et al., 2012; Shi et al., 2012) (**Fig.1**). However, many of the markers used to ascertain the positional identity of in vitro differentiated cells (e.g., Emx2, Foxg1, Tbr1, Ctip2, Satb2) are co-expressed by cortical and hippocampal precursors or neurons (Bulfone et al., 1995; Fukuchi-Shimogori and Grove, 2003; Gyorgy et al., 2008; Hebert and McConnell, 2000; Nielsen et al., 2010), and the exact identity (isocortical versus hippocampal) of the neurons generated in vitro in these studies could not precisely be established.

For this reason, we aimed at precisely identify the molecular identity of our in vitro generated neural progenitor and precursor cells. The analysis of specific markers of hippocampal versus isocortical differentiation, and the comparison of the global gene expression profiles of in vitro differentiated cells and of a number of embryonic regions, allowed us to identify a mechanism that is sufficient to refine the dorsal telencephalic positional differentiation. Our results indicate that in a specific time window, which corresponds to DIV8 of our protocol of neuralization, cells can acquire either an isocortical or a hippocampal molecular identity, depending on the degree of Wnt signaling at that time. Markers that show that graded expression levels between the embryonic hippocampus (Lhx9, Lhx2, Lef1, Lmo4) and isocortex (Lmo3) were differentially expressed by WiBi and CHIR8 cells. Moreover, the global gene expression profiles of WiBi and CHIR8 cells clustered with embryonic isocortex and hippocampus, respectively (**Fig.2**). Wnt signaling de-inhibition before DIV8, or later than DIV9, failed to induce a hippocampal gene expression profile, indicating the existence of a time window of cellular competence for the induction of hippocampal identity.

2- Transplantation in healthy and lesioned brain

Both WiBi and CHIR8 precursors survived and fully differentiated in mature neurons after grafting in adult hippocampus and isocortex. However, they showed different capacity for axonal projection. In intact hippocampus, only grafted hippocampal cells were able to extend long-range projections, while isocortical cells failed in sending far-reaching processes (**Fig. 4**). This axonal projection became more robust over time, as shown by the dramatic enhancement of fiber density 2 months versus 1 month after transplant. At least a subpopulation (about 30%) of CHIR8 cells displayed markers of DG granule cells, such as CALB1, and contacted proper targets of adult DG neurons, such as CA3 (**Fig. 5**).

ESC-derived isocortical cells transplanted into either intact or photothrombotic motor cortex failed in sending projections to thalamic nuclei and midbrain, according to previous observations (Michelsen et al., 2015). In addition, a significant number of processes were found in the internal capsule of photothrombotic brains one month after stroke. Based on these observations, we might speculate that our cells acquired a motor identity. However, we cannot exclude that they might simply have maintained a general isocortical identity and that a further specification step would have been required to generate also thalamic and midbrain projections. Their layer identity remains to be assessed, but we speculate that a majority of them differentiated as deep-layer neurons, because at the time of their transplantation they were mostly expressing TBR1 and CTIP2 markers (**Fig. 2C**).

The results obtained after transplantation in photothrombotic motor cortex indicate that the normal cortical environment retains some cues inhibiting the extension of new processes from WiBi cells and that such cues are somehow removed after the photothrombotic damage. However, it is interesting to note that, after a first early phase when WiBi processes were much denser than CHIR8 processes both in cortical and extra-cortical regions one month after grafting, two months after, the density of CHIR8 fibers in hippocampus and septal nuclei was significantly higher than the density of WiBi processes. We speculate that, in addition to a differential capacity of axonal extension, WiBi and CHIR8 cells hold some ability in selecting specific targets of innervation that is refined over time. This is also supported by the observation that WiBi processes were less dense than CHIR8 processes in healthy motor cortex and corpus callosum one month after graft, but they increase dramatically at 2 months. These data suggest that isocortical and hippocampal cells display different degrees of axonal pruning/ plasticity in specific brain regions.

Altogether, our observations indicate that the distinct molecular identities acquired by CHIR8 and WiBi cells paralleled their different behavior after transplantation and suggest that WiBi and CHIR8 cells might be very similar to naive isocortical and hippocampal precursor cells respectively. A number of experiments of grafting into mouse isocortex of either fetal cells or neural precursors originated in vitro by pluripotent cells have been performed. Overall, these studies show that embryonic or fetal neural precursors transplanted in the intact adult hippocampus integrate efficiently in the host circuitry and contact the correct target in the host tissue displaying specific patterns of long range projections, whereas the intact adult cortical parenchyma appears to be poorly permissive with the transplanted cells (Avaliani et al., 2014; Fricker-Gates et al., 2002; Gage et al., 1995; Guitet et al., 1994; Rosario et al., 1997; Sheen et al., 1999; Shetty and Turner, 1996; Shin et al., 2000). Indeed, this behavior suits well with the natural capability of the hippocampal niche, unlike the cortical environment, to support adult neurogenesis.

In addition, several studies reported that experimentally induced cortical damage (e.g., aspiration, experimental ischemia, or chemically induced neurodegeneration) resulted in functional integration and higher connectivity of the transplanted cells, thus suggesting the

existence of inhibitory cues in the healthy isocortex removed by the lesion (Espuny-Camacho et al., 2013; Falkner et al., 2016; Gaillard et al., 2007; Michelsen et al., 2015; Tornero et al., 2013). Our results, which are consistent with these observations, indicate that the inhibitory effect of the intact cortical environment affects isocortical but not hippocampal cells, although the signals mediating such inhibition are currently unknown. The possibility to successfully transplant neural precursors originated in vitro from ESCs or iPSCs into damaged isocortex has opened new opportunities for therapeutic approaches for cortical stroke. Previous studies have highlighted that transplantation of different cell types induce amelioration of motor symptoms. However, the early appearance of functional improvements can be hardly explained by the replacement of lost neurons by the transplanted ones. Here, we showed that grafting WiBi cells promoted some functional restoration of forelimb function after ischemic damage to the motor cortex. Improvements in motor output were already apparent as early as 16 days after stroke, suggesting that, in addition to network rewiring due to axon extension by the transplanted cells, bystander effects (e.g., release of trophic factors, modulation of inflammation; Borlongan et al., 1998; Chen et al., 2003; Lee et al., 2008; George and Steinberg, 2015) likely play a key role in the observed recovery (**Fig.7O**). Finally, we speculate that the specificity of innervation that we found for WiBi and CHIR8 cells might affect later processes of motor recovery. These and other functional aspects of cell transplantation in ischemic motor cortex are currently under investigation.

The results obtained from the projection analysis clearly indicate that our in vitro protocol is effective at generate neuronal populations that maintained their different molecular identity also when transplanted in vivo. Since the final goal of neuroscientists working in cell therapy for brain diseases is to restore injured neural circuits, we can speculate that these data represents promising results for the clinical use by means of IPSC. For this reason, we are planning to significantly modify our transplantation protocol. Firstly, we will implant a lower number of cells and we will perform multiple injections sites: this way, we expect to abolish or at least reduce the bystander effect and, at the same time, favour neurons integration in the surrounding tissue. In addition, we will implement a double (excitatory/inhibitory – DREADD/KORD, Vardy et al., 2015) chemogenetic approach to modulate grafted neurons activity. In particular, we will selectively stimulate them in phase with a rehabilitative motor task execution (skilled reaching or retraction onto the M-platform). Due to Hebbian plasticity, this strategy is expected to guide their proper integration into spared cortical networks, thus improving functional recovery. Finally, their acute silencing at the completion of rehabilitation will unambiguously demonstrate their role in functional recovery, inducing a re-establishment of the motor deficit.

In parallel, to directly demonstrate the integration of grafted cells in the host circuitry, we are currently exploiting the transplantation of channelrhodopsin-expressing neurons and assessing their functional electrophysiological communication with the surrounding neural tissue. By using optogenetic stimulation and high-resolution electrophysiology, I plan to evaluate whether these cells generate action potentials and send information to post-synaptic partners. Preliminary data support this view are reported in Figure 8.

Bibliography

Agius Anastasi A, Falzon O, Camilleri K, Vella M, Muscat R. 2017. Brain Symmetry Index in Healthy and Stroke Patients for Assessment and Prognosis. Stroke Res Treat. 2017:8276136.

Aisen ML, Krebs HI, Hogan N, McDowell F, Volpe BT. 1997. The Effect of Robot-Assisted Therapy and Rehabilitative Training on Motor Recovery Following Stroke. Arch Neurol. 54:443–446.

Alexandrov A V, Burgin WS, Demchuk AM, El-Mitwalli A, Grotta JC. 2001. Speed of intracranial clot lysis with intravenous tissue plasminogen activator therapy: sonographic classification and short-term improvement. Circulation. 103:2897–2902.

Alia C, Spalletti C, Lai S, Panarese A, Micera S, Caleo M. 2016. Reducing GABAA-mediated inhibition improves forelimb motor function after focal cortical stroke in mice. Sci Rep. 6:37823.

Alia C, Terrigno M, Busti I, Cremisi F, Caleo M. 2019. Pluripotent Stem Cells for Brain Repair: Protocols and Preclinical Applications in Cortical and Hippocampal Pathologies. Front Neurosci. 13:684.

Almeida A, Delgado-Esteban M, Bolaños JP, Medina JM. 2002. Oxygen and glucose deprivation induces mitochondrial dysfunction and oxidative stress in neurones but not in astrocytes in primary culture. J Neurochem. 81:207–217.

Alstermark B, Ogawa J. 2004. In Vivo Recordings of Bulbospinal Excitation in Adult Mouse Forelimb Motoneurons. J Neurophysiol. 92:1958–1962.

Alstermark B, Ogawa J, Isa T. 2004. Lack of Monosynaptic Corticomotoneuronal EPSPs in Rats: Disynaptic EPSPs Mediated Via Reticulospinal Neurons and Polysynaptic EPSPs Via Segmental Interneurons. J Neurophysiol. 91:1832–1839.

Andrew James G, Lu Z-L, VanMeter JW, Sathian K, Hu XP, Butler AJ. 2009. Changes in Resting State Effective Connectivity in the Motor Network Following Rehabilitation of Upper Extremity Poststroke Paresis. Top Stroke Rehabil. 16:270–281.

Arumugam T V., Baik S-H, Balaganapathy P, Sobey CG, Mattson MP, Jo D-G. 2018. Notch signaling and neuronal death in stroke. Prog Neurobiol. 165–167:103–116.

Assenza G, Zappasodi F, Pasqualetti P, Vernieri F, Tecchio F. 2013. A contralesional EEG power increase mediated by interhemispheric disconnection provides negative prognosis in acute stroke. Restor Neurol Neurosci. 31:177–188.

Avaliani N, Sørensen AT, Ledri M, Bengzon J, Koch P, Brüstle O, Deisseroth K, Andersson M, Kokaia M. 2014. Optogenetics Reveal Delayed Afferent Synaptogenesis on Grafted Human-Induced Pluripotent Stem Cell-Derived Neural Progenitors. Stem Cells. 32:3088–3098.

Baldassarre A, Ramsey LE, Siegel JS, Shulman GL, Corbetta M. 2016. Brain connectivity and neurological disorders after stroke. Curr Opin Neurol. 29:706–713.

Barker AT, Jalinous R, Freeston IL. 1985. Non-invasive magnetic stimulation of human motor cortex. Lancet (London, England). 1:1106–1107.

Barreca S, Wolf SL, Fasoli S, Bohannon R. 2003. Treatment Interventions for the Paretic Upper Limb of Stroke Survivors: A Critical Review. Neurorehabil Neural Repair. 17:220–226.

Basic Kes V, Simundic A-M, Nikolac N, Topic E, Demarin V. 2008. Pro-inflammatory and anti-inflammatory cytokines in acute ischemic stroke and their relation to early neurological deficit and stroke outcome. Clin Biochem. 41:1330–1334.

Bembenek JP, Kurczych K, Karli Nski M, Czlonkowska A. 2012. The prognostic value of motor-evoked potentials in motor recovery and functional outcome after stroke − a systematic review of the literature. Funct Neurol. 27:79–84.

Berkhemer OA, et al., 2015. A Randomized Trial of Intraarterial Treatment for Acute Ischemic Stroke. N Engl J Med. 372:11–20.

Bernhardt J, Borschmann K, Boyd L, Carmichael ST, Corbett D, Cramer SC, Hoffmann T, Kwakkel G, Savitz S, Saposnik G, Walker M, Ward N. 2017. Moving Rehabilitation Research Forward: Developing Consensus Statements for Rehabilitation and Recovery Research. Neurorehabil Neural Repair. 31:694–698.

Bernhardt J, Hayward KS, Kwakkel G, Ward NS, Wolf SL, Borschmann K, Krakauer JW, Boyd LA, Carmichael ST, Corbett D, Cramer SC. 2017a. Agreed definitions and a shared vision for new standards in stroke recovery research: The Stroke Recovery and Rehabilitation Roundtable taskforce. Int J Stroke. 12:444–450.

Bertacchi M, Pandolfini L, D'Onofrio M, Brandi R, Cremisi F. 2015. The double inhibition of endogenously produced BMP and Wnt factors synergistically triggers dorsal telencephalic differentiation of mouse ES cells. Dev Neurobiol. 75:66–79.

Biernaskie J, Chernenko G, Corbett D. 2004. Efficacy of rehabilitative experience declines with time after focal ischemic brain injury. J Neurosci. 24:1245–1254.

Biernaskie J, Szymanska A, Windle V, Corbett D. 2005. Bi-hemispheric contribution to functional motor recovery of the affected forelimb following focal ischemic brain injury in rats. Eur J Neurosci. 21:989–999.

Bigourdan A, Munsch F, Coupé P, Guttmann CRG, Sagnier S, Renou P, Debruxelles S, Poli M, Dousset V, Sibon I, Tourdias T. 2016. Early Fiber Number Ratio Is a Surrogate of Corticospinal Tract Integrity and Predicts Motor Recovery After Stroke. Stroke. 47:1053–1059.

Binkofski F, Seitz RJ, Arnold S, Classen J, Benecke R, Freund H-J. 1996. Thalamic metabolism and corticospinal tract integrity determine motor recovery in stroke. Ann Neurol. 39:460–470.

Bodmer B, Beste C. 2017. On the dependence of response inhibition processes on sensory modality. Hum Brain Mapp. 38:1941–1951.

Boggio PS, Nunes A, Rigonatti SP, Nitsche MA, Pascual-Leone A, Fregni F. 2007. Repeated sessions of noninvasive brain DC stimulation is associated with motor function improvement in stroke patients. Restor Neurol Neurosci. 25:123–129.

Borlongan C V, Tajima Y, Trojanowski JQ, Lee VM, Sanberg PR. 1998. Cerebral ischemia and CNS transplantation: differential effects of grafted fetal rat striatal cells and human neurons derived from a clonal cell line. Neuroreport. 9:3703–3709.

Boyd LA, Hayward KS, Ward NS, Stinear CM, Rosso C, Fisher RJ, Carter AR, Leff AP, Copland DA, Carey LM, Cohen LG, Basso DM, Maguire JM, Cramer SC. 2017. Biomarkers of stroke recovery: Consensus-based core recommendations from the Stroke Recovery and Rehabilitation Roundtable. Int J Stroke. 12:480–493.

Bradnam L V., Stinear CM, Barber PA, Byblow WD. 2012. Contralesional Hemisphere Control of the Proximal Paretic Upper Limb following Stroke. Cereb Cortex. 22:2662–2671.

Braeuninger S, Kleinschnitz C. 2009. Rodent models of focal cerebral ischemia: procedural pitfalls and translational problems. Exp Transl Stroke Med. 1:8.

Brewer L, Horgan F, Hickey A, Williams D. 2013. Stroke rehabilitation: recent advances and future therapies. QJM. 106:11–25.

Broeks G, Lankhorst J, , Rumping GJ, , Prevo K. 1999. The long-term outcome of arm function after stroke: results of a follow-up study. Disabil Rehabil. 21:357–364.

Bühnemann C, Scholz A, Bernreuther C, Malik CY, Braun H, Schachner M, Reymann KG, Dihné M. 2006. Neuronal differentiation of transplanted embryonic stem cell-derived precursors in stroke lesions of adult rats. Brain. 129:3238–3248.

Bulfone A, Smiga SM, Shimamura K, Peterson A, Puelles L, Rubenstein JLR. 1995. T-Brain-1: A homolog of Brachyury whose expression defines molecularly distinct domains within the cerebral cortex. Neuron. 15:63–78.

Bütefisch CM, Weβling M, Netz J, Seitz RJ, Hömberg V. 2008. Relationship Between Interhemispheric Inhibition and Motor Cortex Excitability in Subacute Stroke Patients. Neurorehabil Neural Repair. 22:4–21.

Buzsáki G, Wang X-J. 2012. Mechanisms of Gamma Oscillations. Annu Rev Neurosci. 35:203–225.

Byblow WD, Stinear CM, Barber PA, Petoe MA, Ackerley SJ. 2015. Proportional recovery after stroke depends on corticomotor integrity. Ann Neurol. 78:848–859.

Calautti C, Baron J-C. 2003. Functional neuroimaging studies of motor recovery after stroke in adults: a review. Stroke. 34:1553–1566.

Calautti C, Naccarato M, Jones PS, Sharma N, Day DD, Carpenter AT, Bullmore ET, Warburton EA, Baron J-C. 2007. The relationship between motor deficit and hemisphere activation balance after stroke: A 3T fMRI study. Neuroimage. 34:322–331.

Caleo M. 2015. Rehabilitation and plasticity following stroke: Insights from rodent models. Neuroscience. 311:180–194.

Cardin JA, Carlén M, Meletis K, Knoblich U, Zhang F, Deisseroth K, Tsai L-H, Moore CI. 2009. Driving fast-spiking cells induces gamma rhythm and controls sensory responses. Nature. 459:663–667.

Carmichael ST. 2005. Rodent models of focal stroke: size, mechanism, and purpose. NeuroRx. 2:396–409.

Carmichael ST. 2006. Cellular and molecular mechanisms of neural repair after stroke: Making waves. Ann Neurol. 59:735–742.

Carter AR, Astafiev S V., Lang CE, Connor LT, Rengachary J, Strube MJ, Pope DLW, Shulman GL, Corbetta M. 2009. Resting state inter-hemispheric fMRI connectivity predicts performance after stroke. Ann Neurol. NA-NA.

Cassidy JM, Cramer SC. 2017. Spontaneous and Therapeutic-Induced Mechanisms of Functional Recovery After Stroke. Transl Stroke Res. 8:33–46.

Chambers SM, Fasano CA, Papapetrou EP, Tomishima M, Sadelain M, Studer L. 2009. Highly efficient neural conversion of human ES and iPS cells by dual inhibition of SMAD signaling. Nat Biotechnol. 27:275–280.

Chang D-J, Lee N, Park I-H, Choi C, Jeon I, Kwon J, Oh S-H, Shin DA, Do JT, Lee DR, Lee H, Hong KS, Daley GQ, Song J, Moon H. 2013. Therapeutic Potential of Human Induced Pluripotent Stem Cells in Experimental Stroke. Cell Transplant. 22:1427–1440.

Chen H, Lin W, Zhang Y, Lin L, Chen J, Zeng Y, Zheng M, Zhuang Z, Du H, Chen R, Liu N. 2016. IL-10 Promotes Neurite Outgrowth and Synapse Formation in Cultured Cortical Neurons after the Oxygen-Glucose Deprivation via JAK1/STAT3 Pathway. Sci Rep. 6:30459.

Chen J, Du H, Zhang Y, Chen H, Zheng M, Lin P, Lan Q, Yuan Q, Lai Y, Pan X, Chen R, Liu N. 2017. Netrin-1 Prevents Rat Primary Cortical Neurons from Apoptosis via the DCC/ERK Pathway. Front Cell Neurosci. 11:387.

Chen Y, Swanson RA. 2003. Astrocytes and Brain Injury. J Cereb Blood Flow Metab. 23:137–149.

Cheyne D, Ferrari P. 2013. MEG studies of motor cortex gamma oscillations: evidence for a gamma "fingerprint" in the brain? Front Hum Neurosci. 7.

Chollet F, Dipiero V, Wise RJS, Brooks DJ, Dolan RJ, Frackowiak RSJ. 1991. The functional anatomy of motor recovery after stroke in humans: A study with positron emission tomography. Ann Neurol. 29:63–71.

Choudhury GR, Ding S. 2016. Reactive astrocytes and therapeutic potential in focal ischemic stroke. Neurobiol Dis. 85:234–244.

Christie GJ, Tata MS. 2009. Right frontal cortex generates reward-related theta-band oscillatory activity. Neuroimage. 48:415–422.

Chung Y, Klimanskaya I, Becker S, Marh J, Lu S-J, Johnson J, Meisner L, Lanza R. 2006. Embryonic and extraembryonic stem cell lines derived from single mouse blastomeres. Nature. 439:216–219.

Claassen J, Hirsch LJ, Kreiter KT, Du EY, Connolly ES, Emerson RG, Mayer SA. 2004. Quantitative continuous EEG for detecting delayed cerebral ischemia in patients with poor-grade subarachnoid hemorrhage. Clin Neurophysiol. 115:2699–2710.

Clarkson AN, Huang BS, Macisaac SE, Mody I, Carmichael ST. 2010. Reducing excessive GABA-mediated tonic inhibition promotes functional recovery after stroke. Nature. 468:305–309.

Cohen D. 1972. Magnetoencephalography: detection of the brain's electrical activity with a superconducting magnetometer. Science. 175:664–666.

Coupar F, Pollock A, Rowe P, Weir C, Langhorne P. 2012. Predictors of upper limb recovery after stroke: a systematic review and meta-analysis. Clin Rehabil. 26:291–313.

Crafton KR, Mark AN, Cramer SC. 2003. Improved understanding of cortical injury by incorporating measures of functional anatomy. Brain. 126:1650–1659.

Cramer SC, Bastings EP. 2000. Mapping clinically relevant plasticity after stroke. Neuropharmacology. 39:842–851.

Cramer SC, Nelles G, Benson RR, Kaplan JD, Parker RA, Kwong KK, Kennedy DN, Finklestein SP, Rosen BR. 1997. A functional MRI study of subjects recovered from hemiparetic stroke. Stroke. 28:2518–2527.

Cramer SC, Parrish TB, Levy RM, Stebbins GT, Ruland SD, Lowry DW, Trouard TP, Squire SW, Weinand ME, Savage CR, Wilkinson SB, Juranek J, Leu S-Y, Himes DM. 2007. Predicting Functional Gains in a Stroke Trial. Stroke. 38:2108–2114.

Cramer SC, Riley JD. 2008. Neuroplasticity and brain repair after stroke. Curr Opin Neurol. 21:76–82.

Cuspineda E, Machado C, Galán L, Aubert E, Alvarez MA, Llopis F, Portela L, García M, Manero JM, Ávila Y. 2007. QEEG Prognostic Value in Acute Stroke. Clin EEG Neurosci. 38:155–160.

Daadi MM, Li Z, Arac A, Grueter BA, Sofilos M, Malenka RC, Wu JC, Steinberg GK. 2009. Molecular and Magnetic Resonance Imaging of Human Embryonic Stem Cell–Derived Neural Stem Cell Grafts in Ischemic Rat Brain. Mol Ther. 17:1282–1291.

Dancause N, Barbay S, Frost SB, Zoubina E V., Plautz EJ, Mahnken JD, Nudo RJ. 2006. Effects of Small Ischemic Lesions in the Primary Motor Cortex on Neurophysiological Organization in Ventral Premotor Cortex. J Neurophysiol. 96:3506–3511.

Dancause N, Nudo RJ. 2011. Shaping plasticity to enhance recovery after injury. Prog Brain Res. 192:273–295.

Dancause N, Touvykine B, Mansoori BK. 2015. Inhibition of the contralesional hemisphere after stroke: reviewing a few of the building blocks with a focus on animal models. Prog Brain Res. 218:361–387.

Davidoff, MD RA. 1990. The pyramidal tract. Neurology. 40:332–332.

de la Rosa-Prieto C, Laterza C, Gonzalez-Ramos A, Wattananit S, Ge R, Lindvall O, Tornero D, Kokaia Z. 2017. Stroke alters behavior of human skin-derived neural progenitors after transplantation adjacent to neurogenic area in rat brain. Stem Cell Res Ther. 8:59.

de Weerd AW, Veldhuizen RJ, Veering MM, Poortvliet DCJ, Jonkman EJ. 1988. Recovery from cerebral ischaemia. EEG, cerebral blood flow and clinical symptomatology in the first three years after a stroke. Electroencephalogr Clin Neurophysiol. 70:197–204.

Delavaran H, Sjunnesson H, Arvidsson A, Lindvall O, Norrving B, van Westen D, Kokaia Z, Lindgren A. 2013. Proximity of brain infarcts to regions of endogenous neurogenesis and involvement of striatum in ischaemic stroke. Eur J Neurol. 20:473–479.

Di Pino G, Pellegrino G, Assenza G, Capone F, Ferreri F, Formica D, Ranieri F, Tombini M, Ziemann U, Rothwell JC, Di Lazzaro V. 2014. Modulation of brain plasticity in stroke: a novel model for neurorehabilitation. Nat Rev Neurol. 10:597–608.

Dickstein R. 2008. Rehabilitation of Gait Speed After Stroke: A Critical Review of Intervention Approaches. Neurorehabil Neural Repair. 22:649–660.

Dietrich WD, Ginsberg MD, Busto R, Watson BD. 1986. Photochemically Induced Cortical Infarction in the Rat. 1. Time Course of Hemodynamic Consequences. J Cereb Blood Flow Metab. 6:184–194.

Dijkhuizen RM, Ren J, Mandeville JB, Wu O, Ozdag FM, Moskowitz MA, Rosen BR, Finklestein SP. 2001. Functional magnetic resonance imaging of reorganization in rat brain after stroke. Proc Natl Acad Sci. 98:12766–12771.

Dijkhuizen RM, Singhal AB, Mandeville JB, Wu O, Halpern EF, Finklestein SP, Rosen BR, Lo EH. 2003. Correlation between brain reorganization, ischemic damage, and neurologic status after transient focal cerebral ischemia in rats: a functional magnetic resonance imaging study. J Neurosci. 23:510–517.

Ding G, Jiang Q, Li L, Zhang L, Zhang ZG, Ledbetter KA, Panda S, Davarani SP, Athiraman H, Li Q, Ewing JR, Chopp M. 2008. Magnetic Resonance Imaging Investigation of Axonal Remodeling and Angiogenesis after Embolic Stroke in Sildenafil-Treated Rats. J Cereb Blood Flow Metab. 28:1440–1448.

Durukan A, Tatlisumak T. 2007. Acute ischemic stroke: overview of major experimental rodent models, pathophysiology, and therapy of focal cerebral ischemia. Pharmacol Biochem Behav. 87:179–197.

Eckert MA, Vu Q, Xie K, Yu J, Liao W, Cramer SC, Zhao W. 2013. Evidence for High Translational Potential of Mesenchymal Stromal Cell Therapy to Improve Recovery from Ischemic Stroke. J Cereb Blood Flow Metab. 33:1322–1334.

Ekdahl CT, Kokaia Z, Lindvall O. 2009. Brain inflammation and adult neurogenesis: The dual role of microglia. Neuroscience. 158:1021–1029.

Emmons EB, Ruggiero RN, Kelley RM, Parker KL, Narayanan NS. 2016. Corticostriatal Field Potentials Are Modulated at Delta and Theta Frequencies during Interval-Timing Task in Rodents. Front Psychol. 7.

Erdö F, Bührle C, Blunk J, Hoehn M, Xia Y, Fleischmann B, Föcking M, Küstermann E, Kolossov E, Hescheler J, Hossmann K-A, Trapp T. 2003. Host-Dependent Tumorigenesis of Embryonic Stem Cell Transplantation in Experimental Stroke. J Cereb Blood Flow Metab. 23:780–785.

Escudero J V., Sancho J, Bautista D, Escudero M, López-Trigo J. 1998. Prognostic Value of Motor Evoked Potential Obtained by Transcranial Magnetic Brain Stimulation in Motor Function Recovery in Patients With Acute Ischemic Stroke. Stroke. 29:1854–1859.

Espuny-Camacho I, Michelsen KA, Gall D, Linaro D, Hasche A, Bonnefont J, Bali C, Orduz D, Bilheu A, Herpoel A, Lambert N, Gaspard N, Péron S, Schiffmann SN, Giugliano M, Gaillard A, Vanderhaeghen P. 2013. Pyramidal neurons derived from human pluripotent stem cells integrate efficiently into mouse brain circuits in vivo. Neuron. 77:440–456.

Espuny-Camacho I, Michelsen KA, Linaro D, Bilheu A, Acosta-Verdugo S, Herpoel A, Giugliano M, Gaillard A, Vanderhaeghen P. 2018. Human Pluripotent Stem-Cell-Derived Cortical Neurons Integrate Functionally into the Lesioned Adult Murine Visual Cortex in an Area-Specific Way. Cell Rep. 23:2732–2743.

Falkner S, Grade S, Dimou L, Conzelmann K-K, Bonhoeffer T, Götz M, Hübener M. 2016. Transplanted embryonic neurons integrate into adult neocortical circuits. Nature. 539:248–253.

Fanciullacci C, Bertolucci F, Lamola G, Panarese A, Artoni F, Micera S, Rossi B, Chisari C. 2017. Delta Power Is Higher and More Symmetrical in Ischemic Stroke Patients with Cortical Involvement. Front Hum Neurosci. 11:385.

Fang P, Barbay S, Plautz EJ, Hoover E, Strittmatter SM, Nudo RJ. 2010. Combination of NEP 1-40 Treatment and Motor Training Enhances Behavioral Recovery After a Focal Cortical Infarct in Rats. Stroke. 41:544–549.

Fang Y, Daly JJ, Sun J, Hvorat K, Fredrickson E, Pundik S, Sahgal V, Yue GH. 2009. Functional corticomuscular connection during reaching is weakened following stroke. Clin Neurophysiol. 120:994–1002.

Fasoli SE, Krebs HI, Stein J, Frontera WR, Hogan N. 2003. Effects of robotic therapy on motor impairment and recovery in chronic stroke. Arch Phys Med Rehabil. 84:477–482.

Faught E. 1993. Current role of electroencephalography in cerebral ischemia. Stroke. 24:609–613.

Feng W, Wang J, Chhatbar PY, Doughty C, Landsittel D, Lioutas V-A, Kautz SA, Schlaug G. 2015. Corticospinal tract lesion load: An imaging biomarker for stroke motor outcomes. Ann Neurol. 78:860–870.

Feydy A, Carlier R, Roby-Brami A, Bussel B, Cazalis F, Pierot L, Burnod Y, Maier MA. 2002. Longitudinal Study of Motor Recovery After Stroke. Stroke. 33:1610–1617.

Fink JN, Selim MH, Kumar S, Voetsch B, Fong WC, Caplan LR. 2005. Insular Cortex Infarction in Acute Middle Cerebral Artery Territory Stroke. Arch Neurol. 62:1081.

Finnigan S, van Putten MJAM. 2013. EEG in ischaemic stroke: quantitative EEG can uniquely inform (sub-)acute prognoses and clinical management. Clin Neurophysiol. 124:10–19.

Finnigan S, Wong A, Read S. 2016. Defining abnormal slow EEG activity in acute ischaemic stroke: Delta/alpha ratio as an optimal QEEG index. Clin Neurophysiol. 127:1452–1459.

Finnigan SP, Rose SE, Walsh M, Griffin M, Janke AL, McMahon KL, Gillies R, Strudwick MW, Pettigrew CM, Semple J, Brown J, Brown P, Chalk JB. 2004. Correlation of Quantitative EEG in Acute Ischemic Stroke With 30-Day NIHSS Score. Stroke. 35:899–903.

Finnigan SP, Walsh M, Rose SE, Chalk JB. 2007. Quantitative EEG indices of sub-acute ischaemic stroke correlate with clinical outcomes. Clin Neurophysiol. 118:2525–2532.

Fischer U, Arnold M, Nedeltchev K, Brekenfeld C, Ballinari P, Remonda L, Schroth G, Mattle HP. 2005. NIHSS Score and Arteriographic Findings in Acute Ischemic Stroke. Stroke. 36:2121–2125.

Fisher M. 1997. Characterizing the target of acute stroke therapy. Stroke. 28:866–872.

Flor H, Diers M. 2009. Sensorimotor training and cortical reorganization. NeuroRehabilitation. 25:19–27.

Foreman B, Claassen J. 2012a. Quantitative EEG for the detection of brain ischemia. Crit Care. 16:216.

Fox MD, Snyder AZ, Vincent JL, Raichle ME. 2007. Intrinsic fluctuations within cortical systems account for intertrial variability in human behavior. Neuron. 56:171–184.

Fregni F, Boggio PS, Nitsche MA, Rigonatti SP, Pascual-Leone A. 2006. Cognitive effects of repeated sessions of transcranial direct current stimulation in patients with depression. Depress Anxiety. 23:482–484.

Fregni F, Boggio PS, Valle AC, Rocha RR, Duarte J, Ferreira MJL, Wagner T, Fecteau S, Rigonatti SP, Riberto M, Freedman SD, Pascual-Leone A. 2006. A Sham-Controlled Trial of a 5-Day Course of Repetitive Transcranial Magnetic Stimulation of the Unaffected Hemisphere in Stroke Patients. Stroke. 37:2115–2122.

Fricker-Gates RA, Shin JJ, Tai CC, Catapano LA, Macklis JD. 2002. Late-stage immature neocortical neurons reconstruct interhemispheric connections and form synaptic contacts with increased efficiency in adult mouse cortex undergoing targeted neurodegeneration. J Neurosci. 22:4045–4056.

Froehler MT, Ovbiagele B. 2010. Therapeutic hypothermia for acute ischemic stroke. Expert Rev Cardiovasc Ther. 8:593–603.

Frost SB, Barbay S, Friel KM, Plautz EJ, Nudo RJ. 2003. Reorganization of Remote Cortical Regions After Ischemic Brain Injury: A Potential Substrate for Stroke Recovery. J Neurophysiol. 89:3205–3214.

Fukuchi-Shimogori T, Grove EA. 2003. Emx2 patterns the neocortex by regulating FGF positional signaling. Nat Neurosci. 6:825–831.

Gaetz W, Edgar JC, Wang DJ, Roberts TPL. 2011. Relating MEG measured motor cortical oscillations to resting γ-aminobutyric acid (GABA) concentration. Neuroimage. 55:616–621.

Gaetz W, Liu C, Zhu H, Bloy L, Roberts TPL. 2013. Evidence for a motor gamma-band network governing response interference. Neuroimage. 74:245–253.

Gage FH, Coates PW, Palmer TD, Kuhn HG, Fisher LJ, Suhonen JO, Peterson DA, Suhr ST, Ray J. 1995. Survival and differentiation of adult neuronal progenitor cells transplanted to the adult brain. Proc Natl Acad Sci U S A. 92:11879–11883.

Gaillard A, Prestoz L, Dumartin B, Cantereau A, Morel F, Roger M, Jaber M. 2007. Reestablishment of damaged adult motor pathways by grafted embryonic cortical neurons. Nat Neurosci. 10:1294–1299.

George PM, Steinberg GK. 2015. Novel Stroke Therapeutics: Unraveling Stroke Pathophysiology and Its Impact on Clinical Treatments. Neuron. 87:297–309.

Gerloff C, Bushara K, Sailer A, Wassermann EM, Chen R, Matsuoka T, Waldvogel D, Wittenberg GF, Ishii K, Cohen LG, Hallett M. 2006. Multimodal imaging of brain reorganization in motor areas of the contralesional hemisphere of well recovered patients after capsular stroke. Brain. 129:791–808.

Ginsberg MD. 2008. Neuroprotection for ischemic stroke: Past, present and future. Neuropharmacology. 55:363–389.

Gladstone DJ, Danells CJ, Black SE. 2002. The Fugl-Meyer Assessment of Motor Recovery after Stroke: A Critical Review of Its Measurement Properties. Neurorehabil Neural Repair. 16:232–240.

Goldberg MP, Choi DW. 1993. Combined oxygen and glucose deprivation in cortical cell culture: calcium-dependent and calcium-independent mechanisms of neuronal injury. J Neurosci. 13:3510–3524.

Gonzalez MF, Sharp FR, Loken JE. 1988. Fetal frontal cortex transplanted to injured motor/sensory cortex of adult rats: Reciprocal connections with host thalamus demonstrated with WGA-HRP. Exp Neurol. 99:154–165.murriAR. 2004. Protecting the brain: the search for a clinically effective neuroprotective drug for stroke. Crit Rev Neurobiol. 16:91–97.

Green JB. 2003. Brain Reorganization After Stroke. Top Stroke Rehabil. 10:1–20.

Greicius MD, Krasnow B, Reiss AL, Menon V. 2003. Functional connectivity in the resting brain: A network analysis of the default mode hypothesis. Proc Natl Acad Sci. 100:253–258.

Gresham GE, Kelly-Hayes M, Wolf PA, Beiser AS, Kase CS, D'Agostino RB. 1998. Survival and Functional Status 20 or More Years After First Stroke. Stroke. 29:793–797.

Guitet J, Garnier C, Ebrahimi-Gaillard A, Roger M. 1994. Efferents of frontal or occipital cortex grafted into adult rat's motor cortex. Neurosci Lett. 180:265–268.

Guye M, Bettus G, Bartolomei F, Cozzone PJ. 2010. Graph theoretical analysis of structural and functional connectivity MRI in normal and pathological brain networks. Magn Reson Mater Physics, Biol Med. 23:409–421.

Gyorgy AB, Szemes M, de Juan Romero C, Tarabykin V, Agoston D V. 2008. SATB2 interacts with chromatin-remodeling molecules in differentiating cortical neurons. Eur J Neurosci. 27:865–873.

Hall SD, Stanford IM, Yamawaki N, McAllister CJ, Rönnqvist KC, Woodhall GL, Furlong PL. 2011. The role of GABAergic modulation in motor function related neuronal network activity. Neuroimage. 56:1506–1510.

Hamzei F, Liepert J, Dettmers C, Weiller C, Rijntjes M. 2006. Two different reorganization patterns after rehabilitative therapy: an exploratory study with fMRI and TMS. Neuroimage. 31:710–720.

Hanisch U-K, Kettenmann H. 2007. Microglia: active sensor and versatile effector cells in the normal and pathologic brain. Nat Neurosci. 10:1387–1394.

Hansen D V, Rubenstein JLR, Kriegstein AR. 2011. Deriving excitatory neurons of the neocortex from pluripotent stem cells. Neuron. 70:645–660.

Hayakawa K, Nakano T, Irie K, Higuchi S, Fujioka M, Orito K, Iwasaki K, Jin G, Lo EH, Mishima K, Fujiwara M. 2010. Inhibition of Reactive Astrocytes with Fluorocitrate Retards Neurovascular Remodeling and Recovery after Focal Cerebral Ischemia in Mice. J Cereb Blood Flow Metab. 30:871–882.

Hébert JM, McConnell SK. 2000. Targeting of cre to the Foxg1 (BF-1) Locus Mediates loxP Recombination in the Telencephalon and Other Developing Head Structures. Dev Biol. 222:296–306.

Heit JJ, Sussman ES, Wintermark M. 2019. Perfusion Computed Tomography in Acute Ischemic Stroke. Radiol Clin North Am. 57:1109–1116.

Helenius J, Henninger N. 2015. Leukoaraiosis Burden Significantly Modulates the Association Between Infarct Volume and National Institutes of Health Stroke Scale in Ischemic Stroke. Stroke. 46:1857–1863.

Hendricks HT, van Limbeek J, Geurts AC, Zwarts MJ. 2002. Motor recovery after stroke: A systematic review of the literature. Arch Phys Med Rehabil. 83:1629–1637.

Hendrickx M, Van XH, Leyns L. 2009. Anterior-posterior patterning of neural differentiated embryonic stem cells by canonical Wnts, Fgfs, Bmp4 and their respective antagonists. Dev Growth Differ. 51:687–698.

Henninger N, Bouley J, Nelligan JM, Sicard KM, Fisher M. 2007. Normobaric Hyperoxia Delays Perfusion/Diffusion Mismatch Evolution, Reduces Infarct Volume, and Differentially Affects Neuronal Cell Death Pathways after Suture Middle Cerebral Artery Occlusion in Rats. J Cereb Blood Flow Metab. 27:1632–1642.

Henninger N, Fisher M. 2007. Stimulating Circle of Willis Nerve Fibers Preserves the Diffusion-Perfusion Mismatch in Experimental Stroke. Stroke. 38:2779–2786.

Henninger N, Lin E, Haussen DC, Lehman LL, Takhtani D, Selim M, Moonis M. 2013. Leukoaraiosis and sex predict the hyperacute ischemic core volume. Stroke. 44:61–67.

Herman JP, Abrous ND. 1994. Dopaminergic neural grafts after fifteen years: results and perspectives. Prog Neurobiol. 44:1–35.

Hermanto Y, Sunohara T, Faried A, Takagi Y, Takahashi J, Maki T, Miyamoto S. 2018. Transplantation of feeder-free human induced pluripotent stem cell-derived cortical neuron progenitors in adult male Wistar rats with focal brain ischemia. J Neurosci Res. 96:863–874.

Hernit-Grant CS, Macklis JD. 1996. Embryonic neurons transplanted to regions of targeted photolytic cell death in adult mouse somatosensory cortex re-form specific callosal projections. Exp Neurol. 139:131–142.

Hinman JD, Rasband MN, Carmichael ST. 2013. Remodeling of the Axon Initial Segment After Focal Cortical and White Matter Stroke. Stroke. 44:182–189.

Hirsch LJ, LaRoche SM, Gaspard N, Gerard E, Svoronos A, Herman ST, Mani R, Arif H, Jette N, Minazad Y, Kerrigan JF, Vespa P, Hantus S, Claassen J, Young GB, So E, Kaplan PW, Nuwer MR, Fountain NB, Drislane FW. 2013. American Clinical Neurophysiology Society's Standardized Critical Care EEG Terminology. J Clin Neurophysiol. 30:1–27.

Hofmeijer J, van Putten MJAM. 2012. Ischemic Cerebral Damage. Stroke. 43:607–615.

Hong JM, Lee JS, Song H-J, Jeong HS, Choi HA, Lee K. 2014. Therapeutic Hypothermia After Recanalization in Patients With Acute Ischemic Stroke. Stroke. 45:134–140.

Hope TMH, Friston K, Price CJ, Leff AP, Rotshtein P, Bowman H. 2019. Recovery after stroke: not so proportional after all? Brain. 142:15–22.

Hossmann K-A. 2012. The Two Pathophysiologies of Focal Brain Ischemia: Implications for Translational Stroke Research. J Cereb Blood Flow Metab. 32:1310–1316.

Howells DW, Sena ES, Macleod MR. 2014. Bringing rigour to translational medicine. Nat Rev Neurol. 10:37–43.

Hsu JE, Jones TA. 2006. Contralesional neural plasticity and functional changes in the less-affected forelimb after large and small cortical infarcts in rats. Exp Neurol. 201:479–494.

Hummel F, Celnik P, Giraux P, Floel A, Wu W-H, Gerloff C, Cohen LG. 2005. Effects of non-invasive cortical stimulation on skilled motor function in chronic stroke. Brain. 128:490–499.

Hummel F, Cohen LG. 2005. Improvement of Motor Function with Noninvasive Cortical Stimulation in a Patient with Chronic Stroke. Neurorehabil Neural Repair. 19:14–19.

Hummel FC, Cohen LG. 2006. Non-invasive brain stimulation: a new strategy to improve neurorehabilitation after stroke? Lancet Neurol. 5:708–712.

Isacson O, Wictorin K, Fischer W, Sofroniew M V, Björklund A. 1988. Fetal cortical cell suspension grafts to the excitotoxically lesioned neocortex: anatomical and neurochemical studies of trophic

interactions. Prog Brain Res. 78:13–26.

Jeffers MS, Hoyles A, Morshead C, Corbett D. 2014. Epidermal Growth Factor and Erythropoietin Infusion Accelerate Functional Recovery in Combination With Rehabilitation. Stroke. 45:1856–1858.

Jeffers MS, Karthikeyan S, Corbett D. 2018. Does Stroke Rehabilitation Really Matter? Part A: Proportional Stroke Recovery in the Rat. Neurorehabil Neural Repair. 32:3–6.

Jendelová P, Kubinová Š, Sandvig I, Erceg S, Sandvig A, Syková E. 2016. Current developments in cell- and biomaterial-based approaches for stroke repair. Expert Opin Biol Ther. 16:43–56.

Jenkins WM, Merzenich MM. 1987. Reorganization of neocortical representations after brain injury: a neurophysiological model of the bases of recovery from stroke. Prog Brain Res. 71:249–266.

Johnson NW, Özkan M, Burgess AP, Prokic EJ, Wafford KA, O'Neill MJ, Greenhill SD, Stanford IM, Woodhall GL. 2017. Phase-amplitude coupled persistent theta and gamma oscillations in rat primary motor cortex in vitro. Neuropharmacology. 119:141–156.

Jones TA, Kleim JA, Greenough WT. 1996. Synaptogenesis and dendritic growth in the cortex opposite unilateral sensorimotor cortex damage in adult rats: a quantitative electron microscopic examination. Brain Res. 733:142–148.

Jones TA, Schallert T. 1992. Overgrowth and pruning of dendrites in adult rats recovering from neocortical damage. Brain Res. 581:156–160.

Jordan KG. 2004. Emergency EEG and continuous EEG monitoring in acute ischemic stroke. J Clin Neurophysiol. 21:341–352.

Joundi RA, Jenkinson N, Brittain J-S, Aziz TZ, Brown P. 2012. Driving oscillatory activity in the human cortex enhances motor performance. Curr Biol. 22:403–407.

Kashyap R, Purohit H, Daginawala H, Nayak A, Kabra D, Taori G. 2012. Time course of inflammatory cytokines in acute ischemic stroke patients and their relation to inter-alfa trypsin inhibitor heavy chain 4 and outcome. Ann Indian Acad Neurol. 15:181.

Kawai H, Yamashita T, Ohta Y, Deguchi K, Nagotani S, Zhang X, Ikeda Y, Matsuura T, Abe K. 2010. Tridermal Tumorigenesis of Induced Pluripotent Stem Cells Transplanted in Ischemic Brain. J Cereb Blood Flow Metab. 30:1487–1493.

Kawamata T, Dietrich WD, Schallert T, Gotts JE, Cocke RR, Benowitz LI, Finklestein SP, Finklestein SP. 1997. Intracisternal basic fibroblast growth factor enhances functional recovery and up-regulates the expression of a molecular marker of neuronal sprouting following focal cerebral infarction. Proc Natl Acad Sci U S A. 94:8179–8184.

Kerr AL, Cheng S-Y, Jones TA. 2011. Experience-dependent neural plasticity in the adult damaged brain. J Commun Disord. 44:538–548.

Kettenmann H, Verkhratsky A. 2008. Neuroglia: the 150 years after. Trends Neurosci. 31:653–659.

Kim SY, Jones TA. 2010. Lesion size-dependent synaptic and astrocytic responses in cortex contralateral to infarcts in middle-aged rats. Synapse. 64:NA-NA.

Kinsbourne M. 1974. Mechanisms of hemispheric interaction in man.

Kitano H, Young JM, Cheng J, Wang L, Hurn PD, Murphy SJ. 2007. Gender-Specific Response to Isoflurane Preconditioning in Focal Cerebral Ischemia. J Cereb Blood Flow Metab. 27:1377–1386.

Klamroth-Marganska V, Blanco J, Campen K, Curt A, Dietz V, Ettlin T, Felder M, Fellinghauer B, Guidali M, Kollmar A, Luft A, Nef T, Schuster-Amft C, Stahel W, Riener R. 2014. Three-dimensional, task-specific robot therapy of the arm after stroke: a multicentre, parallel-group

randomised trial. Lancet Neurol. 13:159–166.

Kobayashi M, Pascual-Leone A. 2003. Transcranial magnetic stimulation in neurology. Lancet Neurol. 2:145–156.

Kokaia Z, Darsalia V. 2018. Human Neural Stem Cells for Ischemic Stroke Treatment. In: Results and problems in cell differentiation. p. 249–263.

Kokaia Z, Lindvall O. 2012. Stem cell repair of striatal ischemia. Prog Brain Res. 201:35–53.

Kokaia Z, Llorente IL, Carmichael ST. 2018. Customized Brain Cells for Stroke Patients Using Pluripotent Stem Cells. Stroke. 49:1091–1098.

Kokaia Z, Tornero D, Lindvall O. 2017. Transplantation of reprogrammed neurons for improved recovery after stroke. Prog Brain Res. 231:245–263.

Kordower JH, Freeman TB, Chen E-Y, Mufson EJ, Sanberg PR, Hauser RA, Snow B, Warren Olanow C. 1998. Fetal nigral grafts survive and mediate clinical benefit in a patient with Parkinson's disease. Mov Disord. 13:383–393.

Krakauer J, Marshall R. 2015. The proportional recovery rule for stroke revisited. Ann Neurol. 78:845–847.

Krnjević K. 2008. Electrophysiology of cerebral ischemia. Neuropharmacology. 55:319–333.

Kwakkel G, Kollen BJ, van der Grond J, Prevo AJH. 2003. Probability of Regaining Dexterity in the Flaccid Upper Limb. Stroke. 34:2181–2186.

Lai S, Panarese A, Spalletti C, Alia C, Ghionzoli A, Caleo M, Micera S. 2015. Quantitative Kinematic Characterization of Reaching Impairments in Mice After a Stroke. Neurorehabil Neural Repair. 29:382–392.

Lai TW, Zhang S, Wang YT. 2014. Excitotoxicity and stroke: identifying novel targets for neuroprotection. Prog Neurobiol. 115:157–188.

Lämmer AB, Beck A, Grummich B, Förschler A, Krügel T, Kahn T, Schneider D, Illes P, Franke H, Krügel U. 2011. The P2 Receptor Antagonist PPADS Supports Recovery from Experimental Stroke In Vivo. PLoS One. 6:e19983.

Lazar RM, Minzer B, Antoniello D, Festa JR, Krakauer JW, Marshall RS. 2010. Improvement in Aphasia Scores After Stroke Is Well Predicted by Initial Severity. Stroke. 41:1485–1488.

Lee J-K, Kim J-E, Sivula M, Strittmatter SM. 2004. Nogo receptor antagonism promotes stroke recovery by enhancing axonal plasticity. J Neurosci. 24:6209–6217.

Lee M, Hong K-S, Chang S-C, Saver JL. 2010. Efficacy of Homocysteine-Lowering Therapy With Folic Acid in Stroke Prevention. Stroke. 41:1205–1212.

Lee S-T, Chu K, Jung K-H, Kim S-J, Kim D-H, Kang K-M, Hong NH, Kim J-H, Ban J-J, Park H-K, Kim SU, Park C-G, Lee SK, Kim M, Roh J-K. 2008. Anti-inflammatory mechanism of intravascular neural stem cell transplantation in haemorrhagic stroke. Brain. 131:616–629.

Lees KR. 1997. Cerestat and other NMDA antagonists in ischemic stroke. Neurology. 49:S66-9.

Lemon RN. 2008a. Descending Pathways in Motor Control. Annu Rev Neurosci. 31:195–218.

Leon-Carrion J, Martin-Rodriguez JF, Damas-Lopez J, Barroso y Martin JM, Dominguez-Morales MR. 2009a. Delta-alpha ratio correlates with level of recovery after neurorehabilitation in

Li P, Murphy TH. 2008. Two-photon imaging during prolonged middle cerebral artery occlusion in mice reveals recovery of dendritic structure after reperfusion. J Neurosci. 28:11970–11979.

Li S, Carmichael ST. 2006. Growth-associated gene and protein expression in the region of axonal

sprouting in the aged brain after stroke. Neurobiol Dis. 23:362–373.

Liepert J, Graef S, Uhde I, Leidner O, Weiller C. 2000. Training-induced changes of motor cortex representations in stroke patients. Acta Neurol Scand. 101:321–326.

Lim JH, Lee J-C, Lee YH, Choi IY, Oh Y-K, Kim H-S, Park J-S, Kim W-K. 2006. Simvastatin prevents oxygen and glucose deprivation/reoxygenation-induced death of cortical neurons by reducing the production and toxicity of 4-hydroxy-2E-nonenal. J Neurochem. 97:140–150.

Lindvall O, Kokaia Z. 2010. Stem cells in human neurodegenerative disorders--time for clinical translation? J Clin Invest. 120:29–40.

Lindvall O, Kokaia Z. 2011. Stem Cell Research in Stroke. Stroke. 42:2369–2375.

Lindvall O, Kokaia Z. 2015. Neurogenesis following Stroke Affecting the Adult Brain. Cold Spring Harb Perspect Biol. 7:a019034.

Lindvall O, Rehncrona S, Brundin P, Gustavii B, Astedt B, Widner H, Lindholm T, Björklund A, Leenders KL, Rothwell JC. 1990. Neural transplantation in Parkinson's disease: the Swedish experience. Prog Brain Res. 82:729–734.

Lisman J, Redish AD. 2009. Prediction, sequences and the hippocampus. Philos Trans R Soc B Biol Sci. 364:1193–1201.

Liu L, Liu H, Yang F, Chen G, Zhou H, Tang M, Zhang R, Dong Q. 2011. Tissue kallikrein protects cortical neurons against hypoxia/reoxygenation injury via the ERK1/2 pathway. Biochem Biophys Res Commun. 407:283–287.

Liu X, Tian F, Wang S, Wang F, Xiong L. 2018. Astrocyte Autophagy Flux Protects Neurons Against Oxygen-Glucose Deprivation and Ischemic/Reperfusion Injury. Rejuvenation Res. 21:405–415.

Liu Z, Chopp M. 2016. Astrocytes, therapeutic targets for neuroprotection and neurorestoration in ischemic stroke. Prog Neurobiol. 144:103–120.

Liu Z, Li Y, Cui Y, Roberts C, Lu M, Wilhelmsson U, Pekny M, Chopp M. 2014. Beneficial effects of gfap/vimentin reactive astrocytes for axonal remodeling and motor behavioral recovery in mice after stroke. Glia. 62:2022–2033.

Llovera G, Roth S, Plesnila N, Veltkamp R, Liesz A. 2014. Modeling stroke in mice: permanent coagulation of the distal middle cerebral artery. J Vis Exp. e51729.

Lo AC, Guarino PD, Richards LG, Haselkorn JK, Wittenberg GF, Federman DG, Ringer RJ, Wagner TH, Krebs HI, Volpe BT, Bever CT, Bravata DM, Duncan PW, Corn BH, Maffucci AD, Nadeau SE, Conroy SS, Powell JM, Huang GD, Peduzzi P. 2010. Robot-Assisted Therapy for Long-Term Upper-Limb Impairment after Stroke. N Engl J Med. 362:1772–1783.

Longa EZ, Weinstein PR, Carlson S, Cummins R. 1989. Reversible middle cerebral artery occlusion without craniectomy in rats. Stroke. 20:84–91.

Lopes da Silva F. 2013. EEG and MEG: relevance to neuroscience. Neuron. 80:1112–1128.

Lotze M, Markert J, Sauseng P, Hoppe J, Plewnia C, Gerloff C. 2006. The role of multiple contralesional motor areas for complex hand movements after internal capsular lesion. J Neurosci. 26:6096–6102.

Lu X-CM, Williams AJ, Tortella FC. 2001. Quantitative electroencephalography spectral analysis and topographic mapping in a rat model of middle cerebral artery occlusion. Neuropathol Appl Neurobiol. 27:481–495.

Lum PS, Godfrey SB, Brokaw EB, Holley RJ, Nichols D. 2012. Robotic Approaches for Rehabilitation of Hand Function After Stroke. Am J Phys Med Rehabil. 91:S242–S254.

Lupo G, Bertacchi M, Carucci N, Augusti-Tocco G, Biagioni S, Cremisi F. 2014. From pluripotency to forebrain patterning: an in vitro journey astride embryonic stem cells. Cell Mol Life Sci. 71:2917–2930.

Luu P, Tucker DM, Englander R, Lockfeld A, Lutsep H, Oken B. 2001. Localizing acute stroke-related EEG changes: assessing the effects of spatial undersampling. J Clin Neurophysiol. 18:302–317.

Maciejasz P, Eschweiler J, Gerlach-Hahn K, Jansen-Troy A, Leonhardt S. 2014. A survey on robotic devices for upper limb rehabilitation. J Neuroeng Rehabil. 11:3.

Mackay J, Mensah G. 2004. The atlas of heart disease and stroke.

Mah Y-H, Husain M, Rees G, Nachev P. 2014. Human brain lesion-deficit inference remapped. Brain. 137:2522–2531.

Majid A, He YY, Gidday JM, Kaplan SS, Gonzales ER, Park TS, Fenstermacher JD, Wei L, Choi DW, Hsu CY. 2000. Differences in vulnerability to permanent focal cerebral ischemia among 3 common mouse strains. Stroke. 31:2707–2714.

Mansoori BK, Jean-Charles L, Touvykine B, Liu A, Quessy S, Dancause N. 2014. Acute inactivation of the contralesional hemisphere for longer durations improves recovery after cortical injury. Exp Neurol. 254:18–28.

Mariani J, Simonini MV, Palejev D, Tomasini L, Coppola G, Szekely AM, Horvath TL, Vaccarino FM. 2012. Modeling human cortical development in vitro using induced pluripotent stem cells. Proc Natl Acad Sci U S A. 109:12770–12775.

Marshall RS, Perera GM, Lazar RM, Krakauer JW, Constantine RC, DeLaPaz RL. 2000. Evolution of Cortical Activation During Recovery From Corticospinal Tract Infarction. Stroke. 31:656–661.

Masiero S, Celia A, Rosati G, Armani M. 2007. Robotic-Assisted Rehabilitation of the Upper Limb After Acute Stroke. Arch Phys Med Rehabil. 88:142–149.

Massensini AR, Ghuman H, Saldin LT, Medberry CJ, Keane TJ, Nicholls FJ, Velankar SS, Badylak SF, Modo M. 2015. Concentration-dependent rheological properties of ECM hydrogel for intracerebral delivery to a stroke cavity. Acta Biomater. 27:116–130.

Mathis MW, Mathis A, Uchida N. 2017. Somatosensory Cortex Plays an Essential Role in Forelimb Motor Adaptation in Mice. Neuron. 93:1493–1503.e6.

McCabe C, Gallagher L, Gsell W, Graham D, Dominiczak AF, Macrae IM. 2009. Differences in the Evolution of the Ischemic Penumbra in Stroke-Prone Spontaneously Hypertensive and Wistar-Kyoto Rats. Stroke. 40:3864–3868.

McKeon RJ, Schreiber RC, Rudge JS, Silver J. 1991. Reduction of neurite outgrowth in a model of glial scarring following CNS injury is correlated with the expression of inhibitory molecules on reactive astrocytes. J Neurosci. 11:3398–3411.

Medberry CJ, Crapo PM, Siu BF, Carruthers CA, Wolf MT, Nagarkar SP, Agrawal V, Jones KE, Kelly J, Johnson SA, Velankar SS, Watkins SC, Modo M, Badylak SF. 2013. Hydrogels derived from central nervous system extracellular matrix. Biomaterials. 34:1033–1040.

Meng X, Fisher M, Shen Q, Sotak CH, Duong TQ. 2004. Characterizing the diffusion/perfusion mismatch in experimental focal cerebral ischemia. Ann Neurol. 55:207–212.

Meyer S, Kessner SS, Cheng B, Bönstrup M, Schulz R, Hummel FC, De Bruyn N, Peeters A, Van Pesch V, Duprez T, Sunaert S, Schrooten M, Feys H, Gerloff C, Thomalla G, Thijs V, Verheyden G. 2016. Voxel-based lesion-symptom mapping of stroke lesions underlying somatosensory deficits. NeuroImage Clin. 10:257–266.

Meyniel F, Pessiglione M. 2014. Better get back to work: a role for motor beta desynchronization in incentive motivation. J Neurosci. 34:1–9.

Merton PA, Morton HB. 1980. Stimulation of the cerebral cortex in the intact human subject. Nature. 285:227–227.

Michelsen KA, Acosta-Verdugo S, Benoit-Marand M, Espuny-Camacho I, Gaspard N, Saha B, Gaillard A, Vanderhaeghen P. 2015. Area-Specific Reestablishment of Damaged Circuits in the Adult Cerebral Cortex by Cortical Neurons Derived from Mouse Embryonic Stem Cells. Neuron. 85:982–997.

Modo M, Stroemer RP, Tang E, Patel S, Hodges H. 2002. Effects of Implantation Site of Stem Cell Grafts on Behavioral Recovery From Stroke Damage. Stroke. 33:2270–2278.

Mohajerani MH, Aminoltejari K, Murphy TH. 2011. Targeted mini-strokes produce changes in interhemispheric sensory signal processing that are indicative of disinhibition within minutes. Proc Natl Acad Sci U S A. 108:E183-91.

Mohamad O, Drury-Stewart D, Song M, Faulkner B, Chen D, Yu SP, Wei L. 2013. Vector-Free and Transgene-Free Human iPS Cells Differentiate into Functional Neurons and Enhance Functional Recovery after Ischemic Stroke in Mice. PLoS One. 8:e64160.

Moretti A, Ferrari F, Villa RF. 2015a. Neuroprotection for ischaemic stroke: current status and challenges. Pharmacol Ther. 146:23–34.

Morrison HW, Filosa JA. 2013. A quantitative spatiotemporal analysis of microglia morphology during ischemic stroke and reperfusion. J Neuroinflammation. 10:782.

Moyanova S, Kortenska L, Kirov R, Iliev I. 1998. Quantitative Electroencephalographic Changes Due To Middle Cerebral Artery Occlusion By Endothelin 1 In Conscious Rats. Arch Physiol Biochem. 106:384–391.

Mozaffarian D, et al., 2016. Heart Disease and Stroke Statistics—2016 Update. Circulation. 133:e38-360.

Muñetón-Gómez VC, Doncel-Pérez E, Fernandez AP, Serrano J, Pozo-Rodrigálvarez A, Vellosillo-Huerta L, Taylor JS, Cardona-Gómez GP, Nieto-Sampedro M, Martínez-Murillo R. 2012. Neural differentiation of transplanted neural stem cells in a rat model of striatal lacunar infarction: light and electron microscopic observations. Front Cell Neurosci. 6.

Murase N, Duque J, Mazzocchio R, Cohen LG. 2004. Influence of interhemispheric interactions on motor function in chronic stroke. Ann Neurol. 55:400–409.

Murphy TH, Corbett D. 2009. Plasticity during stroke recovery: from synapse to behaviour. Nat Rev Neurosci. 10:861–872.

Murphy TH, Li P, Betts K, Liu R. 2008. Two-photon imaging of stroke onset in vivo reveals that NMDA-receptor independent ischemic depolarization is the major cause of rapid reversible damage to dendrites and spines. J Neurosci. 28:1756–1772.

Murri L, Gori S, Massetani R, Bonanni E, Marcella F, Milani S. 1998. Evaluation of acute ischemic stroke using quantitative EEG: a comparison with conventional EEG and CT scan. Neurophysiol Clin. 28:249–257.

Nakayama H, Jørgensen HS, Raaschou HO, Olsen TS. 1994. The influence of age on stroke outcome. The Copenhagen Stroke Study. Stroke. 25:808–813.

Nicolo P, Rizk S, Magnin C, Pietro M Di, Schnider A, Guggisberg AG. 2015. Coherent neural oscillations predict future motor and language improvement after stroke. Brain. 138:3048–3060.

Nielsen J V., Blom JB, Noraberg J, Jensen NA. 2010. Zbtb20-Induced CA1 Pyramidal Neuron Development and Area Enlargement in the Cerebral Midline Cortex of Mice. Cereb Cortex. 20:1904–1914.

Nijboer TCW, Kollen BJ, Kwakkel G. 2013. Time course of visuospatial neglect early after stroke: a longitudinal cohort study. Cortex. 49:2021–2027.

Nitsche MA, Cohen LG, Wassermann EM, Priori A, Lang N, Antal A, Paulus W, Hummel F, Boggio PS, Fregni F, Pascual-Leone A. 2008. Transcranial direct current stimulation: State of the art 2008. Brain Stimul. 1:206–223.

Nitsche MA, Doemkes S, Karaköse T, Antal A, Liebetanz D, Lang N, Tergau F, Paulus W. 2007. Shaping the Effects of Transcranial Direct Current Stimulation of the Human Motor Cortex. J Neurophysiol. 97:3109–3117.

Nitsche MA, Fricke K, Henschke U, Schlitterlau A, Liebetanz D, Lang N, Henning S, Tergau F, Paulus W. 2003. Pharmacological Modulation of Cortical Excitability Shifts Induced by Transcranial Direct Current Stimulation in Humans. J Physiol. 553:293–301.

Nouri S, Cramer SC. 2011. Anatomy and physiology predict response to motor cortex stimulation after stroke. Neurology. 77:1076–1083.

Novak D, Nagle A, Keller U, Riener R. 2014. Increasing motivation in robot-aided arm rehabilitation with competitive and cooperative gameplay. J Neuroeng Rehabil. 11:64.

Nowak M, Zich C, Stagg CJ. 2018. Motor Cortical Gamma Oscillations: What Have We Learnt and Where Are We Headed? Curr Behav Neurosci Reports. 5:136–142.

Nudo RJ. 2003. Functional and structural plasticity in motor cortex: implications for stroke recovery. Phys Med Rehabil Clin N Am. 14:S57-76.

Nudo RJ. 2006. Mechanisms for recovery of motor function following cortical damage. Curr Opin Neurobiol. 16:638–644.

Nudo RJ. 2007. Postinfarct Cortical Plasticity and Behavioral Recovery. Stroke. 38:840–845.

Nudo RJ, Milliken GW. 1996. Reorganization of movement representations in primary motor cortex following focal ischemic infarcts in adult squirrel monkeys. J Neurophysiol. 75:2144–2149.

Oki K, Tatarishvili J, Wood J, Koch P, Wattananit S, Mine Y, Monni E, Tornero D, Ahlenius H, Ladewig J, Brüstle O, Lindvall O, Kokaia Z. 2012. Human-Induced Pluripotent Stem Cells form Functional Neurons and Improve Recovery After Grafting in Stroke-Damaged Brain. Stem Cells. 30:1120–1133.

Orzyłowska O, Oderfeld-Nowak B, Zaremba M, Januszewski S, Mossakowski M. 1999. Prolonged and concomitant induction of astroglial immunoreactivity of interleukin-1beta and interleukin-6 in the rat hippocampus after transient global ischemia. Neurosci Lett. 263:72–76.

Overman JJ, Carmichael ST. 2014. Plasticity in the Injured Brain. Neurosci. 20:15–28.

Overman JJ, Clarkson AN, Wanner IB, Overman WT, Eckstein I, Maguire JL, Dinov ID, Toga AW, Carmichael ST. 2012. A role for ephrin-A5 in axonal sprouting, recovery, and activity-dependent plasticity after stroke. Proc Natl Acad Sci U S A. 109:E2230-9.

Paciaroni M, Caso V, Agnelli G. 2009. The Concept of Ischemic Penumbra in Acute Stroke and Therapeutic Opportunities. Eur Neurol. 61:321–330.

Park C, Chang WH, Ohn SH, Kim ST, Bang OY, Pascual-Leone A, Kim Y-H. 2011. Longitudinal Changes of Resting-State Functional Connectivity During Motor Recovery After Stroke. Stroke. 42:1357–1362.

Pasquini M, Lai S, Spalletti C, Cracchiolo M, Conti S, Panarese A, Caleo M, Micera S. 2018. A Robotic System for Adaptive Training and Function Assessment of Forelimb Retraction in Mice. IEEE Trans Neural Syst Rehabil Eng. 26:1803–1812.

Pearson-Fuhrhop KM, Kleim JA, Cramer SC. 2009. Brain Plasticity and Genetic Factors. Top Stroke Rehabil. 16:282–299.

Peters AJ, Liu H, Komiyama T. 2017. Learning in the Rodent Motor Cortex. Annu Rev Neurosci. 40:77–97.

Petrof I, Viaene AN, Sherman SM. 2015. Properties of the primary somatosensory cortex projection to the primary motor cortex in the mouse. J Neurophysiol. 113:2400–2407.

Pfurtscheller G, Graimann B, Huggins JE, Levine SP, Schuh LA. 2003. Spatiotemporal patterns of beta desynchronization and gamma synchronization in corticographic data during self-paced movement. Clin Neurophysiol. 114:1226–1236.

Pfurtscheller G, Lopes da Silva FH. 1999. Event-related EEG/MEG synchronization and desynchronization: basic principles. Clin Neurophysiol. 110:1842–1857.

Pocock JM, Kettenmann H. 2007. Neurotransmitter receptors on microglia. Trends Neurosci. 30:527–535.

Poli P, Morone G, Rosati G, Masiero S. 2013. Robotic technologies and rehabilitation: new tools for stroke patients' therapy. Biomed Res Int. 2013:153872.

Pomper MG, Hammond H, Yu X, Ye Z, Foss CA, Lin DD, Fox JJ, Cheng L. 2009. Serial imaging of human embryonic stem-cell engraftment and teratoma formation in live mouse models. Cell Res. 19:370–379.

Popivanov D, Mineva A, Krekule I. 1999. EEG patterns in theta and gamma frequency range and their probable relation to human voluntary movement organization. Neurosci Lett. 267:5–8.

Post-stroke rehabilitation: assessment, referral, and patient management. U.S. Department of Health and Human Services Public Health Service. Agency for Health Care Policy and Research. 1995. . Clin Pract Guidel Quick Ref Guide Clin. i–iii, 1-32.

Posteraro F, Mazzoleni S, Aliboni S, Cesqui B, Battaglia A, Dario P, Micera S. 2009. Robot-mediated therapy for paretic upper limb of chronic patients following neurological injury. J Rehabil Med. 41:976–980.

Prabhakaran S, Zarahn E, Riley C, Speizer A, Chong JY, Lazar RM, Marshall RS, Krakauer JW. 2008. Inter-individual Variability in the Capacity for Motor Recovery After Ischemic Stroke. Neurorehabil Neural Repair. 22:64–71.

Puig J, Blasco G, Daunis-I-Estadella J, Thomalla G, Castellanos M, Figueras J, Remollo S, van Eendenburg C, Sánchez-González J, Serena J, Pedraza S. 2013. Decreased Corticospinal Tract Fractional Anisotropy Predicts Long-term Motor Outcome After Stroke. Stroke. 44:2016–2018.

Puig J, Blasco G, Schlaug G, Stinear CM, Daunis-i-Estadella P, Biarnes C, Figueras J, Serena J, Hernández-Pérez M, Alberich-Bayarri A, Castellanos M, Liebeskind DS, Demchuk AM, Menon BK, Thomalla G, Nael K, Wintermark M, Pedraza S. 2017. Diffusion tensor imaging as a prognostic biomarker for motor recovery and rehabilitation after stroke. Neuroradiology. 59:343–351.

Quartarone A, Siebner HR, Rothwell JC. 2006. Task-specific hand dystonia: can too much plasticity be bad for you? Trends Neurosci. 29:192–199.

Raffin E, Hummel FC. 2018. Restoring Motor Functions After Stroke: Multiple Approaches and

Opportunities. Neurosci. 24:400–416.

Ramos-Cabrer P, Justicia C, Wiedermann D, Hoehn M. 2010. Stem Cell Mediation of Functional Recovery after Stroke in the Rat. PLoS One. 5:e12779.

Ratcliffe E, Glen KE, Naing MW, Williams DJ. 2013. Current status and perspectives on stem cell-based therapies undergoing clinical trials for regenerative medicine: case studies. Br Med Bull. 108:73–94.

Rathelot J-A, Strick PL. 2009. Subdivisions of primary motor cortex based on cortico-motoneuronal cells. Proc Natl Acad Sci U S A. 106:918–923.

Rijntjes M, Weiller C. 2002. Recovery of motor and language abilities after stroke: the contribution of functional imaging. Prog Neurobiol. 66:109–122.

Risedal A, Mattsson B, Dahlqvist P, Nordborg C, Olsson T, Johansson BB. 2002. Environmental influences on functional outcome after a cortical infarct in the rat. Brain Res Bull. 58:315–321.

Robertson JA. 2001. Human embryonic stem cell research: ethical and legal issues. Nat Rev Genet. 2:74–78.

Rondina JM, Park C-H, Ward NS. 2017a. Brain regions important for recovery after severe post-stroke upper limb paresis. J Neurol Neurosurg Psychiatry. 88:737–743.

Rosario CM, Yandava BD, Kosaras B, Zurakowski D, Sidman RL, Snyder EY. 1997. Differentiation of engrafted multipotent neural progenitors towards replacement of missing granule neurons in meander tail cerebellum may help determine the locus of mutant gene action. Development. 124:4213–4224.

Rossini PM, Calautti C, Pauri F, Baron J-C. 2003. Post-stroke plastic reorganisation in the adult brain. Lancet Neurol. 2:493–502.

Rossiter HE, Boudrias M-H, Ward NS. 2014. Do movement-related beta oscillations change after stroke? J Neurophysiol. 112:2053–2058.

Rosso C, Samson Y. 2014. The ischemic penumbra. Curr Opin Neurol. 27:35–41.

Saletti A, Morghen I, Finessi L, Fainardi E. 2011. Angioplasty in acute middle cerebral artery stroke due to atrial fibrillation selected by CT perfusion: a case report. Int J Emerg Med. 4:23.

Samdani AF, Dawson TM, Dawson VL. 1997. Nitric oxide synthase in models of focal ischemia. Stroke. 28:1283–1288.

Sandvig I, Augestad IL, Håberg AK, Sandvig A. 2018. Neuroplasticity in stroke recovery. The role of microglia in engaging and modifying synapses and networks. Eur J Neurosci. 47:1414–1428.

Sandvig I, Gadjanski I, Vlaski-Lafarge M, Buzanska L, Loncaric D, Sarnowska A, Rodriguez L, Sandvig A, Ivanovic Z. 2017. Strategies to Enhance Implantation and Survival of Stem Cells After Their Injection in Ischemic Neural Tissue. Stem Cells Dev. 26:554–565.

Sandvig I, Karstensen K, Rokstad AM, Aachmann FL, Formo K, Sandvig A, Skjåk-Braek G, Strand BL. 2015. RGD-peptide modified alginate by a chemoenzymatic strategy for tissue engineering applications. J Biomed Mater Res Part A. 103:896–906.

Sauter A, Rudin M. 1995. Strain-dependent drug effects in rat middle cerebral artery occlusion model of stroke. J Pharmacol Exp Ther. 274:1008–1013.

Saver JL. 2010. Targeting the Brain: Neuroprotection and Neurorestoration in Ischemic Stroke. Pharmacotherapy. 30:62S–69S.

Schaechter JD, Fricker ZP, Perdue KL, Helmer KG, Vangel MG, Greve DN, Makris N. 2009. Microstructural status of ipsilesional and contralesional corticospinal tract correlates with motor skill in chronic stroke patients. Hum Brain Mapp. 30:3461–3474.

Schleiger E, Sheikh N, Rowland T, Wong A, Read S, Finnigan S. 2014a. Frontal EEG delta/alpha ratio and screening for post-stroke cognitive deficits: the power of four electrodes. Int J Psychophysiol. 94:19–24.

Schroeter M, Jander S, Stoll G. 2002. Non-invasive induction of focal cerebral ischemia in mice by photothrombosis of cortical microvessels: characterization of inflammatory responses. J Neurosci Methods. 117:43–49.

Schulz R, Park E, Lee J, Chang WH, Lee A, Kim Y-H, Hummel FC. 2017. Interactions Between the Corticospinal Tract and Premotor–Motor Pathways for Residual Motor Output After Stroke. Stroke. 48:2805–2811.

Seniów J, Bilik M, Leśniak M, Waldowski K, Iwański S, Członkowska A. 2012. Transcranial Magnetic Stimulation Combined With Physiotherapy in Rehabilitation of Poststroke Hemiparesis. Neurorehabil Neural Repair. 26:1072–1079.

Sheen VL, Arnold MW, Wang Y, Macklis JD. 1999. Neural Precursor Differentiation Following Transplantation into Neocortex Is Dependent on Intrinsic Developmental State and Receptor Competence. Exp Neurol. 158:47–62.

Shen Q, Meng X, Fisher M, Sotak CH, Duong TQ. 2003. Pixel-by-Pixel Spatiotemporal Progression of Focal Ischemia Derived Using Quantitative Perfusion and Diffusion Imaging. J Cereb Blood Flow Metab. 23:1479–1488.

Shenoy K V., Sahani M, Churchland MM. 2013. Cortical Control of Arm Movements: A Dynamical Systems Perspective. Annu Rev Neurosci. 36:337–359.

Sheorajpanday RVA, Nagels G, Weeren AJTM, De Deyn PP. 2011a. Quantitative EEG in ischemic stroke: correlation with infarct volume and functional status in posterior circulation and lacunar syndromes. Clin Neurophysiol. 122:884–890.

Shetty AK, Turner DA. 1996. Development of fetal hippocampal graft in intact and lesioned hippocampus. Prog Neurobiol. 50:597–653.

Shi Y, Kirwan P, Smith J, Robinson HPC, Livesey FJ. 2012. Human cerebral cortex development from pluripotent stem cells to functional excitatory synapses. Nat Neurosci. 15:477–486.

Shin JJ, Fricker-Gates RA, Perez FA, Leavitt BR, Zurakowski D, Macklis JD. 2000. Transplanted neuroblasts differentiate appropriately into projection neurons with correct neurotransmitter and receptor phenotype in neocortex undergoing targeted projection neuron degeneration. J Neurosci. 20:7404–7416.

Shiner CT, Tang H, Johnson BW, McNulty PA. 2015. Cortical beta oscillations and motor thresholds differ across the spectrum of post-stroke motor impairment, a preliminary MEG and TMS study. Brain Res. 1629:26–37.

Shintani Y, Terao Y, Ohta H. 2011. Molecular Mechanisms Underlying Hypothermia-Induced Neuroprotection. Stroke Res Treat. 2011:1–9.

Siesjo BK, Siesjo P. 1996. Mechanisms of secondary brain injury. Eur J Anaesthesiol. 13:247–268.

Sigler A, Murphy TH. 2010. In Vivo 2-Photon Imaging of Fine Structure in the Rodent Brain: Before, During, and After Stroke. Stroke. 41:S117–S123.

Singh V, Roth S, Veltkamp R, Liesz A. 2016. HMGB1 as a Key Mediator of Immune Mechanisms in Ischemic Stroke. Antioxid Redox Signal. 24:635–651.

Smith GM, Strunz C. 2005. Growth factor and cytokine regulation of chondroitin sulfate proteoglycans by astrocytes. Glia. 52:209–218.

Sohal VS, Zhang F, Yizhar O, Deisseroth K. 2009. Parvalbumin neurons and gamma rhythms enhance cortical circuit performance. Nature. 459:698–702.

Sohn H-M, Hwang J-Y, Ryu J-H, Kim J, Park S, Park J, Han S-H. 2017. Simvastatin protects ischemic spinal cord injury from cell death and cytotoxicity through decreasing oxidative stress: in vitro primary cultured rat spinal cord model under oxygen and glucose deprivation-reoxygenation conditions. J Orthop Surg Res. 12:36.

Soleman S, Yip PK, Duricki DA, Moon LDF. 2012. Delayed treatment with chondroitinase ABC promotes sensorimotor recovery and plasticity after stroke in aged rats. Brain. 135:1210–1223.

Spalletti C, Alia C, Lai S, Panarese A, Conti S, Micera S, Caleo M. 2017. Combining robotic training and inactivation of the healthy hemisphere restores pre-stroke motor patterns in mice. Elife. 6.

Spalletti C, Lai S, Mainardi M, Panarese A, Ghionzoli A, Alia C, Gianfranceschi L, Chisari C, Micera S, Caleo M. 2014. A Robotic System for Quantitative Assessment and Poststroke Training of Forelimb Retraction in Mice. Neurorehabil Neural Repair. 28:188–196.

Sterr A, Dean PJA, Szameitat AJ, Conforto AB, Shen S. 2014. Corticospinal Tract Integrity and Lesion Volume Play Different Roles in Chronic Hemiparesis and Its Improvement Through Motor Practice. Neurorehabil Neural Repair. 28:335–343.

Sterr A, Shan Shen S, Szameitat AJ, Herron KA. 2010. The Role of Corticospinal Tract Damage in Chronic Motor Recovery and Neurorehabilitation: A Pilot Study. Neurorehabil Neural Repair. 24:413–419.

Stinear CM. 2017. Prediction of motor recovery after stroke: advances in biomarkers. Lancet Neurol. 16:826–836.

Stinear CM, Barber PA, Petoe M, Anwar S, Byblow WD. 2012. The PREP algorithm predicts potential for upper limb recovery after stroke. Brain. 135:2527–2535.

Stinear CM, Barber PA, Smale PR, Coxon JP, Fleming MK, Byblow WD. 2006. Functional potential in chronic stroke patients depends on corticospinal tract integrity. Brain. 130:170–180.

Stinear CM, Fleming MK, Barber PA, Byblow WD. 2007. Lateralization of motor imagery following stroke. Clin Neurophysiol. 118:1794–1801.

Stroemer RP, Kent TA, Hulsebosch CE. 1993. Acute increase in expression of growth associated protein GAP-43 following cortical ischemia in rat. Neurosci Lett. 162:51–54.

Sutherland BA, Neuhaus AA, Couch Y, Balami JS, DeLuca GC, Hadley G, Harris SL, Grey AN, Buchan AM. 2016. The transient intraluminal filament middle cerebral artery occlusion model as a model of endovascular thrombectomy in stroke. J Cereb Blood Flow Metab. 36:363–369.

Takahashi K, Yamanaka S. 2006. Induction of Pluripotent Stem Cells from Mouse Embryonic and Adult Fibroblast Cultures by Defined Factors. Cell. 126:663–676.

Takeuchi N, Izumi S-I. 2012. Maladaptive Plasticity for Motor Recovery after Stroke: Mechanisms and Approaches. Neural Plast. 2012:1–9.

Takeuchi N, Izumi S-I. 2013. Rehabilitation with Poststroke Motor Recovery: A Review with a Focus on Neural Plasticity. Stroke Res Treat. 2013:1–13.

Talelli P, Greenwood RJ, Rothwell JC. 2006. Arm function after stroke: neurophysiological correlates and recovery mechanisms assessed by transcranial magnetic stimulation. Clin Neurophysiol. 117:1641–1659.

Tamura A, Graham DI, McCulloch J, Teasdale GM. 1981. Focal Cerebral Ischaemia in the Rat: 1. Description of Technique and Early Neuropathological Consequences following Middle Cerebral Artery Occlusion. J Cereb Blood Flow Metab. 1:53–60.

Tarr D, Graham D, Roy LA, Holmes WM, McCabe C, Macrae IM, Muir KW, Dewar D. 2013. Hyperglycemia Accelerates Apparent Diffusion Coefficient-Defined Lesion Growth after Focal Cerebral Ischemia in Rats with and Without Features of Metabolic Syndrome. J Cereb Blood Flow Metab. 33:1556–1563.

Tatarishvili J, Oki K, Monni E, Koch P, Memanishvili T, Buga A-M, Verma V, Popa-Wagner A, Brüstle O, Lindvall O, Kokaia Z. 2014. Human induced pluripotent stem cells improve recovery in stroke-injured aged rats. Restor Neurol Neurosci. 32:547–558.

Teasell R, Bayona NA, Bitensky J. 2005. Plasticity and Reorganization of the Brain Post Stroke. Top Stroke Rehabil. 12:11–26.

Teasell RW, Foley NC, Salter KL, Jutai JW. 2008. A blueprint for transforming stroke rehabilitation care in Canada: the case for change. Arch Phys Med Rehabil. 89:575–578.

Tecchio F, Pasqualetti P, Zappasodi F, Tombini M, Lupoi D, Vernieri F, Rossini PM. 2007. Outcome prediction in acute monohemispheric stroke via magnetoencephalography. J Neurol. 254:296–305.

Tedesco Triccas L, Meyer S, Mantini D, Camilleri K, Falzon O, Camilleri T, Verheyden G. 2019. A systematic review investigating the relationship of electroencephalography and magnetoencephalography measurements with sensorimotor upper limb impairments after stroke. J Neurosci Methods. 311:318–330.

Teng H, Zhang ZG, Wang L, Zhang RL, Zhang L, Morris D, Gregg SR, Wu Z, Jiang A, Lu M, Zlokovic B V, Chopp M. 2008. Coupling of Angiogenesis and Neurogenesis in Cultured Endothelial Cells and Neural Progenitor Cells after Stroke. J Cereb Blood Flow Metab. 28:764–771.

Terrigno M, Busti I, Alia C, Pietrasanta M, Arisi I, D'Onofrio M, Caleo M, Cremisi F. 2018. Neurons Generated by Mouse ESCs with Hippocampal or Cortical Identity Display Distinct Projection Patterns When Co-transplanted in the Adult Brain. Stem cell reports. 10:1016–1029.

Theodore WH, Hunter K, Chen R, Vega-Bermudez F, Boroojerdi B, Reeves-Tyer P, Werhahn K, Kelley KR, Cohen L. 2002. Transcranial magnetic stimulation for the treatment of seizures: A controlled study. Neurology. 59:560–562

Thomson JA, Itskovitz-Eldor J, Shapiro SS, Waknitz MA, Swiergiel JJ, Marshall VS, Jones JM. 1998. Embryonic Stem Cell Lines Derived from Human Blastocysts. Science (80-). 282:1145–1147.

Tornero D, Tsupykov O, Granmo M, Rodriguez C, Grønning-Hansen M, Thelin J, Smozhanik E, Laterza C, Wattananit S, Ge R, Tatarishvili J, Grealish S, Brüstle O, Skibo G, Parmar M, Schouenborg J, Lindvall O, Kokaia Z. 2017. Synaptic inputs from stroke-injured brain to grafted human stem cell-derived neurons activated by sensory stimuli. Brain. 140:692–706.

Tornero D, Wattananit S, Grønning Madsen M, Koch P, Wood J, Tatarishvili J, Mine Y, Ge R, Monni E, Devaraju K, Hevner RF, Brüstle O, Lindvall O, Kokaia Z. 2013. Human induced pluripotent stem cell-derived cortical neurons integrate in stroke-injured cortex and improve functional recovery. Brain. 136:3561–3577.

Touvykine B, Mansoori BK, Jean-Charles L, Deffeyes J, Quessy S, Dancause N. 2016. The Effect of Lesion Size on the Organization of the Ipsilesional and Contralesional Motor Cortex. Neurorehabil Neural Repair. 30:280–292.

Traversa R, Cicinelli P, Bassi A, Rossini PM, Bernardi G. 1997. Mapping of Motor Cortical Reorganization After Stroke. Stroke. 28:110–117.

Trounson A, DeWitt ND. 2016. Pluripotent stem cells progressing to the clinic. Nat Rev Mol Cell Biol. 17:194–200.

Truelsen T, Piechowski-Jozwiak B, Bonita R, Mathers C, Bogousslavsky J, Boysen G. 2006. Stroke incidence and prevalence in Europe: a review of available data. Eur J Neurol. 13:581–598.

Tsujimoto T, Shimazu H, Isomura Y. 2006. Direct Recording of Theta Oscillations in Primate Prefrontal and Anterior Cingulate Cortices. J Neurophysiol. 95:2987–3000.

Turak B, Louvel J, Buser P, Lamarche M. 2001. Parieto-temporal rhythms in the 6–9 Hz band recorded in epileptic patients with depth electrodes in a self-paced movement protocol. Clin Neurophysiol. 112:2069–2074.

Tuttolomondo A, Di Raimondo D, di Sciacca R, Pinto A, Licata G. 2008. Inflammatory Cytokines in Acute Ischemic Stroke. Curr Pharm Des. 14:3574–3589.

Tzvetanov P, Rousseff RT, Atanassova P. 2005. Prognostic value of median and tibial somatosensory evoked potentials in acute stroke. Neurosci Lett. 380:99–104.

Uhlhaas PJ, Pipa G, Neuenschwander S, Wibral M, Singer W. 2011. A new look at gamma? High-(>60 Hz) γ-band activity in cortical networks: function, mechanisms and impairment. Prog Biophys Mol Biol. 105:14–28.

Vallone F, Lai S, Spalletti C, Panarese A, Alia C, Micera S, Caleo M, Di Garbo A. 2016a. Post-Stroke Longitudinal Alterations of Inter-Hemispheric Correlation and Hemispheric Dominance in Mouse Pre-Motor Cortex. PLoS One. 11:e0146858.

van Meer MPA, van der Marel K, Wang K, Otte WM, El Bouazati S, Roeling TAP, Viergever MA, Berkelbach van der Sprenkel JW, Dijkhuizen RM. 2010. Recovery of sensorimotor function after experimental stroke correlates with restoration of resting-state interhemispheric functional connectivity. J Neurosci. 30:3964–3972.

van Putten MJAM. 2007. The revised brain symmetry index. Clin Neurophysiol. 118:2362–2367.

van Putten MJAM, Tavy DLJ. 2004. Continuous Quantitative EEG Monitoring in Hemispheric Stroke Patients Using the Brain Symmetry Index. Stroke. 35:2489–2492.

Vardy E, Robinson JE, Li C, Olsen RHJ, DiBerto JF, Giguere PM, Sassano FM, Huang X-P, Zhu H, Urban DJ, White KL, Rittiner JE, Crowley NA, Pleil KE, Mazzone CM, Mosier PD, Song J, Kash TL, Malanga CJ, Krashes MJ, Roth BL. 2015. A New DREADD Facilitates the Multiplexed Chemogenetic Interrogation of Behavior. Neuron. 86:936–946.

Volpe BT, Krebs HI, Hogan N, Edelstein L, Diels C, Aisen M. 2000. A novel approach to stroke rehabilitation: Robot-aided sensorimotor stimulation. Neurology. 54:1938–1944.

Wahl A-S, Schwab ME. 2014. Finding an optimal rehabilitation paradigm after stroke: enhancing fiber growth and training of the brain at the right moment. Front Hum Neurosci. 8.

Wang L, Yu C, Chen H, Qin W, He Y, Fan F, Zhang Y, Wang M, Li K, Zang Y, Woodward TS, Zhu C. 2010. Dynamic functional reorganization of the motor execution network after stroke. Brain. 133:1224–1238.

Wang T, Cui W, Xie Y, Zhang W, Sci SD-AJB, 2010. Controlling the volume of the focal cerebral ischemic lesion through photothrombosis. researchgate.net.

Ward NS. 2017. Restoring brain function after stroke — bridging the gap between animals and humans. Nat Rev Neurol. 13:244–255.

Ward NS, Brown MM, Thompson AJ, Frackowiak RSJ. 2003. Neural correlates of motor recovery after stroke: a longitudinal fMRI study. Brain. 126:2476–2496.

Watson BD, Dietrich WD, Busto R, Wachtel MS, Ginsberg MD. 1985. Induction of reproducible brain infarction by photochemically initiated thrombosis. Ann Neurol. 17:497–504.

Weinrich M, Good DC, Reding M, Roth EJ, Cifu DX, Silver KH, Craik RL, Magaziner J, Terrin M,

Schwartz M, Gerber L. 2004. Timing, Intensity, and Duration of Rehabilitation for Hip Fracture and Stroke: Report of a Workshop at the National Center for Medical Rehabilitation Research. Neurorehabil Neural Repair. 18:12–28.

Westlake KP, Hinkley LB, Bucci M, Guggisberg AG, Findlay AM, Henry RG, Nagarajan SS, Byl N. 2012a. Resting state alpha-band functional connectivity and recovery after stroke. Exp Neurol. 237:160–169.

Wintermark M, Reichhart M, Cuisenaire O, Maeder P, Thiran J-P, Schnyder P, Bogousslavsky J, Meuli R. 2002. Comparison of Admission Perfusion Computed Tomography and Qualitative Diffusion- and Perfusion-Weighted Magnetic Resonance Imaging in Acute Stroke Patients. Stroke. 33:2025–2031.

Winters C, Heymans MW, van Wegen EEH, Kwakkel G. 2016. How to design clinical rehabilitation trials for the upper paretic limb early post stroke? Trials. 17:468.

Wittenberg GF. 2010. Experience, cortical remapping, and recovery in brain disease. Neurobiol Dis. 37:252–258.

Wobus AM, Boheler KR. 2005. Embryonic Stem Cells: Prospects for Developmental Biology and Cell Therapy. Physiol Rev. 85:635–678.

Wu J, Srinivasan R, Burke Quinlan E, Solodkin A, Small SL, Cramer SC. 2016. Utility of EEG measures of brain function in patients with acute stroke. J Neurophysiol. 115:2399–2405.

Wu O, Cloonan L, Mocking SJT, Bouts MJRJ, Copen WA, Cougo-Pinto PT, Fitzpatrick K, Kanakis A, Schaefer PW, Rosand J, Furie KL, Rost NS. 2015. Role of Acute Lesion Topography in Initial Ischemic Stroke Severity and Long-Term Functional Outcomes. Stroke. 46:2438–2444.

Yao H, Gao M, Ma J, Zhang M, Li S, Wu B, Nie X, Jiao J, Zhao H, Wang S, Yang Y, Zhang Y, Sun Y, Wicha MS, Chang AE, Gao S, Li Q, Xu R. 2015. Transdifferentiation-Induced Neural Stem Cells Promote Recovery of Middle Cerebral Artery Stroke Rats. PLoS One. 10:e0137211.

Zeiler SR, Krakauer JW. 2013. The interaction between training and plasticity in the poststroke brain. Curr Opin Neurol. 26:609–616.

Zeiler SR, Hubbard R, Gibson EM, Zheng T, Ng K, O'Brien R, Krakauer JW. 2016. Paradoxical Motor Recovery From a First Stroke After Induction of a Second Stroke. Neurorehabil Neural Repair. 30:794–800.

Zhang J, Chopp M. 2013. Cell-based therapy for ischemic stroke. Expert Opin Biol Ther. 13:1229–1240.

Zhu LL, Lindenberg R, Alexander MP, Schlaug G. 2010. Lesion Load of the Corticospinal Tract Predicts Motor Impairment in Chronic Stroke. Stroke. 41:910–915.

Zhu M, HajiHosseini A, Baumeister TR, Garg S, Appel-Cresswell S, McKeown MJ. 2019. Altered EEG alpha and theta oscillations characterize apathy in Parkinson's disease during incentivized movement. NeuroImage Clin. 23:101922.

Ziemann U, Ishii K, Borgheresi A, Yaseen Z, Battaglia F, Hallett M, Cincotta M, Wassermann EM. 1999. Dissociation of the pathways mediating ipsilateral and contralateral motor-evoked potentials in human hand and arm muscles. J Physiol. 518:895–906.

Zigmond M, Coyle J, Rowland L. 2014. Neurobiology of brain disorders: biological basis of neurological and psychiatric disorders.

Acknowledgements

First, I want to thank Professor Ubaldo Bonuccelli for giving me the opportunity to carry out my PhD at University of Florence.

The results obtained in this thesis have been collected at the Neuroscience Institute of the CNR of Pisa. I would like to thank all the people from IN for their help, support and suggestions. Especially, my second supervisor, Professor Matteo Caleo. I spent four years in your group and I couldn't do a better choice, not only for your scientific knowledge that, everybody knows, is absolute, but also because every time I needed to be listened and supported, you were present and it's something I have never taken for granted. I have learnt a lot from you and there are not enough thanks for this.

Thanks also to our collaborators who gave an important contribute to my thesis: Dr Federico Cremisi (Scuola Normale Superiore, Pisa), Dr Angelo Di Garbo and Marco Carloni (Biophysics Institute, CNR, Pisa), Maria Grazia De Simoni and Carlo Perego (Mario Negri Institute, Milano).

A big thank to Claudia. I remember the first day at CNR and you were there. I didn't know you, but I immediately felt admiration for you, so young (let me say younger than now XD) and so good and passionate in what you did. I wasn't wrong. I had always great respect for you as a tutor for your patient guide, as a friend for your simplicity and altruism and as a scientist for the passion you put into your work, despite the sacrifices. For these reasons, I wish you, from my heart, to obtain the satisfactions you deserve.

Thanks to Alessio, you saved me in a period where I felt scientifically lost. You, with your 'I know everything' and your determination and ambition, gave me the enthusiasm to start our project that couldn't be in this way if it wasn't also for you.

Thanks to Verediana and Daniele who took care of this project when I wasn't in Italy, giving a great input and also to Maria, my favorite engineer, who never gives up and she is always ready to help.

Thanks to Laura, for your wise advises and our 'gossip' chats. Even if I tease you saying you are old, the truth is that I never felt distance between us.

Nadia, thank you for your 'not scientific' support and for our authentic friendship. During these years I learned to understand you and your silences and I realized that there is no need for so many words between two people who love each other. Sara, on the contrary, you always speak a lot (fortunately) and bring a bit of good madness between our three. I admire your ability to not be afraid to put you on the line.

Thanks to people I met during my PhD in the lab that made my work more pleasant: Elena, Manuella, Cristina, Marco, Claudia, Eleonora, Laura B and many others. A special thanks to Miriam with whom I shared only one year but it was enough to understand our great complicity.

During my PhD I had the opportunity to spend seven months abroad, in Norway at NTNU Institute of Trondheim. Before leaving I couldn't imagine to be so good in a place that was

not my home but I fell in love with this amazing country. This is mostly because I was lucky enough to work with Ioanna and Axel Sandvig who immediately made me feel part of their group and gave me the possibility to do a scientific and formative experience that I never forgot. Thanks to all the people in your lab: Ola, Janelle, Lars, Ulrich, Kristine, Vegard and Nicholas.
Vibeke, this experience couldn't be so beautiful if it wasn't for you and also Eirik. From the first day I came, you have been so kind to help me and guide me into something that was completely unknown for me. I enjoyed our early lunches and very early dinners, the walks into the woods with Navdi and the days spent in your wonderful cabin. Even if this experience is finished I know that now I have a true friend.

Thanks to my distant but close friends: Federica and Francesca. Fede we started this experience almost together and during these years we shared our satisfactions and disappointments. I always knew I could count on you for everything and I couldn't be more grateful for our friendship. Fra, instead, you have always dampened my pessimism with your smile and positivity and it's something for which I will always thank you.

Thanks to my certainty, Camilla, always with me in everything I do.

A special thanks to my family. You have always trusted me and believed in me more than I did.

Finally, thanks to Tommaso. I know you from exactly ten years. Since the beginning, you have been, probably without knowing, my polar star. You have endured me and supported into my troubles and paranoia and you were my first fan for my little successes. You, with your laugh, bring joy to my life and now I know that whatever the future holds for us, we will be together.

Appendix

During my PhD, I was also involved in a different project about a mouse model of X-linked Intellectual Disability caused by the loss of Oligophrenin-1(Ophn-1) gene.

I started this project during my master thesis in collaboration with the group of Dr. Billuart (Institut Cochin, Paris). Firstly, we exploited adult hippocampal neurogenesis to dissect the steps of neuronal differentiation that were affected by Ophn-1 deletion. Since Ophn-1 KO mice displayed over-activation of Rho-associated protein kinase (ROCK) and protein kinase A (PKA) signaling, we administered a clinically approved ROCK/PKA inhibitor (fasudil) to correct the neurogenesis defects.
The results obtained during this work were published in the following paper:
M. Allegra, C. Spalletti, B. Vignoli, S. Azzimondi, **I. Busti**, P. Billuart, M. Caleo,
Neurobiol. Dis. **2017**, *100*, 75-86

In this article we demonstrated alterations of adult neurogenesis in the hippocampus of Ophn1- deficient mice. Specifically, Ophn1 deletion reduced the survival of newly generated neurons and impacted both dendritic and axonal outgrowth. Importantly, these defects could be significantly attenuated by administration of fasudil in the drinking water. In particular, my contribution consisted in the histological analysis of newly generated neurons in Ophn-1 -/y and Ophn-1 +/y in physiological and Fasudil-treated conditions.
Then, we investigated whether the loss of function of Ophn-1 can alter inhibitory hippocampal circuitry and enhance seizure propensity and we assessed the possibility to rescue network defects by using fasudil, a clinically approved drug already used.
The final paper was submitted to the '*Journal of Neuroscience'* and it was recently accepted.

ROCK/PKA inhibition rescues hippocampal hyperexcitability and GABAergic neuron alterations in Oligophrenin-1 Knock-out mouse model of X-linked intellectual disability

Irene Busti[1,2,*], *Manuela Allegra*[1,*,§], *Cristina Spalletti*[1], *Pierre Billuart*[3], *Matteo Caleo*[1,4]

[1] Neuroscience Institute, National Research Council (CNR), via G.Moruzzi 1, 56124 Pisa, Italy
[2] NEUROFARBA, University of Florence, via G. Pieraccini 6, 50134 Florence, Italy
[3]Institute of Psychiatry and Neuroscience of Paris, INSERM UMR1266, Paris Descartes University, 102-108 rue de la Santé, 75014 Paris, France
[4] Department of Biomedical Sciences, University of Padua, via G. Colombo 3, 35121 Padua, Italy

*I.B. and M.A. share equal contribution as first authors
[§]M.A. present address: Institut Pasteur, 25 Rue du Dr Roux, 75015 Paris, France

Abbreviated title: Rescue of hyperexcitability in Ophn1 KO mice

Abstract

Oligophrenin-1 (Ophn1) encodes a Rho GTPase activating protein whose mutations cause X-linked intellectual disability (XLID) in humans. Loss of function of Ophn1 leads to impairments in the maturation and function of excitatory and inhibitory synapses, causing deficits in synaptic structure, function and plasticity. Epilepsy is a frequent co-morbidity in patients with Ophn1-dependent XLID, but the cellular bases of hyperexcitability are poorly understood. Here we report that male mice knock-out (KO) for Ophn1 display hippocampal epileptiform alterations, which are associated with changes in parvalbumin- and neuropeptide Y-positive interneurons. Since loss of function of Ophn1 is related to enhanced activity of Rho-associated protein kinase (ROCK) and protein kinase A (PKA), we attempted to rescue Ophn1-dependent pathological phenotypes by treatment with the ROCK/PKA inhibitor Fasudil. We found that seven weeks of Fasudil treatment in adulthood were able to correct the electrographic and neuroanatomical alterations of Ophn1 deficient mice. These data demonstrate that hyperexcitability and the associated changes in GABAergic markers can be rescued at the adult stage in Ophn1-dependent XLID through ROCK/PKA inhibition.

Key words: hippocampus, interneurons, epilepsy, Fasudil

Significance Statement: In this study we demonstrate enhanced seizure propensity and impairments in hippocampal GABAergic circuitry in Ophn1 mouse model of XLID. Importantly, the enhanced susceptibility to seizures, accompanied by an alteration of GABAergic markers were rescued by ROCK/PKA inhibitor Fasudil, a drug already tested on humans. Since seizures can significantly impact the quality of life of XLID patients, the present data suggest a potential therapeutic pathway to correct alterations in GABAergic networks and dampen pathological hyperexcitability in adults with XLID.